Summary of climate- and geohazard-related vulnerabilities for the Dempster Highway corridor

YC-2018-100

Yukon

Transport
Canada

Transports
Canada

PROJECT TEAM

Authors

Fabrice Calmels	Northern Climate ExChange, Yukon Research Centre, Yukon College
Louis-Philippe Roy	Northern Climate ExChange, Yukon Research Centre, Yukon College
Katerine Grandmont	Northern Climate ExChange, Yukon Research Centre, Yukon College
Rachel Pugh	Northern Climate ExChange, Yukon Research Centre, Yukon College

Disclaimer

Acknowledgments

TABLE OF CONTENTS

1   INTRODUCTION

The Dempster Highway is the only road connection to the western Arctic. Now connected with the Inuvik-Tuktoyaktuk Highway, it is part of the infrastructure linking southern Canada with the Arctic Ocean. Extensive reconstruction of the Dempster Highway has been completed on the NWT side of the territorial border in response to degradation of the road surface and embankment. Recognizing the need to ensure year-round availability of the Dempster Highway in the context of increasing traffic and a changing climate, Yukon Government Department of Highways and Public Works (HPW) has initiated a project to create a functional plan that specifically considers contributions of climate change to geohazards along the highway. Research and analysis required to assess climate and geohazard vulnerability have been carried out by the Northern Climate ExChange, part of the Yukon Research Centre at Yukon College, feeding into the functional planning process carried out by an engineering consultant. This report is a summary of climate- and geohazard-related vulnerabilities for the highway corridor.

This project included various activities. The first step consisted of a preliminary assessment and literature review, where data and report from previous surveys and studies pertaining to the study area and its surroundings were reviewed. Additional information such as articles, air photos, satellite imagery, geological and surficial geological maps have been reviewed to gain insight about the geomorphologic and surficial geologic conditions of the area.

The preliminary assessment was followed by field assessments which took place during the summer and fall, 2017. Field work included a combination of drilling, electrical resistivity tomography (ERT), and installation of ground temperature monitoring instruments. Core samples collected during drilling were kept frozen and returned to the Northern Climate ExChange (NCE) lab in Whitehorse for further analyses including soil grain-size analysis, cryostructure, volumetric excess ice content and gravimetric ice content. Ground temperature data was downloaded in the fall from monitoring instruments installed earlier in the summer, and from those installed in previous years.

This report presents the results of the field, laboratory, and desktop assessment. Subsequent sections include a review of methodology, summarizing the techniques used for the surveys and their underlying principles; a presentation and discussion of the existing and newly collected data for each site; and, hypotheses and discussion of supporting evidence of the origin and processes leading to the identified geohazards at each site.

The present work is only intended to determine the nature of the issues at each site. Further investigations may be required. It remains HPW's prerogative to determine the action to take to deal with the issues at each site.

2   METHODOLOGY

The objective of this project was to understand the issues contributing to identified geo-hazards along the Dempster Highway. To achieve this objective, a combination of desktop study and field investigation were used.

2.1   ASSESSMENT OF EXISTING DATA

Surficial geology maps prepared by the Yukon Geological Survey, as well as aerial and satellite images were interpreted as part of this project. These data were supplemented with geotechnical reports from consultants and discussion with civil engineers and maintenance crew from HPW. Data and personal communications were combined, analyzed and interpreted to complement previous efforts.

2.2   FIELD SURVEYS

Field investigation was focused largely on the acquisition of new geophysical information using electrical resistivity tomography (ERT) surveys. In addition, shallow drilling was used to verify interpretations of geophysical information and to develop cryostratigraphic logs. Importantly, the work focuses on areas proximal to the highway embankment either in the field parallel to the highway, or at the toe and on the shoulder of the embankment, where minimal information is currently available. This information is key because it will allow project researchers to infer the probability of permafrost presence under the highway embankment.

2.2.1   Electrical Resistivity Tomography

Electrical resistivity tomography (ERT) is a geophysical method that passes electrical current through stainless steel electrodes that are driven into the ground surface. A central "station" measures the resistivity distribution of the subsurface between electrode pairs. Resistivity is the mathematical inverse of conductivity and indicates the ability of an electrical current to pass through a material. Mineral materials (except for specific substances such as metallic ores) are mostly non-conductive. Therefore, variation in the resistivity of a soil or rock profile is governed primarily by the amount and resistivity of pore water present in the profile, and the arrangement of the pores. This makes ERT very well suited to permafrost and hydrology applications. Because most water content in frozen ground is in the solid phase and typically has a higher resistivity than unfrozen water content, permafrost distribution can be inferred based on changes in resistivity between frozen and unfrozen ground.

An ERT system consists of an automated imaging unit and a set of wires connected to an electrode array. The system used for the surveys presented in this report is an ABEM Terrameter LS electrical resistivity and tomography system, consisting of a four-channel imaging unit and four electrode cables, each with 21 take-outs at five-metre intervals. To conduct a survey, 81 electrodes are driven into the ground along a survey line and connected to the electrode cables (Figure 2.2.1).
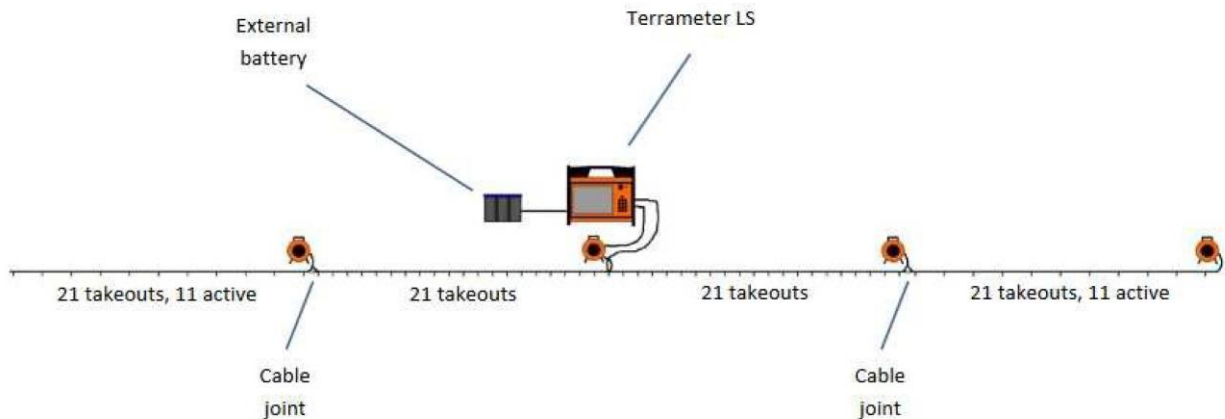
Figure 2.2.1 Instrument set-up for ERT surveying

Three different types of electrode configurations or arrays were used during the surveys: the "Wenner", "Dipole-dipole", and "gradient" arrays. These arrays differ in how they pair current and potential electrodes (Figure 2.2.2). A direct current electrical pulse is sent from the resistivity meter along the survey line in two current electrodes (C1 and C2), and the measurement is performed by two potential electrodes (P1 and P2). The resulting data consists of a cross-sectional (2D) plot of the ground's resistivity (ohm·m) versus depth (m) for the length of the survey.

4
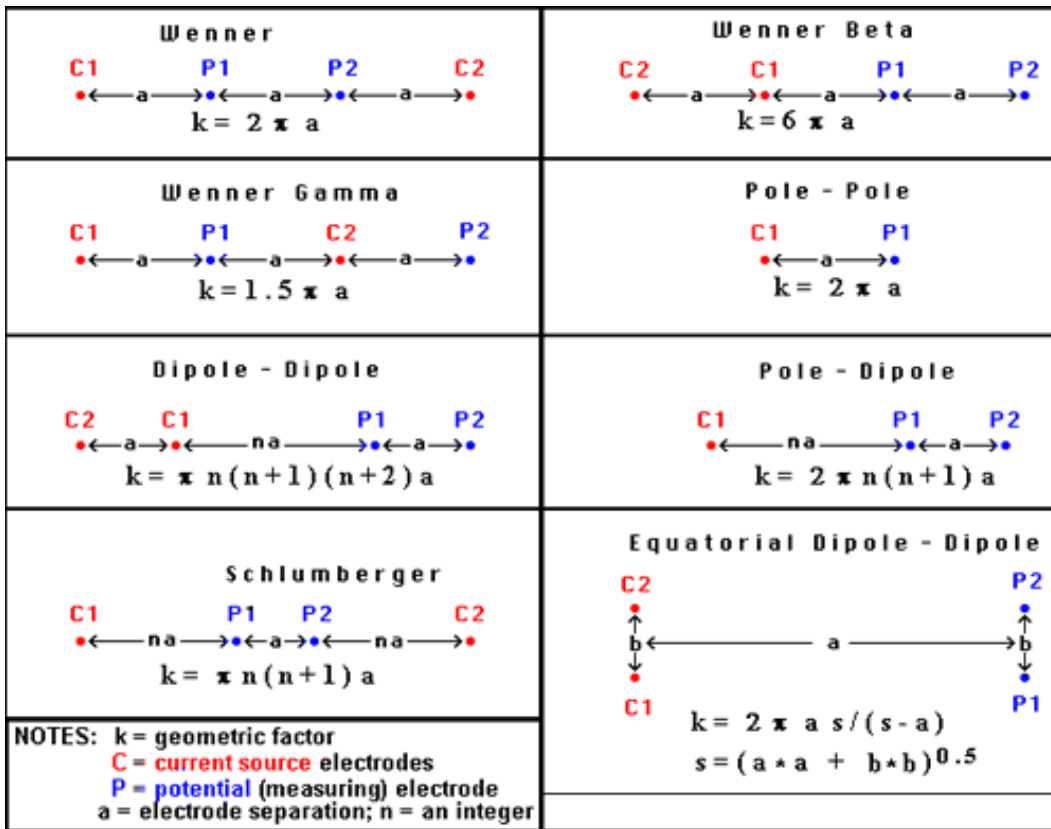
Figure 2.2.2 Survey configurations or "arrays" for ERT surveying.

In general, the Wenner array is good in resolving vertical changes (i.e. horizontal structures), but relatively poor in detecting horizontal changes (i.e. narrow vertical structures). Compared to other arrays, the Wenner array has a moderate depth of investigation. Among the common arrays, the Wenner array has the strongest signal strength. This can be an important factor if the survey is carried in areas with high background noise. Relatively small current magnitudes are needed to produce measurable potential differences. The disadvantage is that to image deep into the earth, it is necessary to use longer current cables. The Wenner array is also very sensitive to near surface inhomogeneities which may skew deeper electrical responses. One disadvantage of this array for 2-D surveys is the relatively poor horizontal coverage as the electrode spacing is increased, which can be a problem when using a system with a relatively small number of electrodes.

The dipole-dipole array is very sensitive to horizontal changes in resistivity, but relatively insensitive to vertical changes in the resistivity. That means that it is good for mapping vertical structures, such as dykes and cavities, but relatively poor in mapping horizontal structures such

as sills or sedimentary layers. This array can have a shallower depth of investigation compared to the Wenner array, but it has better horizontal data coverage than the Wenner, which can be an advantage when the number of nodes available with the multi-electrode system is small. One possible disadvantage can be a very small signal strength. With the proper field equipment and survey techniques, this array has been successfully used in many areas to detect structures such as cavities where the good horizontal resolution of this array is a major advantage.

The "gradient" array is similar to the Wenner array, but with asymmetrical electrode pairs. The "Gradient" array is less conventional, but was tested due to its efficiency and fast data acquisition time. Compared together, the data obtained by the three types of surveys allow a more comprehensive interpretation of each study sites.

Results of the surveys are post-treated and analyzed at the NCE using inversion software (Res2DInv 64 and Res3DInv 32).

2.2.2   Permafrost drilling and sample collection

A light and portable GÖLZ Earth-drill system was used to drill shallow boreholes. The borehole was initiated by shoveling a fore hole down to the thaw front. At the thaw front, the Earth-drill system was used. The drill uses a small Stihl engine with a high-speed transmission (600 rpm). The drill is coupled to stainless steel rods (1 metre in length and 4.5 cm in diameter) and a core barrel (40 cm long and 10 cm in diameter) with diamonds set in carbide alloy teeth. The drill is used in unconsolidated, fine to medium-grain material (sand to clay). A core catcher tool was used to extract frozen core from the borehole, allowing for the collection of continuous, undisturbed permafrost samples. This type of drilling is limited to a maximum drilling depth of approximately 5 to 6 m under optimal conditions. To drill boreholes at deeper depths, a conventional water-jet diamond drill was used. Details regarding these tools and the drilling methodology are provided in Calmels, Gagnon and Allard (2005).

The same sampling and drilling protocols were followed for each borehole. The site was first described (e.g., hydrology, vegetation type and density, topography), photos were taken, and locations were recorded using a hand-held GPS. Each core sample was photographed and described in situ (e.g., soil type, soil moisture, presence or absence of organic matter, any notable features). Each sample extracted from a borehole was identified by borehole name and depth. Samples were put in polybags and sealed immediately after being extracted. Samples were kept frozen and stored in a freezer that was taken back to the laboratory for further analyses. In the laboratory, each core was cleaned with cold water to remove drilling mud and then photographed.

2.3   PERMAFROST SAMPLE ANALYSIS

Laboratory analyses were carried out to measure the properties of the permafrost samples. Both soil grain characteristics and ice characteristics were evaluated. To evaluate soil grain characteristics, a grain-size analysis was performed on selected samples. To evaluate ice characteristics in permafrost samples, the cryostructure, volumetric excess ice content and gravimetric ice content were quantified. These methods are described below. For more information, please refer to Andersland and Ladanyi (2004).

Grain-size analysis
Sieve and hydrometer analyses of grain size were performed following a specifically modified American Standard and Testing Method protocol (ASTM D422-63, 2000). The sieves used were 4, 2, 1, 0.5, 0.25, 0.125 and 0.063 mm.

Cryostructure
Permafrost cryostructure (the geometry of the ice in the permafrost) depends on water availability, the soil's ice-segregation potential, and the time of freezing, all of which affect the development of ice structures in the soil matrix. Information such as soil genesis, climate conditions at the time of freezing, permafrost development history, and ground vulnerability when permafrost degrades can be interpreted from cryostructure (the shape of the ground ice), cryofacies (groups of cryostructures) analysis, and general cryostratigraphy (assemblages of cryofacies).

Because field descriptions are based only on a visual interpretation of the core, the samples were described a second time more thoroughly in the laboratory using standard terminology (Murton and French 1994). Frozen core samples were warmed to near 0°C and any refrozen mud was scraped off before the sample was described.

Gravimetric ice content
Ice content was calculated using:

$$u1 = \frac{(M_i)}{(M_s)}$$

where M_i is the ice weight, measured as weight loss after drying (g), and M_s is dry soil weight in grams. Results are expressed as percentages (dimensionless).

Volumetric excess ice content

The volumetric excess ice content was calculated by immersing the frozen sample, bagged in vacuum- sealed polybags, in a recipient to measure its volume (V_{tot}). The sample was then thawed and put in the oven to dry. The remaining dry material was immersed again to determinate its volume (V_{sed}). The volume of excess content was calculated using:

$$V_{tot} - V_{sed} = V_{ice}$$

The volumetric excess ice content is expressed as percentages (fundamentally meaning cm^3/cm^3).

2.4   BOREHOLE LOGS

A log for each permafrost borehole was created by assembling laboratory photos of the cores. Borehole logs include maximal depths, grain size ratio and volumetric excess ice content. These logs were used as supporting data for mapping.

2.5   GROUND TEMPERATURE AND CLIMATE MONITORING

For ground temperature monitoring, newly-drilled boreholes are instrumented with a HOBO (U12-008) four-channel external data logger. This stand-alone weatherproof logger can record data at various intervals and uses a direct USB interface for fast data offload. The logger requires one three-volt CR-2032 lithium battery. Each battery will typically last one year when logging intervals are greater than one minute. To ensure uninterrupted operation, the data loggers are placed in a sealed 15-cm x 15-cm junction box that is connected to the borehole casing. All borehole casings are made of electrical-grade PVC filled with silicone oil. The temperature sensors (TMC6-HD to TMC50-HD) can accurately record temperatures ranging from −20°C to +70°C, with interchangeability to a tolerance of +/−0.25°C from 0°C to 50°C. They have a resolution of 0.03°C at 20°C.

The ground surface temperature is monitored using a HOBO Pendant data logger (UA-002-08). This miniature waterproof two-channel data logger can accurately record temperatures ranging from −20°C to +70°C with interchangeability to a tolerance of +/− 0.53°C from 0°C to 50°C. The UA-002-08 loggers have a resolution of 0.14°C at 25°C.

3   RESULTS

Over 30 sites were visited with the HPW staff in charge of management of each of the three-maintenance areas of the Dempster Highway (Klondike, Ogilvie, and Eagle Plains). Seventeen sites were retained for further geotechnical and/or geophysical investigations. The selection was made based on the following criteria:

- Recurring issues likely to persist over a multi-year period;

- Requiring intensive maintenance in term of magnitude and duration;

- Being representative in terms of geomorphologic and environmental setting of other sites with similar issues.

Table 1 is a list of the 30 sites with notes on the types of degradation issues at the site, and any temperature monitoring measures underway. The 17 sites selected for investigation are indicated with an asterisk*.

Table 1. Dempster Highway locations showing potential permafrost-related degradation

Km Post	Location	Degradation type	Comments	Survey	Temperature Monitoring
82*	-138.277208W 64.586202N	Sinkholes	Recurring at RHS (uphill), depression forming in field at LHS (downhill)	ERT	HPW
95*	-138.398027W 64.677519N	Subsidence, cracking	Failure 20 m long at RHS	ERT, Drilling	NCE, field
102.5*	-138.361639W 64.732985N	Subsidence	Ice wedge field degrading at LHS, lakes at RHS	ERT, Drilling	NCE, field
103*	-138.360546W 64.736358N	Subsidence	Sagging where Two Moose Lake touch the embankment.	ERT	
103.5	-138.365217W 64.740842N	Thermokarst, thaw lakes	A thermokarst lake located at RHS is expanding northward		
104.5	-138.373087W 64.749559N	Erosion	The river eroding embankment at RHS		
109.4	-138.350782W 64.789328N	Slide	Slide at LHS on hill slope - new from this year		

109.6	-138.350733W 64.791175N	Slide	Debris flow at LHS		
116.5*	-138.336849W 64.843072N	Subsidence	Lost of ground, the embankment was moved	ERT, Drilling	NCE, field
117	-138.323624W 64.845332N	Water ponding	Standing water at RHS, smaller at LHS - new of this year (2016)		
119.5	-138.296320W 64.864069N	Water ponding	Lake touching the embankment at LHS, small ponds at RHS		
121.5	-138.286917W 64.882431N	Water ponding, gaining on road	Water level higher at LHS, culvert does not seem flowing		
123.8*	-138.277402W 64.901459N	Depression, Channel forming	Repairs crossing airstrip, longitudinal depression mimicking ice wedge.	ERT	
124*	-138.277826W 64.903173N	Major depression - transversal	Ice wedge degrading in field at LHS	ERT	HPW Met station
125	-138.280323W 64.908234N	General subsidence	As embankment is built up, the road is becoming narrower		
126*	-138.277803W 64.918621N	Sinkhole	Deep excavation (ca. 6 m), did not find ice.	ERT, Drilling	NCE, field
129	-138.270686W 64.94307N	Cracking	Cracking RHS at Culvert, thick embankment (high grade)		
135	-138.201989W 64.98399N	Washout	Repaired - debris flow?		
166	-138.336622W 65.142857N	Subsidence	The road is sinking, berm at both side, peat deposit at LHS		
192*	-138.256425W 65.3466N	Subsidence, Sinkhole	The road is sinking. Presence of a hole in the middle of the road	ERT	
264	-137.773054W 65.826508N	Sinkhole	Cones at LHS, water ponding, water disappearing in holes at LHS		

375*	-136.719994W 66.418483N	Thermokarst ponds - Slide	Thermokarst ponds forming at both sides of the road	ERT, Drilling	NCE, field
381*	-136.664156W 66.446562N	N/A	Recently built and instrumented culvert	ERT	NCE, field
421*	-136.358622W 66.700926N	Ponds, subsidence	Thermokarst ponds at both sides, ice wedges degrading	ERT	HPW Met station
424*	-136.357464W 66.722663N	Slope movement, thermal erosion	Water ponding at RHS, sign of thermal erosion at LHS	ERT, Drilling	
438*	-136.346322W 66.852419N	Degradation	Degradation in the field, 500 m at LHS	ERT, Drilling	NCE, field
442*	-136.338391W 66.883582N	Subsidence	Located in field at RHS	ERT, Drilling	NCE, field
447*	-136.337862W 66.920699N	Sinkhole	Material keeps disappearing	ERT	
454*	-136.229042W 66.956397N	Thaw lake, subsidence	Ice wedge degradation in field	ERT, Drilling	NCE, field
458*	-136.215026W 66.994515N	Sinkhole, thaw lake, subsidence	Water disappears at RHS, depression at LHS, snow patch on LHS shoulder	ERT	NCE, field

Each of the 17 investigated sites is presented individually in the following text, starting with a quick summary of identified geo-hazard issues at the site, and the most pertinent findings of the study. This is intended to provide a quick site reference for readers. Following the summary is a more detailed presentation of the site information, investigations, and conclusions.

3.1   SITE 1: DH 82 – KM82

Issues

- Recurring formation of sinkholes over a small section of highway

Summary of Findings

- Relatively high ground temperatures and course materials suggest permafrost is vulnerable to thawing
- Of the two hypotheses for the cause of the sinkholes, fine material leaching and ground ice thaw, investigations favour fine material leaching as the main cause
- With either hypothetical cause, permafrost degradation contributes to the problem
- Permafrost degradation at this site is potentially influenced by:
  - The road cut on the RHS increasing the active layer
  - Snow accumulation on the shoulder increasing the active layer
  - New pathways for ground infiltration by precipitation due to retreating permafrost
  - Increase in annual precipitation in the region

3.1.1   Introduction

This site has already been extensively addressed in the report "Investigation of Dempster Highway Sinkholes" (Calmels et al. 2016). This section can be considered as an addendum; reprising some results and adding new insights from ground temperature monitoring.
The reported issue at the site is the recurring formation of sinkholes at the right-hand side of the road (Fig. 3.1.1). The most affected area being located between the two HPW-contracted boreholes, BH 876-5321 and BH 841-4949.

3.1.2   Geology

The area where the sinkholes occur is located on a colluvial deposit, a mix of coarse hetero granular material in a fine-grained matrix. It is a slope deposit that overlays and is surrounded by till, a morainal deposit laid by glacier (Fig. 3.1.2). The biophysical context is present in the 2016 report, from page 3 to 9.

3. Results

3.1.3   Aerial imagery

No obvious permafrost-related features or landforms can be observed from the aerial imagery (Fig. 3.1.3).

3.1.4   Borehole geotechnical data

The logs of boreholes BH 876-5321 and BH 841-4949 are presented in figure 3.1.4. The notable findings from the borehole are:

- A localized decrease of fine material content observed in the borehole log 876-5321 (mostly gravel with silt and sand from 3 to 10 m depth) versus stable fine content in borehole log 841-4949 (silty-sand with gravel, all along the profile);

- No ground ice was sampled or reported in either borehole.

The depletion in coarse material suggest leaching of sediments by ground water. The absence of ice suggests that ground ice thaw is not the cause of the observed subsidence and subsequent sinkhole formation.

3.1.5   Ground temperature

Ground temperature profiles suggest a thermal effect of subsurface water movement on ground temperature (Fig. 3.1.5). Comparison of ground temperature records with precipitation records from Dawson City Airport, 80 km away, during summer 2016 suggested that the infiltration can be fast and that there might be a flow sufficient to either thermally erode permafrost and/or leach out fine sediment particles (Calmels et al. 2016, figure 5.5 p. 29).

For this study, the ground temperatures recorded from September 2016 to September 2017 have been plotted in a diagram of depth vs. time (Fig. 3.1.5b). It clearly shows the thermal impact of underground water during freshet, starting mid-May, with a peak early June, when ground temperature goes as high as 3 °C. The area between 7 to 11 m depth seems the most impacted.

3.1.6   ERT survey

ERT resistivity values are generally relatively low in this area, consistent with an ice-poor permafrost (Figs. 3.1.6 and 3.1.7). The low resistivity does not support the hypothesis of a thawing massive ice body as the cause of subsidence. However, some highly resistive areas may indicate either a more ice-rich permafrost or a coarser sediment at those specific locations.

13

ERT surveys carried in the field generally show lower resistivity values deeper in the profile. At the survey done along the road (S3), low resistivity values are concentrated in the upper parts of the profile and the higher resistivity values are concentrated in the lower parts. These observations indicate that the upper ground is likely permafrost free at the toe of the road due to the impact of the embankment. By comparing ground temperature records from the borehole and resistivity values measured at the same depth, it is probable that areas with resistivity values below 600 to 800 ohm·m (depending on the type of survey array) are not frozen.

3.1.7   Synthesis

The fact that sediment is generally gravely, with ground temperature very close to 0°C suggests that, where present, permafrost is highly vulnerable to thawing.

Results from the ERT surveys could support either of the two hypotheses for causes of sinkhole formation (i.e., either fine material being leached away, or ground ice being thawed). However, the borehole data favor the leaching hypothesis.

In both cases permafrost degradation is contributing to the issue. The cut on the right-hand side may have triggered active layer thickening, but also favors the presence of snow accumulating on the shoulder of the embankment, promoting thickening of the active layer. The retreat of the permafrost table may have opened new pathways for the ground water originating from precipitation to flow through and leach sediments. Similarly, an increase of the precipitation in the area over decades may have led to the situation. Ground temperature records prove that infiltrating water is significantly impacting permafrost at this site and is likely responsible for the sinkhole by leaching fine sediment between approximately 6 and 12 m depth.

Figure 3.1.1 Degradation observed at site DH82 in 2014 and 2015.
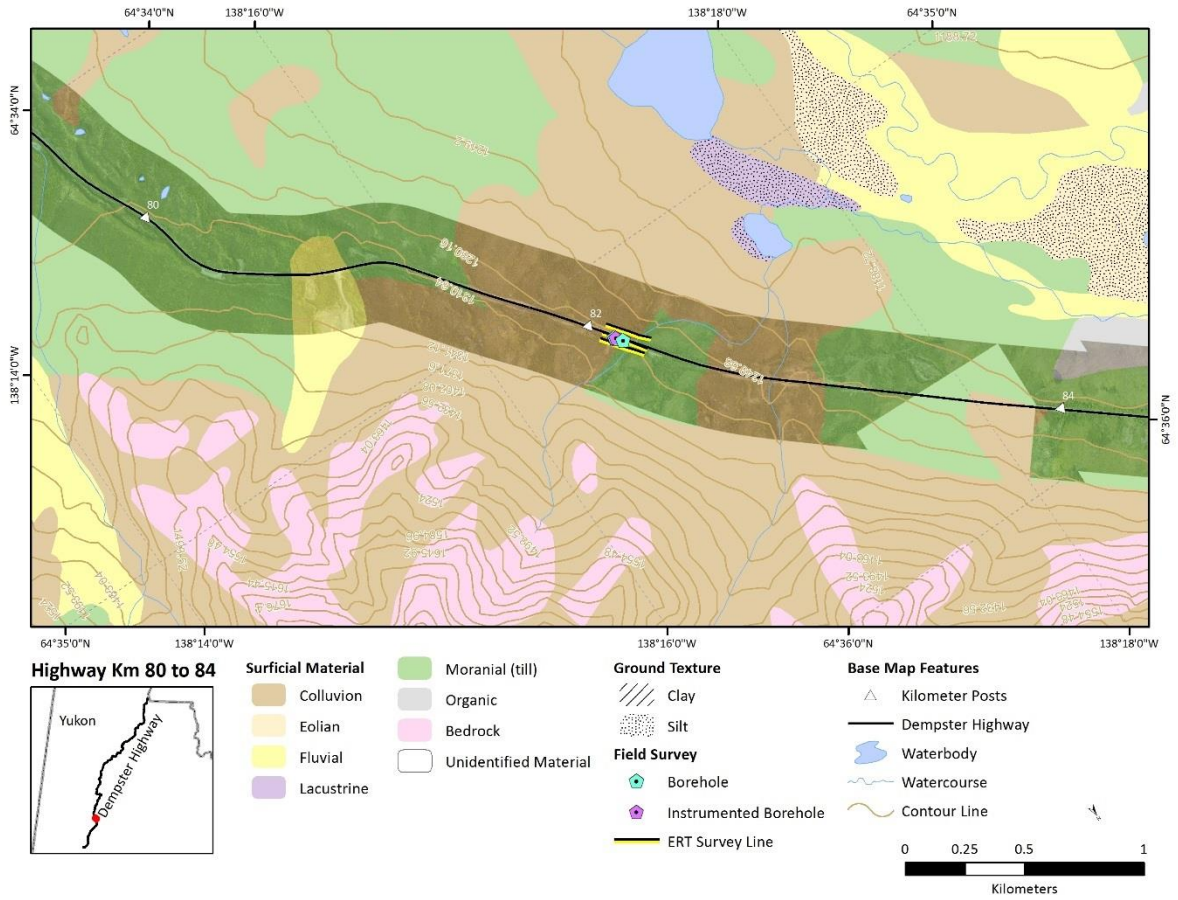
Figure 3.1.2 Surficial geology map of the site 1 DH82 area

Figure 3.1.3 Aerial view of site DH82

Borehole 876-5321

Log	Grain size

0.2 to 0.4 m
0% 20% 40% 60% 80% 100%
SILTY SAND with GRAVEL

3.1 to 3.3 m
0% 20% 40% 60% 80% 100%
GRAVEL with SILT and SAND

6.8 to 7.0 m
0% 20% 40% 60% 80% 100%
GRAVEL with SILT and SAND

8.8 to 9.0 m
0% 20% 40% 60% 80% 100%
SILTY GRAVEL with SAND

10.4 to 10.6 m
0% 20% 40% 60% 80% 100%
SILTY SAND with GRAVEL

Frozen

13.7 m

Depth (m): 0 1 2 3 4 5 6 7 8 9 10 11 12 13 14

Borehole 841-4949

Log	Grain size

0.4 to 0.6 m
0% 20% 40% 60% 80% 100%
SILTY SAND with GRAVEL

3.0 to 3.2 m
0% 20% 40% 60% 80% 100%
SILTY SAND with GRAVEL

5.0 to 5.2 m
0% 20% 40% 60% 80% 100%
SILTY SAND with GRAVEL

6.6 to 6.8 m
0% 20% 40% 60% 80% 100%

Frozen

7.3 m

Depth (m): 0 1 2 3 4 5 6 7 8

■ Gravel

■ Sand

■ Silt & Clay

Figure 3.1.4 Logs of boreholes BH 876-5321 and BH 841-4949

18

a Ground temperature at km 82
September 1st 2016 to August 31st 2017

b

c

Depth		0.0 m	0.5 m	2.0 m	3.0 m	5.0 m	8.0 m	10.0 m	13.5 m
2016	Sep.	4.1 °C	4.8 °C	5.6 °C	5.7 °C	3.6 °C	1.1 °C	0.4 °C	0.0 °C
	Oct.	-5.1 °C	-1.7 °C	0.7 °C	2.5 °C	2.9 °C	1.4 °C	0.6 °C	0.0 °C
	Nov.	-8.3 °C	-3.3 °C	-1.0 °C	0.7 °C	1.8 °C	1.4 °C	0.6 °C	0.0 °C
	Dec.	-12.5 °C	-5.8 °C	-2.7 °C	0.0 °C	1.1 °C	1.1 °C	0.6 °C	0.1 °C
2017	Jan.	-9.7 °C	-5.1 °C	-3.1 °C	-0.8 °C	0.6 °C	0.8 °C	0.4 °C	0.0 °C
	Feb.	-9.5 °C	-4.9 °C	-3.2 °C	-1.2 °C	0.4 °C	0.7 °C	0.4 °C	0.1 °C
	Mar.	-12.9 °C	-7.0 °C	-4.5 °C	-1.9 °C	0.2 °C	0.5 °C	0.3 °C	0.1 °C
	Apr.	-4.2 °C	-3.3 °C	-3.0 °C	-2.0 °C	0.1 °C	0.4 °C	0.2 °C	0.0 °C
	May.	6.4 °C	4.1 °C	2.2 °C	0.1 °C	0.1 °C	0.9 °C	0.7 °C	0.0 °C
	Jun.	11.9 °C	9.5 °C	6.6 °C	2.2 °C	0.3 °C	2.1 °C	1.7 °C	0.0 °C
	Jul.	15.2 °C	12.9 °C	10.2 °C	5.6 °C	0.8 °C	1.1 °C	0.9 °C	0.0 °C
	Aug.	12.0 °C	11.6 °C	10.6 °C	7.8 °C	2.9 °C	0.9 °C	0.5 °C	0.0 °C
	Sep.	7.2 °C	7.2 °C	7.4 °C	6.6 °C	3.7 °C	1.1 °C	0.4 °C	0.0 °C
Sept. 1st to Aug. 31st									
Max		15.2 °C	12.9 °C	10.6 °C	7.8 °C	3.6 °C	2.1 °C	1.7 °C	0.1 °C
Min		-12.9 °C	-7.0 °C	-4.5 °C	-2.0 °C	0.1 °C	0.4 °C	0.2 °C	0.0 °C
Mean		-1.0 °C	1.0 °C	1.6 °C	1.6 °C	1.2 °C	1.0 °C	0.6 °C	0.0 °C

Figure 3.1.5 Ground temperature at site DH82. a- trumpet diagram; b- depth vs. time temperature diagram; c- monthly mean ground temperature
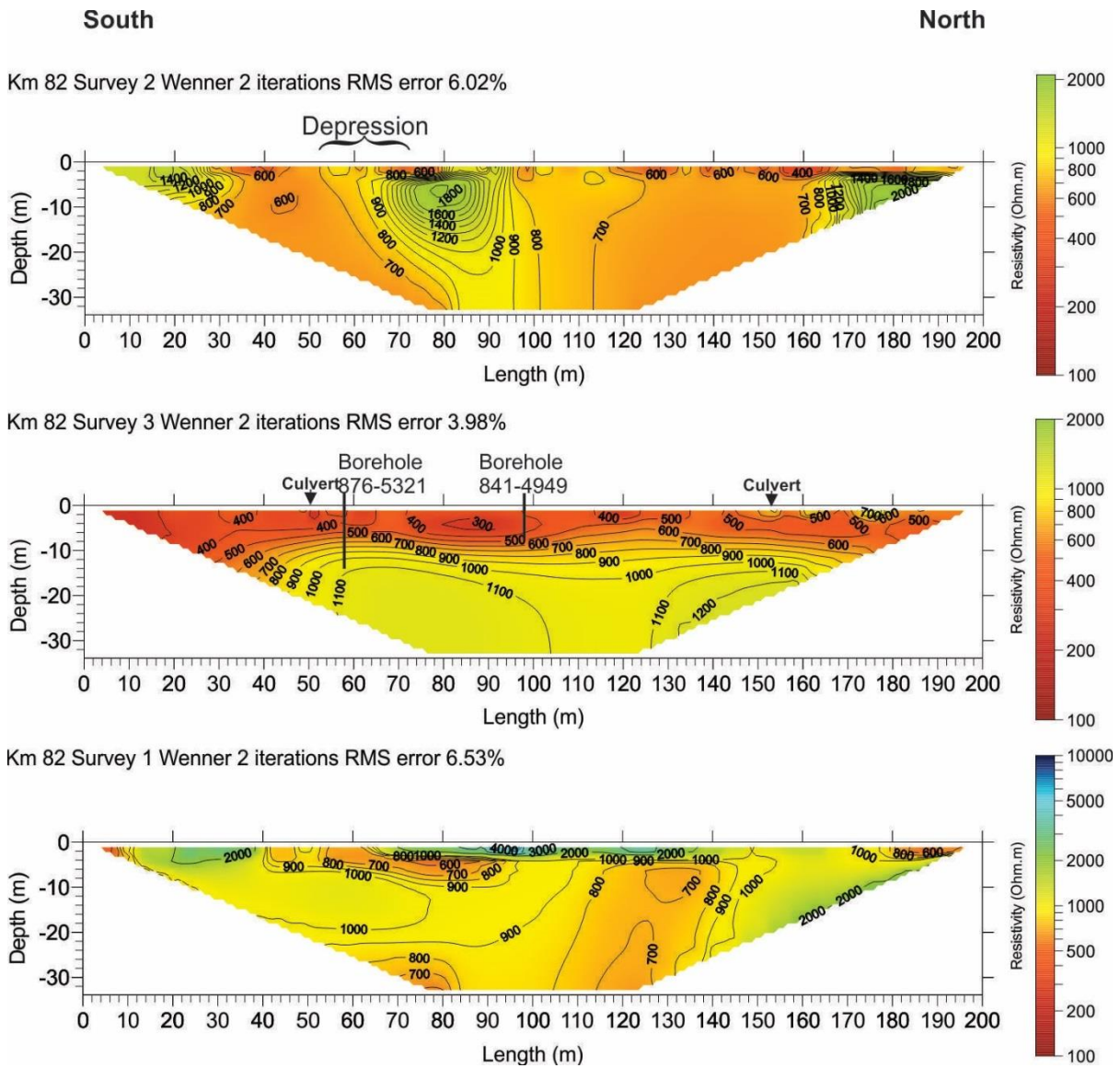
Figure 3.1.6 Wenner ERT surveys at site DH82
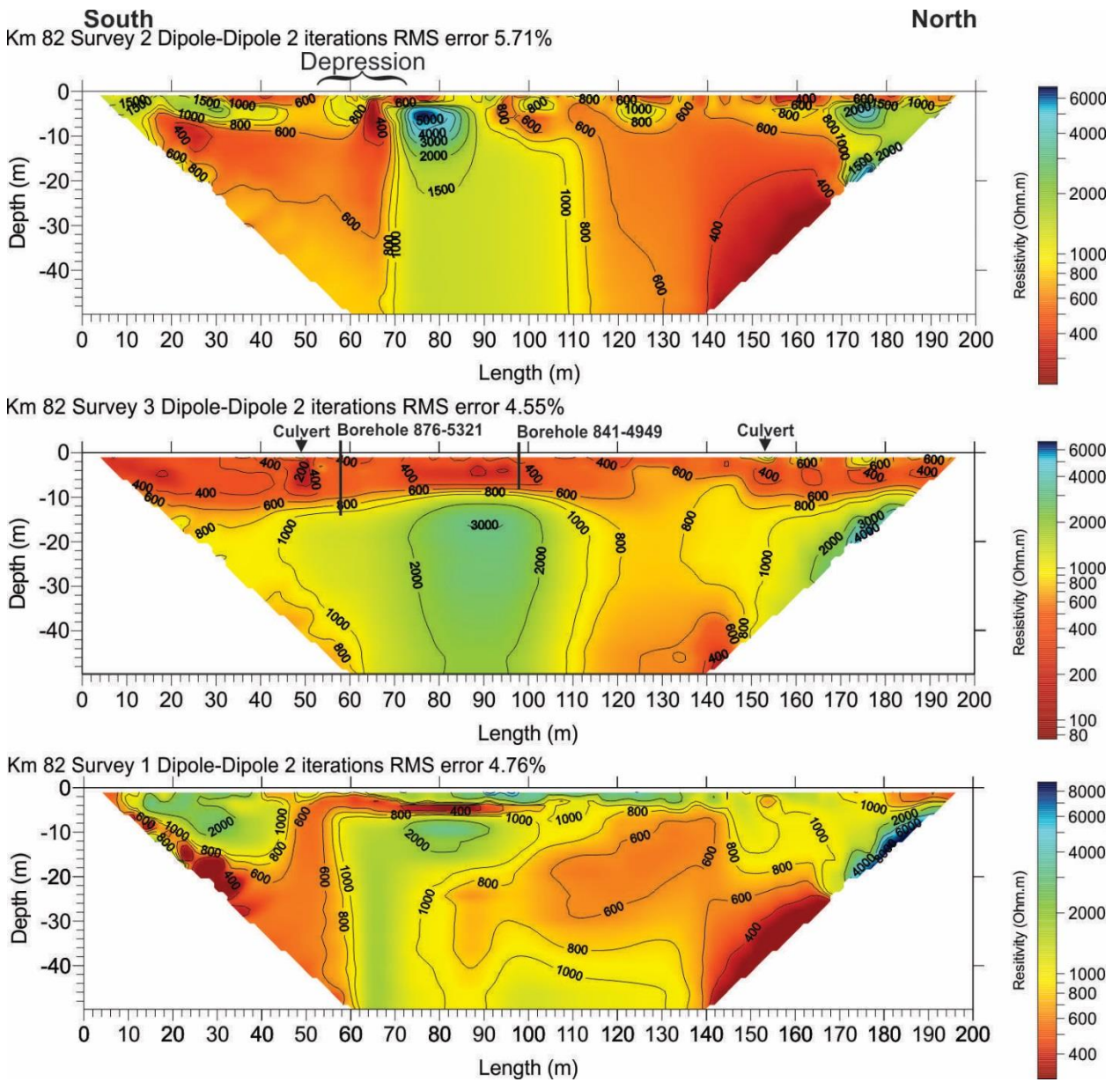
Figure 3.1.7 Dipole-dipole ERT surveys at site DH82

3.2   SITE 2: DH95 – KM 95.2

Issues

- Reoccurring ground movement and settling

Summary of Findings

- Settling can be attributed to both thawing of ground ice and leaching of sediment

- While potentially causing major settling in the nearer term, once the active layer reaches below 2m, the thawing of ground ice and settling close to the surface should cease to be an issue

- Groundwater movement causing both fine material leaching and the thawing of deeper ice bodies may continue to cause loss of volume and settling at the site in the long-term

3.2.1   Introduction

This site is located 7-8 kilometers southward of Two Moose Lake, an area investigated in the Report "Investigation of Dempster Highway Sinkholes" (Calmels et al. 2016). [1] This site has been assessed because of recurring issues of ground movement and settling. At the time of the field visit with HPW, a failure roughly 20 m long located at the Right-hand side was observed (Fig 3.2.1). The field survey consisted of one shallow borehole and one ERT survey using both Wenner and dipole-dipole arrays.

3.2.2   Geology

The area were the sinkholes occur is located on a colluvial deposit, a mix of coarse hetero granular material in a fine-grained matrix. It is a slope deposit that overlays and is surrounded by till, a morainal deposit laid by a glacier (Fig. 3.2.2). The biophysical context is present in the 2016 report, pages 3 to 9.

---

[1] The sinkholes report provides the biophysical context to an area between km 74 and km 160, of which the site under scrutiny is part. The reader should refer to this report to get additional information on general geology and glacial history.

3.2.3   Aerial imagery

Figure 3.2.3 presents an aerial view of site DH95. A polygonal ground pattern attributable to the presence of ice wedges is visible on both sides of the road in the aerial imagery. The pattern is especially apparent at the Right-hand side, as the troughs are wetter, and channeled water thaws the wedge ice. Some ponds also are visible in the landscape, forming in the troughs. The site is located in a wetter area; where water tracks are visible, the drainage is eastward.

3.2.4   Borehole geotechnical data

The Borehole DH95 BH1 was drilled in the field at the Left-hand side; cores being collected down to 2.60 m depth. The log (Fig. 3.2.3) shows a 30 cm organic layer followed by a silty sand and sandy silt, having volumetric excess ice content ranging from 34 to 70%, down to 2.50 m depth. The mean volumetric excess ice content is 40%. The borehole ends in the ice-poor gravelly sediment.

3.2.5   Ground temperature

Ground temperature was recorded from June 5th to September 17th, 2017, the date of the last downloading (Fig. 3.2.4). Although very partial with just 3-months of monitoring, the record shows that from June 15th to September 15th, the ground temperature at the deepest 2.6 m depth, increases from -3.2 to -1.6 °C. The active layer has a thickness of 60 cm on September 15th. We can hypothesize that the permafrost is relatively cold with temperature lower than -2.0 °C.

3.2.6   ERT survey

Figure 3.2.5 shows both the Wenner and dipole-dipole ERT surveys. For each array, two profiles are shown, the first with an iteration number sufficient to reach a RMS error inferior to 5% and a second with an additional iteration cycle to try to develop sharper boundaries between resistivity values.

The results obtained with the Wenner and dipole-dipole arrays are very similar, yet the dipole-dipole shows more detail on the vertical boundaries.

The darkest blue colors are the highest resistivity values, and can be interpreted as cold and/or ice rich permafrost. They are mainly concentrated in the south side of the profiles and in the first 6-8 m of the profile. It can be assumed that the ice wedges are located in the first 3 m of

the profile and do not propagate into the gravelly sediment. Without direct observation below 3 m, it can only be assumed that the high resistivity is attributable to an ice-rich, colder, and coarser sediment. The presence of a buried ice body cannot be disproved.

The reddish areas can be interpreted as thawed, wetter ground, that mainly occur at two locations: in the middle of the survey; and, in the northern end. These locations line up with the presence of two channels/water tracks. Therefore, these low resistivity areas could be indicative of underground water movement.

3.2.7 Synthesis

The observed settling along the road section can be attributable to two phenomena:

- The thawing of ground ice; i.e. a loss of volume of ice;

- The leaching of sediment, i.e. a loss of volume of fine sediment.

Results from the ERT surveys could support either of the two hypotheses for causes of settling. The surveys show high resistivity areas likely representative of ice-rich ground, and also low resistivity areas likely attributable to ground water movements capable of leaching sediment. Although gravelly, the deeper coarse sediment contains a significant fraction of fine sediment.

The ice wedges are of unknown width and probably don't exceed 2 m high. The loss of this volume of ice could induce major settling in the road. However, when the active layer reaches a little bit lower than 2m (i.e. the height of the ice wedge), the degradation due to their thawing should cease. Water leaching and the thawing of deeper ice bodies could be a greater concern in the long term.

Figure 3.2.1 20m failure located on the RHS of the road at site DH95.
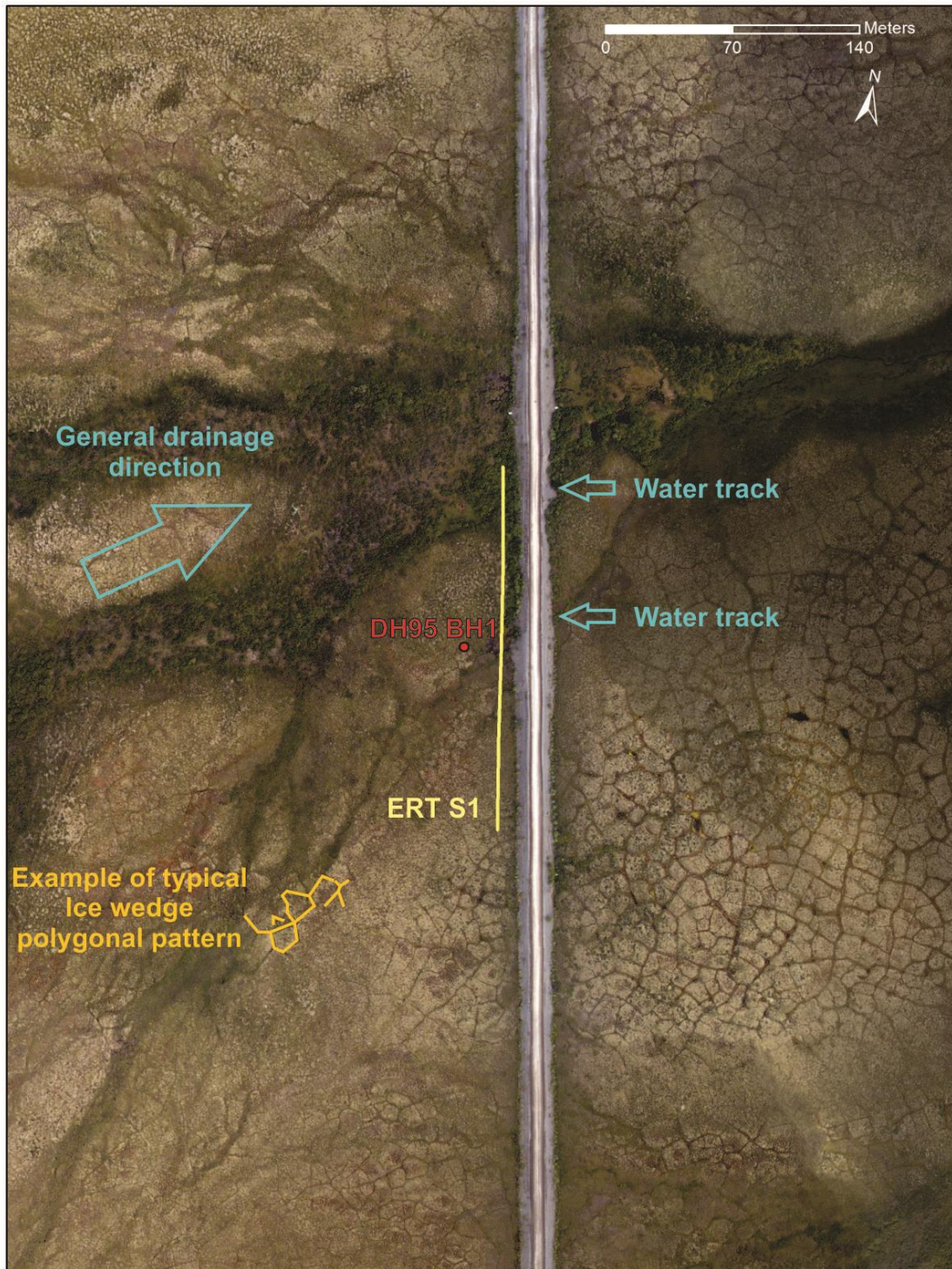
Figure 3.2.2 Aerial view of site DH95
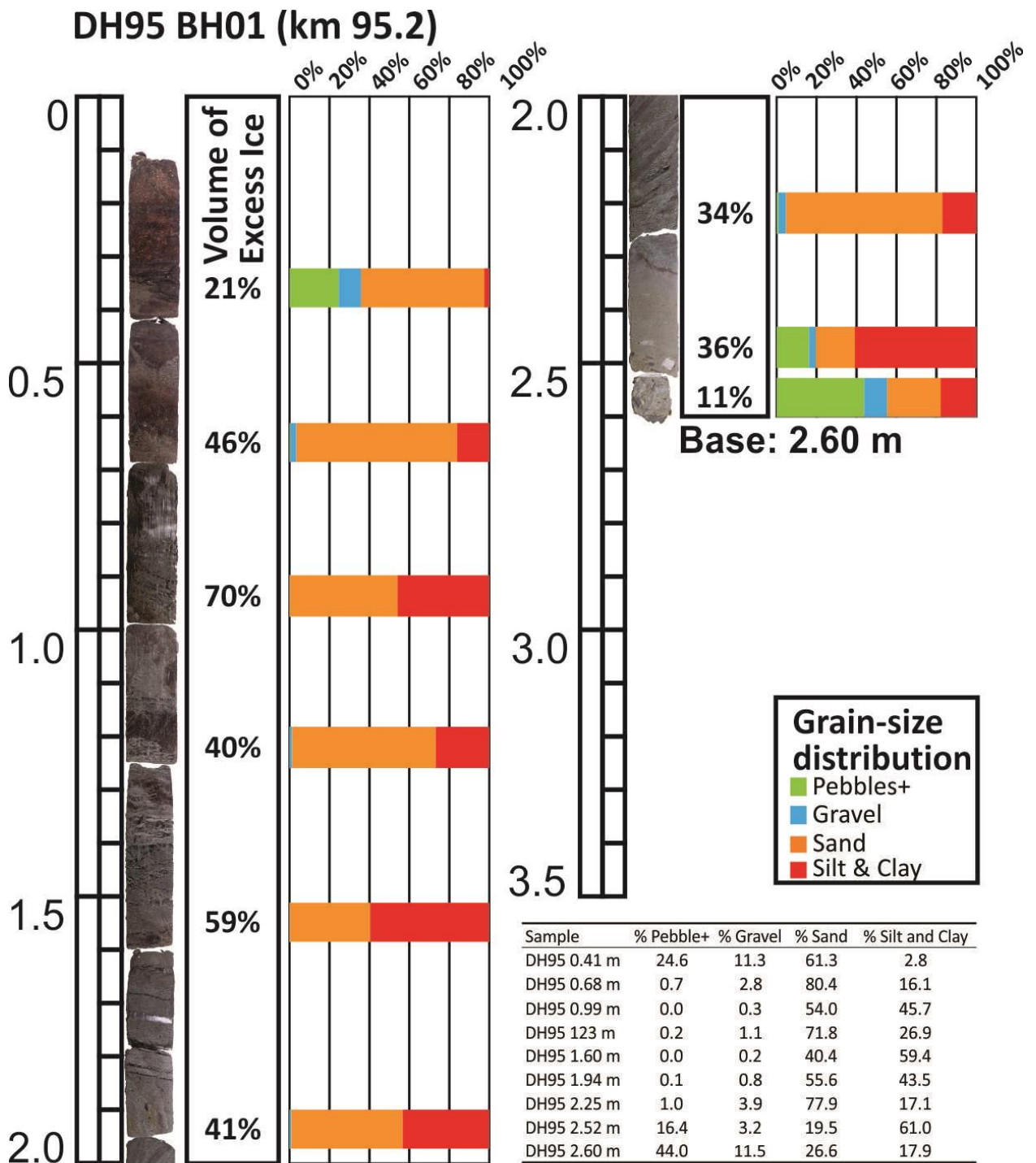
Figure 3.2.3 Logs of borehole DH95 BH1, with volumetric excess ice content and grain size distribution.

Sample	% Pebble+	% Gravel	% Sand	% Silt and Clay
DH95 0.41 m	24.6	11.3	61.3	2.8
DH95 0.68 m	0.7	2.8	80.4	16.1
DH95 0.99 m	0.0	0.3	54.0	45.7
DH95 123 m	0.2	1.1	71.8	26.9
DH95 1.60 m	0.0	0.2	40.4	59.4
DH95 1.94 m	0.1	0.8	55.6	43.5
DH95 2.25 m	1.0	3.9	77.9	17.1
DH95 2.52 m	16.4	3.2	19.5	61.0
DH95 2.60 m	44.0	11.5	26.6	17.9

Ground temperature at km 95
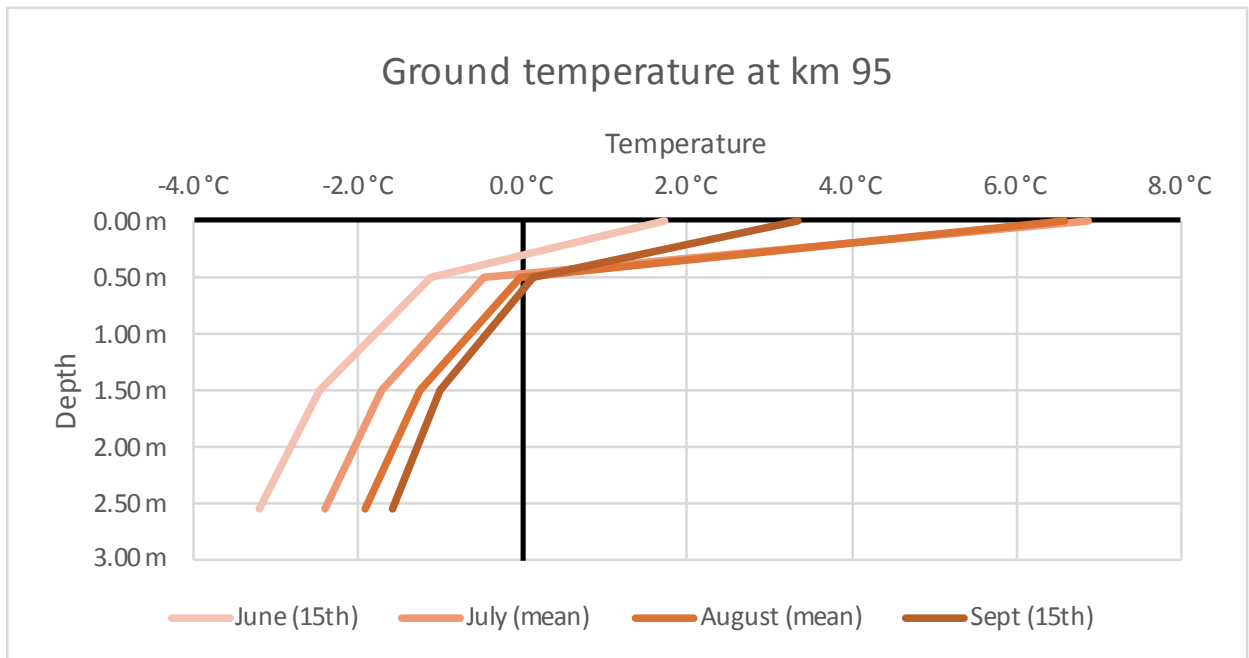
Depth	June (15th)	July (mean)	August (mean)	Sept (15th)
0.00 m	1.7 °C	6.9 °C	6.6 °C	3.3 °C
0.50 m	-1.1 °C	-0.5 °C	0.0 °C	0.1 °C
1.50 m	-2.5 °C	-1.7 °C	-1.3 °C	-1.0 °C
2.55 m	-3.2 °C	-2.4 °C	-1.9 °C	-1.6 °C

Figure 3.2.4 Ground temperature at site DH95, based on a record from June 15th to September 15th, 2017.
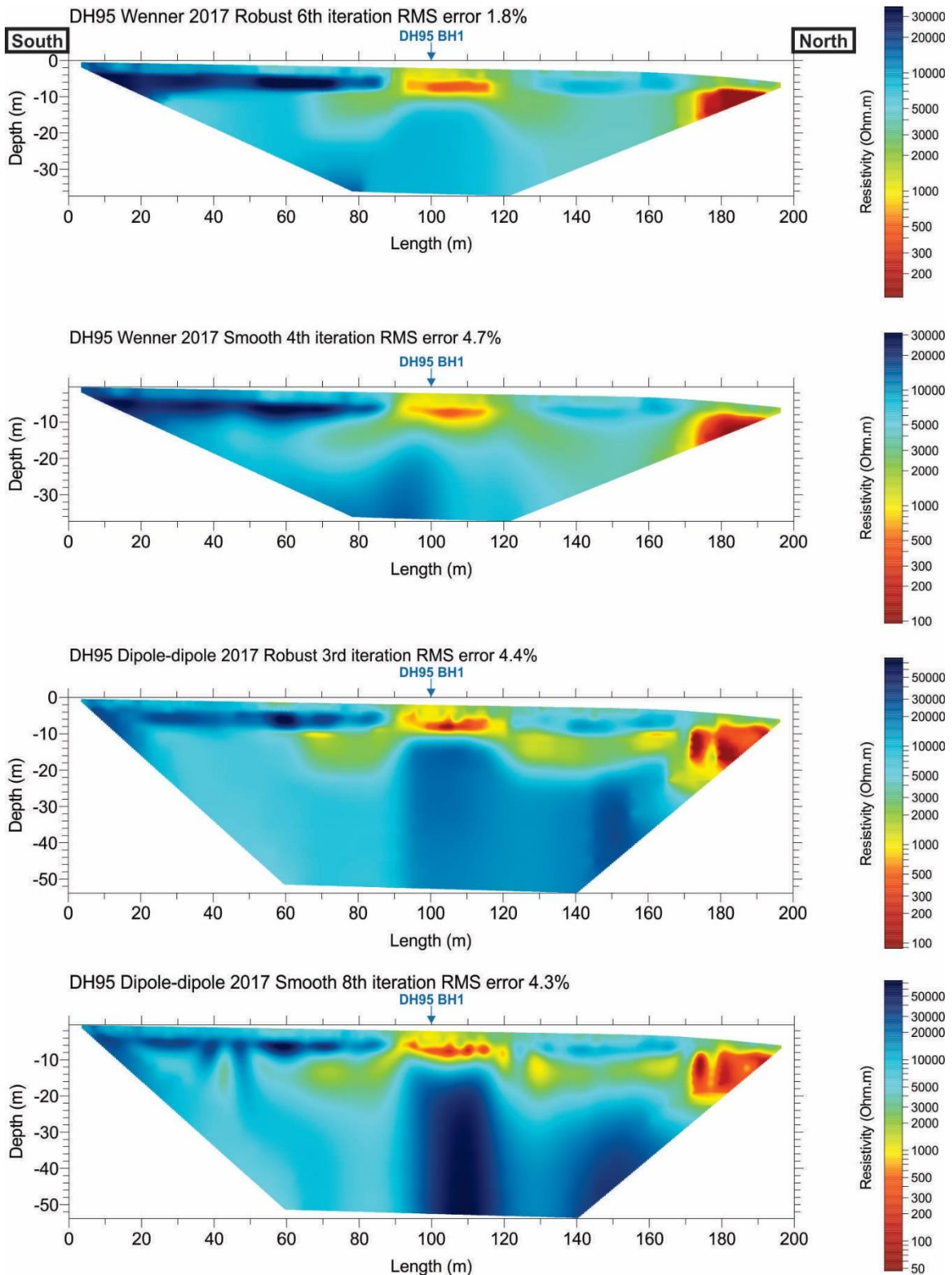
Figure 3.2.5 Wenner and dipole-dipole ERT surveys at site DH95.

3.3   SITE 3: DH102 – KM 102

Issues

- No specific site issues; it was investigated to better understand the permafrost characteristics of the area.

Summary of Findings

- The area shows higher resistivity in the ERT surveys compared to site DH95, likely due to more ice-rich, coarser material, and/or colder ground.

- High resistivity areas likely represent ice-rich ground; and lower resistivity areas are likely attributable to unfrozen ground associated with ground water movement.

3.3.1   Introduction

This site is located 350 m south of the Two Moose Lake rest area, which was investigated in 2016 as it was impacted by the formation of sinkhole. The results of the 2016 survey are presented in the Report "Investigation of Dempster Highway Sinkholes" (Calmels et al. 2017). [2]

Site 3 DH102 has not been reported as having specific issues, yet it offers the possibility to gather further understanding of permafrost characteristic for this area where polygonal ground seems to undergo degradation.

The field survey consisted of one ERT survey using both Wenner and dipole-dipole arrays. The survey was made perpendicular to the embankment, starting from the toe and going in the field.

3.3.2   Geology

The site is located on fluvial deposits (Fig. 3.3.1). The YGS surficial geology map reports that it consists of a gravely sediment overlaying a glacial till, and is surrounded by aeolian, fine-grained deposits. The biophysical context is present in the 2016 report, pages 3 to 9.

---

[2] A summary of this study is presented in the next section, 3.4 Site 4: DH103. The 2017 report provides the biophysical context to the area between km 74 and km 160, in which DH102 is located. Refer to this report to get additional information on general geology and glacial history.

3.3.3   Aerial imagery

A polygonal ground pattern attributable to the presence of wedge ice (similar to that observed at site 2 DH95), is visible most prominently on the left-hand side of the road on the aerial imagery (Fig. 3.3.2). This pattern is especially apparent where the troughs are wetter, as channelled water is thawing the ice wedges. Some ponding is visible in the field, forming in the troughs. The drainage direction is seemingly parallel to the road, flowing eastward into Two Moose lake.

3.3.4   Borehole geotechnical data

There was no borehole drilled at this site.

3.3.5   Ground temperature

There was no ground temperature monitoring implemented at this site.

3.3.6   ERT survey

Figure 3.3.3 shows both Wenner and dipole-dipole ERT surveys. For each array, two profiles are shown; the first is produced using a robust inversion, and the second is created with a smoothness constraint in the inversion process. The robust inversion is typically used when sharp boundaries are expected, like in between ice and unfrozen ground. A smoothness constraint tends to ensure that the resulting model shows a smooth variation in the resistivity values, which usually produces a model with a larger apparent resistivity RMS error.

The general results obtained with the Wenner and dipole-dipole arrays are very similar with regards to the patterns, yet the dipole-dipole arrays show more details on the vertical boundaries, and provide higher resistivity values in the upper limit of the resistivity scale. The robust inversions show sharper definition in the boundaries than the smoothed inversion. The smoothed inversion has higher resistivity values in the lower limits of the resistivity scale. Overall, resistivity values are high, from 1000s to 100 000s.

If focusing only on the patterns of resistivity, it appears that the most resistive material (the darkest blue colors) is located between approximately 2 and 10 m, slightly deeper in the northwestern part of the profile. It likely coincides with the presence of ice wedges. Generally, the dark blue colour can be interpreted as cold and/or ice rich permafrost.

Some red/orange lower resistivity areas appear above the higher resistivity layers, likely due to thawed, wetter ground, especially in the northwestern area, which is consistent with the observations drawn from the aerial imagery. Similar low resistivity areas appear at locations below 10 m depth in the southeastern section and the northwestern end of the profile. This indicates unfrozen ground and underground water flow.

Without direct investigation, it can only be assumed that the high resistivity is attributable to an ice-rich, colder, and coarser sediment. The presence of a buried ice body can not be discarded.

3.3.7 Synthesis

Results from the ERT surveys are somewhat like those at DH95; yet with higher overall resistivity values which could be due more ice-rich, coarser, and/and colder ground, all of which could impact inversion processes.

High resistivity areas likely represent ice-rich ground; and lower resistivity areas are likely attributable to unfrozen ground associated with ground water movement.
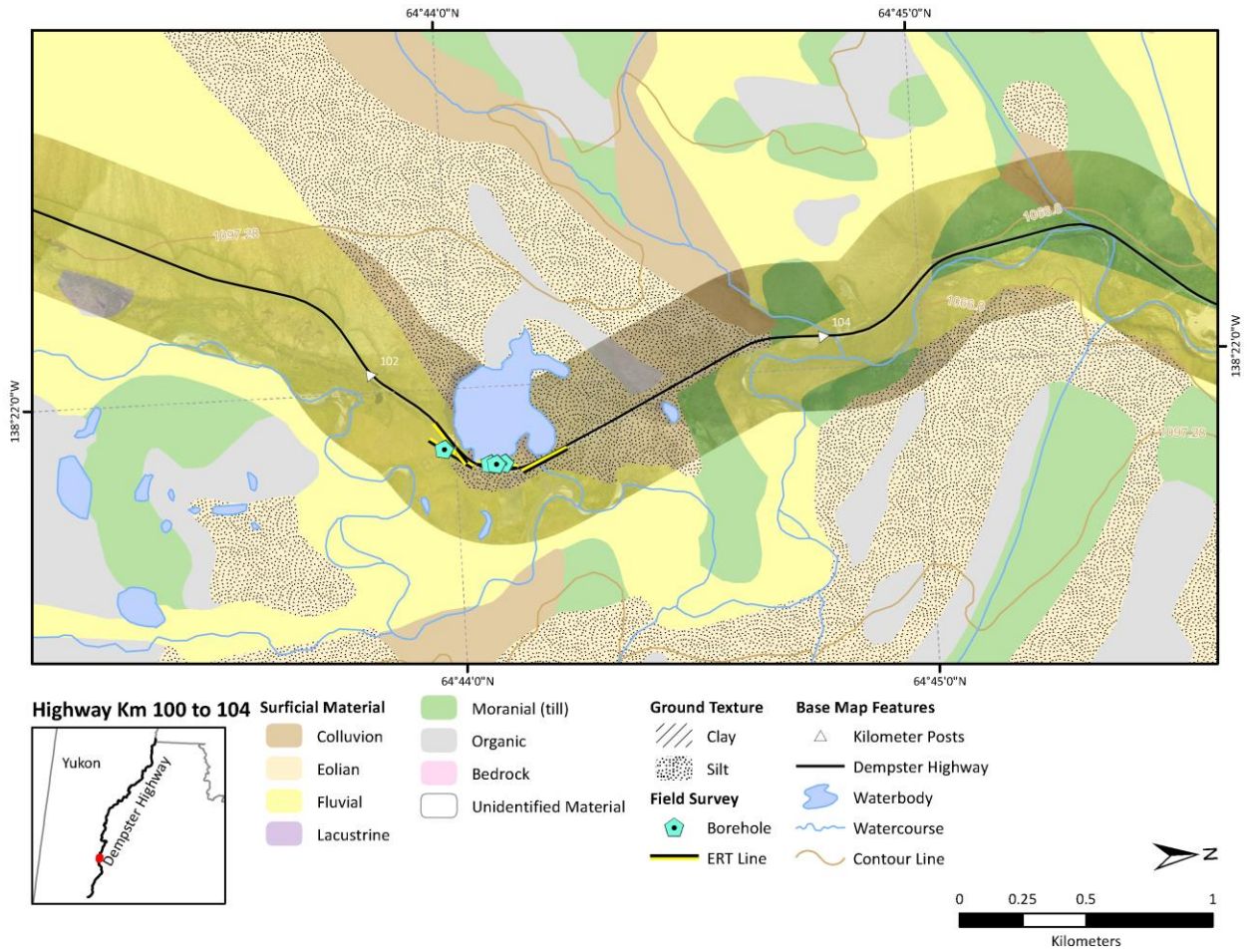
Figure 3.3.1 Surficial geology map of the site 3 DH102 area

Figure 3.3.2 Aerial view of site DH102
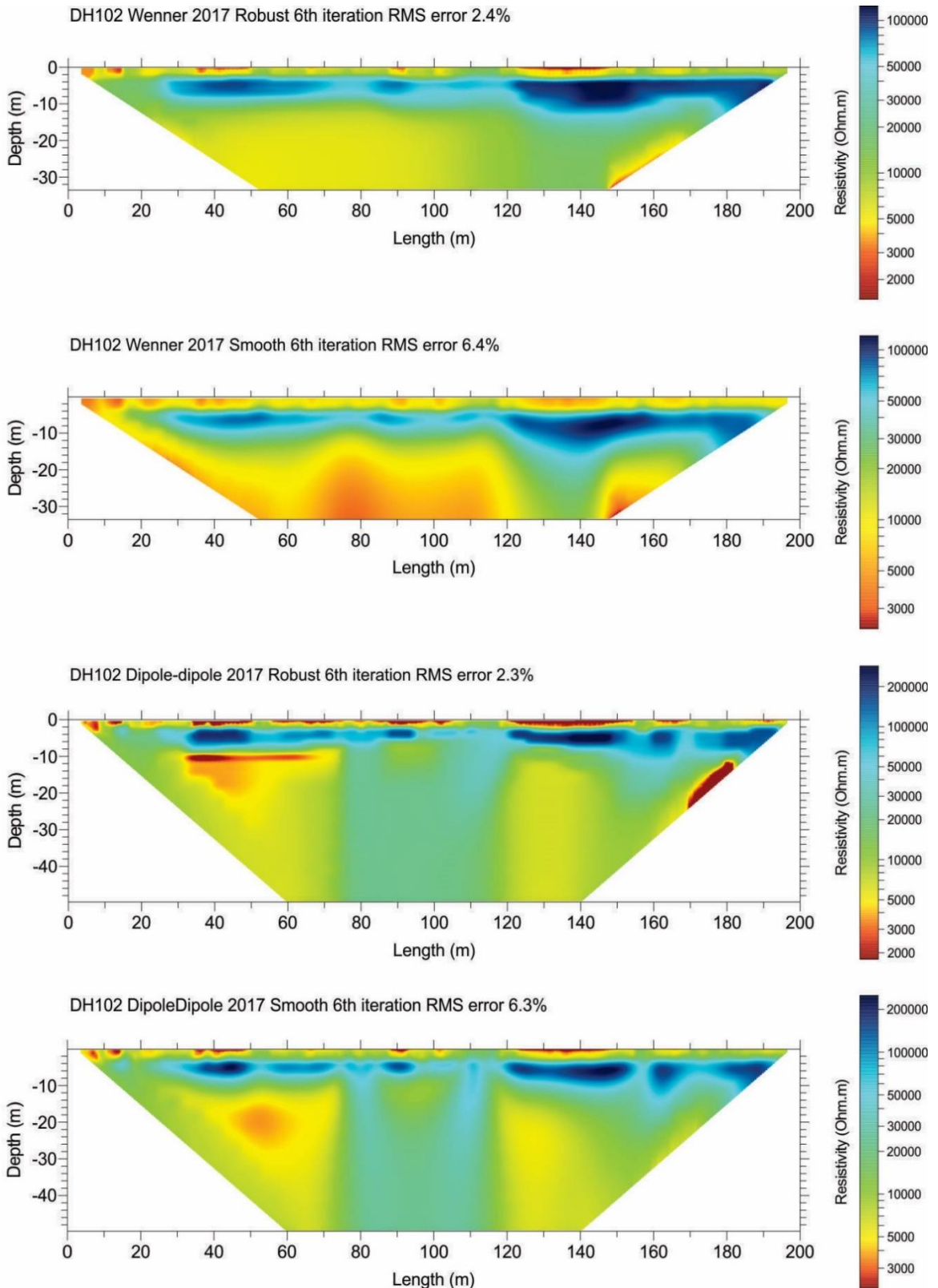
Figure 3.3.3 Wenner and dipole-dipole ERT surveys at site DH102

35

3.4   SITE 4: DH103 – KM 102

Issues

- This section has a history of road subsidence, particularly at km 102.7.

Summary of Findings

- ERT surveys at km 102-103 indicate 3 possible features: 1- Ice-rich permafrost; 2- massive ground ice bodies - either ice wedges or buried ice; and 3- possible ground water movement

- The ice rich permafrost and massive ground ice bodies may be responsible for the general subsidence observed on this section on the road.

- Groundwater movement may be an additional influence on ground movement in a section of the study area where permafrost is absent, between the lake and the river (see Fig 3.4.3, ERT S4).

- The permafrost at this site is relatively cold, below -2 °C, and therefore can be more resilient to an increase in air temperature in the future.

3.4.1   Introduction

This site has already been extensively addressed in the Report "Investigation of Dempster Highway Sinkholes" (Calmels et al. 2017). This section can be considered as an addendum; reprising some results and adding new insights from ground temperature monitoring.

This site is located between km 102.3 and km 103. The issue largely entails subsidence of the road. The phenomenon is especially pronounced at km 102.7, where the lake reach the foot of the embankment. At the time of the survey, no damage was observed on the road, on its shoulders, or at the toe of the embankment, as the road is regularly re-leveled by HPW services. However, indicators of a 50 cm re-leveling were observable on site (Fig. 3.4.1).

Shallow boreholes were drilled. One of them, DH103 BH1 (named DH102 BH1 in the Sinkhole Report), was drilled and instrumented with a 4-channel Hobo logger. The site was investigated by ERT survey lines. Because the configuration of the road includes a broad bend, 4 ERT surveys with differing orientations were done to cover the length of the site.

3.4.2   Geology

The area were the sinkholes occur is located on aeolian deposits, mostly fine, silty material, overlaying a fluvial deposit consisting of a gravelly sediment (Fig. 3.4.2). The aeolian deposit is frost susceptible and often associated with syngenetic ice wedges. The gravel is less frost susceptible, but, if it is fluvioglacial in nature, it may contain buried massive ice. The biophysical context is presented in the 2017 report, from page 3 to 9.

3.4.3   Aerial imagery

Referencing Fig. 3.4.3, ice wedge polygons are present but hardly visible in the aerial imagery where ERT survey 1 is located, between the lake and the highway. However, their surficial expression can be observed close to the lake, where flooded troughs are apparent. There is also polygonal ground where ERT survey 3 is located, which is hard to discern in the aerial imagery but is evidenced on site by subtle surficial expression on a small plateau about 2 m higher in elevation than the road embankment, right-hand side. Therefore, although the surficial expression is less obvious than at previous sites, ice wedges are present in the area. The area that is reportedly the most affected by subsidence is where the lake is touching the road, approximately in the middle of the ERT survey 4.

3.4.4   Borehole geotechnical data

Borehole DH103-BH1 was drilled along ERT survey 3 in the middle of an ice wedge polygon. The thaw front was at 44 cm depth at the end of July 2016. The soil stratigraphy consisted of moss and peat from 0 to 20 cm, organic rich silty sand from 20 to 75 cm, and sediment alternating between silty sand and sandy silt down to about 290 cm. The lower part of the profile had a layer of sand from 290 cm down to termination on a gravel layer at 316 cm. Excess ice content ranged from 12 to 63%, the lowest content being in the lower part of the profile (Fig. 3.4.4). The mean volumetric excess ice content is 42%.

3.4.5   Ground temperature

Borehole DH103-BH1 was lined with PVC piping and instrumented with a 4-channel Hobo logger to record ground temperatures at 0, 0.5, 1.5, and 3.16 m depths. The recording started July 30th, 2016, at 4:00 pm. Data were downloaded September 17th, 2017, providing 13 months of monitoring. Figure 3.4.5 presents ground temperature data from August 2016 to August 2017, inclusively. The trumpet diagram was designed using a 12-month record, from September 1st, 2016 to August 31st, 2017. The minimum and maximum monthly mean temperatures at 3.16 m,

the deepest sensor, are -5.4 and -1.6 °C respectively, with a mean annual ground temperature of -3.1 °C.

3.4.6   ERT survey

Figure 4.5 and 4.6 show both Wenner and dipole-dipole ERT surveys. The profiles were produced using a robust inversion, usually used where sharp boundaries are expected, like in between ice and unfrozen ground. Below is a repeat of the interpretations found in Calmels et al. (2017)

Survey 2 – RHS – Shoulder of the embankment

Wenner array - Survey 2 (Fig. 3.4.5): The resistivity profile can be interpreted along either vertical or horizontal orientations. Vertically, there is an upper area showing lower resistivity values of the survey, ≤1000 ohm·m, which can be found down to 6 m depth, as well as a deeper area where the resistivity values can be tens of thousands ohm·m. Horizontally, the southern part of the profile shows the highest resistivity values in the shape of a high-resistivity block, while the northern part has generally smaller resistivity values, but with another very high-resistivity area between about 130 and 170 m chaining. The south and north parts are separated by a vertical boundary located at approximately 100 m chaining. The blocky appearance of the profile may be because the electrical current cannot pass through the ground. In this area, the magnitude of the resistivity may be overestimated due to the inability of the current to pass to greater depth. Even with this in mind, the profile can be interpreted as showing massive ground ice at relatively shallow depth approximately between chaining 0-100 m and 125-180 m. While its vertical extent cannot be estimated at the southern portion of the survey, it does not extend deeper than 13 to 17 m in the northern section.

Dipole-dipole array - Survey 2 (Fig. 3.4.7): The dipole-dipole resistivity profile shows the same type of resistivity distribution as the Wenner survey, but with a sharper image of the permafrost conditions. In the southern section of the profile, two very high-resistivity zones occur from approximately chaining 16 to 38 m, and chaining 50 to 106 m, within a larger zone of generally higher resistivity. In the northern section, a large higher-resistivity area spreads from chaining 110 to 168 m, with a very high-resistivity area from approximately chaining 124 to 148 m. A final smaller area of high resistivity is present between approximately chaining 174 and 180 m. The high-resistivity areas are between approximately 3 and 16 m depths. The presence of a culvert at 170 m chaining may be contributing to lower resistivity, either because of the influence of the metallic pipe, or because of the thermal effect of the culvert and the induced thaw, as a small pond is present here. At the depth of roughly 20 m, the resistivity values drop drastically.

A plausible interpretation of this profile is that the high resistivity areas are bodies of massive ice, with maximum thickness that may range between 6 m and 10 m. The lower-resistivity areas may be either bedrock or unfrozen ground.

Survey 3 – RHS – Field – 5 to 50 m away from the embankment

Wenner array - Survey 3 (Fig. 3.4.5): The surface conditions of the survey length vary significantly along the profile. From chaining 0 to about 64 m, there is a low-elevation marshy area, then a higher, polygonal plateau until about chaining 100 m. Beyond this small plateau, a downhill slope leads to a lower marshy area and a small pond between chaining 135 and 140 m (the same pond as the one described in Survey 2), and finally to a flat shrub-covered area until the survey end. The ERT survey seems to partially reflect these surficial conditions. The southern end of the section shows low resistivity values in the marshy area down to about 6 m depth. Resistivity values are much higher below this depth. Over the dry polygonal ground, the resistivity values are high from the surface down. The first 4 m of the profile may reflect the presence of frozen, ice-rich fine sediment. This is consistent with the observation made from borehole DH102-BH1. Below this depth, the resistivity increases considerably down to approximately 16 m depth. This could be attributed to frozen gravel or the presence of massive ice. Further north along the survey, the resistivity generally decreases, the lowest values being recorded at the level of the ponded water. Overall, below 16 m depth, the resistivity value decreases progressively but remains relatively high (between 5,000+ and 2,000 ohm·m). This could be attributable to coarse sediment, bedrock, or the influence of the overlying very resistive layer. Considering the geomorphological context and the subsidence occurring in the whole area, it can be assumed that the very high-resistivity zones are massive ice.

Dipole-dipole array - Survey 3 (Fig. 3.4.7): Survey S3 was similar to S2 in that the dipole-dipole array appears to be better defined than the Wenner array. In general, the pattern of resistivity is very similar, with the dipole-dipole array resistivity values slightly higher than the Wenner array. However, two significant differences can be reported. First, the area of high resistivity below the polygonal ground extends further north that what was detected using the Wenner survey (as far as chaining 125 m). The very highly-resistive core of this area is detected between 4 m and 12 m depth. In addition, between 0 and 4 m depth, there is a pattern of lower and higher resistivity values along the survey length. It is probable that the higher resistivity values represent ice wedges. The second difference is that there is a low-resistivity area located between 100 m and 130 m chaining, at depths ranging between approximately 12 m and 20 m. To the North, lower resistivity values continue in the deeper part of the profile. Laterally, this low-resistivity zone coincides with the presence of a sequence of ponds located about 25 m east of the survey. It can be hypothesized that the low resistivity area between 100-130 m is an

unfrozen area where subsurface water from Two Moose Lake connects with the biggest pond in the field.

Survey 1 – LHS – Field – 5 to 25 m away from the embankment

Wenner array - Survey 1 (Fig. 3.4.6): The ERT profile show mostly higher resistivity values in the upper part of the profile, and lower values deeper down. Three areas at approximately chaining 20-40 m, 65-90 m, and 100-125 m show resistivity values ranging from 6,000 to 10,000+ ohm·m. These areas occur between approximately 2 and 6 m depth, and could coincide with ice wedge polygons. The surrounding ground could also be ice-rich as the resistivity values are above 2,000 ohm·m. There is a horizontal 2000 ohm·m boundary at about 8 m depth. This boundary underlies almost the entire profile, clearly separating shallow resistive ground from deeper, low-resistivity ground. The northern section of the profile, past chaining 60 m, has resistivity values lower than 400 ohm·m. The area might be unfrozen, and even wet, because this part of the survey is located between Two Moose Lake to the west and pond formed within an excavation to the east. The presence of nearby water bodies may contribute to lower resistivity values by warming permafrost, either through infiltration of ground water or by thermal influence.

Dipole-dipole array - Survey 1 (Fig. 3.4.7): Adding to the results from the Wenner array, the dipole-dipole array results indicate that there are high-resistivity areas at both southern and northern ends of the survey. These observations should be considered cautiously because these areas are located at the edge of the profile and it could be an artefact of the inversion process. The dipole-dipole array results also show another low resistivity area located between chaining 50 and 60 m, between approximately 6 and 26 m depth. At this location, the lake is just over 10 m to the west of the survey. Finally, the large, low-resistivity area located north of chaining 70 m has better defined lower boundaries than the Wenner survey. Resistivity values appear to slightly increase below 20 m depth, between approximately chaining 66 and 96 m. High-resistivity zones still are present all along the length of the profile between 1 and 6 m depth; they may represent massive ice, either buried or wedge ice.

Survey 4 – RHS – Shoulder of the embankment

Wenner array - Survey 4 (Fig. 3.4.6): The major feature of this ERT profile is a large, low-resistivity area spreading from chaining 40 m to 130 m, and from the top of the profile to the bottom. Only one high resistivity area appears in this section of the profile between chaining 100 to 130 m, from approximately 2 to 7 m depth. Each end of the profile shows higher-resistivity areas, from 10 to 40 m chaining at the south, and from 130 m to the end of the survey

40

at the north. In the northern end, resistivity values increase to over 9,000 ohm·m, suggesting the presence of massive ground ice or very ice-rich permafrost. The very low-resistivity values observed between chaining 40-130 m suggest the possibility that groundwater passes under the embankment.

Dipole-dipole array - Survey 4 (Fig. 3.4.7): Because the dipole-dipole array provides a deeper and wider window of investigation than the Wenner array, it better shows the high-resistivity area in the southern end which was not apparent in the Wenner survey. The resistivity values are over 10,000 ohm·m, suggesting the presence of massive ice. North of this, resistivity decreases drastically, even in the deepest part of the profile, with resistivity values <200 ohm·m. Within this relatively low-resistivity environment, three high-resistivity areas are present: one between chaining 95-108 m from 4 to 12 m depth, another between chaining 132-154 m from 4 to 25 m depth, and a last one between chaining 165 m to the end of the survey, from 4 to 20+ m depth. While ice wedges are suspected to the south end, the two last northern areas could also be attributable to the presence of massive buried ice.

3.4.7   Synthesis

The ERT surveys at km 102-103 indicate 3 possible features: 1- ice-rich permafrost; 2- massive ground ice bodies - either ice wedges or buried ice; and 3- possible groundwater movement. Figure 3.4.8 shows the plan view of the site with the plausible locations of these features as suggested by merging the observations from the three ERT arrays.

The ice rich permafrost and massive ground ice bodies may be responsible for the general subsidence observed on this section on the road. Groundwater movement may also be influencing ground movement in the northern part of the study area. This is the location where the lake is at the west foot of the road embankment. In this area, the northern-most section may be partly underlain by ice-rich permafrost and massive ice which may contribute to subsidence when they thaw. In the southern part of ERT S4 permafrost is absent; here, groundwater seeping from the lake to the river nearby may be responsible for leaching sediment and contributing to the subsidence.

The permafrost at this site is relatively cold, below -2 °C, and therefore can be more resilient to an increase of air temperature in the next decades.

Figure 3.4.1 Subsidence observed at site DH103.
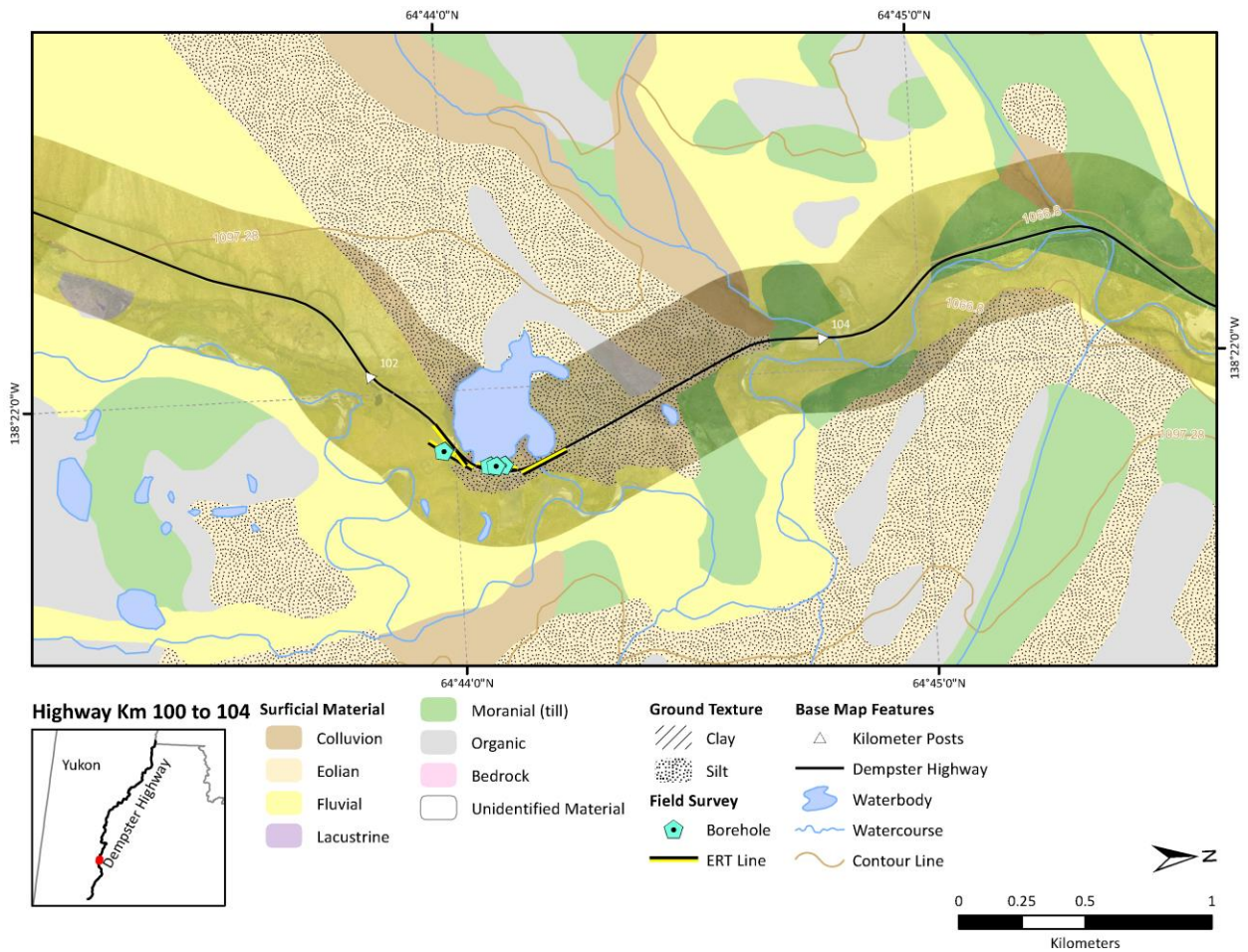
Figure 3.4.2 Surficial geology map of the site 4 DH103 area (same as DH102)

42

Figure 3.4.3 Aerial view of site DH103
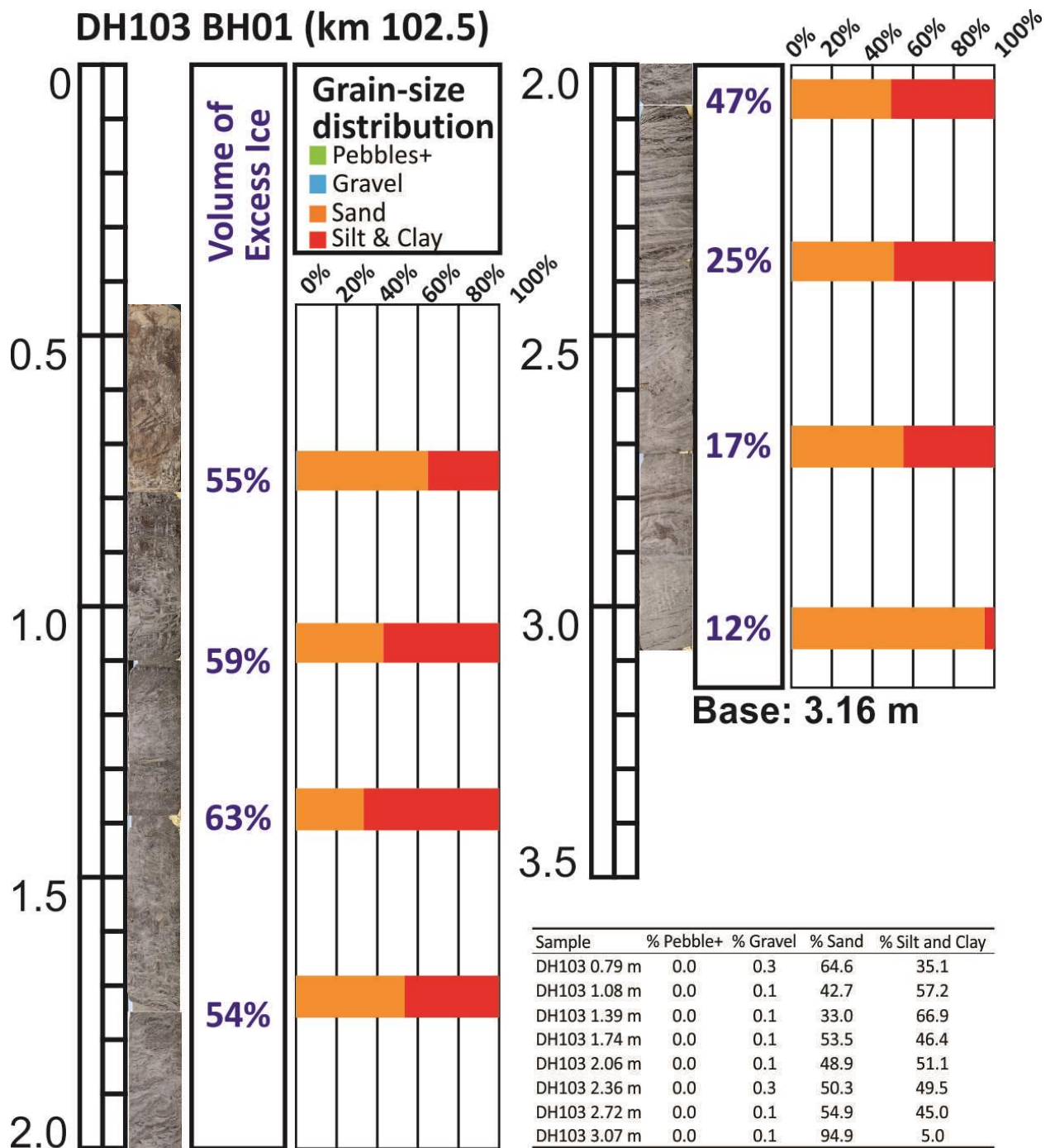
Figure 3.4.4 Log of borehole DH103 BH1, with volumetric excess ice content and grain size distribution.

Sample	% Pebble+	% Gravel	% Sand	% Silt and Clay
DH103 0.79 m	0.0	0.3	64.6	35.1
DH103 1.08 m	0.0	0.1	42.7	57.2
DH103 1.39 m	0.0	0.1	33.0	66.9
DH103 1.74 m	0.0	0.1	53.5	46.4
DH103 2.06 m	0.0	0.1	48.9	51.1
DH103 2.36 m	0.0	0.3	50.3	49.5
DH103 2.72 m	0.0	0.1	54.9	45.0
DH103 3.07 m	0.0	0.1	94.9	5.0

Ground temperature at km 103 2016/2017
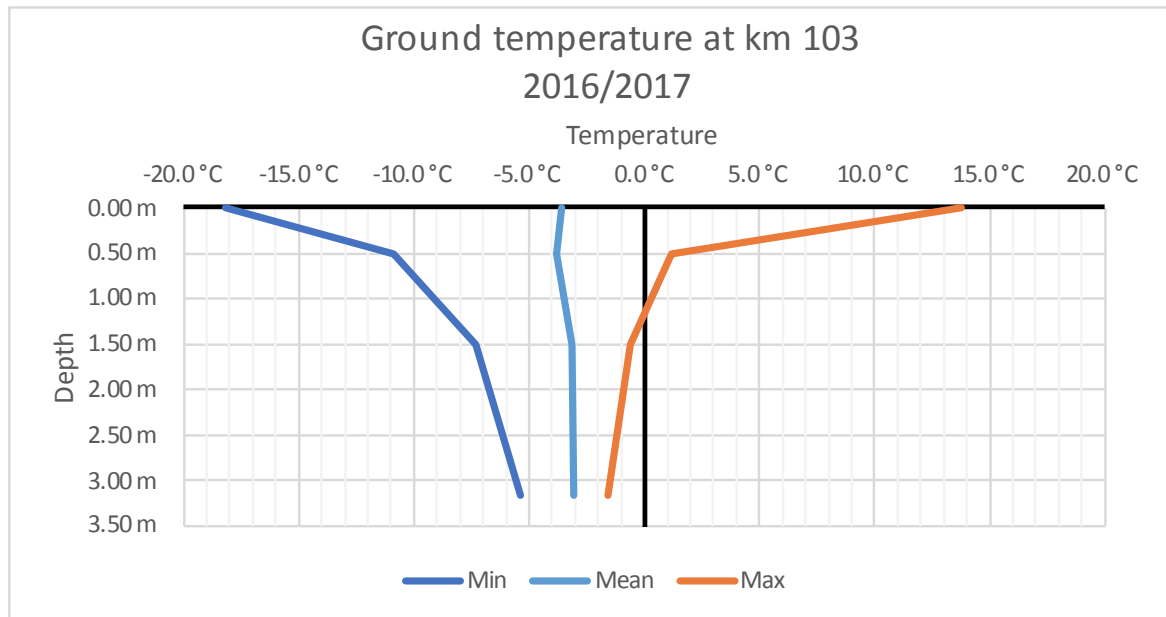
	0.00 m	0.50 m	1.50 m	3.16 m
2016				
August	9.8 °C	0.2 °C	-0.8 °C	-2.0 °C
September	3.2 °C	0.2 °C	-0.7 °C	-1.8 °C
October	-5.7 °C	-0.9 °C	-0.6 °C	-1.7 °C
November	-9.3 °C	-2.0 °C	-0.6 °C	-1.6 °C
December	-14.5 °C	-6.4 °C	-2.5 °C	-1.7 °C
2017				
January	-13.6 °C	-7.6 °C	-4.7 °C	-2.8 °C
February	-14.3 °C	-8.4 °C	-5.7 °C	-3.7 °C
March	-18.2 °C	-10.9 °C	-7.3 °C	-4.6 °C
April	-9.2 °C	-7.9 °C	-7.0 °C	-5.4 °C
May	4.6 °C	-1.9 °C	-4.0 °C	-4.8 °C
June	9.4 °C	-0.7 °C	-2.1 °C	-3.5 °C
July	13.8 °C	0.0 °C	-1.4 °C	-2.9 °C
August	10.8 °C	1.2 °C	-1.0 °C	-2.4 °C
Sept 1st to Aug 31st				
Max	13.8 °C	1.2 °C	-0.6 °C	-1.6 °C
Min	-18.2 °C	-10.9 °C	-7.3 °C	-5.4 °C
Mean	-3.6 °C	-3.8 °C	-3.1 °C	-3.1 °C

Figure 3.4.5 Ground temperature at site DH103, based on a record from August 2016 to August 2017.
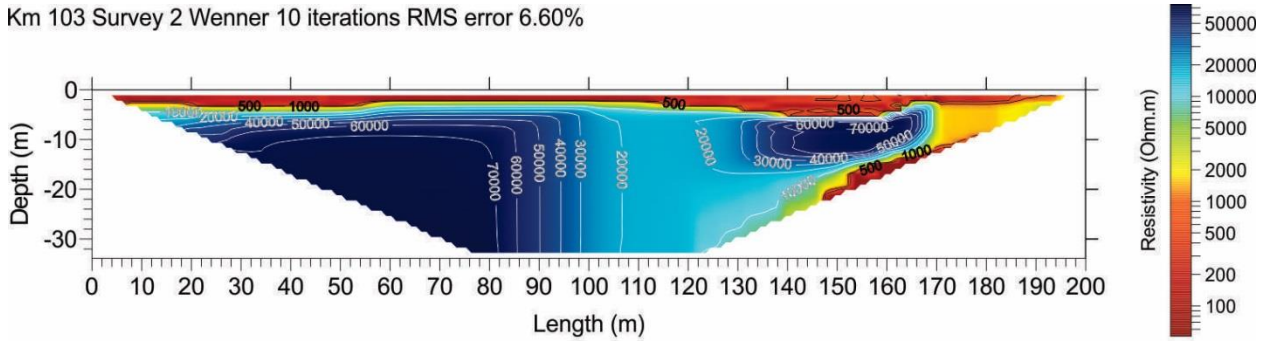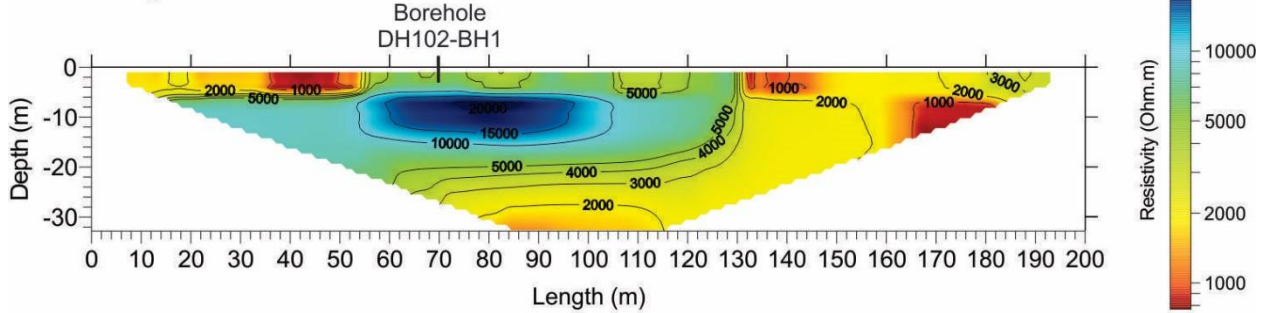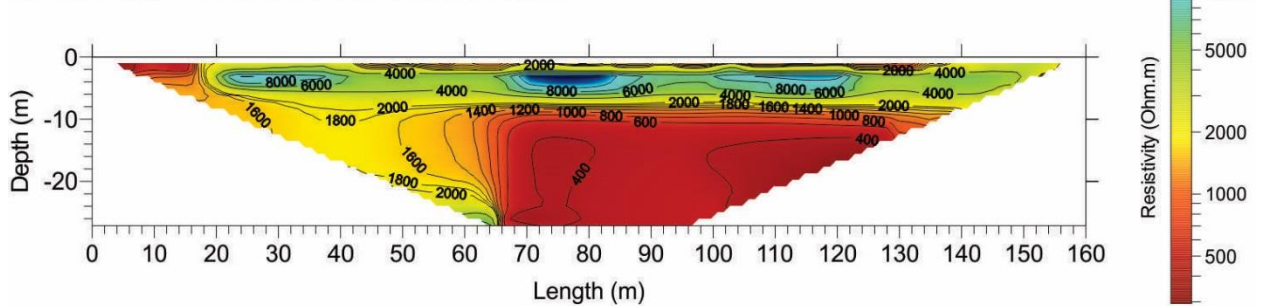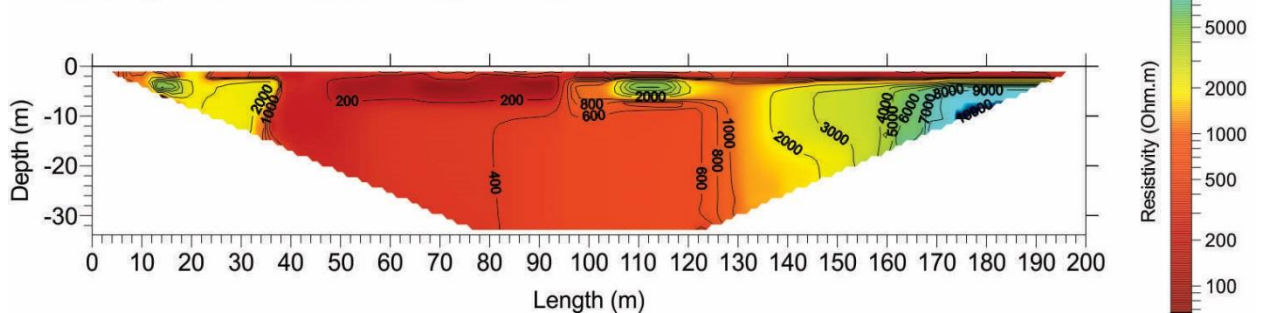
Figure 3.4.6 Wenner ERT surveys at site DH103.
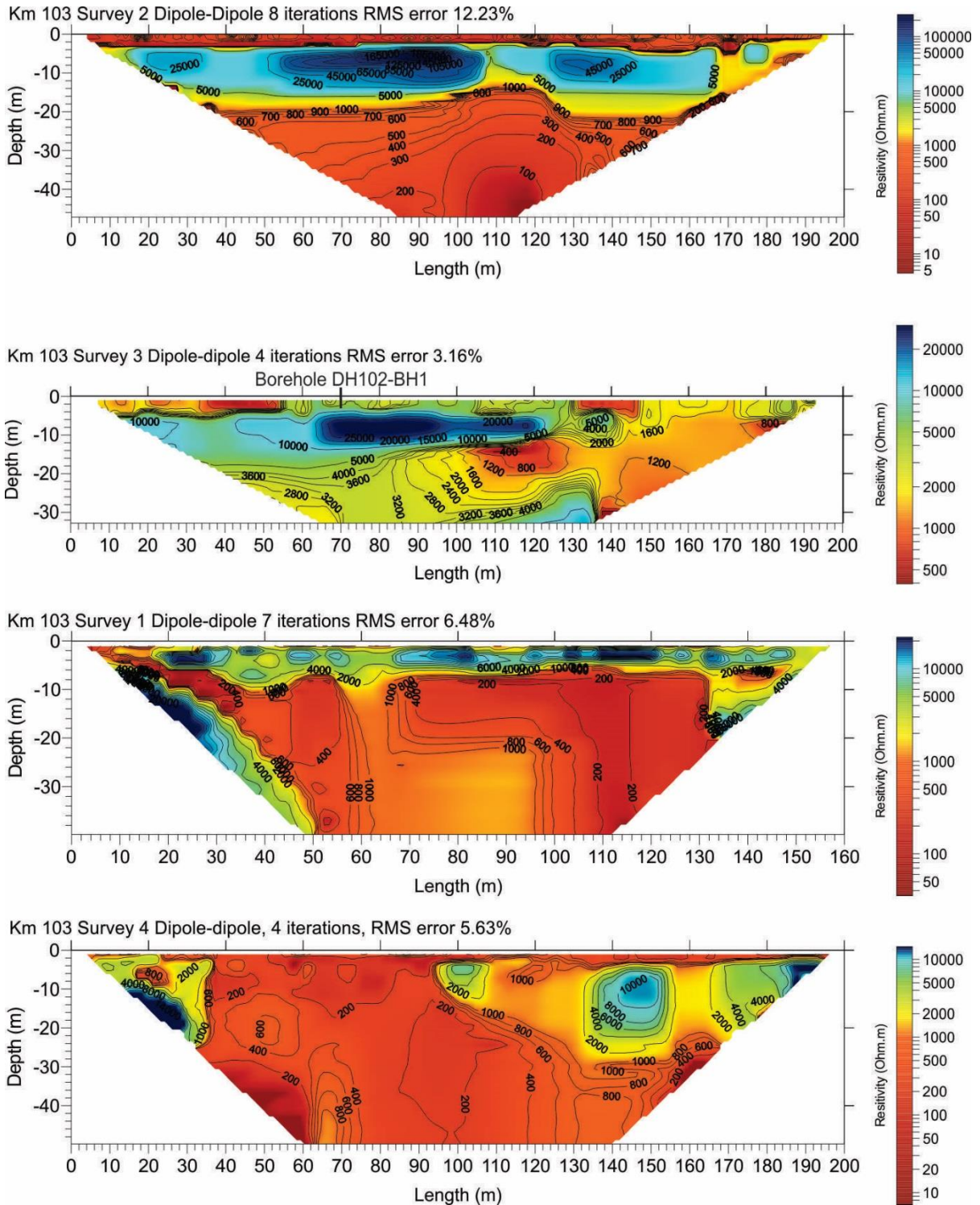
Figure 3.4.7 Dipole-dipole ERT surveys at site DH103**.**
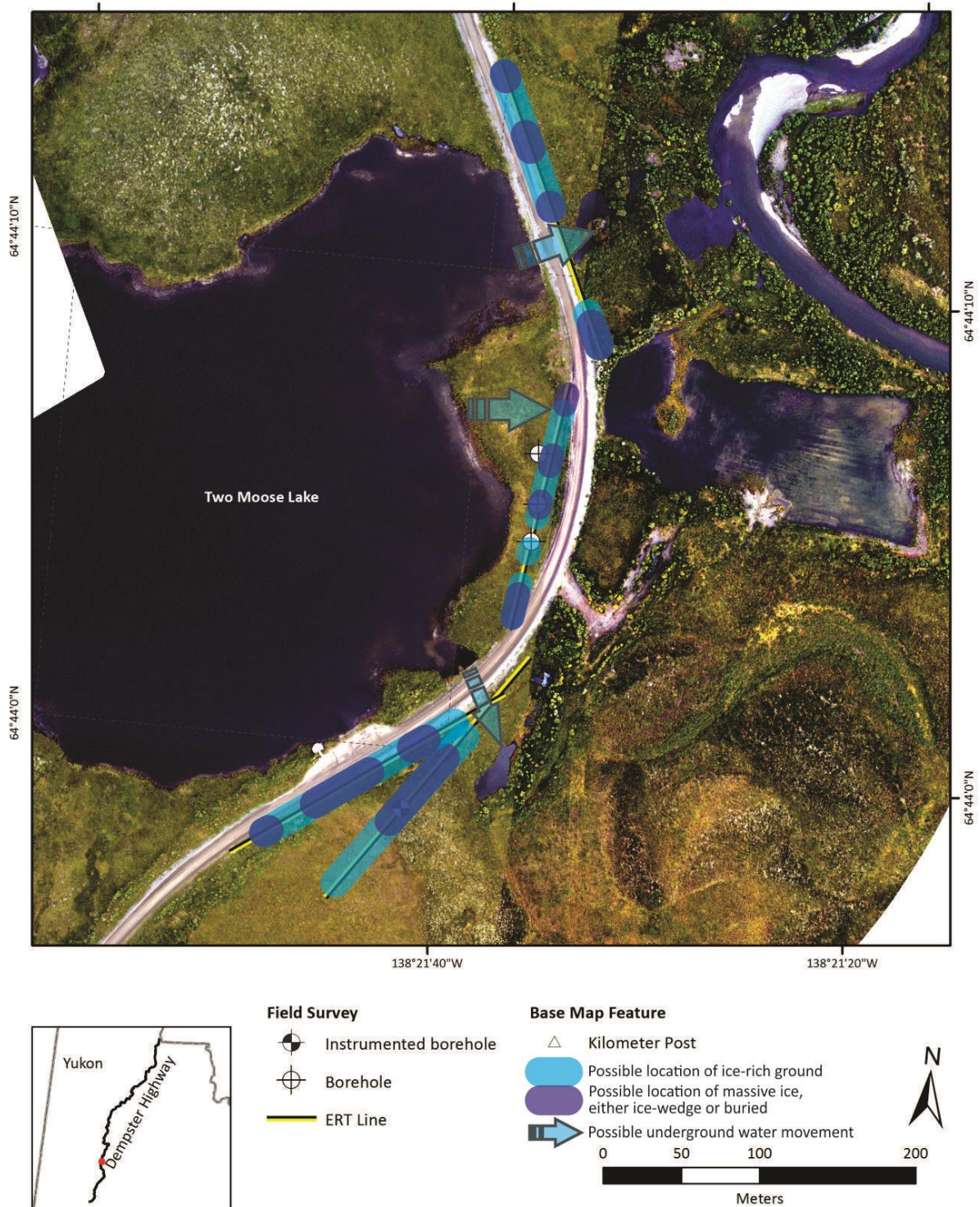
Figure 3.4.8 Site DH103 view with features inferred from the ERT surveys.

3.5   SITE 5: DH116 – KM 116

Issues

- Major subsidence is occurring along this section of the highway including multiple landslides in the slope between Chapman Lake and the Blackstone River.

Summary of Findings

- ERT surveys and a drill core at 100m identified a high-resistivity area as an ice wedge. This leads to the interpretation of similar high-resistivity areas as ice wedges.

- Massive ice is present at 14m depth, extending below the lower borehole limit at 20m.

- An unfrozen layer between 9 and 12m found in DH116 BH2 may be attributable to groundwater infiltration from the lake to the river.

- Permafrost is cold (below -2°C) and may therefore be resilient in the face of rising air temperatures; however, groundwater movement may contribute to permafrost thaw and further landslides.

- The thaw of ice-rich permafrost and massive ground ice bodies is responsible for subsidence and landslides in the area. Groundwater movement may contribute to permafrost degradation.

- If significant ice thaw and water seepage occur in the area between Chapman Lake and the Blackstone River, severe ground instability and catastrophic drainage of the lake could occur. Monitoring of this section is recommended to prevent or anticipate such an event.

3.5.1   Introduction

This site is located at km 116, approximately 13 km north of Two Moose Lake, an area investigated during summer 2016 and previously reported in "Investigation of Dempster Highway Sinkholes" (Calmels et al. 2017).[3]

---

[3] The sinkholes report provides the biophysical context to the area between km 74 and km 160, of which the site under scrutiny is part. Please refer to that report to get additional information on general geology and glacial history. This section can be considered as an addendum, reprising some results and adding new insights from ground temperature monitoring.

There are several issues at this site. Major subsidence is occurring along some sections of the highway. Where the road passes between Chapman Lake (north/left-hand side) and the Blackstone River (south/right-hand side). HPW was forced to realign the highway to the north (Fig. 3.5.1A) as a result of landslides that occurred along the cliff (river side – Fig. 3.5.1.B).

The field survey conducted for this report consisted of one shallow borehole that was instrumented with two 4-channel Hobo loggers, and two ERT surveys (one on each side of the road), using both Wenner and dipole-dipole arrays. An additional geotechnical borehole was drilled by a contractor for HPW; its preliminary results are presented below.

3.5.2   Geology

The Yukon Geological Survey surficial materials map (Fig. 3.5.2) indicates that this section of the road crosses over a lacustrine silt deposit. The lacustrine unit borders on aeolian deposits to the north and fluvial deposits to the south. A patch of morainal material is indicated to the west. The sediment deposition sequence is likely to start with a glacial deposit (moraine), followed by lacustrine, then fluvial, and aeolian at the top. Lacustrine and aeolian material are fine-grained and frost susceptible, and are likely to be associated with ground ice such as wedge ice. The moraine and fluvial deposits are coarser and less frost susceptible; nevertheless, such deposits can contain massive ice bodies. Additional biophysical context can be found from page 3 to 9 of Calmels et al. 2017.

3.5.3   Aerial imagery

The surveyed area is shown in Figure 3.5.3. Three notable features provide important information on the site. First, a polygonal pattern is visible in the area between Chapman Lake and the road, showing the presence of ice wedges throughout the whole area. Second, landslides are visible at several locations along the cliff between the road and the Blackstone River. Field observation indicates that these slides are attributable to the thaw of ice wedges (Fig. 3.5.4). The widths of the ice wedges are variable, one being measured to be 3.2 m wide, and their height can reach 6 m. based on field observations from cuts. Third, an area where gravel was excavated shows signs of intense subsidence (Fig. 3.5.2, northeast), likely due to the thaw of massive ice of an unknown nature.

3.5.4   Borehole geotechnical data

Borehole DH116-BH1 was drilled along ERT survey LHS, between the road and Chapman Lake (Figure 3.5.3). The thaw front was at 12 cm depth on June 6th, 2017. The soil stratigraphy

consisted of moss and peat from 0 to 0.30 m, followed by a sand mixed with organics down to 0.90 m. Deeper down, the soil became a sandy silt down to 1.35 m, at which depth a contact with wedge ice was found. Wedge ice was continuous down to 4.50 m depth. Below, a silty and sandy gravel was present down to 4.68 m, the end of the borehole. Excess ice content ranged from 27% in the sediment, to 100% in the ice wedge (Fig. 3.5.5). The mean volumetric excess ice content is 47%, without taking in account the ice-wedge cores.

Two boreholes were contracted by HPW and drilled on October 28th, 2017. The first, BH5566, was located based on ERT surveys (Fig. 3.5.6 - see Fig. 3.5.3 for location). The active layer thickness was 38 cm at the time. The profile consisted of organic cover from 0 to 0.30 m, organic sandy-silt from 0.30 to 1.9 m, sandy silt with gravel from 1.9 to 7.50 m, then a layer of ice (possibly wedge ice) from 7.50 to 8.80 m, then a gravelly sandy-silt, possibly unfrozen from 8.80 to12.20 m, followed by a silty-sand and a sandy silt with gravel down to 13.70 m. Finally, massive ice occurs from 13.7 m to 19.81 m, the end of the drilling. The nature of this massive ice is undetermined, although the absence of foliation and presence of granular material within the ice seems to disprove wedge ice. The second borehole, BH5567 (Fig. 3.5.7), was drilled in the field, left-hand side, facing the major slide that occurred this summer, about 0.6 km south to the two previous boreholes. It showed the presence on wedge ice from 4 m to 7.5 m depths, approximately, but no buried ice was found deeper, down to 19.8 m, end of the borehole.

3.5.5   Ground temperature

Borehole DH116-BH1 was lined with PVC piping and instrumented with two 4-channel Hobo loggers to record air temperature and ground temperatures at 0, 0.5, 1.0, 1.5, 2.0, 3.0, and 4.65 m depths. The recording started June 8th, 2017, at 3:00 pm. Data were downloaded September 17th, 2017, providing a little more than 3 months of monitoring. Figure 3.5.8 presents ground temperature data from June 15th, 2017 to September 15th, 2017. The records show that temperatures at the deepest point, 4.65 m, increased from -2.8 to -1.9 °C, and suggest a mean annual ground temperature below -2 °C.

3.5.6   ERT survey

Two ERT lines were surveyed at DH116, one in the field on the left-hand side (Fig. 3.5.9), and the other in the former embankment on the right-hand side of the road (Fig. 3.5.10). Both lines were surveyed with Wenner and dipole-dipole ERT arrays. For each array, two profiles are shown; the first is produced using a robust inversion, and the second one is created with a smoothness constraint in the inversion process. The robust inversion is typically used when sharp boundaries are expected, like in between ice and unfrozen ground, while a smoothness

constraint tends to ensure that the resulting model shows a smooth variation in the resistivity values, usually producing a model with a larger apparent resistivity RMS error.

Left-hand side ERT survey (Fig. 3.5.9)

Both Wenner and dipole-dipole surveys show similar results, however, the dipole-dipole appears to show more distinct boundaries than the Wenner array. The robust inversion provides the sharpest boundaries for both arrays. In general, several highly resistive areas (blue in color) are present between the ground surface and 10 m depth, all along the profile. Below 10 m depth, there is a clear difference between the western and eastern halves of the survey, with the west side showing lower resistivity values and the east side showing higher resistivity values. The red/orange lower resistivity value areas could be due to a decrease in ice content, warmer permafrost, or a presence of liquid water; while the darkest blue higher resistivity value areas could be resulting from coarser, more ice-rich, and/or colder permafrost.

Right-hand side ERT survey (Fig. 3.5.10)

The ERT survey on the right-hand side was similar to the that on left-hand side in that both Wenner and dipole-dipole surveys show comparable results. However, unlike the left-hand side, the RMS error obtained after several iterations (from 4 to 13) remains relatively high, between 15 and 26 %, for both Wenner and dipole-dipole surveys, regardless of the type of inversion used. Because of this high error, the results of the survey must be considered with caution. In general, the profiles show a red/orange, low-resistivity layer, 4-5 m thick located in the upper part of the profile, overlying a blue, highly resistive material. These results could be interpreted as the ice-poor, now warm relic road embankment overlying relatively ice-rich, colder frozen ground.

3.5.7   Synthesis

The ERT surveys at km 116 on the left-hand side are the most interesting. The high-resistivity area present at 100 m has been identified as an ice wedge complex, drilled and cored in DH116 BH1. Therefore, the other high-resistivity bodies located at similar depth can be interpreted as ice wedges also.

Based on the observation of very high resistivity deeper in the eastern end of the profile, HPW contracted geotechnical drilling located at 160 m of the profile. The drilling of DH116 BH2 showed that massive ice was present much deeper than 10 m. Massive ice starts at about 14 m

depth and extends below the end of the 20 m borehole. Without finding the lower contact of the lower layer of massive ice, it is not possible to infer its thickness.

Lidar data were used to relate the DH116 BH2 log to the surrounding topography. The Blackstone River is at an elevation of 977 m and the surface of Chapman lake is at 987.5 m. The surface of the ground at DH116 BH2 is at an elevation of 1002 m. Consequently, the elevation of the deeper massive ice contact is almost at level with Chapman Lake water level (988.2 m). It is possible that the unfrozen level reported between 9 and 12 m (approximately 990 and 993 m elevation) is attributable to underground water infiltration from the lake to the river (Fig. 3.5.11).

Ground temperature records are short, yet permafrost seems relatively cold, below -2 °C, and therefore may be relatively resilient to an increase of air temperature over the next decades. However, groundwater movement may contribute to permafrost thaw and the further development of landslides. Borehole DH116 BH2 has been temporally instrumented for ground temperature monitoring and should confirm or refute the presence of a talik (unfrozen area) within the profile. If there is a talik, then it is likely that groundwater could move in this layer.

Overall, permafrost is very ice-rich, massive ground ice bodies are present, and there are possible pathways for ground water movement. The thaw of ice-rich permafrost and massive ground ice bodies is responsible for the general subsidence observed all along this section of the road, as well as for the landslides along the cliff. Groundwater movement may contribute to the general permafrost degradation in this area.

The combined thicknesses of upper wedge ice (up to 8 m) and of deeper massive ice bodies (>6 m) may exceed 14 m at some locations. The difference in elevation between the lake surface and the ground surface at DH116 BH2 is 14.5 m. Should the ice thaw or be removed and underground water seepage occur, the possibility of the lake draining cannot be excluded. The situation should be monitored to prevent or anticipate this catastrophic event.
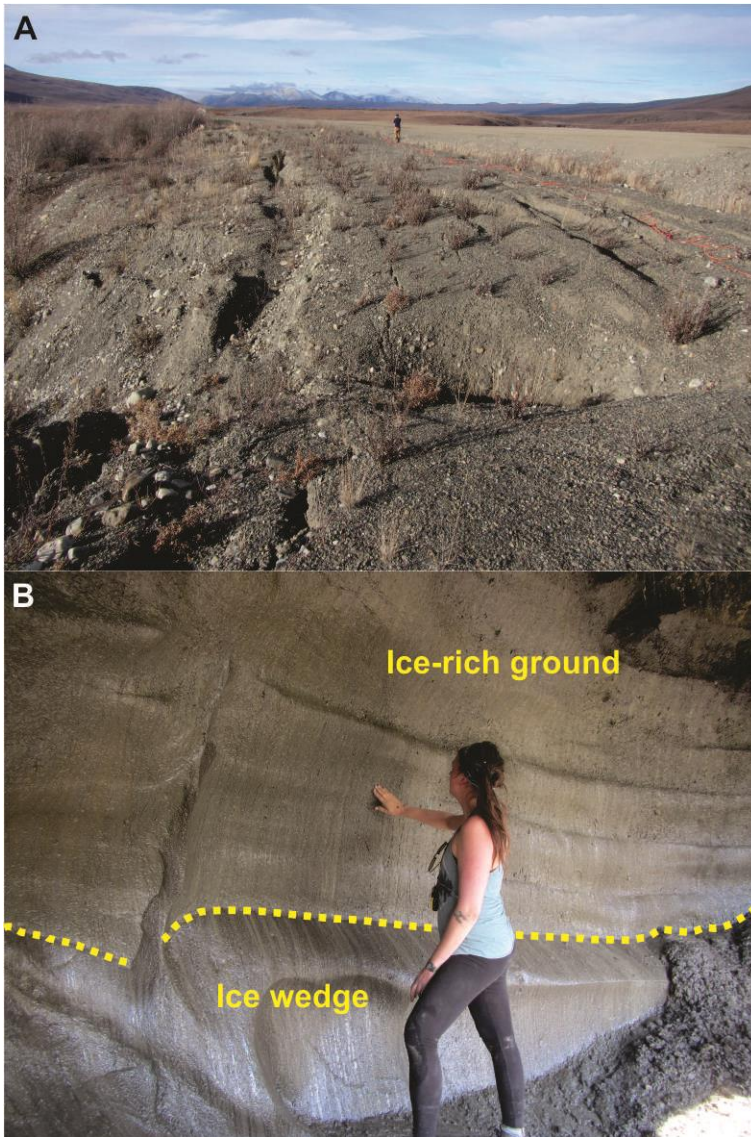
Figure 3.5.1 Degradations observed at DH116. A- Former embankment at right-hand side affected by permafrost degradation; B- ice-rich ground and ice-wedge observed at landslides along the cliff.
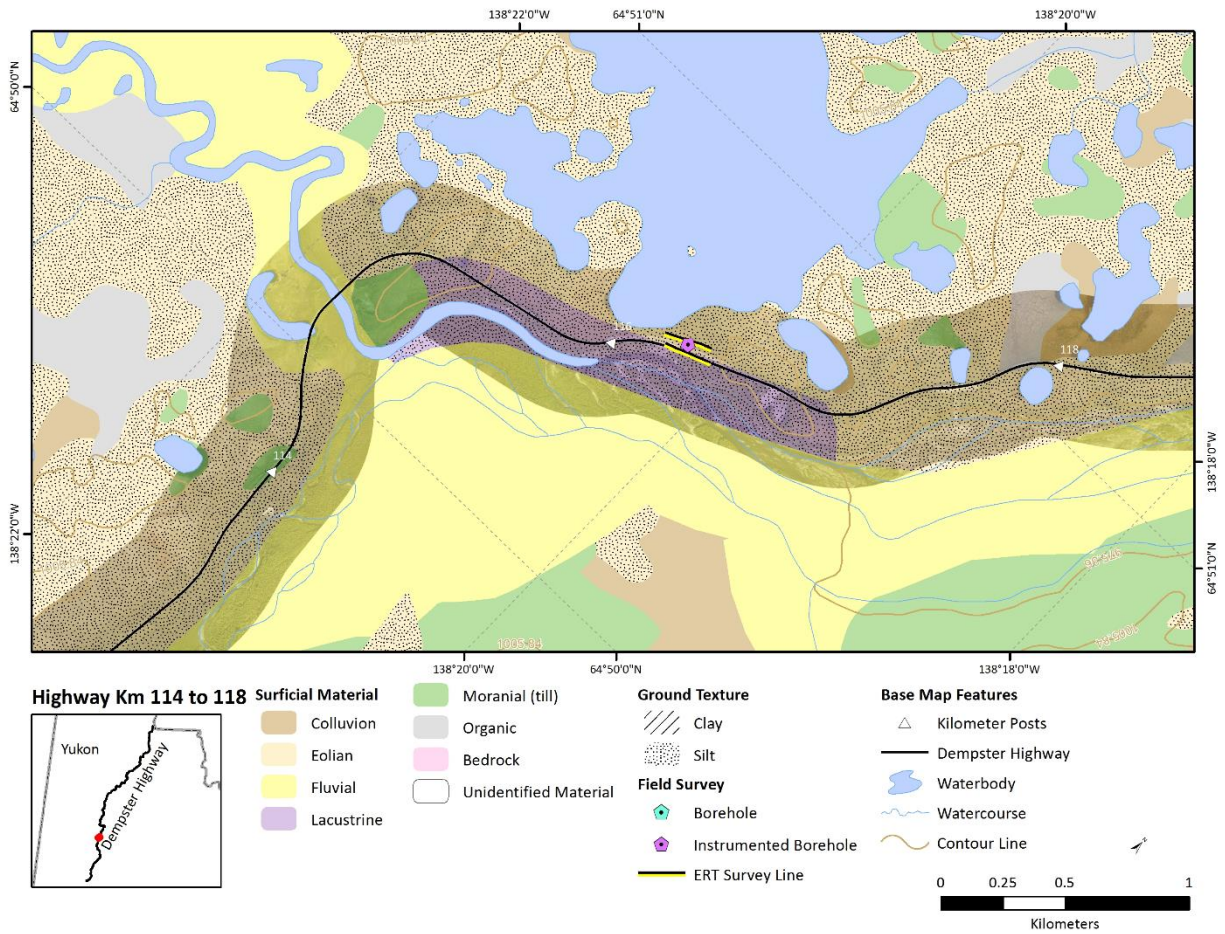
Figure 3.5.2 Surficial geology map of the site 5 DH116 area
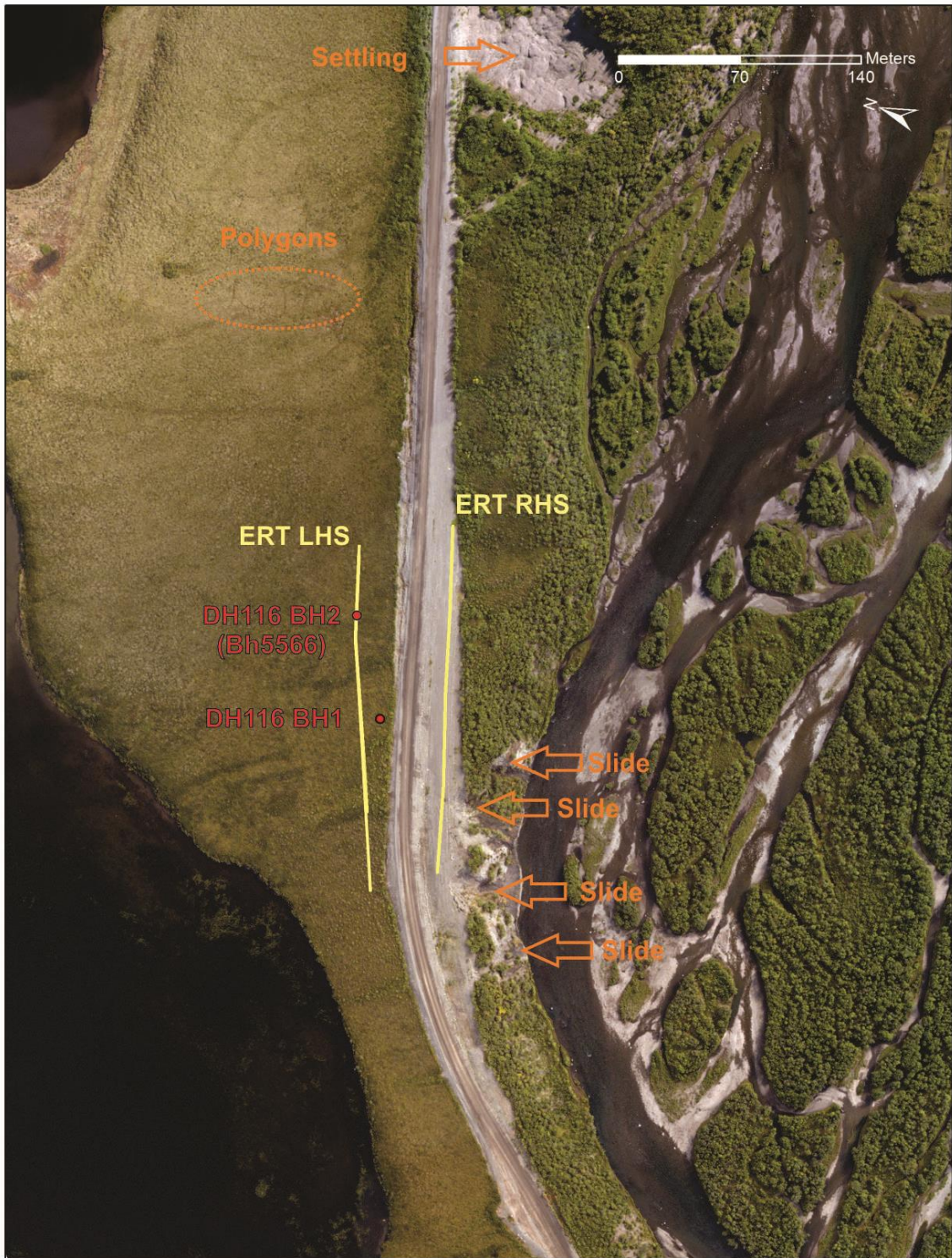
Figure 3.5.3 Aerial view of site DH116
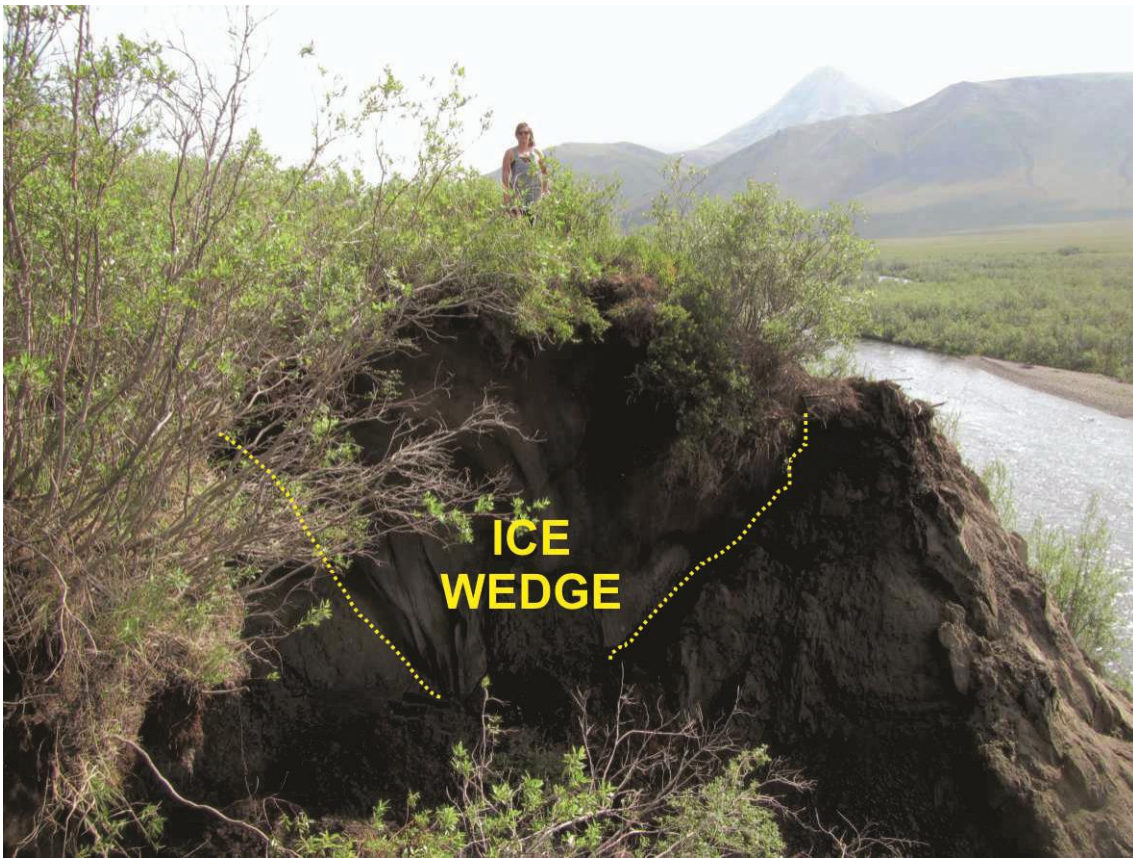
Figure 3.5.4 Slide showing an ice wedge at DH116; its estimated height is 6 m.

Sample	% Pebble+	% Gravel	% Sand	% Silt and Clay
DH116 0.28 m	0.6	7.7	88.6	3.1
DH116 0.60 m	6.5	8.7	82.6	2.3
DH116 0.95 m	34.6	1.7	21.3	42.3
DH116 1.25 m	1.7	0.9	46.4	51.0
DH116 1.49 m	0.0	0.6	39.1	60.3
DH116 4.51 m	38.6	3.1	16.8	41.6
DH116 4.68 m	55.2	4.3	14.5	25.9
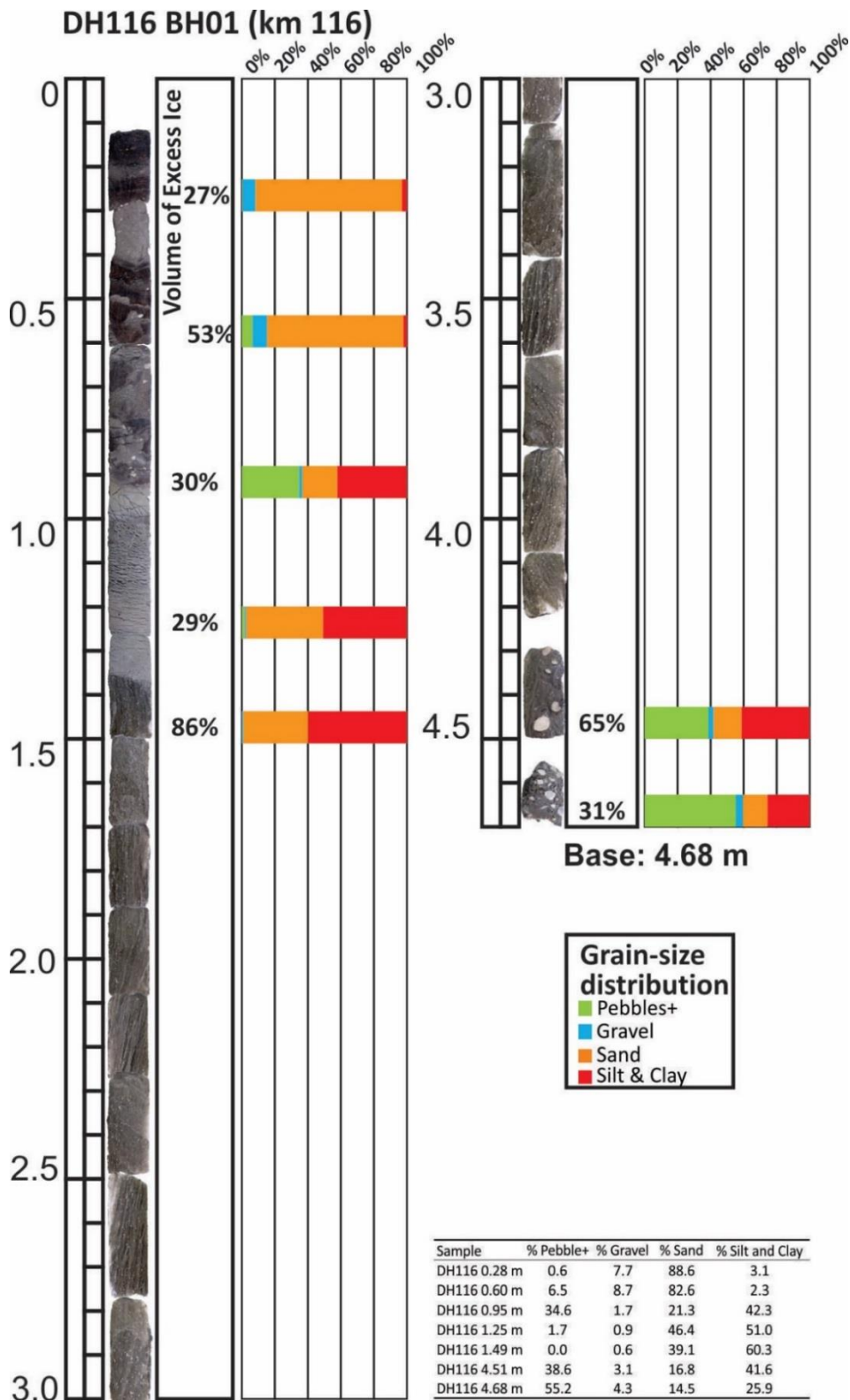
Figure 3.5.5 Log of borehole DH116 BH1, with volumetric excess ice content and grain size distribution.

BH5566 / DH116 BH2

Organic cover
Active Layer (0.38 m)

Organic sandy-silt

Sandy silt + gravel

+ gravelly, sandy-silt

coarse gravel + sandy-silt

Ice wedge / foliations

Unfrozen

Gravelly sandy-silt
Rounded, well-sorted

Silty-sandy gravel

Sandy silt + gravel

Ice wedge (?) / Massive ice
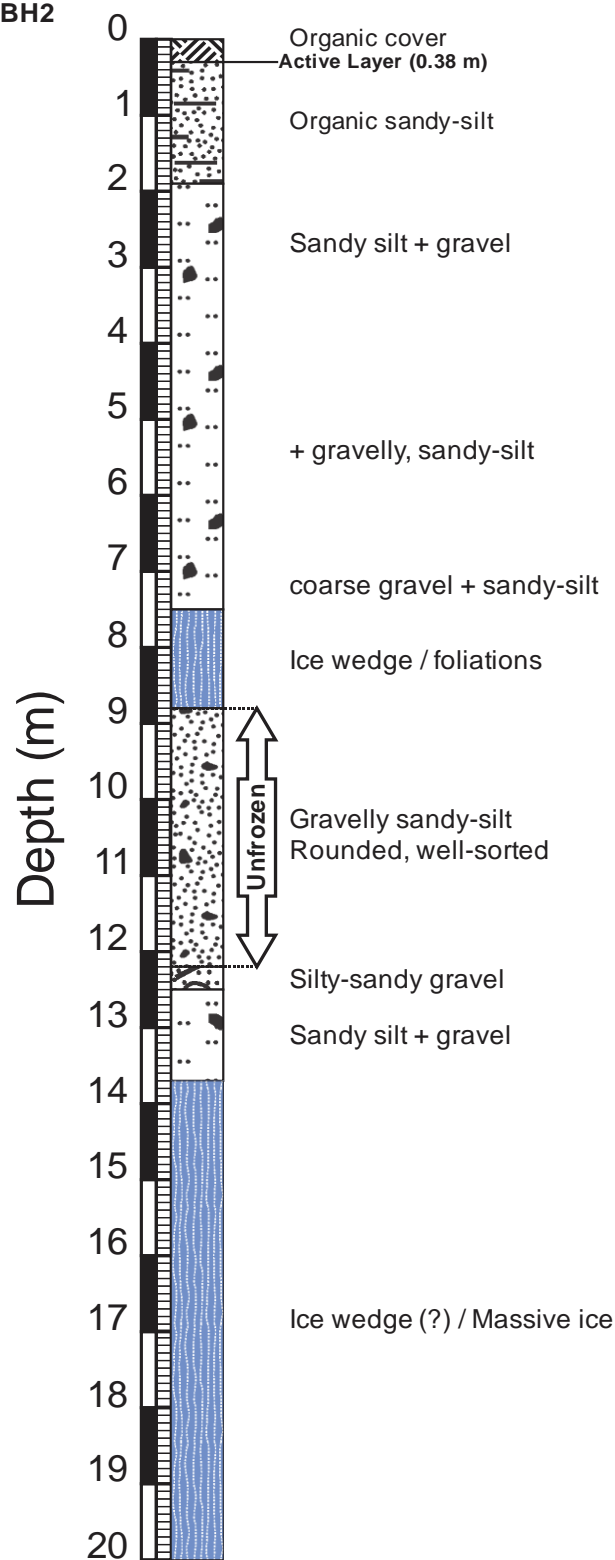
Depth (m)

Figure 3.5.6 Preliminary log of borehole DH116 BH2 (BH5566).

BH5567 / DH116 BH3

Organic cover

Ice-rich silt
(lenticular, maybe reticulate cryost.)

Foliated massive ice / Ice wedge

Organic silt with traces of sand

Potent. unfrozen — Sand and silt with traces of gravel

Silty sand and gravel
(less gravel with depth)

Silt with some gravel and traces of sand
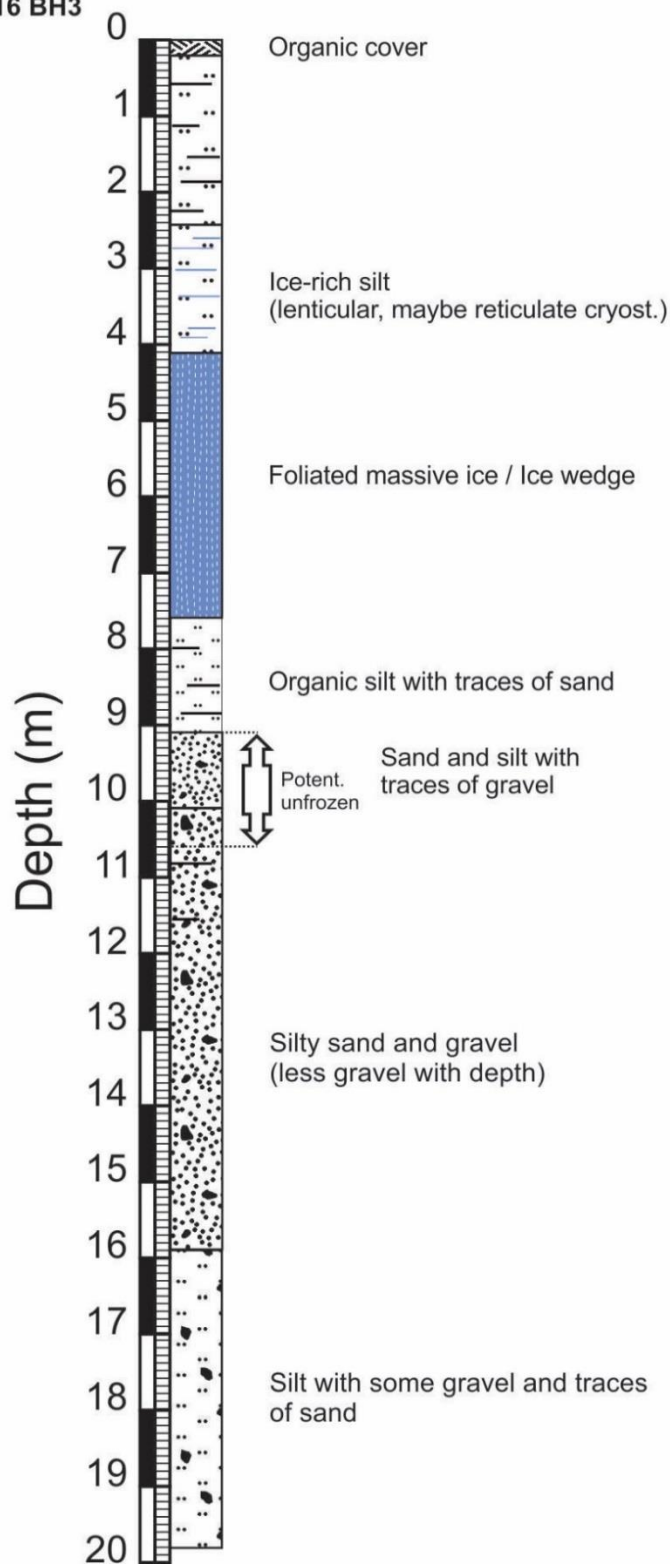
Depth (m)

Figure 3.5.7 Preliminary log of borehole DH116 BH3 (BH5567).
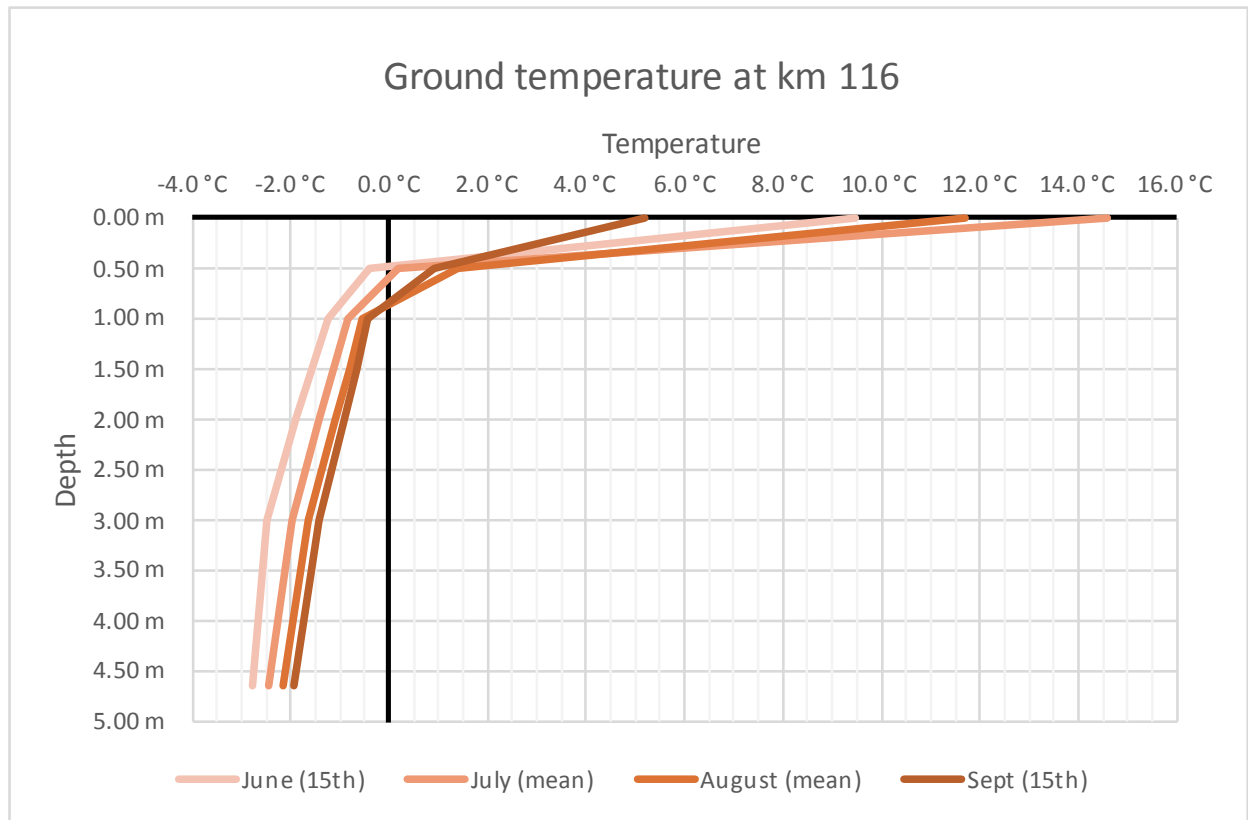
Depth	June (15th)	July (mean)	August (mean)	Sept (15th)
Air Temp	9.8 °C	14.3 °C	11.1 °C	4.7 °C
0.00 m	9.5 °C	14.6 °C	11.7 °C	5.2 °C
0.50 m	-0.4 °C	0.2 °C	1.4 °C	0.9 °C
1.00 m	-1.3 °C	-0.8 °C	-0.6 °C	-0.4 °C
1.50 m	-1.6 °C	-1.1 °C	-0.8 °C	-0.7 °C
2.00 m	-1.9 °C	-1.4 °C	-1.1 °C	-0.9 °C
3.00 m	-2.5 °C	-2.0 °C	-1.6 °C	-1.4 °C
4.65 m	-2.8 °C	-2.4 °C	-2.2 °C	-1.9 °C

Figure 3.5.8 Ground temperature at DH116 BH1, based on a record from June 15th, 2017 to September 15th, 2017.
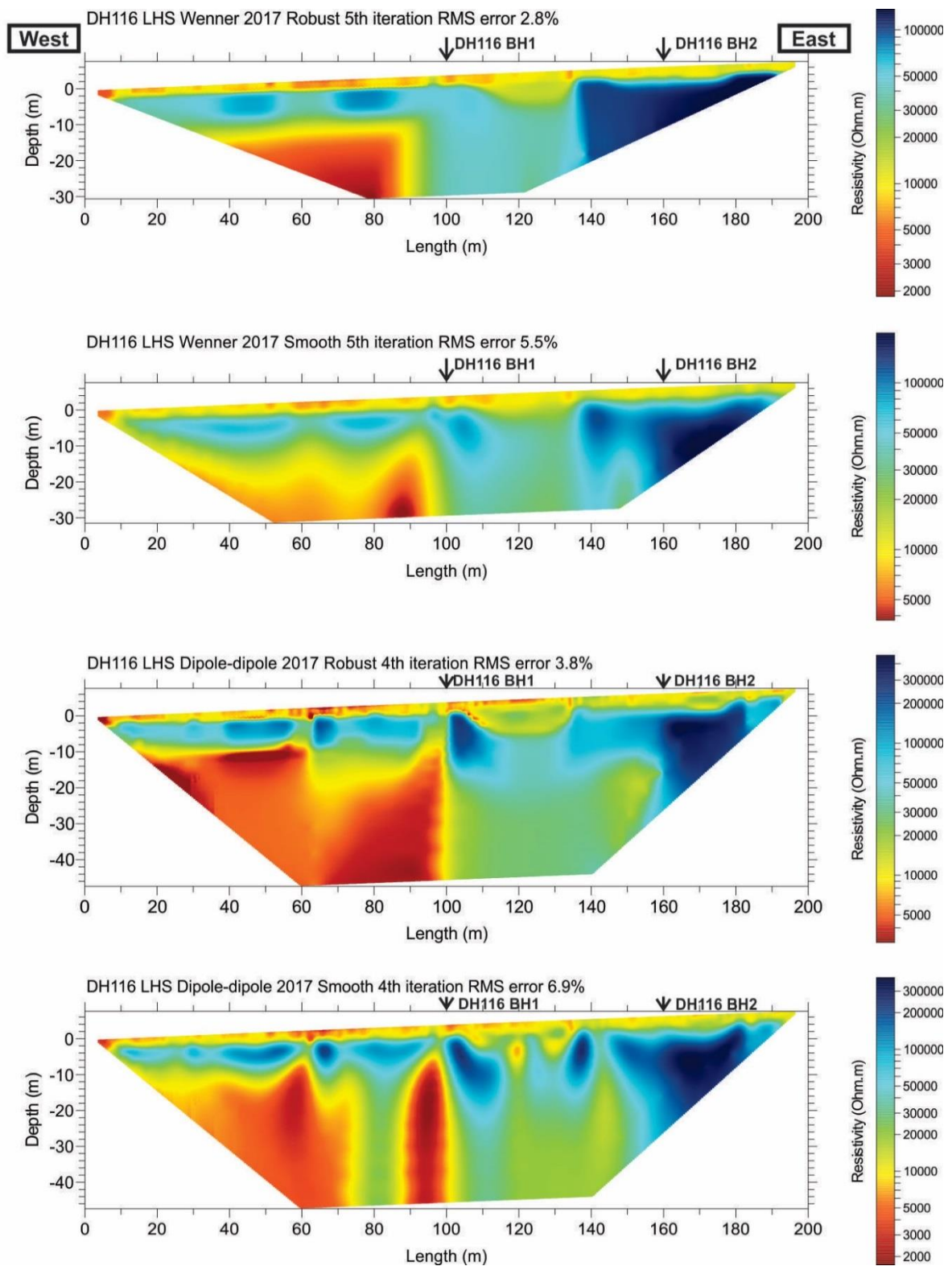
Figure 3.5.9 Wenner and dipole-dipole ERT surveys at site DH116, left-hand side (LHS), using robust and smoothed inversion processes.
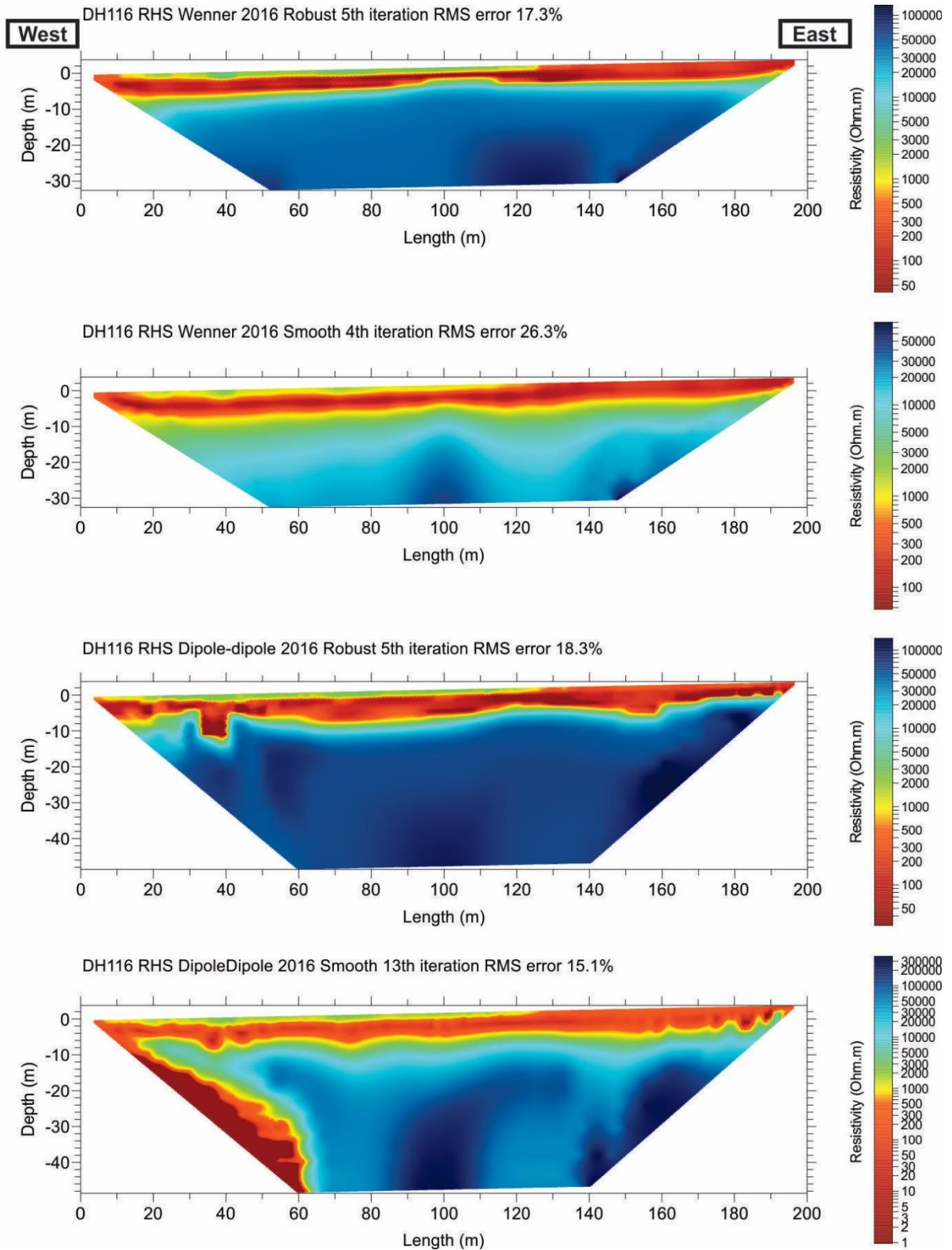
Figure 3.5.10 Wenner and dipole-dipole ERT surveys at site DH116, right-hand side (RHS), using robust and smoothed inversion processes.
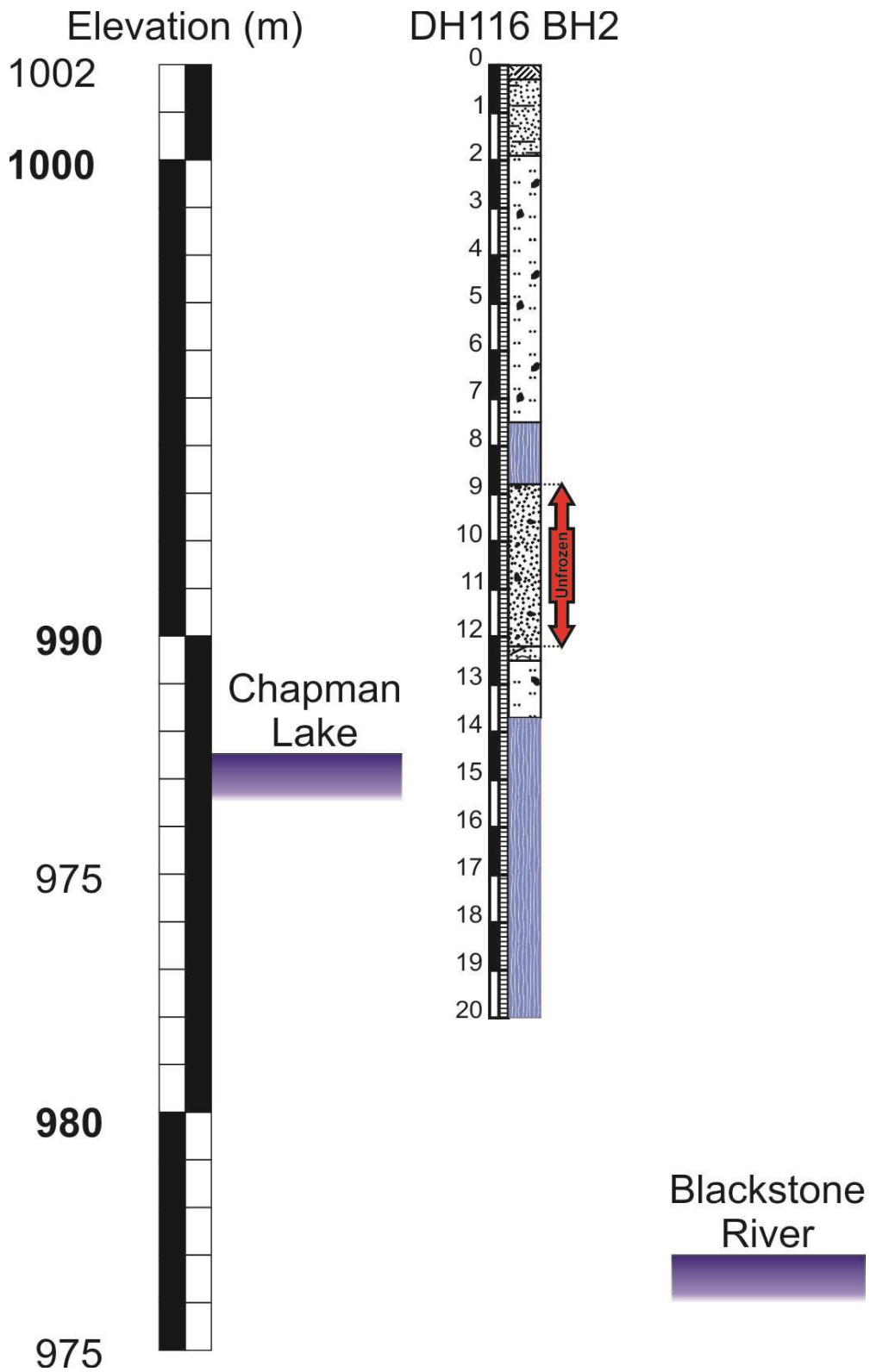
Figure 3.5.11 DH116 BH2 borehole log compared to Blackstone River and Chapman Lake water levels.

3.6   SITE 6: DH124 – KM 124

Issues

- The site shows major subsidence along the highway and airstrip

- Depressions are generally perpendicular to the highway and are accompanied by ponding at the foot of the embankment

Summary of Findings

- Permafrost is cold, but degrading

- Depressions were observed at the south end of the airstrip and around the HPW station

- The first three metres of ground appears to be rich with permafrost and ice wedges

- An ice-poor gravel lays below the top layer ice wedges and may allow for groundwater movement. Water movement cannot be confirmed by the current investigation methods.

- Thaw-sensitivity is likely due entirely to the ice wedges in the top 3m.

- If this top 3m was to thaw completely, the ground would likely become stable.

3.6.1   Introduction

This site was selected for monitoring of permafrost conditions along the highway in 2013. Located in the Blackstone Uplands at the Chapman Lake airstrip (Yukon km 124), results of the borehole drillings and ground temperature monitoring were presented in the GeoQuébec 2015 conference proceedings (Idrees et al. 2015). This section can be considered as an addendum; reprising some results of the proceedings, and adding new insights from the geophysical assessments. The biophysical context provided in the report "Investigation of Dempster Highway Sinkholes" (Calmels et al. 2017) still applies to this area (Blackstone Uplands).[4]

The general issue at this site is major subsidence occurring along some sections of the highway and airstrip (Fig 3.6.1). The depressions are generally perpendicular to the road, incising the shoulder of the embankment, and accompanied by ponding at the foot of the highway.

---

[4] The report provides an overview of the area between km 74 and km 160. Refer to this report for additional information on general geology and glacial history.

The field survey consisted of 4 geotechnical boreholes contracted by HPW, which were instrumented with a Campbell Scientifics logging station. Two ERT surveys, one in the field at the left-hand side, and one on the airstrip at the right-hand side, were performed using both Wenner and dipole-dipole arrays.

3.6.2   Geology

Site DH124 is in the northernmost portion of the Blackstone Uplands, where the road follows the broad Blackstone River valley (Figure 3.6.2). The surficial materials are mostly glaciofluvial outwash, covered by a veneer of silt of aeolian origin. The site has well developed networks of ice wedge polygons. These are outlined at the ground surface by slight depressions in the surface vegetation of mosses and lichens.

3.6.3   Aerial imagery/field observation

The surveyed area is show in Figure 3.6.3. The most noticeable feature is the polygonal ground patterns that are visible in field at the left-hand side of the road, showing the presence of ice wedges throughout the area. These ice wedges are degrading, resulting in the formation of depressions in the troughs, which channel water, creating ponds. In the past year, depressions have formed at the location of the HPW monitoring station. Groundwater discharges from the cliff located at the right-hand side, through the gravel, into the Blackstone River channel, leading to surface icing in winter.

3.6.4   Borehole geotechnical data

The log of the first borehole drilled in the field in November 2013 is presented in figure 3.6.4, with core photos in figure 3.6.5. Because of cold (-4°C) near-surface mean annual ground temperatures in this area, permafrost was anticipated in the surficial materials; however, unfrozen ground and free water were encountered at depth. A thin layer of permafrost was found in the field, where foliated massive ice, interpreted as wedge ice, was recovered in silts (Mod. USC - ML) above gravel, and a 0.35-m layer of pool ice was found within the permafrost (Figure 3.6.4 and 3.6.5). The silts were ice-rich, with two tested samples giving excess ice contents of 49 and 69%. The outwash gravels include a range of clast sizes, including boulders that terminated initial drilling. The exceptionally thin permafrost for a site with T_p of < -4 °C is likely due to convective heat transfer from the groundwater.

A deeper borehole was drilled at the site (BH 876-5320 – Fig. 3.6.6). The results were very similar, with wedge ice between 0.7 and 3.0, followed by gravel below. The material was as unfrozen below about 7 m depth. The water table was observed at 12.2 m.

3.6.5   Ground temperature

Near-surface permafrost temperatures at the field site were low, as anticipated (Fig. 3.6.7). However, it was not anticipated that permafrost would be < 8 m thick at this site, or that it would have degraded completely beneath the toe of the embankment. Maximum temperatures measured over the year indicate the base of the permafrost is at about 7 m depth at both field and centerline sites. The thin layer of permafrost is likely due to heat transfer from groundwater flowing through the glacial outwash at the site. The extensive icing along the bank of the Blackstone River is derived from groundwater discharge throughout winter. Permafrost at the toe cannot be sustained, due to snow accumulation at the edge of the road from ploughing, and trapping of blown snow in willows and alder bushes which insulates the ground from the coldest temperatures. Within the embankment, at the centerline, permafrost is sustained, and permafrost temperature just below the active layer is comparable with the field site (-2.4 °C).

3.6.6   ERT survey

Two ERT lines were surveyed at DH124, one in the field at the left-hand side (Fig. 3.6.8), and the other on the airstrip at the right-hand side of the road (Fig. 3.6.9). Both lines were surveyed with Wenner and dipole-dipole ERT arrays. For each array, two profiles are shown; the first is produced using a robust inversion, and the second is created with a smoothness constraint in the inversion process. The robust inversion is typically used when sharp boundaries are expected, like in between ice and unfrozen ground, while a smoothness constraint tends to ensure that the resulting model shows a smooth variation in the resistivity values which usually produces a model with a larger apparent resistivity RMS error.

Left-hand side ERT survey (Fig. 3.6.8)

Both Wenner and dipole-dipole surveys show similar results; yet the dipole-dipole seems to provide better defined boundaries than the Wenner array. The robust inversion provides the sharpest boundaries for both arrays. The third profile from the top in figure 3.6.8, dipole-dipole with robust inversion seems to be the more realistic representation. In general, several high-resistivity areas, blue in color, are present between the ground surface and a little less than 10 m depth, all along the profile. These areas are thicker in the ends of the profile, and less dense in the middle of the profile. The middle of the profile, which coincides with the location of a

67

HPW permafrost station, shows low-resistivity material starting at about 8 m (green color at about 2000 Ohm·m). This could be the boundary between frozen and unfrozen gravel, the darkest blue bodies being ice-wedges. This observation implies that ice wedges and permafrost could be thicker on both sides of the station; yet following this 2000 ohm·m boundary, permafrost would not go deeper than 15 m, with the ground unfrozen below.

Right-hand side ERT survey (Fig. 3.6.9)

Similar to observations from the left-hand side ERT survey above, in the right-hand side survey, both Wenner and dipole-dipole surveys show comparable results, but the dipole-dipole profile with robust inversion (fig. 3.6.9. third profile from the top) seems to provide the more realistic representation of permafrost conditions. The surveys show low resistivity in the first 4-5 m depth along the survey, which could be attributable to dry, unfrozen gravel in the airstrip. Below the 4-5 m depth, higher-resistivity areas are present, likely attributable to the presence of ice wedge complexes. The base of the permafrost could be located between 15 m to 20 m depth, between approximately 500-1000 ohm·m.

3.6.7   Synthesis

While the permafrost is relatively cold, it is now degrading in this area. Some depressions mimicking an ice wedge network were observed in June 2017 at the southern end of the airstrip, and the ground surface is pitted with depressions at the location of the HPW station.

Borehole logs suggest that the permafrost is ice-rich from the near-ground surface to 3 m depth, in silt. The underlying gravel appears to be ice-poor; and permafrost seems relatively thin. ERT surveys confirm these observations, showing a permafrost thickness between 8 and 15 m. ERT surveys do not allow for the observation of groundwater movement.

There are no indicators of massive ice bodies within the gravel material; therefore, the thaw sensitivity of this site may be entirely attributable to the presence of ice wedge complexes in the first 3 meters. Should the ice wedges completely thaw, the area should become thaw stable. The height of the ice wedge complex is approximately 2.5 m; yet the average width of an individual ice-wedge is unknow. Observations from another site (DH116) suggest that ice wedge widths may average 1-2 m.
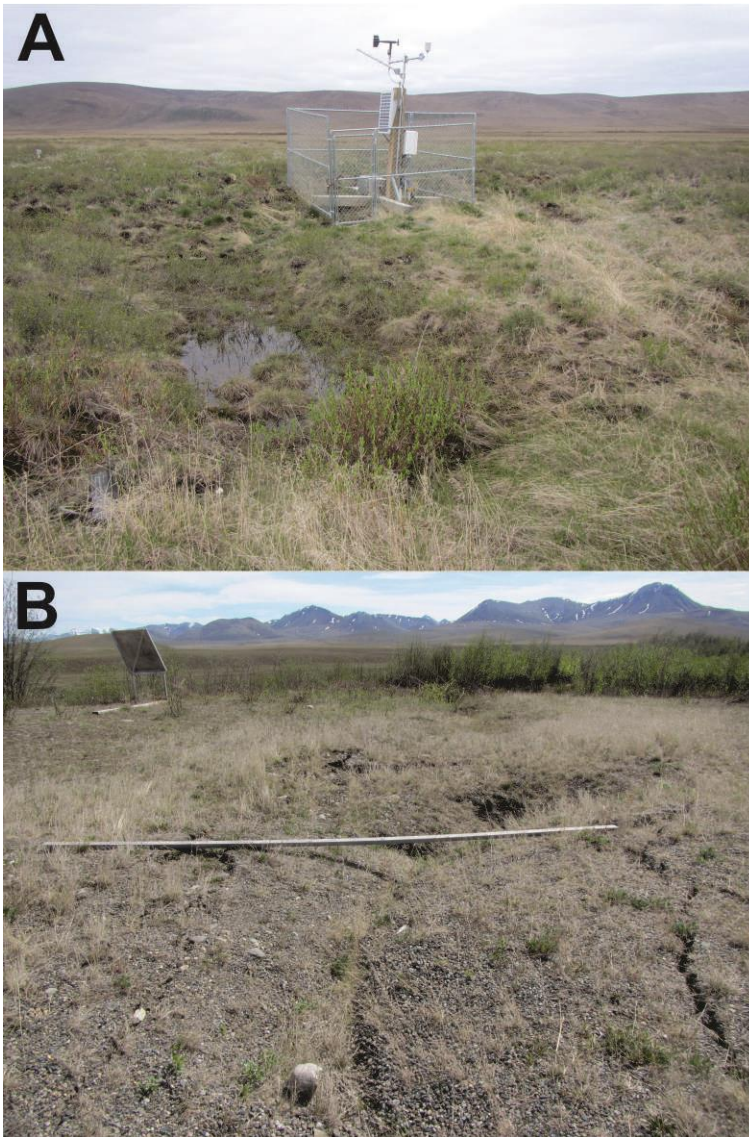
Figure 3.6.1 Degradations observed at the site DH124: A- at HPW met-station; B- at south end of the Chapman Lake airstrip.
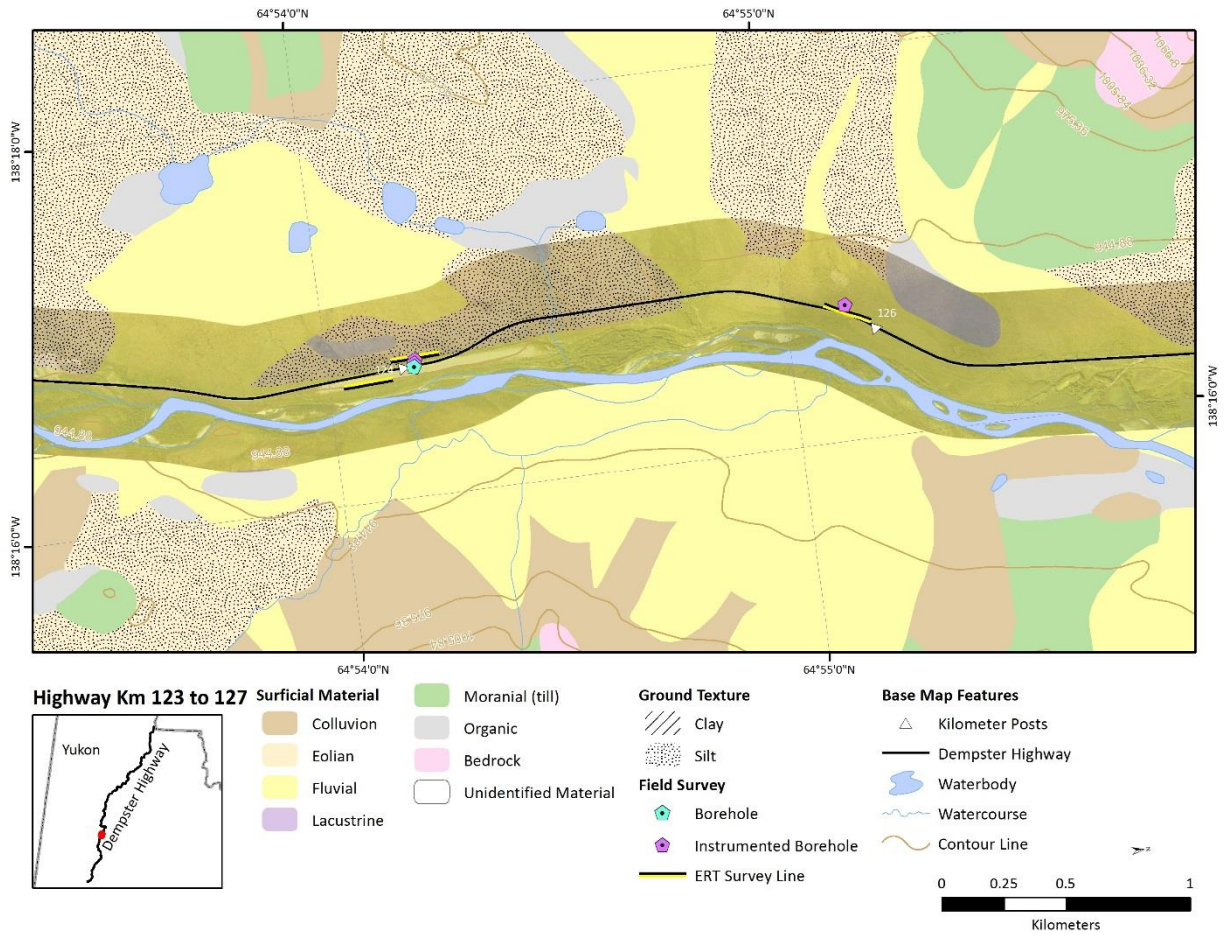
Figure 3.6.2 Surficial geology map of site 6 DH124 area.
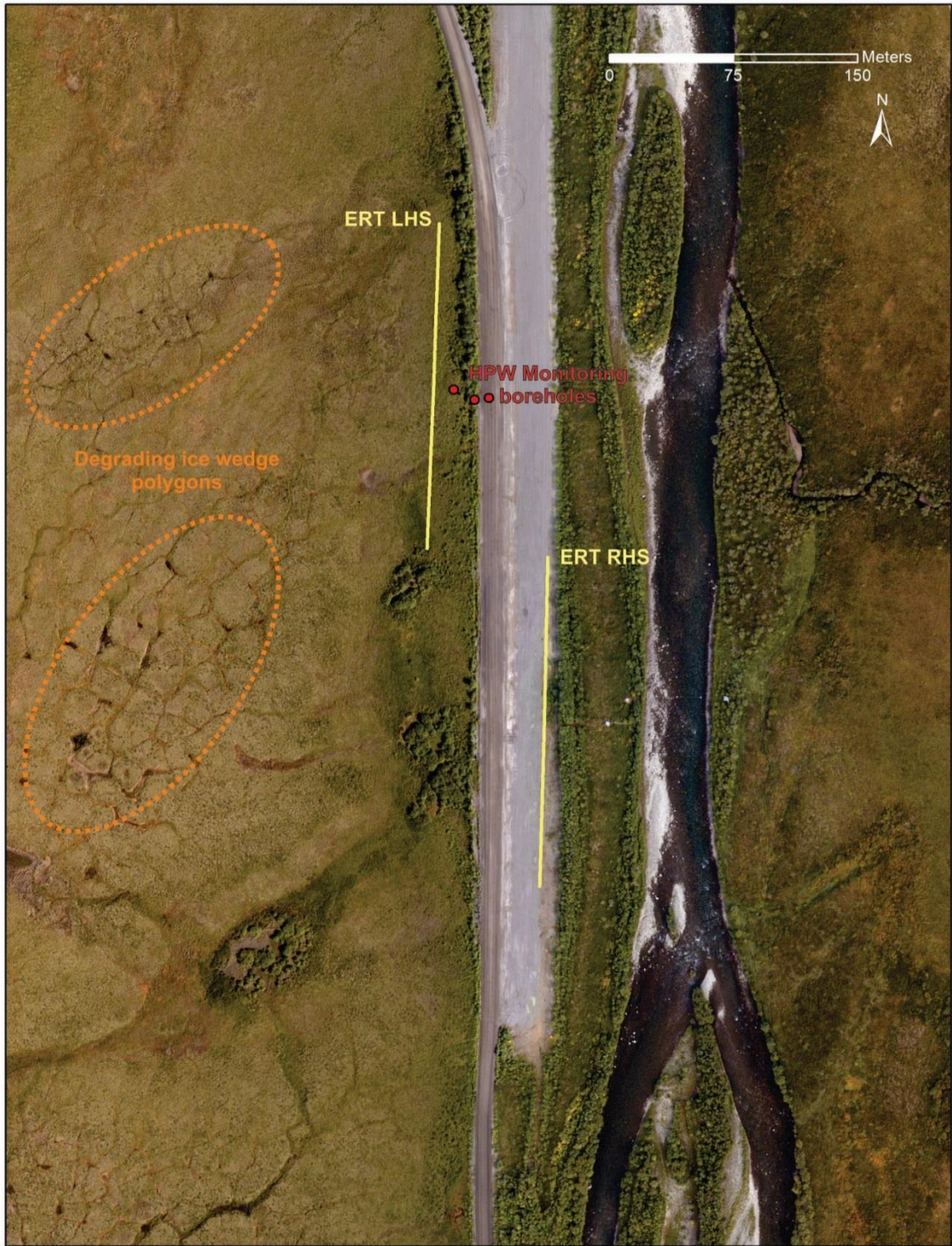
Figure 3.6.3 Aerial view of site DH124
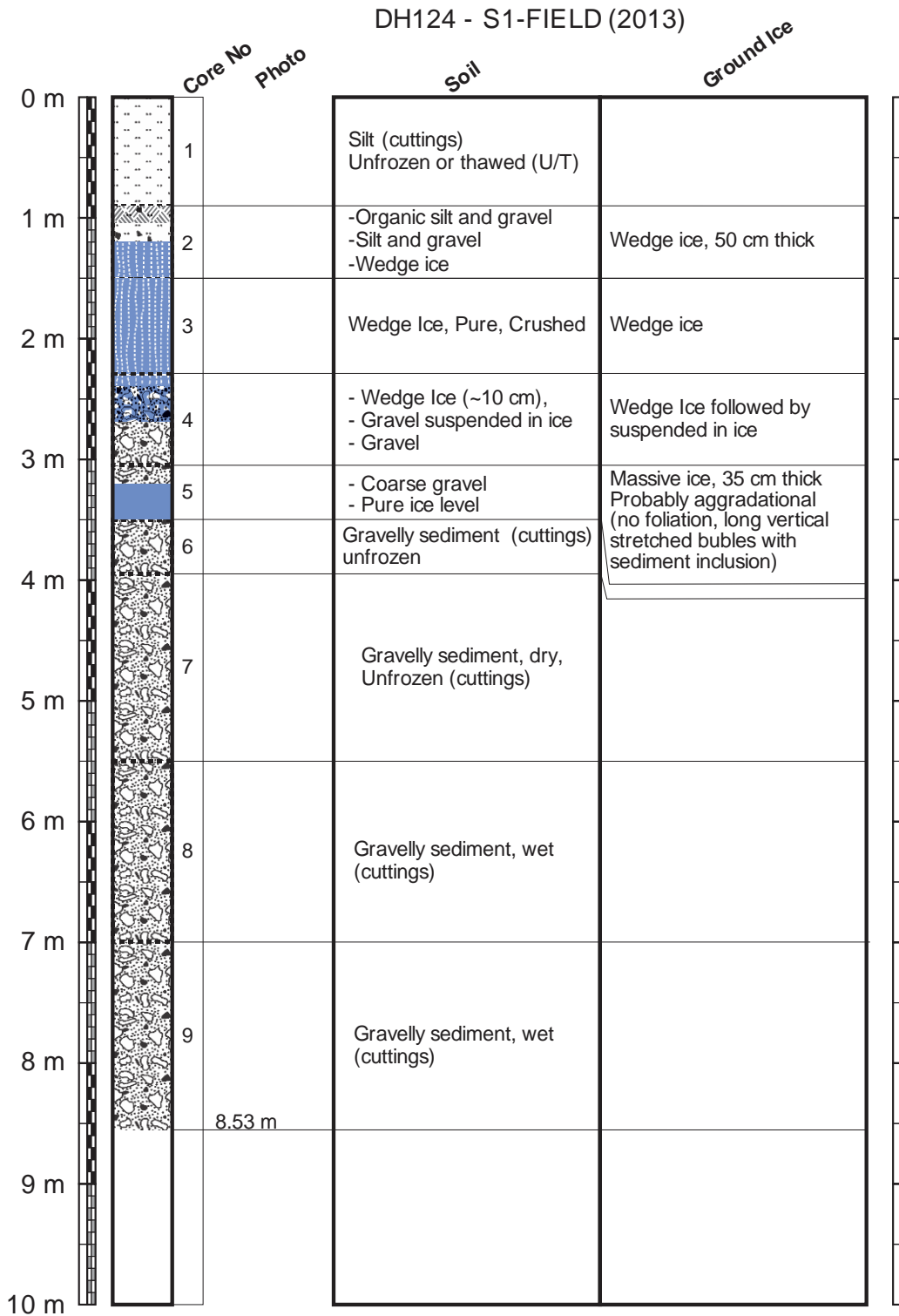
Figure 3.6.4 Log of borehole DH124 BH Field.

DH124 - S1-FIELD (2013)
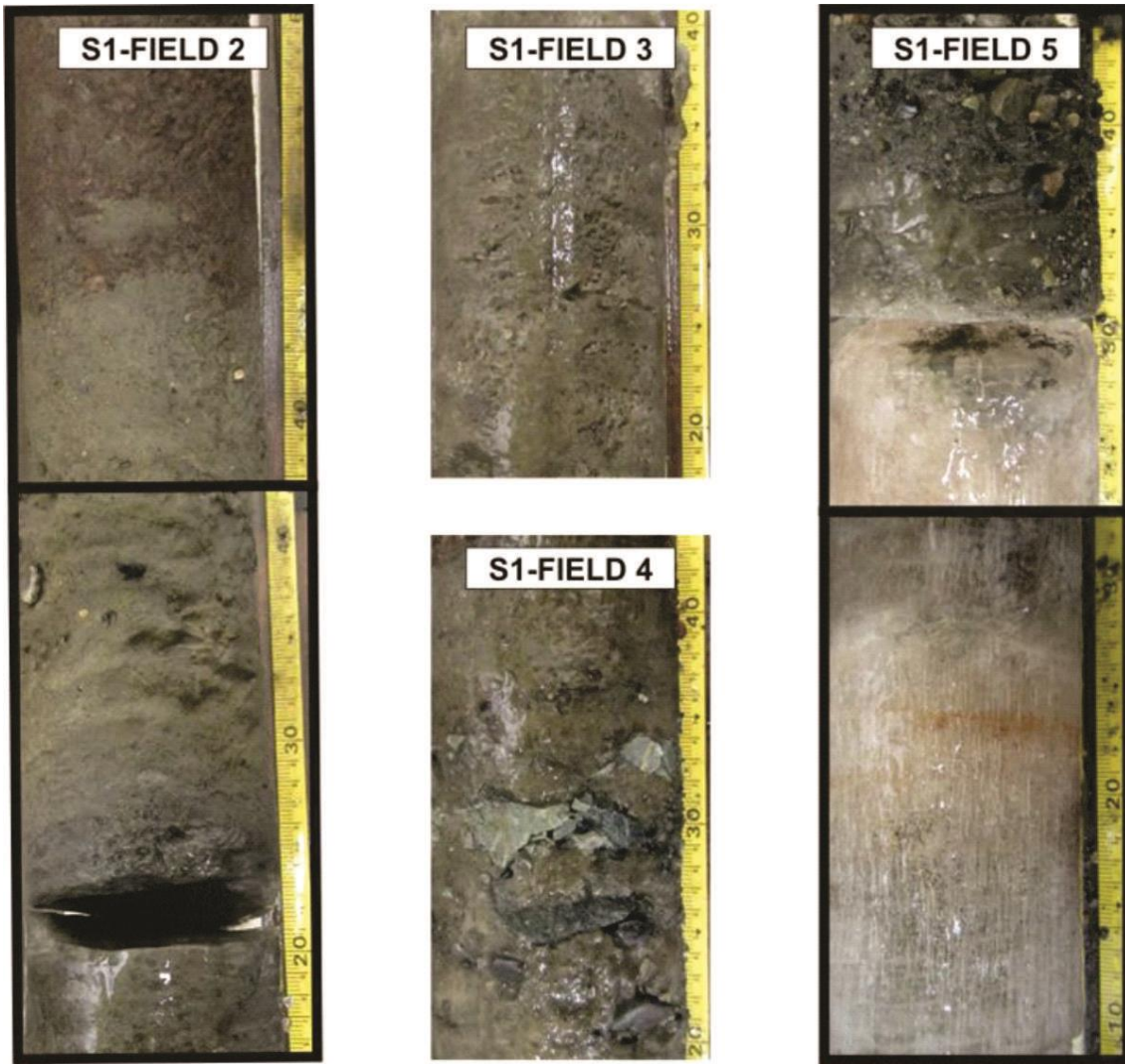
Figure 3.6.5 Core pictures of borehole DH124 BH1 Field.

km 124 LHS - Bh 876-5320
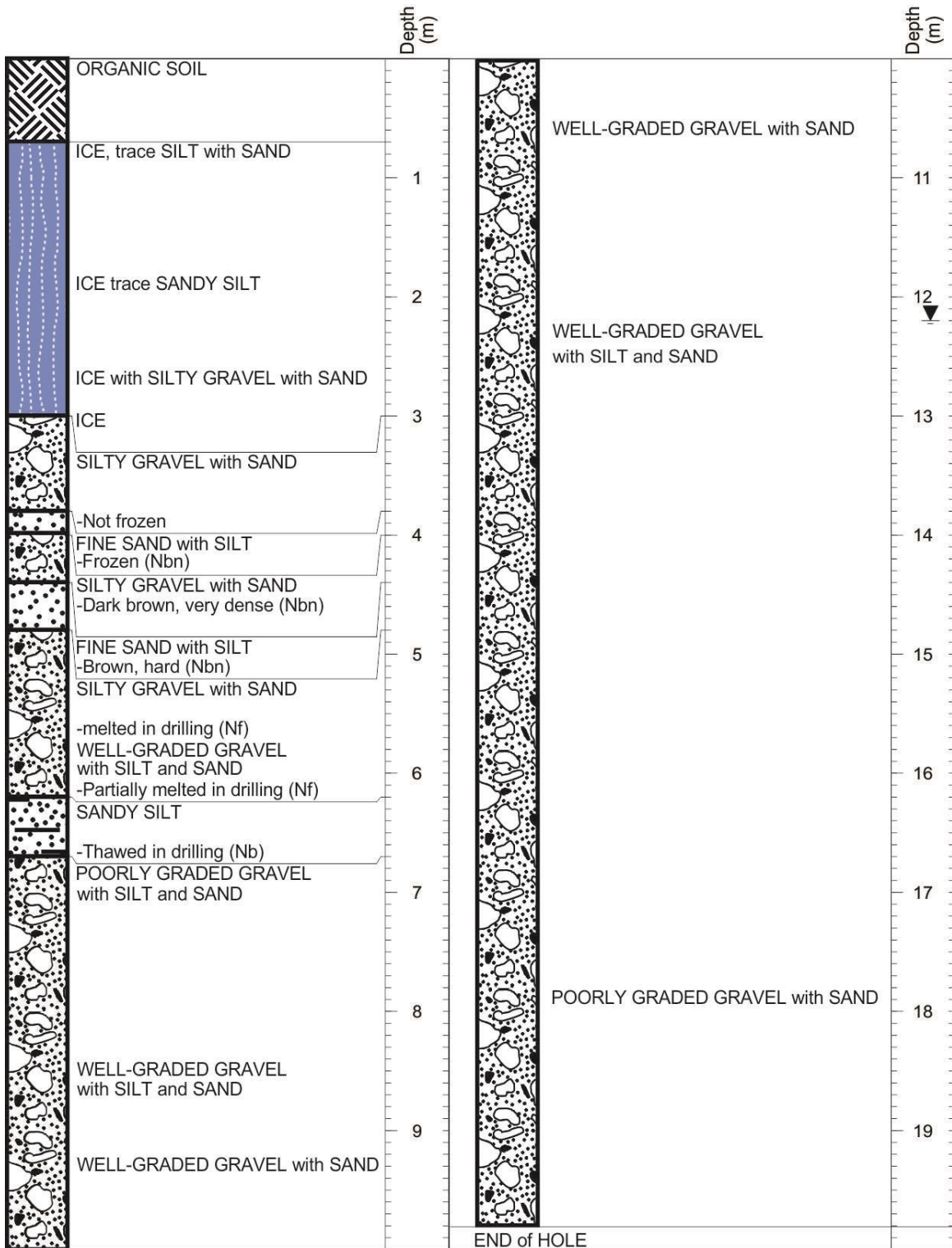
Figure 3.6.6 Log of borehole DH124 – BH 876-5320.
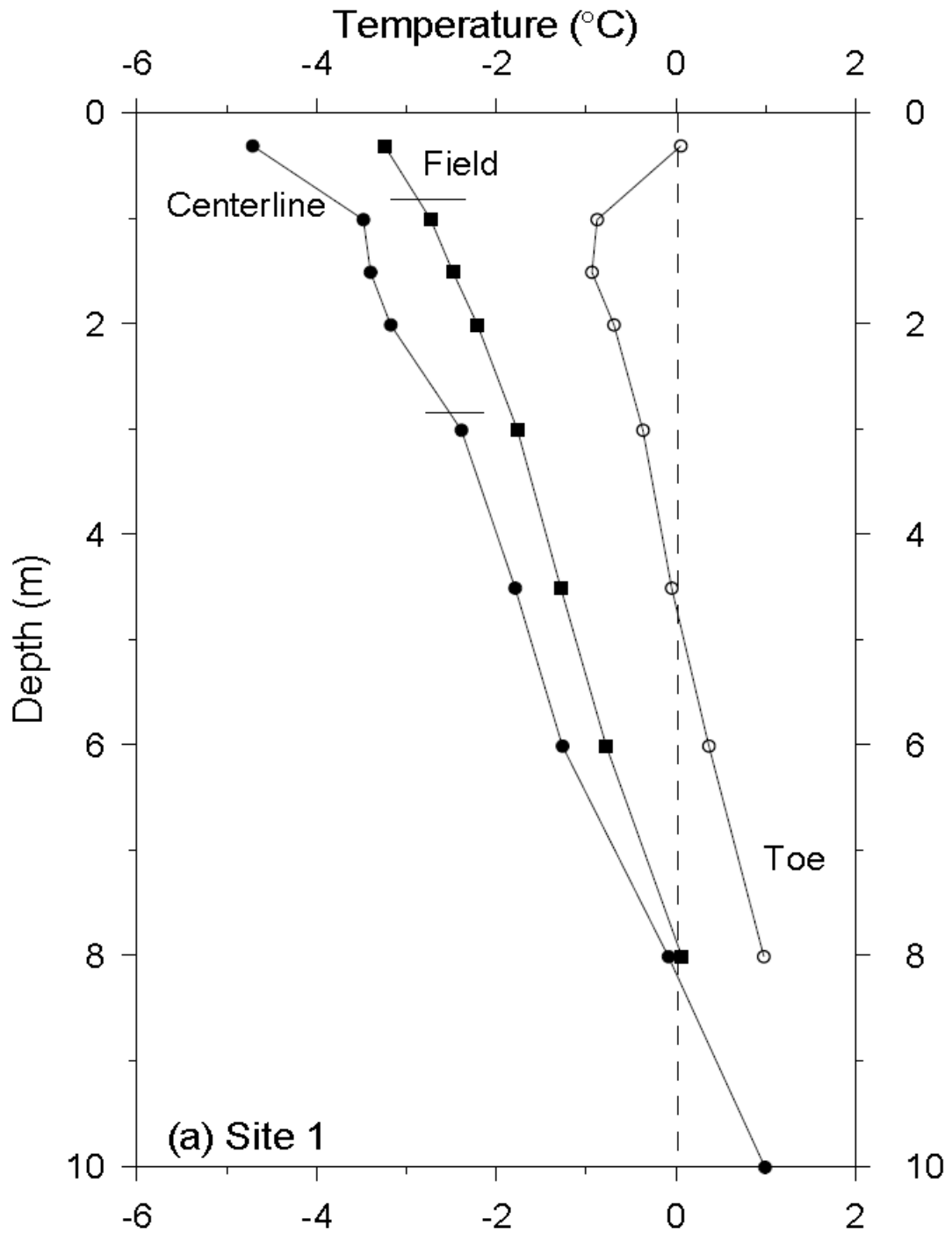
Figure 3.6.7 Annual mean temperature profiles from DH124 for Mar 1st, 2014 – Feb 28th, 2015. Thaw depths are indicated by a horizontal line. Maximum temperatures were > 0 °C throughout the profile at the toe location (from Idrees et al. 2015).
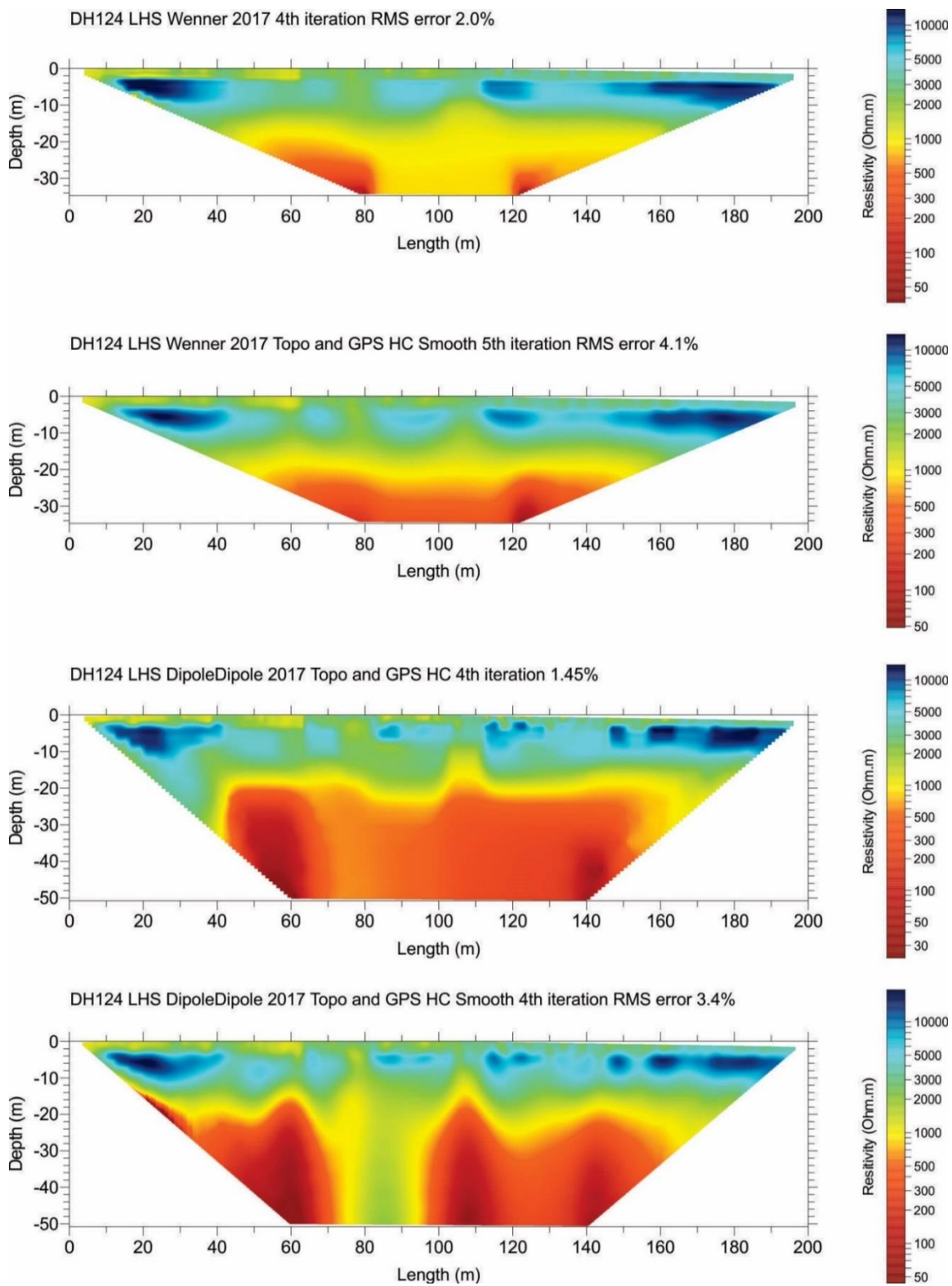
Figure 3.6.8 Wenner and dipole-dipole ERT surveys at site DH124, left-hand side (LHS), using robust and smoothed inversion processes.
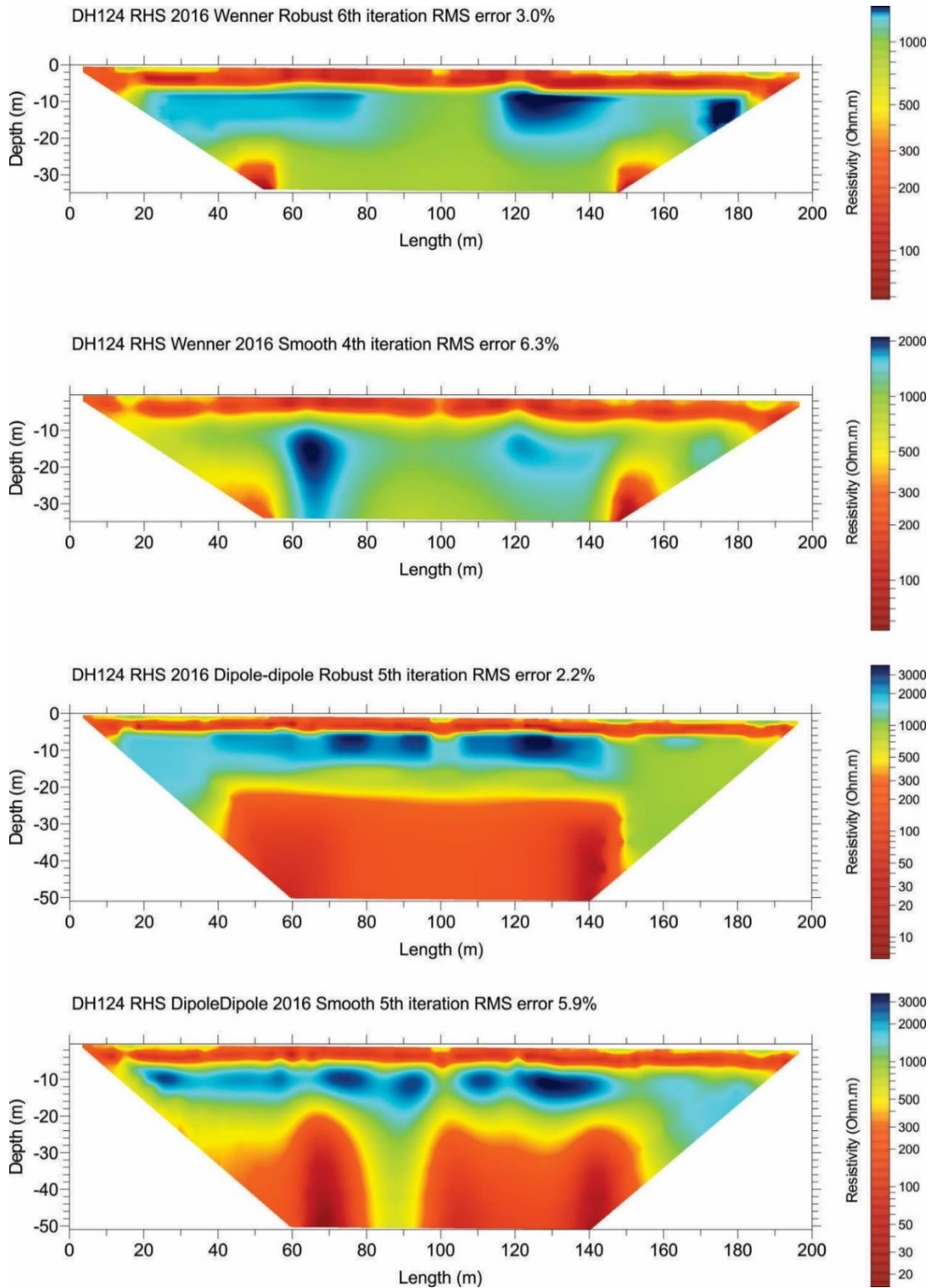
Figure 3.6.9 Wenner and dipole-dipole ERT surveys at site DH124, right-hand side (RHS), using robust and smoothed inversion processes.

3.7   SITE 7: DH126 – KM 126

Issues

- Recurring formation of sinkholes, filled repeatedly

Summary of Findings

- Permafrost is relatively warm in this area (> -1.0 °C), and degrading

- Depressions reflect ice wedge thaw

- Thermokarst ponds are present at the foot of the road embankment and in the RoW

- Permafrost is ice-rich in the top 3m (silt), and this may constitute the entirety of the thaw sensitivity at this site

- Permafrost is likely ice-poor in underlying gravels (below 3m depth), but may have significant fine-sediment

- Fine sediment presents potential for leaching through groundwater movement and may also be a risk for current and future settling at this site.

3.7.1   Introduction

This site is located at km 126 in the Blackstone Uplands only two kilometers north of the Chapman Lake airstrip (km 124).[5] The general issue at this site is the recurring formation of sinkholes, repeatedly filled by HPW. In addition, thermokarst ponds are developing at both sides of the road (Fig 3.7.1). The field survey consisted of one shallow borehole, that was instrumented with a 4-CH Hobo logger. One ERT survey, starting in the field, going on the embankment and finishing in the field was performed at the left-hand side, using both Wenner and Dipole-dipole arrays.

3.7.2   Geology

Site DH126 is in the northernmost portion of the Blackstone Uplands, where the road follows the broad Blackstone River valley (Figure 3.7.2). The surficial materials are mostly glaciofluvial

---

[5] The biophysical context provided in the Report "Investigation of Dempster Highway Sinkholes" (Calmels et al. 2017), still apply to this area (Blackstone Uplands), the report providing an overview comprised between km 74 and km 160. Refer to this report for additional information on general geology and glacial history.

outwash, covered by a veneer of aeolian silt. The site has well developed networks of ice wedge polygons. These are outlined at the ground surface by slight depressions in the covering mosses and lichens.

3.7.3   Aerial imagery/field observation

The surveyed area is show in Figure 3.7.3. The most noticeable feature is the polygonal ground patterns visible in field at the left-hand side of the road. It shows the presence of ice wedges in the whole area. These ice wedges are degrading, which results in the formation of depressions in the troughs, which channelize water and create ponds. Thermokarst ponds are present at the foot of the embankment at the left-hand side, with smaller ones forming in the field, seemingly following the direction of the drainage. A drained lake is observable near the investigation site. The drained lake fills with runoff water during freshet, and drains later in the season when the active layer thickens, opening pathway for the water, likely through the troughs of the ice wedge polygons.

3.7.4   Borehole geotechnical data

The Borehole DH126 BH1 was drilled in the field at the left-hand side, with cores being collected down to 2.66 m depth. The log (Fig. 3.7.4) shows a 1.05 m organic layer interbedded with a gravelly sand at about 0.5 m. Below the organics is a sandy silt, with a volumetric excess ice content ranging from 23 to 68%, down to 2.66 m depth. The mean volumetric excess ice content is 48%. The borehole ends at the contact of an ice-poor gravelly sediment.

3.7.5   Ground temperature

Ground temperatures were recorded from June 5th to September 17th, 2017, the date of the last downloading (Fig. 3.7.5). Although very partial with only 3 months of monitoring, the record shows that from June 15th to September 15th the ground temperature, at the deepest 2.66 m, depth increases from -0.9 to -0.3 °C. The active layer has a thickness of 1.20 m on September 15th. We can hypothesize that permafrost is relatively warm with temperature above -1.0 °C.

3.7.6   ERT survey

Figure 3.7.6 shows both Wenner and dipole-dipole ERT surveys. For each array, two profiles are shown; the first is produced using a robust inversion, and the second one is created with a smoothness constraint in the inversion process. The robust inversion is usually used when sharp boundaries are expected, like in between ice and unfrozen ground; while a smoothness

constraint tends to ensure that the resulting model shows a smooth variation in the resistivity values. This typically produces a model with a larger apparent resistivity RMS error. The results obtained with the Wenner and dipole-dipole arrays are very similar, yet the dipole-dipole shows more details on the vertical boundaries, and robust inversion provides sharper resistivity limits.

The darkest blue colors are the highest resistivity values, and can be interpreted as cold and/or ice rich permafrost. They are mainly concentrated in the south and north ends of the profile. They start between 2 to 5 m depth in the field, but are deeper under the embankment of the road. Note that the profiles are topographically corrected, taking into account the thickness of the road embankment. It can be assumed that the ice wedges are located in the first 3 m of the profile and do not propagate in the gravelly sediment. Without direct observation below 3 m, it can only be assumed that the high resistivity is attributable to an ice-rich, colder, and coarser sediment. The presence of a buried ice body cannot be disregarded.

The reddish areas can be interpreted as thawed, or ice-poor ground which would be consistent with a thickened active layer. There are present in the first few meters, and below 20 m depth. The impact of the road embankment on permafrost clearly appears on the ERT profiles, as in these areas (e.g. 100-150 m), lower resistivity extends down to 8-9 m depth.

3.7.7   Synthesis

Permafrost appears to be relatively warm in this area, and degrading. Some depressions mimicking ice wedge networks are forming, and thermokarst ponds are occurring at the foot of the road embankment as well as in the field.

Borehole logs suggest that the permafrost is ice-rich from the near-ground surface to approximately 3 m depth, in silt. The underlying gravel is assumed to be relatively ice-poor but may contain a significant portion of fine sediment. ERT surveys show that permafrost is even more degraded under the embankment. The darkest blue color is attributable to ice-wedges, and the lighter blue more likely to be frozen gravel. The ERT surveys do not allow for the observation of groundwater movement.

There are no indicators of massive ice bodies within the gravel material, except perhaps in the south end of the profile. The thaw sensitivity of this site may be entirely attributable to the presence of ice wedge complexes in the first 3 meters. It can be assumed that this ice is thawed below the road, and therefore, in the absence of other ice bodies, the subsidence and sinkholes could be attributable to water leaching fine sediment from the gravel, (as is seen at km 82), as the site is located above a drainage path.

Both hypotheses, ice thawing and water seeping may be valid in this site.

Figure 3.7.1 Thermokarst ponds forming at site DH126: A- at Left-hand side; B- at Right-hand side.
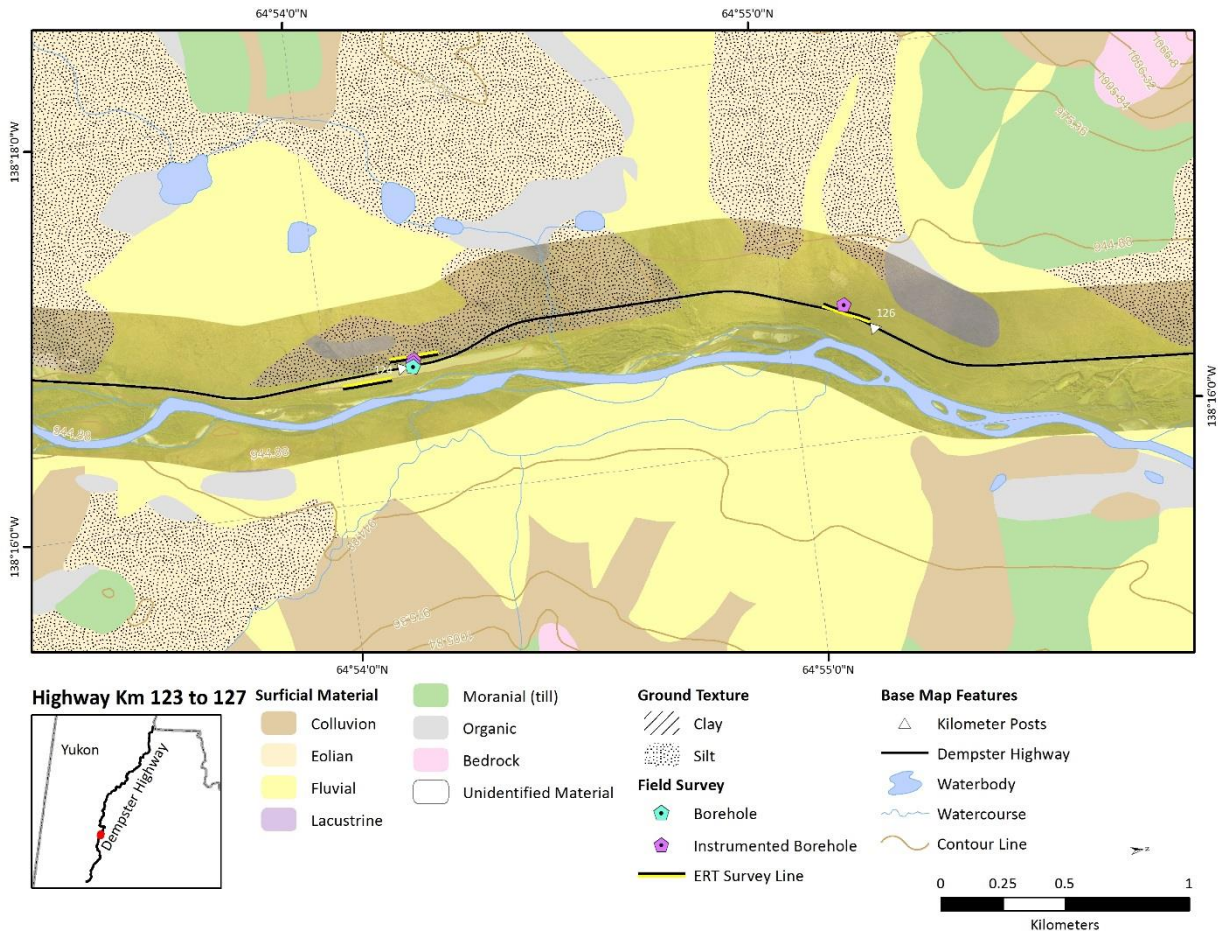
Figure 3.7.2 Surficial geology map of site 7 DH126 area.
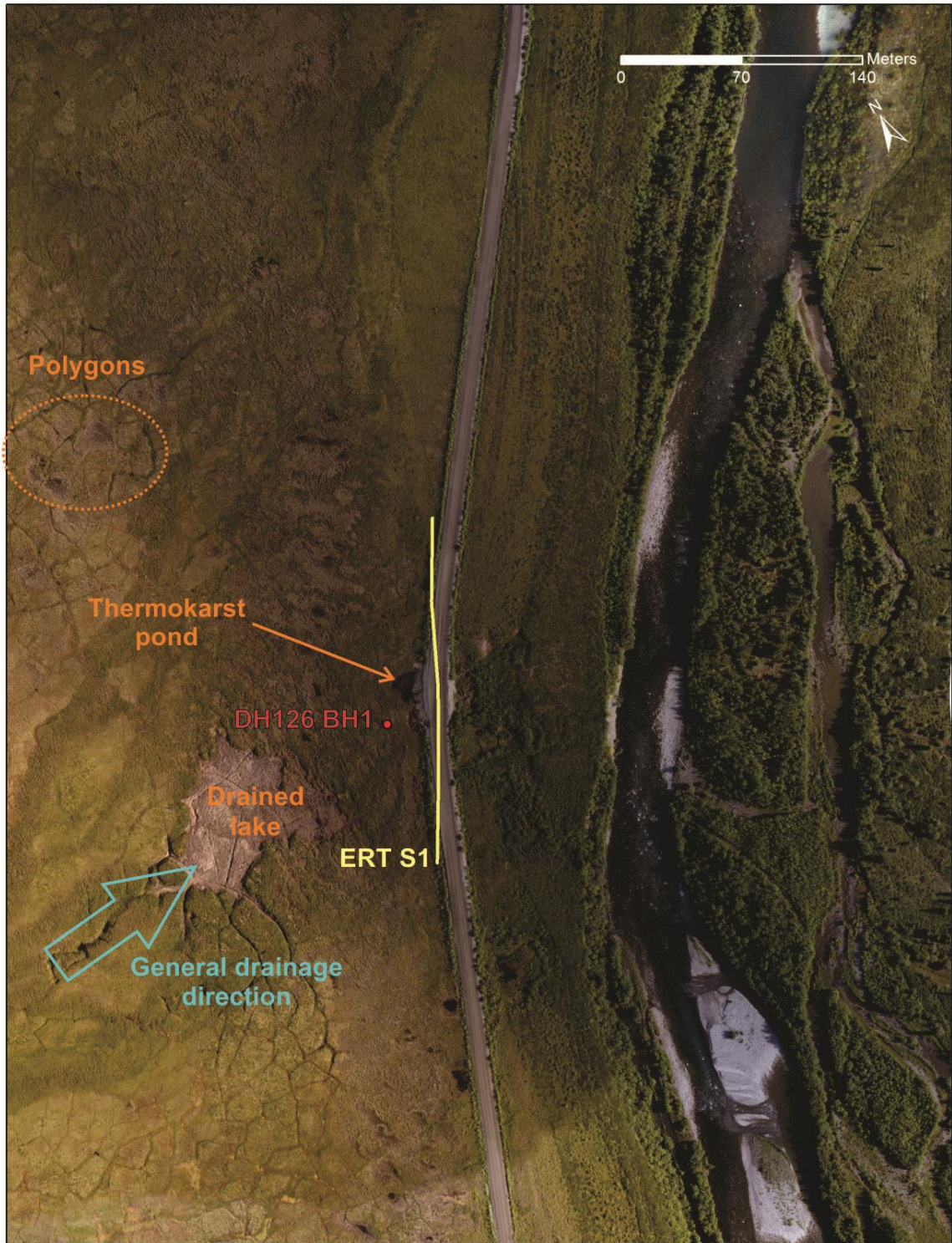
Figure 3.7.3 Aerial view of site DH126.
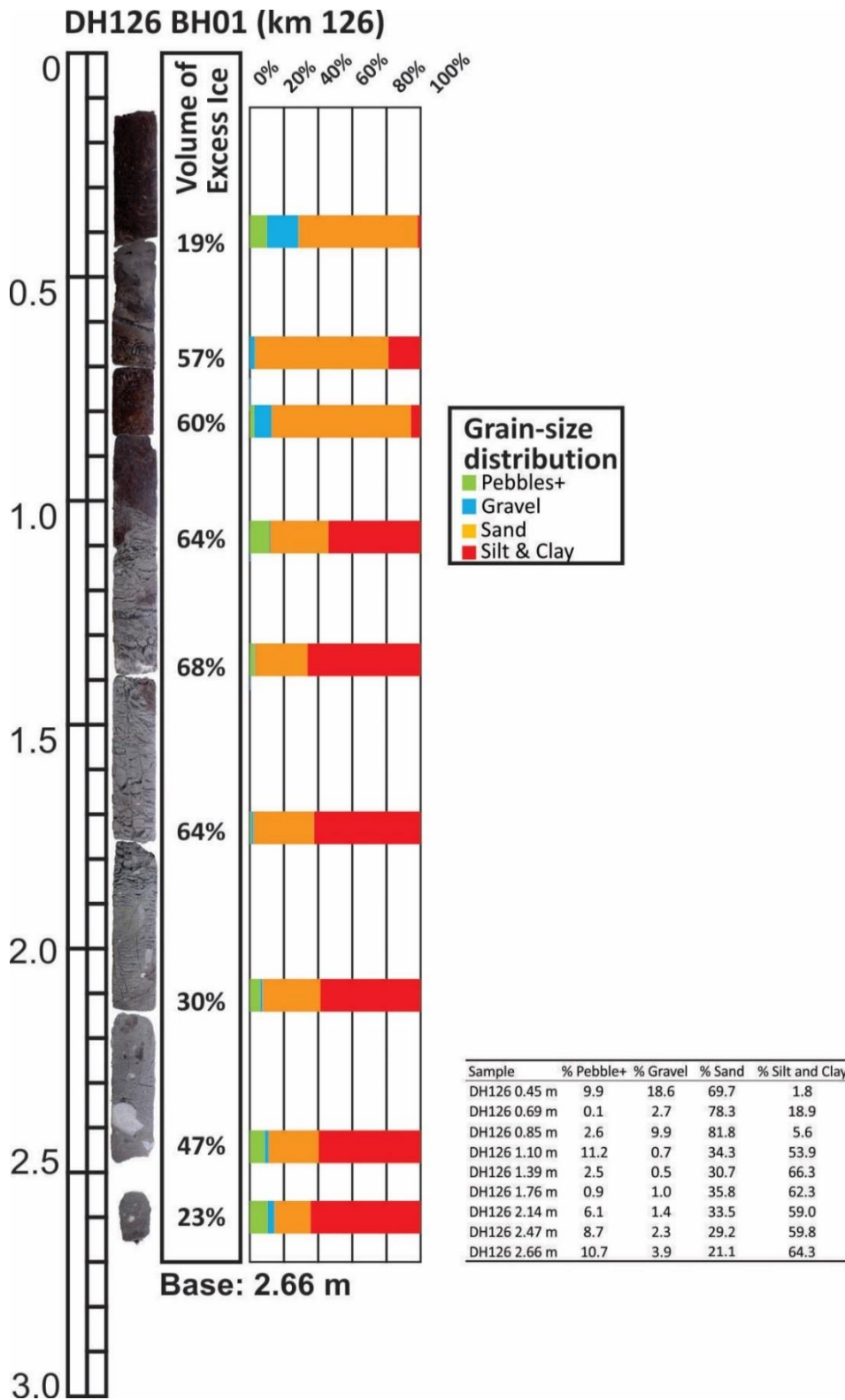
Figure 3.7.4 Log of DH126 BH1, in Field.

Sample	% Pebble+	% Gravel	% Sand	% Silt and Clay
DH126 0.45 m	9.9	18.6	69.7	1.8
DH126 0.69 m	0.1	2.7	78.3	18.9
DH126 0.85 m	2.6	9.9	81.8	5.6
DH126 1.10 m	11.2	0.7	34.3	53.9
DH126 1.39 m	2.5	0.5	30.7	66.3
DH126 1.76 m	0.9	1.0	35.8	62.3
DH126 2.14 m	6.1	1.4	33.5	59.0
DH126 2.47 m	8.7	2.3	29.2	59.8
DH126 2.66 m	10.7	3.9	21.1	64.3
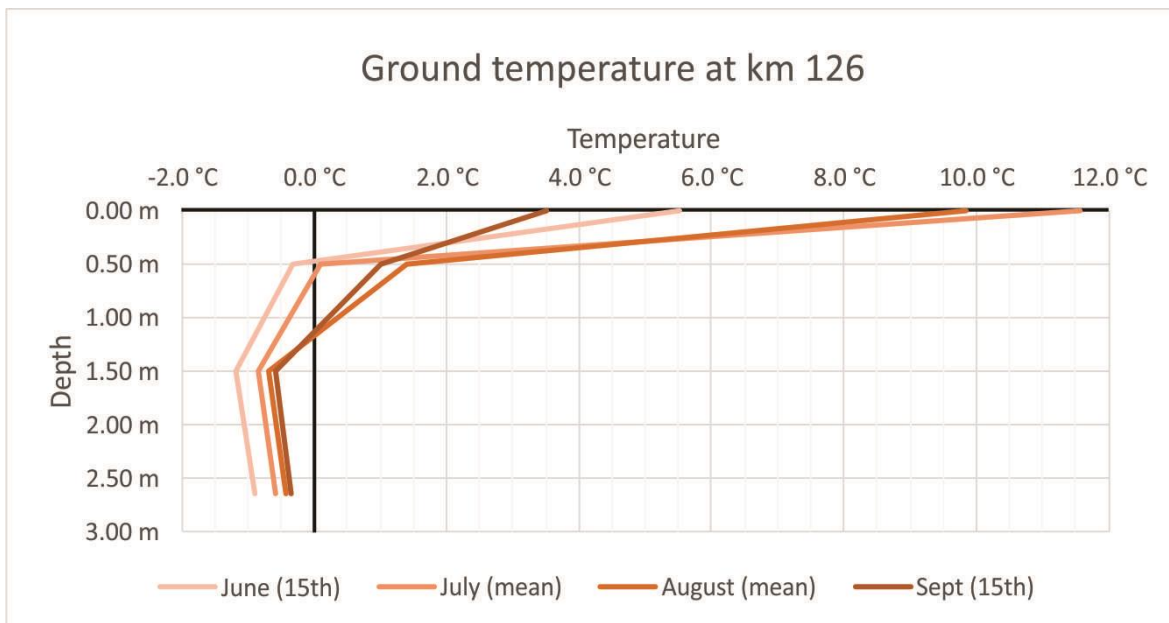
Depth	June (15th)	July (mean)	August (mean)	Sept (15th)
0.00 m	5.5 °C	11.6 °C	9.8 °C	3.5 °C
0.50 m	-0.3 °C	0.1 °C	1.4 °C	1.0 °C
1.50 m	-1.2 °C	-0.9 °C	-0.7 °C	-0.6 °C
2.65 m	-0.9 °C	-0.6 °C	-0.4 °C	-0.3 °C

Figure 3.7.5 Ground temperature from DH126 BH1 from June 15th to September 15th, 2017.
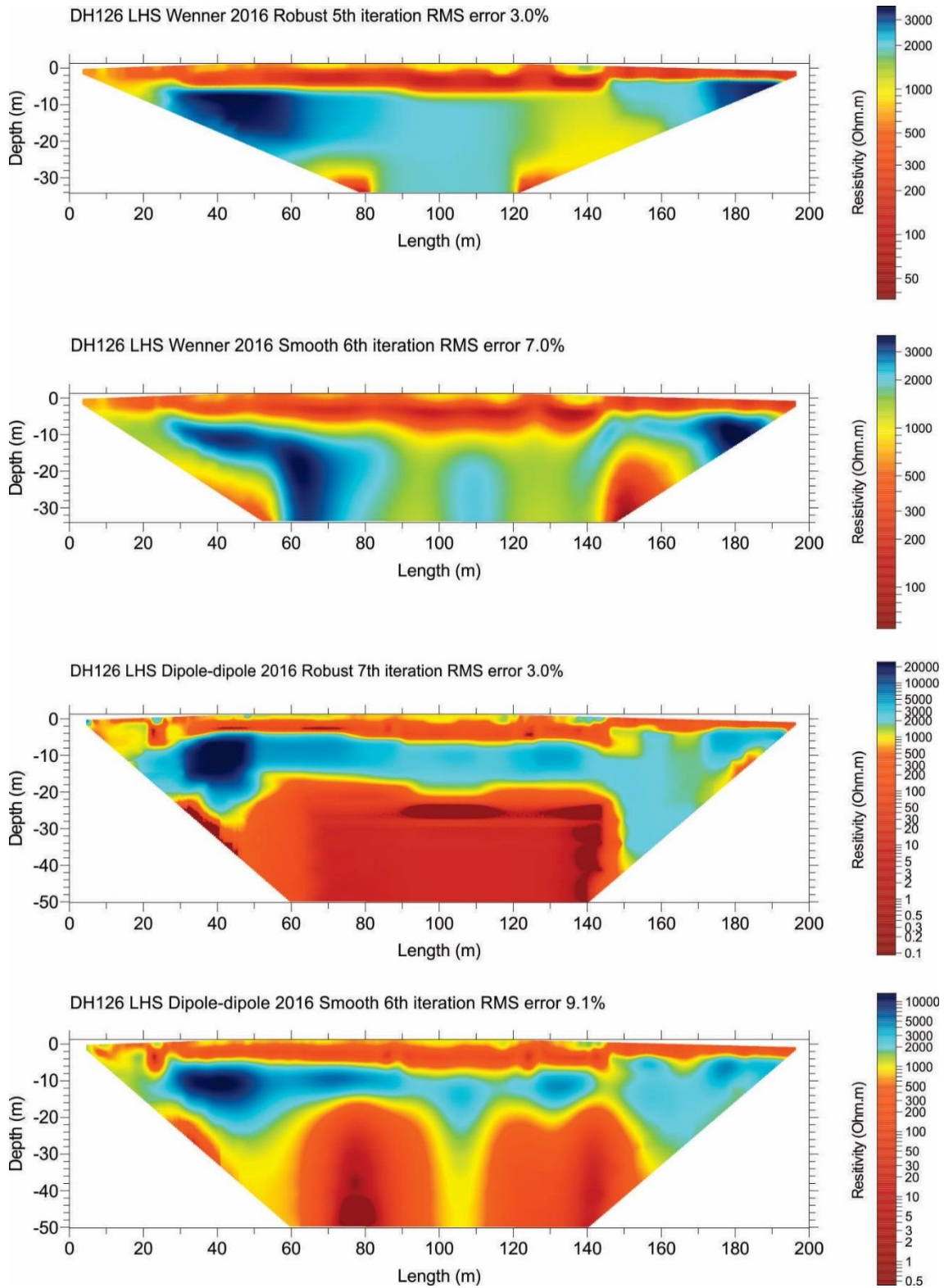
Figure 3.7.6 Wenner and dipole-dipole ERT surveys at site DH126, left-hand side (LHS), using robust and smoothed inversion processes.

3.8   SITE 8: DH192 – KM 192

Issues

- General subsidence and sinkholes

Summary of Findings

- Field observations and surveys suggest groundwater movement and fine material leaching is responsible for subsidence in this area.

3.8.1   Introduction

This site is located at km 192. The physiographic unit is the Engineer/Ogilvie River, which is between km 160 and 246 of the Dempster Highway. The road follows the narrow valleys of Engineer Creek and the Ogilvie River. Surficial material consists of colluvium and alluvium (slope and fluvial deposits).

Mass movement has been identified as the principal geohazard encountered in this area. It can occur in the form of rock falls where the slopes are bare of soil (Burn et al. 2015). Where a surface veneer of soil rests on permafrost, landslides and debris flows may block the road following heavy rain. High discharge and coarse bedload in the streams during freshet and following rain storms may erode the riverbank supporting the highway and bridge abutments, requiring reconstruction of the road bed.

This site was selected because general subsidence and sinkholes have been indicated. As the road seems to be sinking, the presence of holes in the middle of it often has been observed and repaired. The field survey consisted only of an ERT survey following the embankment at the right-hand side, using both Wenner and dipole-dipole arrays. No shallow borehole was drilled for this site.

3.8.2   Geology

The surficial geology map from Yukon Geological Survey shows that the area where the sinkholes occur is located on a fluvial deposit, likely a gravelly sediment (Fig. 3.8.1). However, the road is located at the bottom of a hill slope. On this slope, the surficial material consists of colluvium with a clay. This material is frost susceptible and may extend under the road.

3.8.3   Aerial imagery

There are no noticeable features associated with the presence of ground ice, such as polygonal ground patterns on the aerial imagery (Fig. 3.8.2). However, observation of the image suggests that a lobe of colluvial material may extend under the road embankment. Drainage patterns are visible, extending from the hillslope in direction of an elbow lake within a former river channel.

Field observation suggests that there may be an accumulation of frost susceptible material, from colluvial or fluvial origin, in the field at the right-hand side, close to the southern end of the ERT survey. Water is ponding in the field nearby the centre of the ERT survey, where the sinkholes were reported. Fine, dark brown material, likely an organic rich silt, is visible in the image.

3.8.4   Borehole geotechnical data

No borehole or geotechnical data are available for this section of the road.

3.8.5   Ground temperature

No ground temperature records are available for this section of the road.

3.8.6   ERT survey

Figure 3.8.3 shows both Wenner and dipole-dipole ERT surveys. For each array, two profiles are shown; the first is produced using a robust inversion, and the second is created with a smoothness constraint in the inversion process. The robust inversion is typically used when sharp boundaries are expected, like in between ice and unfrozen ground, while a smoothness constraint tends to ensure that the resulting model shows a smooth variation in the resistivity value, usually producing a model with a larger apparent resistivity RMS error.

The results obtained with Wenner and dipole-dipole array seem inconclusive if we consider that both surveys have relatively high RMS error.

The Wenner survey shows a low-resistivity layer in the first two meters of the profile, followed by higher resistivity below. The southern part of the survey seems more resistive than the northern part. The Wenner and dipole-dipole surveys are very similar, yet the dipole-dipole shows more details in the vertical boundaries and the RMS error is greater. The middle of the

survey length, where the sinkholes are reported, is less resistive, even deeper in the profile. This coincides with a wet area where water is ponding.

3.8.7 Synthesis

Observations carried out in the field, and cautious interpretation of the ERT surveys suggests that the movement of ground water has a major role in the formation of the sinkholes. There are wetlands, yet no obvious indicator of permafrost degradation. This suggests that water seepage and leaching of fine sediment may be responsible of the observed damage.
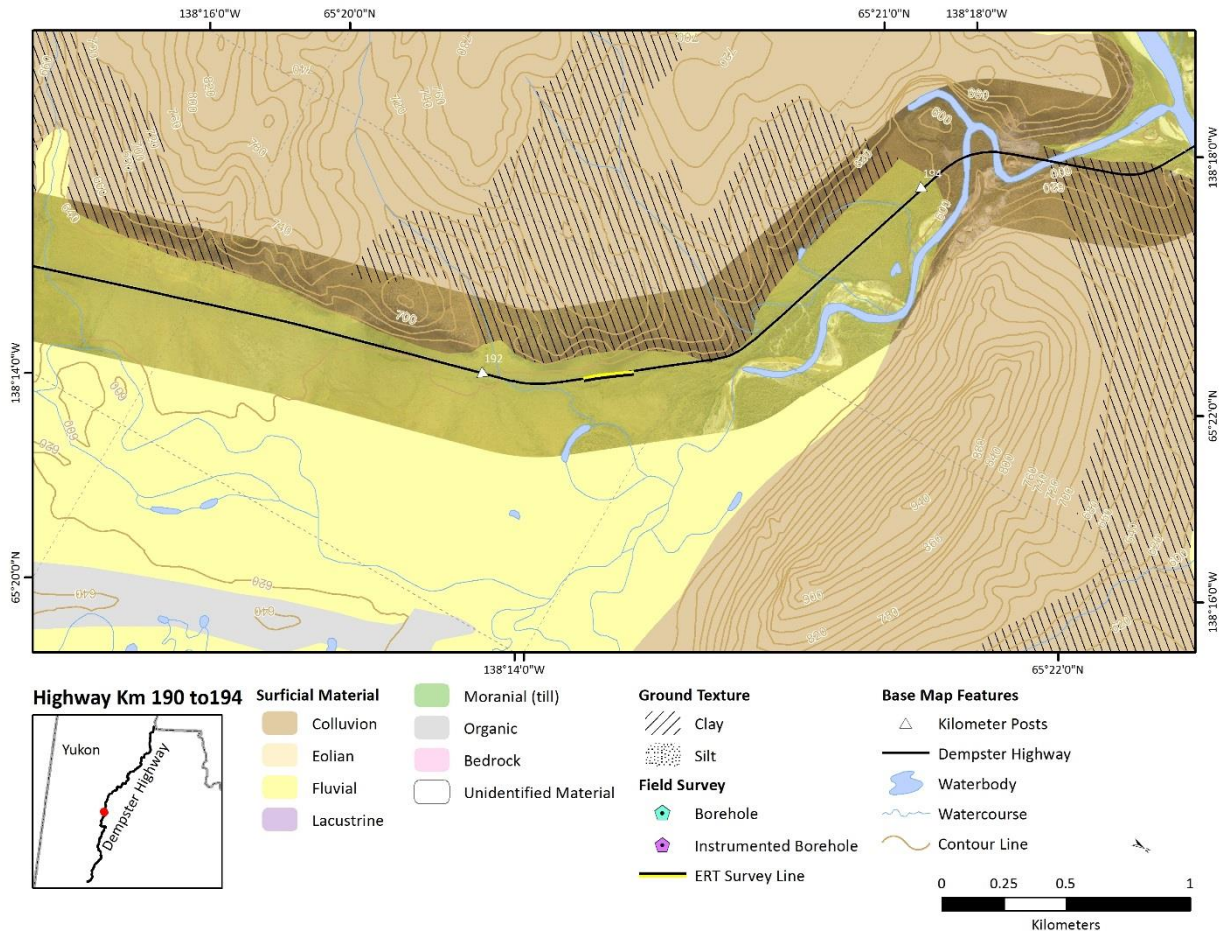
Figure 3.8.1 Surficial geology map of Site 8 DH192 area.
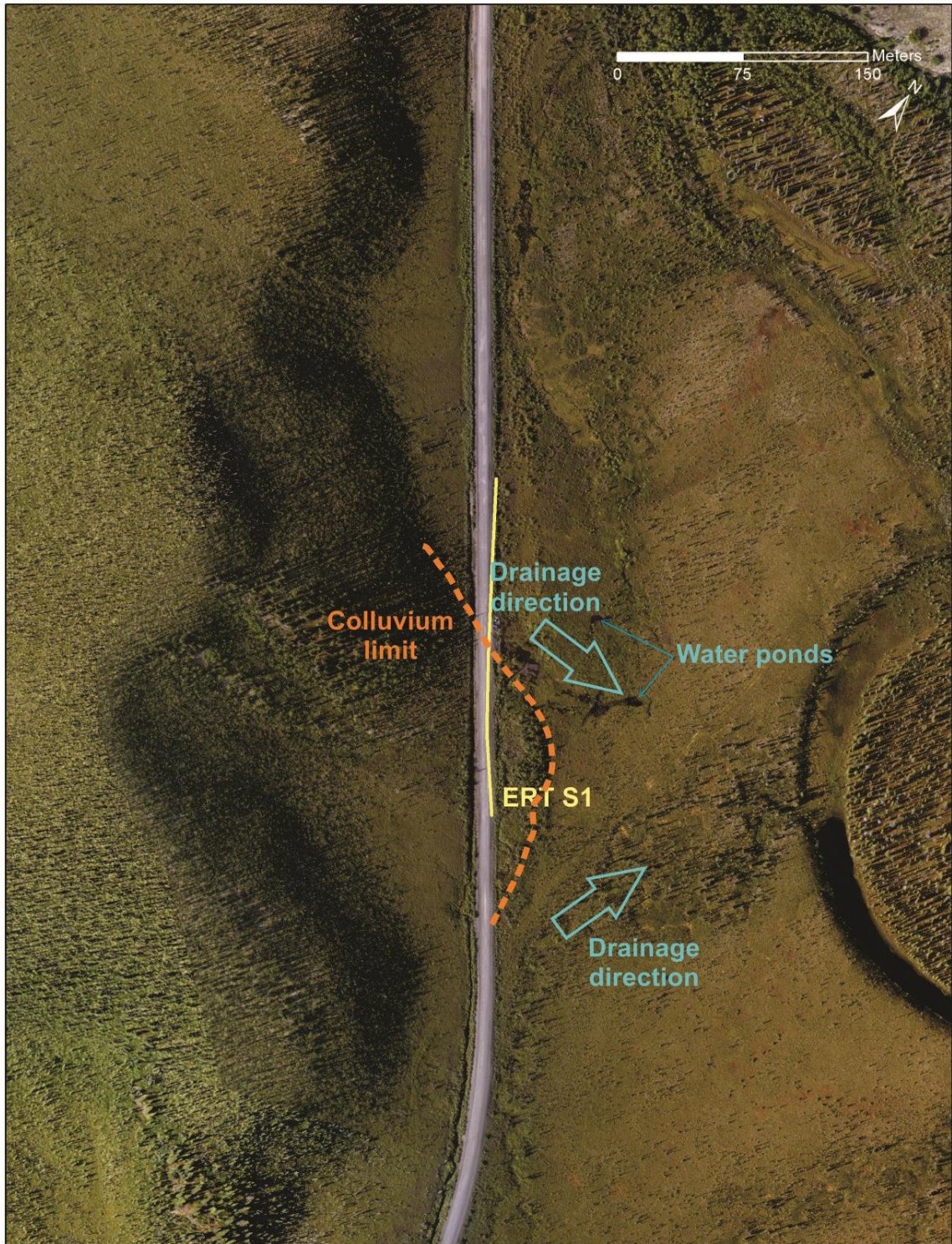
Figure 3.8.2 Aerial view of site DH192.
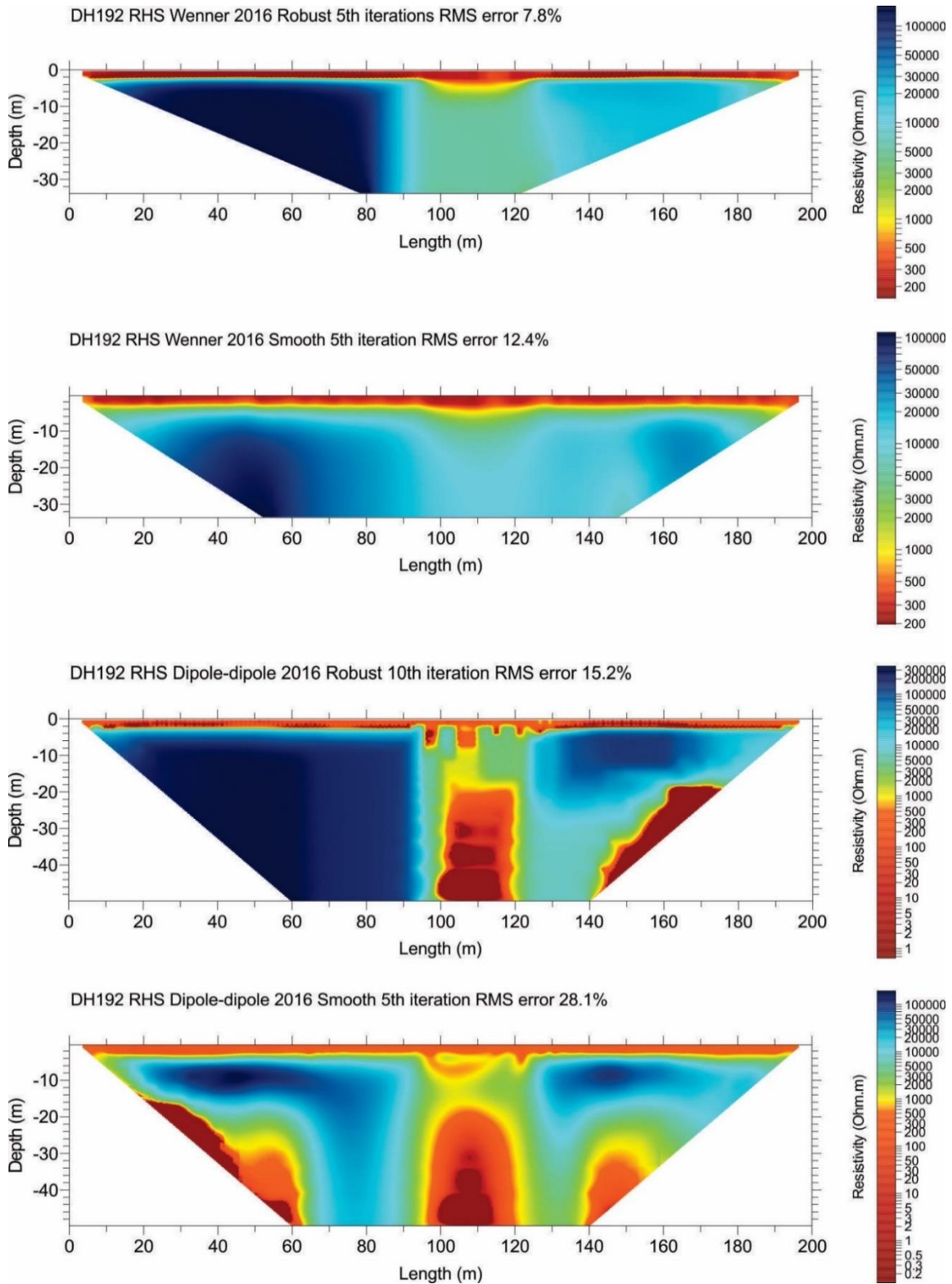
Figure 3.8.3 Wenner and dipole-dipole ERT surveys at site DH192, right-hand side (RHS), using robust and smoothed inversion processes.

3.9   SITE 9: DH375 – KM 375

Issues

- Thermokarst lakes are forming on either side of the highway

- Observed subsidence in the embankment and burying of the culvert

Summary of Findings

- The top 0-10+m of material is fine-grained and ice-rich

- Below 10m the material is coarser, and more ice-poor

- Surface water flow suggests that there may also be groundwater movement in the area, possibly causing the nearby slope failures on the RHS

- Two hazards exist to the highway in this section:

- Subsidence from loss of up to 35-40% of the soil volume with permafrost thaw, more if groundwater movement leaches fine material

- Landslide movement in the direction of the highway

- Roadside drainage remediation should be considered cautiously in order not to exacerbate the adjacent landslide phenomenon

3.9.1   Introduction

This site is located at km 375. The physiographic unit is Eagle Plains, which is between km 246 and 405 of the Dempster Highway. The road follows rolling uplands. Surficial material mostly consists of weathered bedrock (Burn et al. 2015).

Burn et al. (2015) mention that the highway route follows the upper surface of Eagle Plains, and avoids many hazards associated with permafrost due to the shallow soils and absence of water courses. The area around km 375 is an exception, with an abundance of water, and frost-susceptible floodplain deposits. This site was selected because thermokarst lakes are developing on both sides of the road (Fig 3.9.1). Selected late in the 2017 field season, it is unclear yet how it may impact the road, but the embankment seems to be subsiding and burying the culvert.

The field survey consisted of one shallow borehole in the field and one ERT survey using Wenner and Dipole-dipole arrays, both within the field at the right-hand side.

3.9.2   Geology

Based of the surficial geology map from the Yukon Geological Survey, the area were the ponds occur is located at the boundary between a colluvial deposit- a mix of coarse hetero granular material in a fine-grained matrix-, and a fluvial deposit (Fig. 3.9.2). These types of materials are usually coarse in nature and likely not susceptible to frost; yet the fine material contents are variable and can be significant at any location.

3.9.3   Aerial imagery

The aerial imagery of the site shows interesting features related to the presence of permafrost (Fig. 3.9.3). There is a water track, or creek, in the field, at the left-hand side of road that intercepts perpendicularly with the embankment. At the same location, on the opposite side (right-hand side), another pond is forming at the left-hand side foot of the embankment, 50-60 m north to the creek, likely attributable to thaw of ice-rich permafrost. Farther away from the road, at the right-hand side, slides are visible. Some are located as close as 120 m from the road. These cuts display a white, fine-grained sediment; and may be attributable to permafrost thaw.

The aerial imagery assessment of the site suggests the presence of ice-rich ground.

3.9.4   Borehole geotechnical data

Borehole DH375 BH1 was drilled in the field at the right-hand side; cores being collected down to 6.0 m depth. The thaw front was at 30 cm depth at the time of the drilling (July 5th, 2017). The log (Fig. 3.9.4) shows a 1.30 m organic layer followed by a gray sandy-silt alternating with some sandier levels. The borehole ends at 6 m in the ice-poor gravelly sediment, the end of the borehole. Centimeter-scale ice lenses are visible all along the profile in the silty material, with volumetric excess ice content ranging from 14 to 57%. Overall, the borehole has a mean volumetric excess ice content of 37%, which represents a potential subsidence of 2.22 m if permafrost were to thaw.

3.9.5 Ground temperature

Borehole DH375-BH1 was lined with PVC piping and instrumented with two 4-channel Hobo loggers to record ground temperatures at 0, 0.5, 1.0, 2.0, 3.0, 4.0, 5.0 and 6.0 m depths. Ground temperature were recorded from July 5th to September 17th, 2017, the date of the last downloading (Fig. 3.9.5). Although very partial with only two months of monitoring, the record shows that from July 15th to September 15th, the ground temperature at the deepest (6.0 m) point remains relatively stable between -1.2 and -1.1 °C. The active layer had a thickness of 90 cm on September 15th. The permafrost is relatively warms with temperatures above -2.0 °C.

3.9.6 ERT survey

Figure 3.9.6 shows both the Wenner and dipole-dipole ERT surveys. For each array, two profiles are shown. The first is produced using a robust inversion, and the second is created with a smoothness constraint in the inversion process. The robust inversion is usually used when sharp boundaries are expected, like in between ice and unfrozen ground, while a smoothness constraint tends to ensure that the resulting model shows a smooth variation in the resistivity values, typically producing a model with a larger apparent resistivity RMS error.

The results obtained with the Wenner and dipole-dipole arrays mainly show a similar distribution of resistivity in the ground, yet the dipole-dipole shows more details relative to the low resistivity areas.

In the Wenner array, high resistivity values (blue shades), are present all along the profile between approximately 2 and 10 m in depth. The depths are variable, and the thickest high resistivity layer is observable at both end of the profile. The lowest resistivity values (reddish shades), are located deeper in the profile, in the approximate middle of the survey. This is consistent with the positioning of the ERT survey with the thermokarst pond area located in the middle. The observed low-resistivity could be from the thermal effect of the water body as well as underground water movement lowering the resistivity values in this area.

In the dipole-dipole array, high resistivity values are also present all along the profile between 2 and 10 m depths, but are better defined. The depths are variable, and the thickest high-resistivity layer is especially prominent at the north end of the profile, where they reach 12-14 m. The lowest resistivity value areas, are located deeper in the profile, and are better defined than in the Wenner array. Some distinct low-resistivity bodies are apparent, generally located close to the thermokarst pond area but with one additional low-resistivity body at the south end.

Overall, the high-resistivity areas are attributable to ice-rich ground with fine material; they decrease where the soil is gravellier and therefore ice-poor. If lower resistivity values could be attributable to ice poor and/or unfrozen material such as gravel and bedrock, the lowest resistivity values could indicate the presence of unfrozen underground water, passing between permafrost above and bedrock below.

3.9.7   Synthesis

The borehole and ERT data are consistent with each other. Both show the presence of fine-grained, ice-rich material from the surface to a depth that could exceed 10 m around the borehole location (north end of the profile). At greater depth, the ground becomes coarser and more ice-poor.

If water flows at the surface level, it seems likely that some groundwater seepage may also occur. Groundwater could be responsible for the landslides occurring on the hillslope at the right-hand side.

Two hazards threaten the road in this location:
1- subsidence due to permafrost thaw in the order of 35-40% of permafrost thickness, or more if underground water movement leaches sediment;
2- 2- landslide movement in the direction of the highway.

While the slumps still are located at more than 100 m from the road; drainage remediation should be considered cautiously so as not to exacerbate the phenomenon.
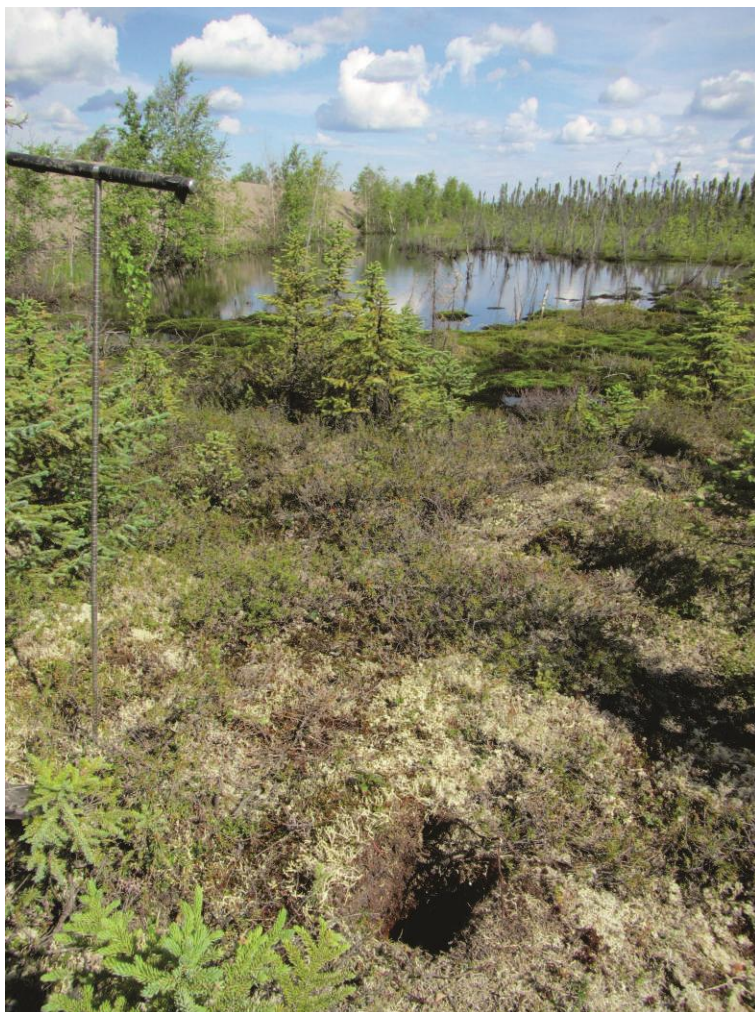
Figure 3.9.1 Thermokarst pond along right-hand side at site DH375 (view from the field).
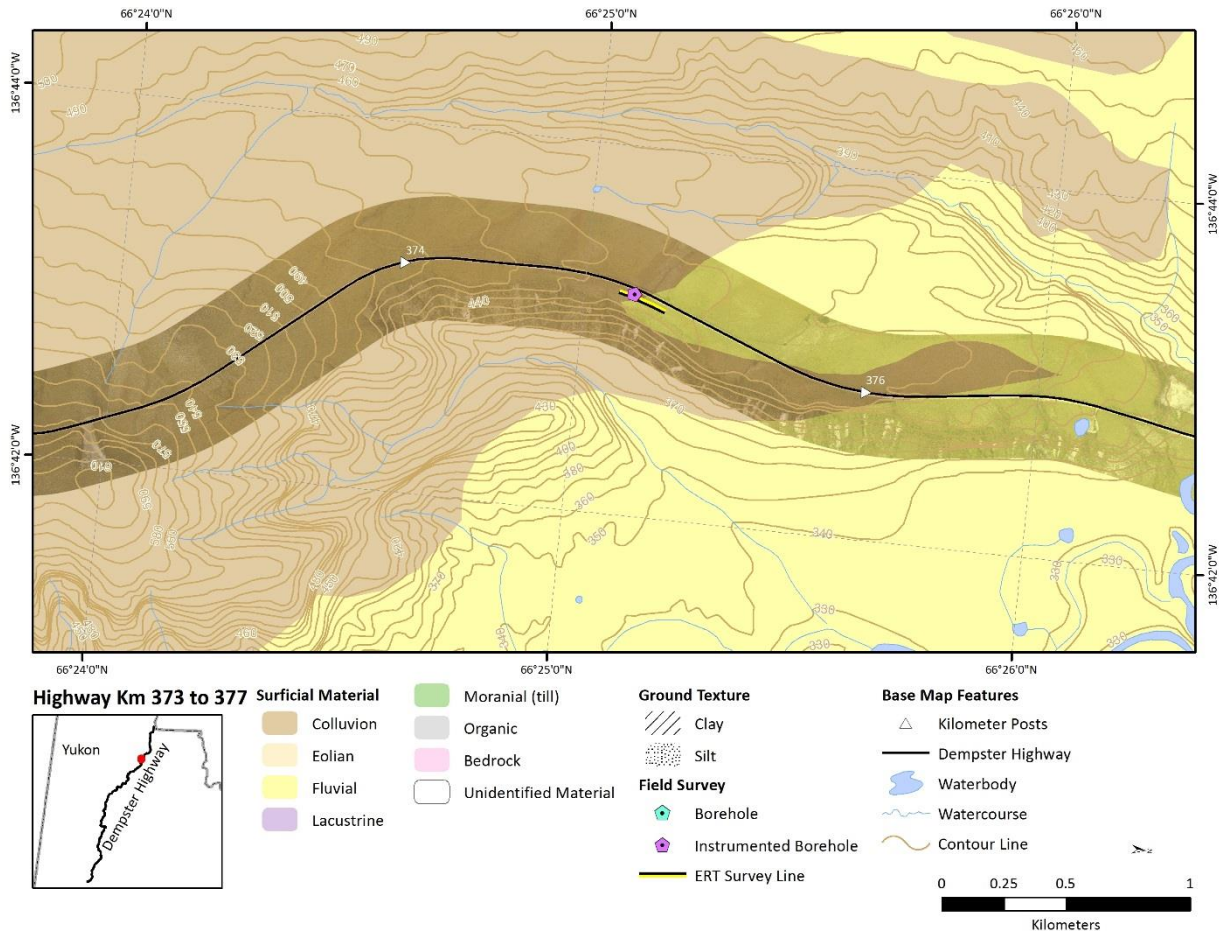
Figure 3.9.2 Surficial geology map for the Site 9 DH375 area
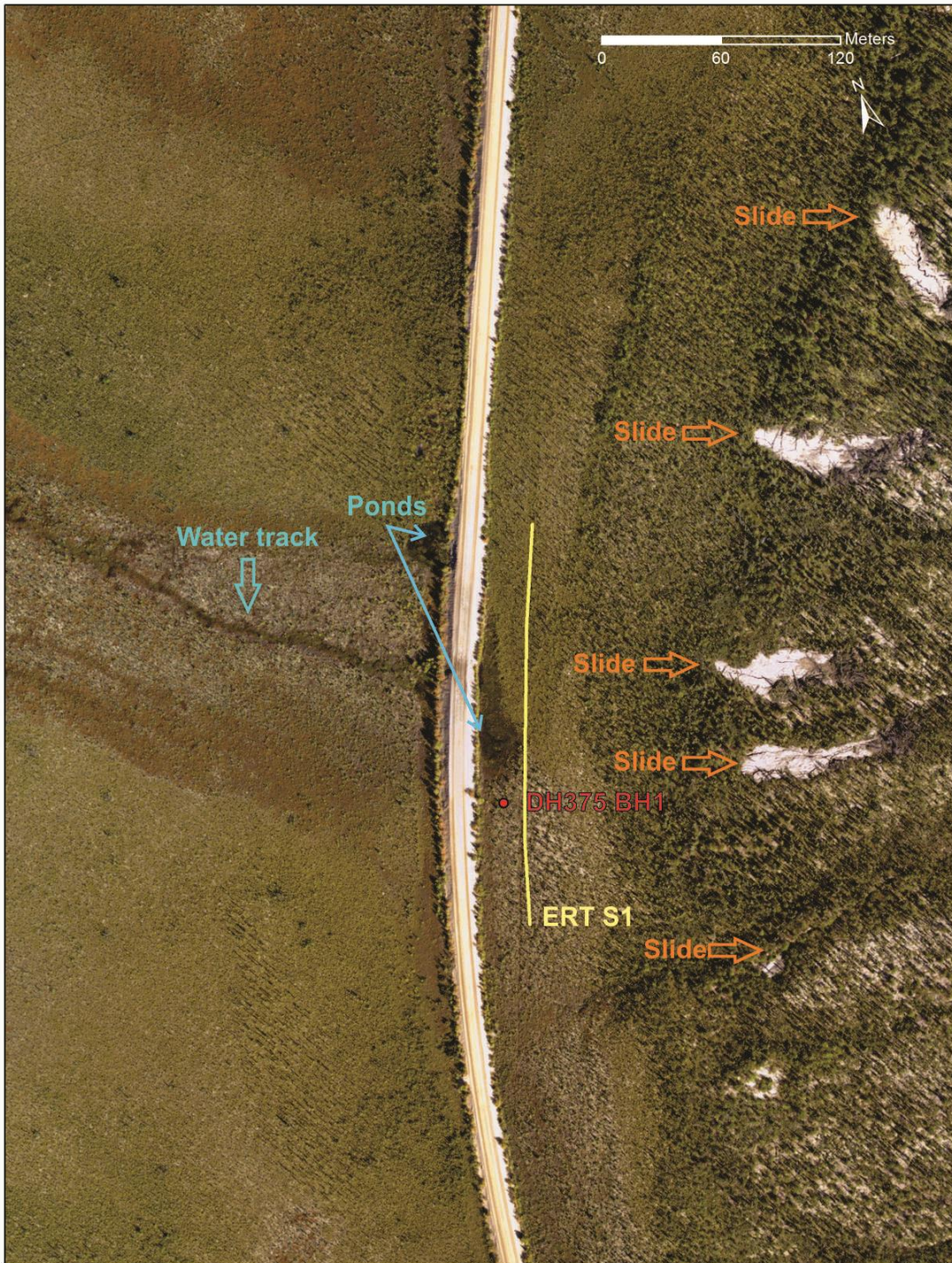
Figure 3.9.3 Aerial view of site DH375
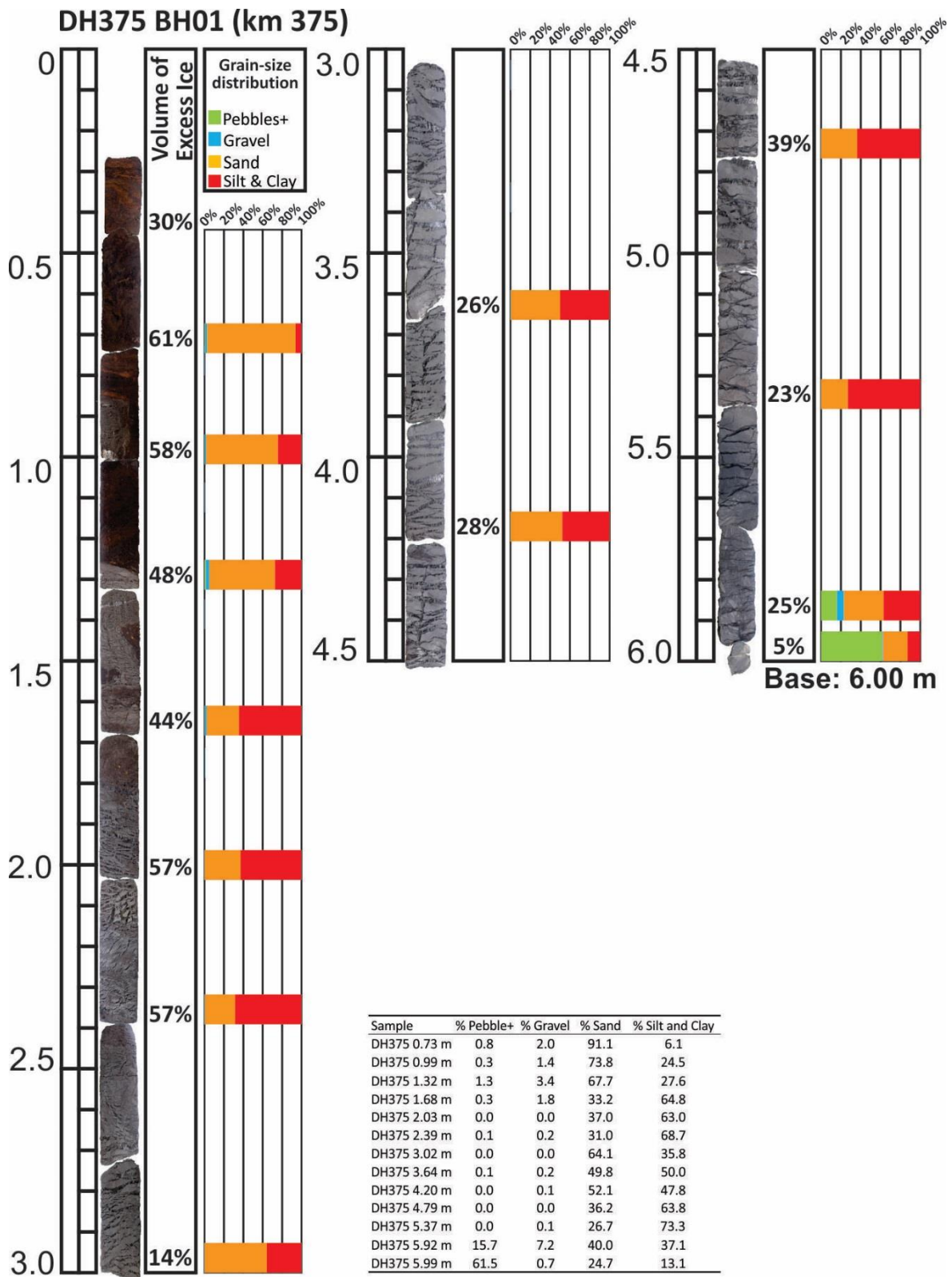
Figure 3.9.4 Log of borehole DH375 BH1, with volumetric excess ice content and grain size distribution.

Sample	% Pebble+	% Gravel	% Sand	% Silt and Clay
DH375 0.73 m	0.8	2.0	91.1	6.1
DH375 0.99 m	0.3	1.4	73.8	24.5
DH375 1.32 m	1.3	3.4	67.7	27.6
DH375 1.68 m	0.3	1.8	33.2	64.8
DH375 2.03 m	0.0	0.0	37.0	63.0
DH375 2.39 m	0.1	0.2	31.0	68.7
DH375 3.02 m	0.0	0.0	64.1	35.8
DH375 3.64 m	0.1	0.2	49.8	50.0
DH375 4.20 m	0.0	0.1	52.1	47.8
DH375 4.79 m	0.0	0.0	36.2	63.8
DH375 5.37 m	0.0	0.1	26.7	73.3
DH375 5.92 m	15.7	7.2	40.0	37.1
DH375 5.99 m	61.5	0.7	24.7	13.1

A Summary of Climate- and Geohazard-Related Vulnerabilities for the Dempster Highway Corridor

Depth	July (15th)	August (mean)	September (15th)
0.00 m	14.2 °C	12.5 °C	6.8 °C
0.50 m	0.1 °C	2.0 °C	1.6 °C
1.00 m	-0.5 °C	-0.3 °C	-0.2 °C
2.00 m	-0.9 °C	-0.8 °C	-0.6 °C
3.00 m	-1.1 °C	-1.0 °C	-0.9 °C
4.00 m	-1.2 °C	-1.1 °C	-1.0 °C
5.00 m	-1.2 °C	-1.2 °C	-1.1 °C
6.00 m	-1.2 °C	-1.2 °C	-1.1 °C

Figure 3.9.5 Ground temperature at site DH375, based on a record from July 15th to September 15th, 2017.
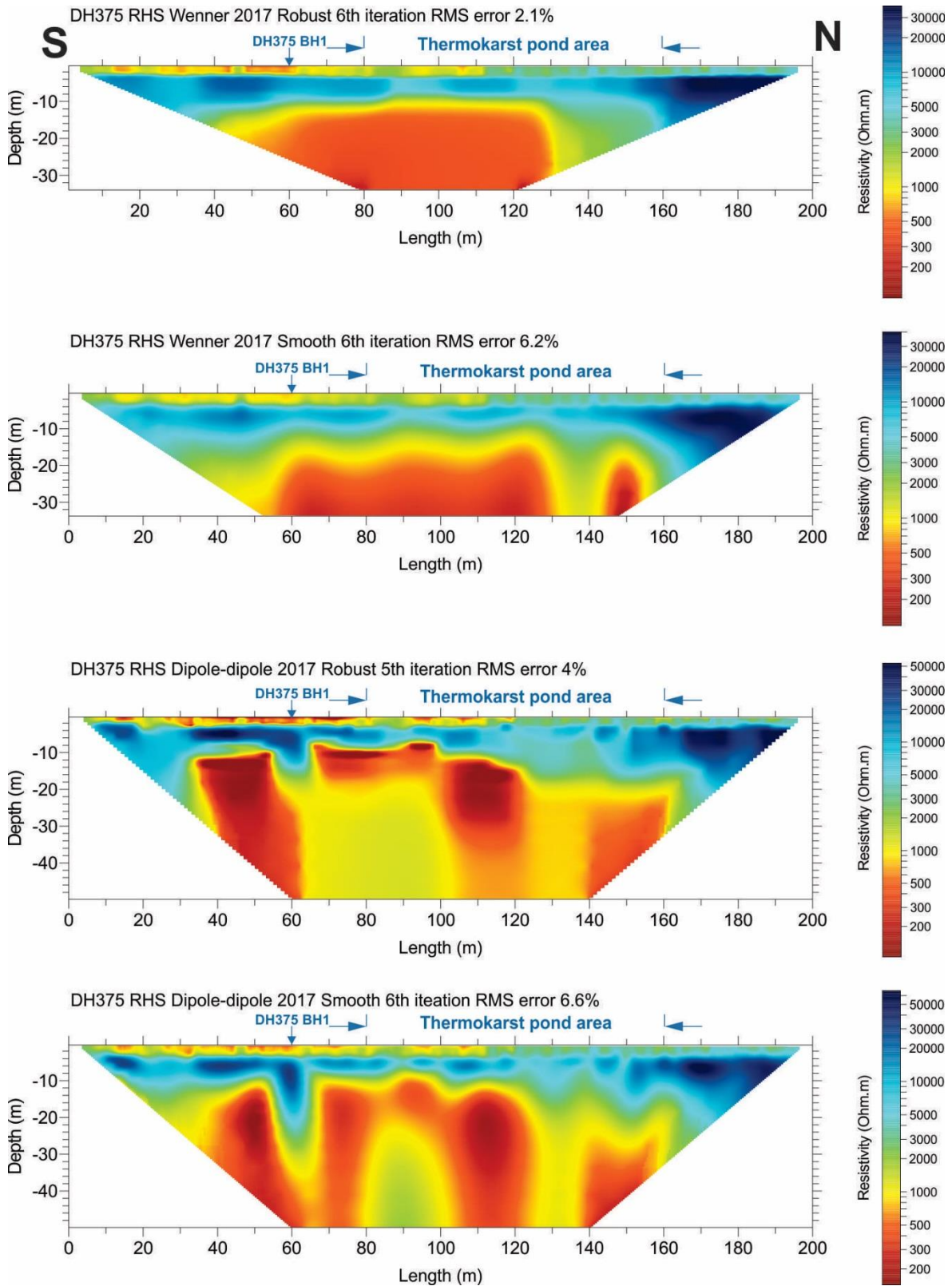
Figure 3.9.6 Wenner and dipole-dipole ERT surveys at site DH375.

3.10   SITE 10: DH381 – KM 381

Issues

- This is the site of a recent insulated culvert installation, which will be monitored via a ground temperature array.

Summary of Findings

- DH 381 has geotechnical similarities to the previous site DH 375, but has warmer permafrost and likely little thermal resiliency to warming influences.

3.10.1   Introduction

This site is located at km 381. The physiographic unit is Eagle Plains, which is between km 246 and 405 of the Dempster Highway. The road follows rolling uplands. Surficial material mostly consists of weathered bedrock (Burn et al. 2015).

Burn et al. (2015) mention that the highway route follows the upper surface of Eagle Plains, and avoids many hazards associated with permafrost due to the shallow soils and absence of water courses. The area around km 381 is an exception, with an abundance of water, and frost-susceptible floodplain deposits. Originally, this site was not selected because the potential geohazard had been reported on already by HPW. Previously, thermal monitoring below the embankment was implemented at this site when a new culvert was installed (Fig 3.10.1). The monitoring aims to evaluate the efficiency of insulating foam positioned between the natural ground and the culvert, in mitigating the heating effect of the culvert on permafrost. For this purpose, a ground temperature monitoring array was installed below and above the foam, under the culvert. In addition, a borehole was waterjet-drilled in the field to provide undisturbed ground temperature data.

The field survey consisted of visual observation of permafrost during installation of the new culvert, and the shallow borehole in the field, at the left-hand side of the road from which the permafrost cores were collected. No ERT survey was done at this location.

3.10.2   Geology

Based of the surficial geology map from the Yukon Geological Survey, the area where the culvert is located is in a colluvial deposit, a mix of coarse hetero granular material in a fine-grained matrix (Fig. 3.10.2). These types of materials are usually coarse in nature but the fine material content can be significant. The geological map points out the presence of clay with the colluvium, all around the studied site.

3.10.3   Aerial imagery

The site is located in the lower part of a small valley. Two interesting features providing information about the geomorphic context can be seen in the aerial imagery (Fig. 3.10.3). First are some mud boils (AKA Frost boils), which are upwellings of mud that occur through frost heave and cryoturbation in permafrost areas. A swarm of them is visible about 100 m into the field at the left-hand side of the road. These are good indicators of a fine-grained, frost-susceptible material, i.e. potentially ice-rich ground. Second, a small slide is visible on the slope about 70-80 m from the road, at its right-hand side. While less developed, this slide is like those observed at site DH375.

Permafrost was directly observed during installation of the culvert, when the excavation extended below the road embankment. The ground was fine-grained and ice-rich, quite similar the sample collected at site DH375 (Fig. 3.10.4).

3.10.4   Borehole geotechnical data

The Borehole DH381 BH1 was drilled in the field at the right-hand side using a waterjet drill; no cores were collected. The borehole was easy to drill down to the depth of 4.55 m, within fine-grained material; after 4.55m the drilling was unable to continue, likely due to the presence of coarser material.

3.10.5   Ground temperature

Borehole DH381-BH1 was lined with PVC piping and instrumented with one 4-channel Hobo logger to record ground temperatures at 0, 1.0, 2.0, and 4.55 m depths. Ground temperatures were recorded from September 29th, 2016 to September 17th, 2017, the date of the last downloading (Fig. 3.10.5). Although the records only cover just under a year, the data show that during this period the ground temperature measured at 4.55 m, the deepest sensor depth, remains relatively stable at -0.2 °C. The depth of the active layer almost reached 4.55 m in

August 2017. While the permafrost may still be recovering from the drilling process, this is attributable to very warm ground temperature, close to 0 °C.

3.10.6   ERT survey

No ERT surveys were performed on site, except of the test survey performed below the culvert.

3.10.7   Synthesis

The site DH381 shares similarities with site DH375, such as fine-grained and ice-rich material in the first 5-6 m of the ground profile.

However, DH381 has a very warm permafrost, 1 °C above DH375, with ground temperature close to 0 °C, and consequently has very limited, possibly even no thermal resiliency to climate warming or other thermal disturbance. This difference could be because DH375 is located at a hillcrest, on a plateau, while DH381 is in a small valley bottom, on its south facing hillslope.

Figure 3.10.1 Culvert at site DH381.
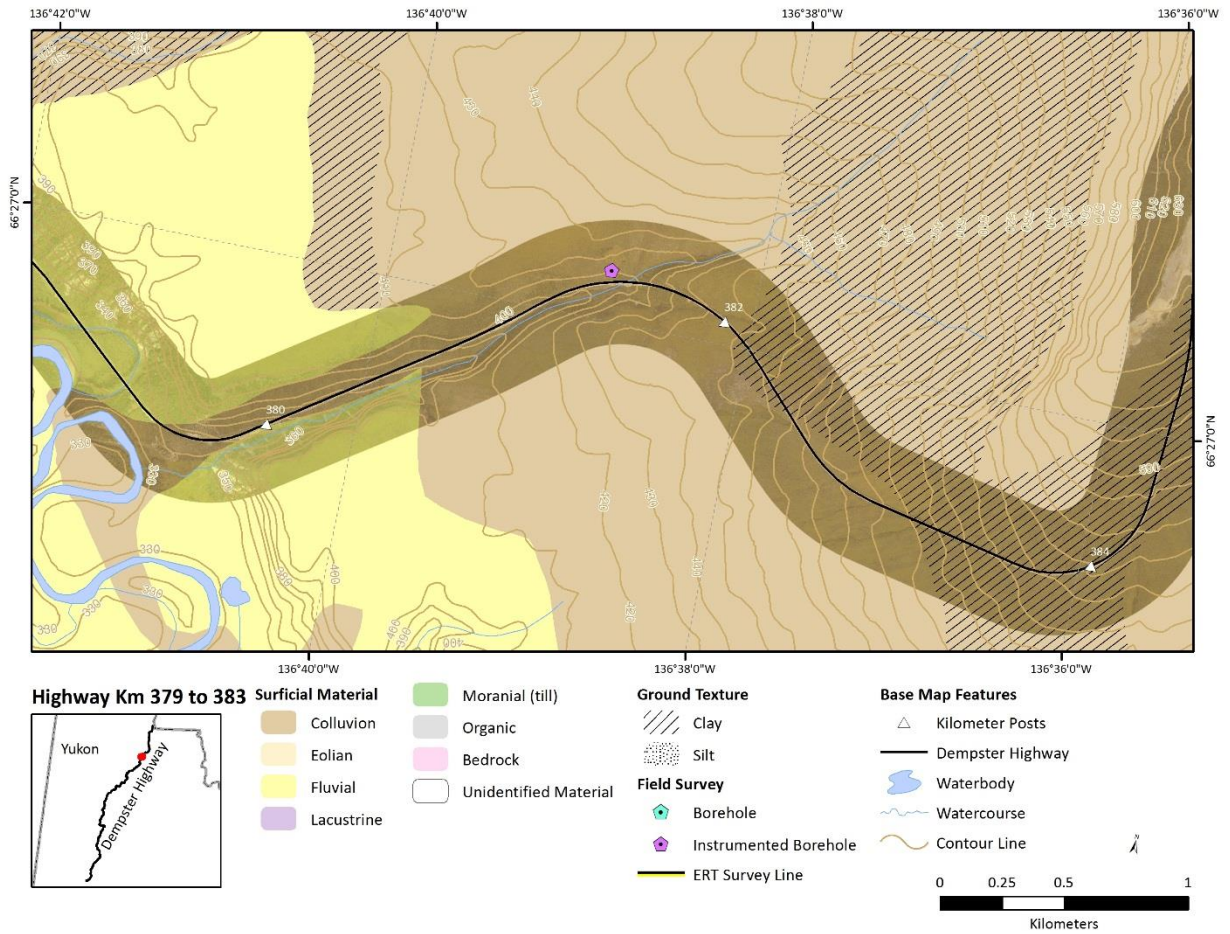
Figure 3.10.2 Surficial geology map for the Site 10 DH381 area

Figure 3.10.3 Aerial view of site DH381.

Figure 3.10.4 Permafrost observed during culvert installation at site DH381. A- ice-rich fine grained soil excavated below the embankment; B- close-up of an ice-rich permafrost sample collected during the excavation works

Ground temperature at km 381
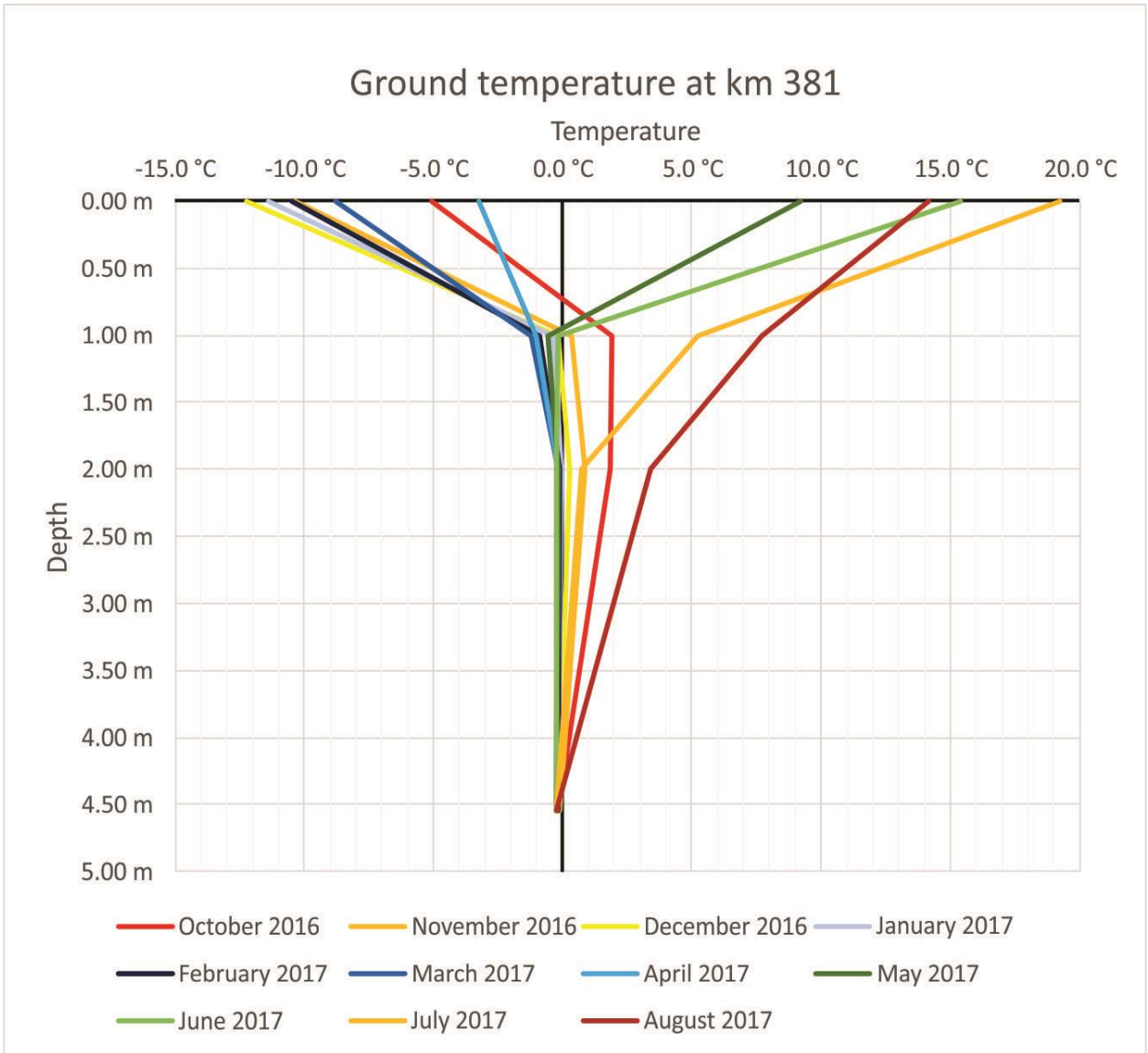
Depth	2016			2017							
	October	November	December	January	February	March	April	May	June	July	August
0.00 m	-5.1 °C	-10.4 °C	-12.2 °C	-11.4 °C	-10.5 °C	-8.8 °C	-3.3 °C	9.2 °C	15.4 °C	19.2 °C	14.2 °C
1.00 m	1.9 °C	0.4 °C	-0.2 °C	-0.4 °C	-0.9 °C	-1.2 °C	-1.0 °C	-0.6 °C	-0.2 °C	5.2 °C	7.7 °C
2.00 m	1.8 °C	0.9 °C	0.3 °C	0.0 °C	-0.1 °C	-0.2 °C	-0.2 °C	-0.2 °C	-0.2 °C	0.7 °C	3.4 °C
4.55 m	-0.2 °C	-0.1 °C	-0.2 °C	-0.2 °C	-0.2 °C	-0.2 °C	-0.2 °C	-0.2 °C	-0.2 °C	-0.2 °C	-0.2 °C

Figure 3.10.5 Ground temperature at site DH381, based on a record from October 2016 to August 2017.

3.11   SITE 11: DH421 – KM 421

Issues

- Thaw of ground ice and subsidence of road embankment

- Repeated need for maintenance

- Shoulder rotation due to thaw settlement

Summary of Findings

- Degradations observed on the road are attributable to the degradation of permafrost induced by surficial and ground water movement.

- Thaw lakes are forming at the toe of the road embankment, resulting in a thermal mass which degrades surrounding permafrost extending into the embankment.

- Water seeps through the embankment and ponds on the other side.

- Groundwater flow may occur at the site, potentially resulting in leaching of fine materials and contributing to subsidence.

- The thaw sensitivity of this site may be entirely attributable to the presence of the ice wedges in the first 3.5 meters. Should this wedge ice wedge completely thaw, the area should become thaw stable.

3.11.1   Introduction

This site was selected in 2013 for monitoring of permafrost conditions along the highway. Located in the Richardson Mountains, 15 km north of the Arctic Circle crossing, results of the borehole drilling and ground temperature monitoring were presented in a GeoQuébec 2015 conference proceedings (Idrees et al. 2015). This section can be considered as an addendum; reprising some results of the proceedings, and adding new insights from the geophysical assessments.

This site is located at km 421, in the Richardson Mountains, a physiographic unit between km 405 and 492, where thaw settlement has been identified as the principal permafrost-related geohazard (Burn et al. 2015). Subsidence of the road embankment due to thaw of ground ice is a principal hazard in this section. Degradation of the driving surface is managed through routine

maintenance along the route. Shoulder rotation due to thaw settlement in the toe may be observed, as well as the formation of thermokarst ponds (Fig 3.11.1).

The field survey consisted of 3 geotechnical boreholes contracted by HPW, instrumented with Campbell Scientifics logging stations. One ERT survey was performed using both Wenner and Dipole-dipole arrays, in the field at the right-hand side.

3.11.2 Geology

Site DH421 is located at the foot of the western escarpment of the Richardson Mountains. Based on the surficial geology map from the Yukon Geological Survey, the road runs on a colluvial deposit, a mix of coarse hetero granular material in a fine-grained matrix (Fig. 3.11.2). These types of material are usually coarse in nature, but the fine material content can be significant. The geological map does not show the presence of fine material in the vicinity of the site.

3.11.3 Aerial imagery/field observation

The road runs across a slope covered by colluvium. The vegetation cover is dominated by mosses and lichen, with few bushes. The ground was not glaciated, so the gentle gradient of the lower slopes is the result of colluvial deposition continuing over millennia. Ice-wedge polygons are apparent, but their form is muted, with little development of bounding ridges and troughs (Fig. 3.11.3).

The polygons are more apparent in the center area of the image, in what appears to be a drainage area (seen as the lightest brown areas) compared to the upper and lower parts of the image (green/darker brown areas). This is because surficial water drainage follows the trough, making the polygons more apparent. Burn et al. (2015) mention that the ground ice is localized because the mountains were not glaciated. Ground ice may occur as ice wedges or bodies of intrusive ice. However, surface expression of the ice formation may be covered by material deposited by hill slope movement during the extensive unglaciated time.

The ice wedges are degrading at the foot of the embankment, which results in the formation of thermokarst ponds at both sides of the road. These ponds have angular edges that reflect the polygon shape.

3.11.4   Borehole geotechnical data

The log of the first borehole, drilled in the field in November 2013, is presented in figure 3.11.4 with core pictures in figure 3.11.5. the ground profile consists in an ice-poor gravelly diamicton which is overlain at the site by a layer of ice-rich organic silt and clay, 1 – 2 m thick (Fig. 3.11.4). The diamicton is interpreted as a colluvial deposit that originated from the nearby slopes of the Richardson Mountains. Wedge and aggradational ice are limited to the upper 3.5 m. The restriction of ice enrichment to this uppermost 3.5 m suggests that the excess ice is associated with permafrost aggradation during deposition of the fine-grained materials. Excess ice content in this material ranged from 20 – 50 %. Wedge ice was recovered in the toe borehole. The organic content of the upper 2 m indicates burial by surface deposition or cryoturbation.

3.11.5   Ground temperature

The 2014-2015 ground temperature monitoring revealed that permafrost is sustained at site DH421, but has been warmed at depth beneath the road and toe, due to the deep snow banks that accumulate on the side slopes (Fig. 3.11.6). The field site appears to be located away from thermal disturbances associated with the embankment (-3.6 °C). The site is exemplary because it demonstrates (1) overall warming of permafrost by the road; (2) relatively cold conditions in the embankment (-2.3 °C); (3) relatively warm conditions at the toe (-1.4 °C).

3.11.6   ERT survey

One ERT line was surveyed at DH421 (Fig. 3.11.7), located in the field at right-hand side, parallel to the road and passing nearby the HPW field monitoring station. The line was surveyed with Wenner and dipole-dipole ERT arrays. For each array, two profiles are shown; the first is produced using a robust inversion, and the second is created with a smoothness constraint in the inversion process. The robust inversion is typically used when sharp boundaries are expected, like in between ice and unfrozen ground, while a smoothness constraint tends to ensure that the resulting model shows a smooth variation in the resistivity values, usually producing a model with a larger apparent resistivity RMS error.

The locations of the HPW station and of possible ice-wedge troughs (visually observed in the field), have been indicated along the profile presented in figure 3.11.7.

Both Wenner and dipole-dipole surveys show similar results. The dipole-dipole seems to provide better defined boundaries than the Wenner array, but also higher resistivity values

within the range of the highest resistivity values. The robust inversion provides the sharpest boundaries for both arrays.

The highest resistivity values (dark blue areas) are concentrated in the top 10 m of the profile, likely due to the presence of cold ice-rich ground, and wedge ice. The dipole-dipole survey with robust inversion limits these areas to between 2 and 7 m. Some low resistivity values (red/orange areas) are present between 0 and 2 m in the north half of the profile, likely due to a wetter environment (i.e. the presence of liquid water), and to warmer permafrost resulting from the presence of water.

Between 130 and 145 m along the profile, a low resistivity area is present; it coincides with the presence of a thermokarst pond forming at the toe of the embankment. A water track is passing through this location.

On the dipole-dipole profiles, a lower resistivity area is present below the higher ones between 40 and 60 m; this low resistivity could be indicative of ground water movement at about 8 m depth.

3.11.7   Synthesis

The surveys suggest that the degradations observed on the road are attributable to the degradation of permafrost induced by surficial and ground water movement.

The presence of the thaw lakes coincides with the location of water tracks. The thaw lakes are shaped in the polygonal pattern found in the surrounding ground. While the surface water flows following the direction of the ground slope, it is likely channelized by the troughs of the ice wedges. When the water reaches the toe of the embankment it forms ponds. The thermal mass of the pond degrades the nearby permafrost, extending below the road embankment, through which the water continues to seep. Another pond is forming on the other side at the outlet point.

The ERT surveys suggest the possibility of underground water flow. As has been observed elsewhere (site DH82) the water seepage can contribute to the removal of fine sediment from the soil, contributing to the subsidence.

However, the thaw sensitivity of this site may be entirely attributable to the presence of ice wedges in the first 3.5 meters. Should this wedge ice completely thaw, the area should become thaw stable. The height of the ice wedges is unknown yet likely does not exceed 3.5 m. The

average width of an individual ice-wedge remains unknown until further observations can confirm it.
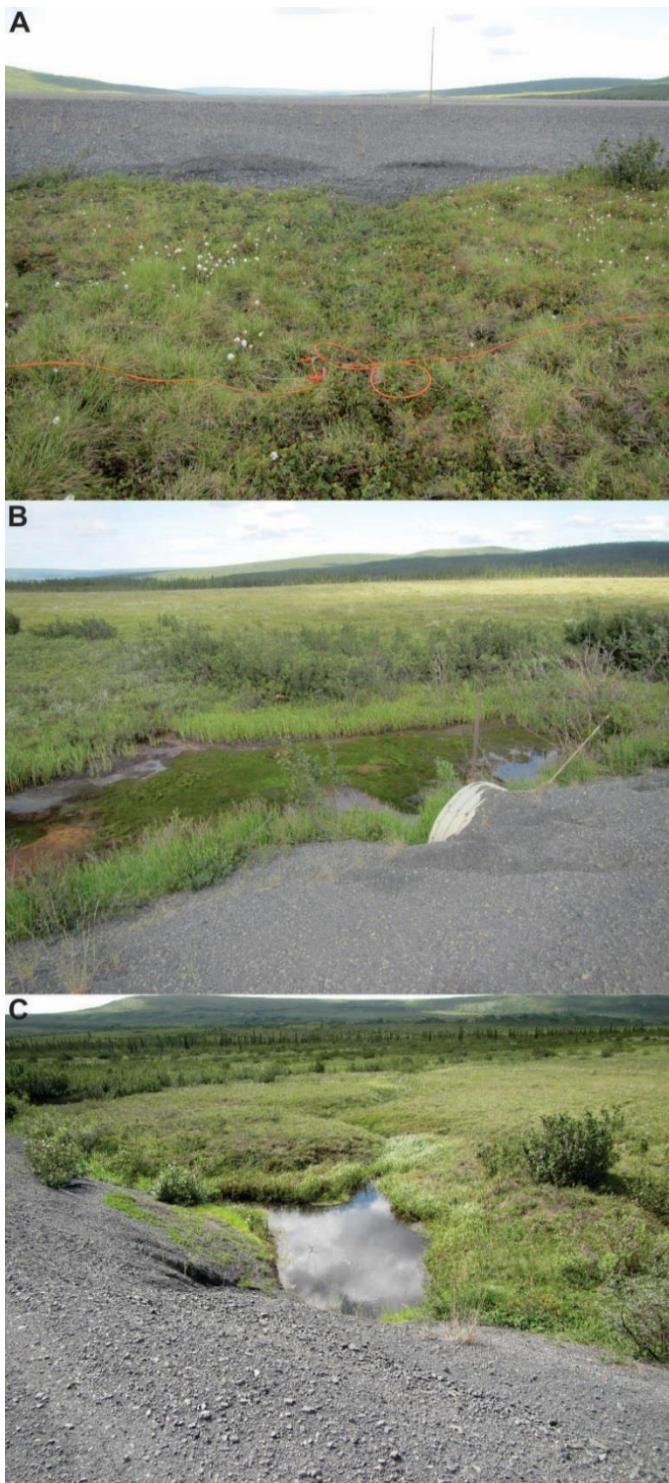
Figure 3.11.1 Degradations observed at site DH421: A- cracks on shoulder of the embankment at right-hand side; B- Settlement and water ponding at a culvert at right-hand side; C- a thermokarst pond and ice wedges degrading at left-hand side.
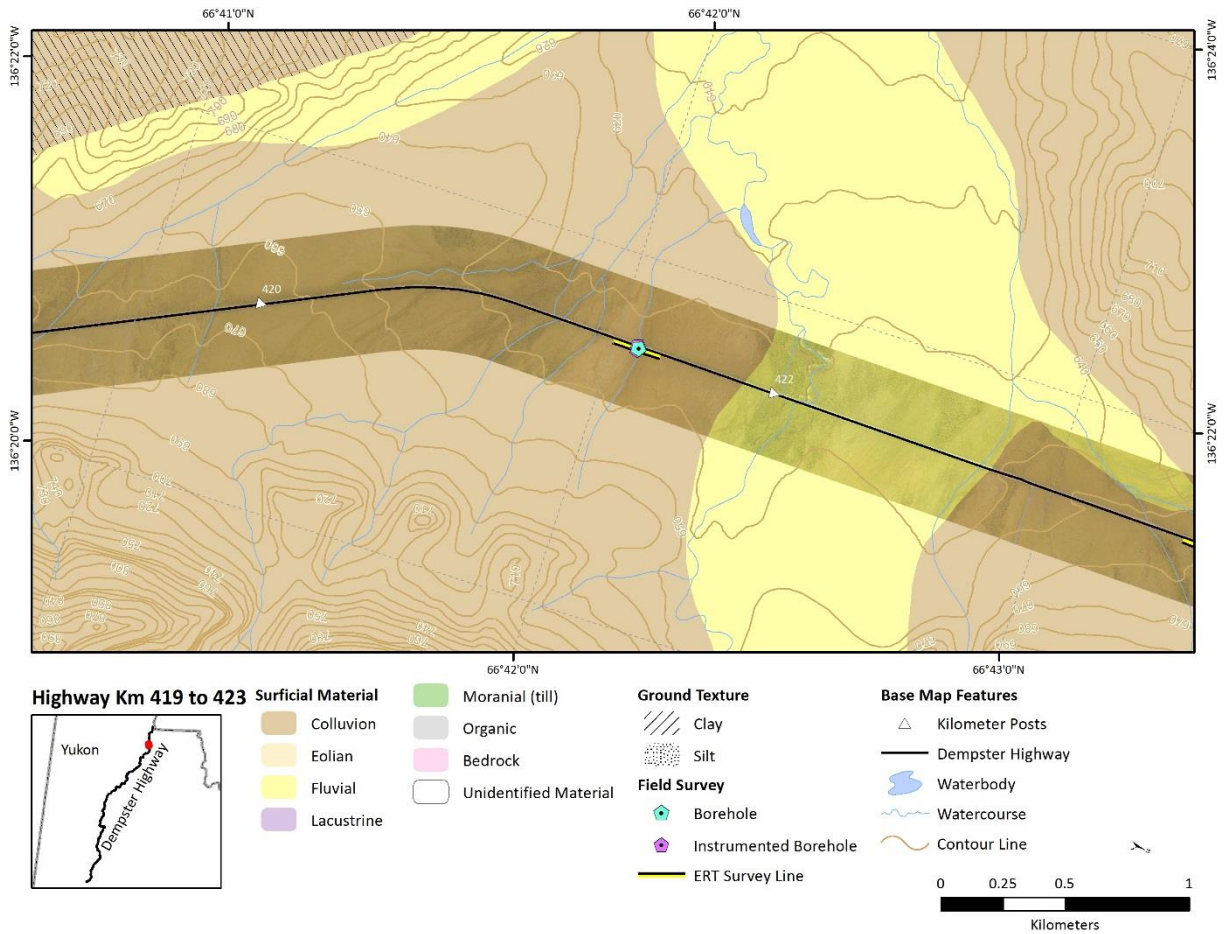
Figure 3.11.2 Surficial geology map of Site 11 DH421 area
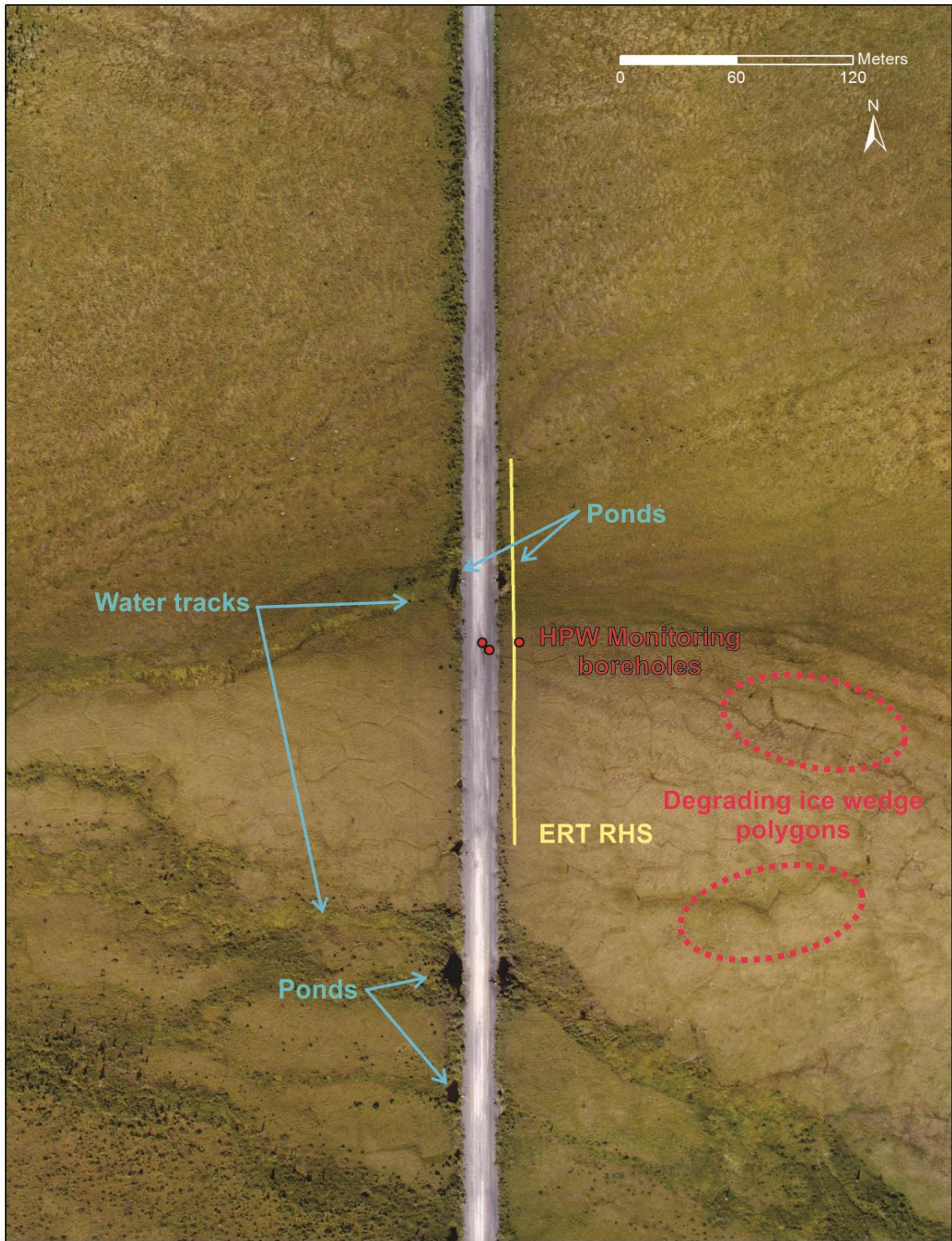
Figure 3.11.3 Aerial view of site DH421.
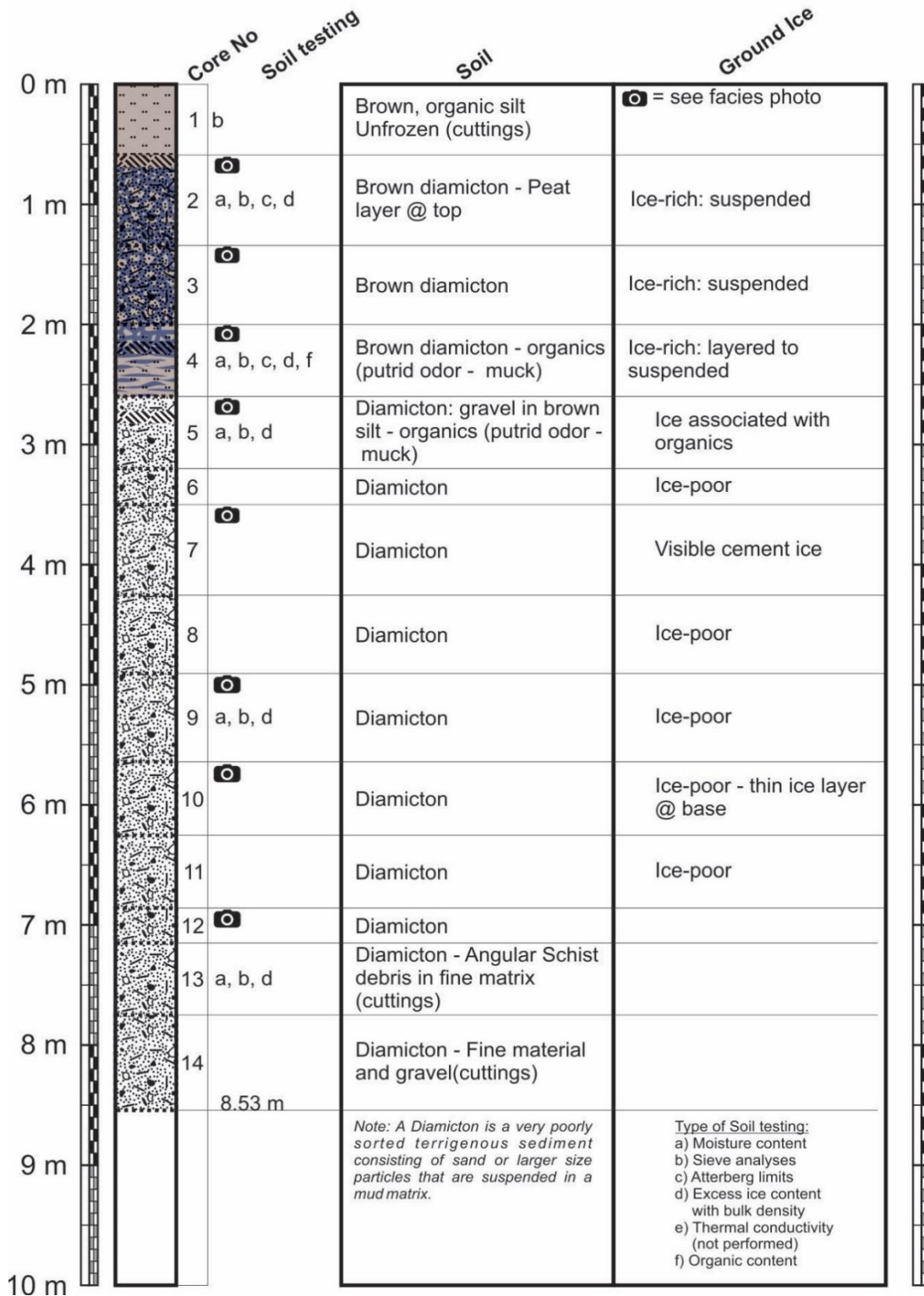
Figure 3.11.4 Log of borehole DH421 BH1 Field.

DH421- S2 - FIELD (2015)
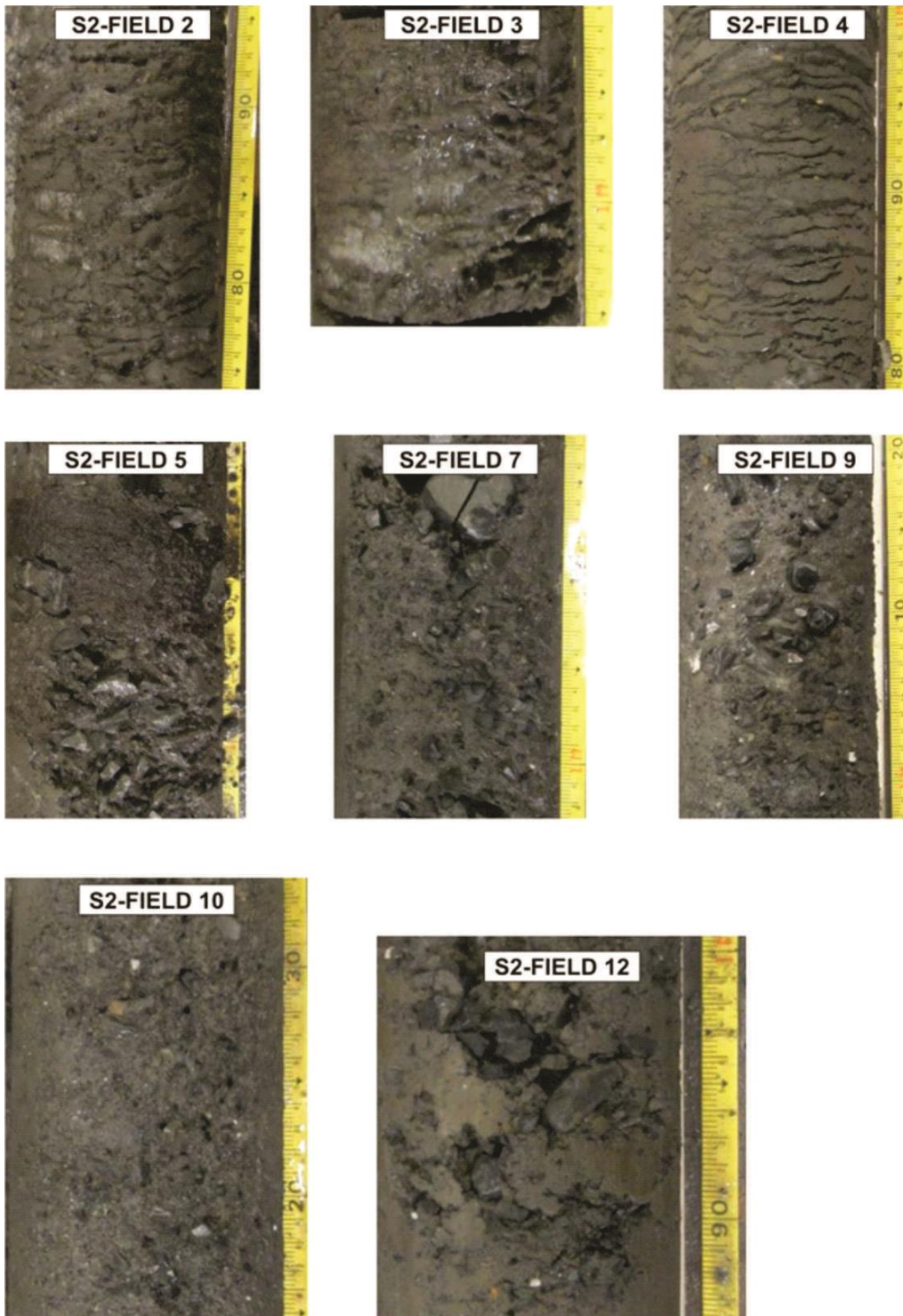
Figure 3.11.5 Core pictures of DH421 BH1 Field.
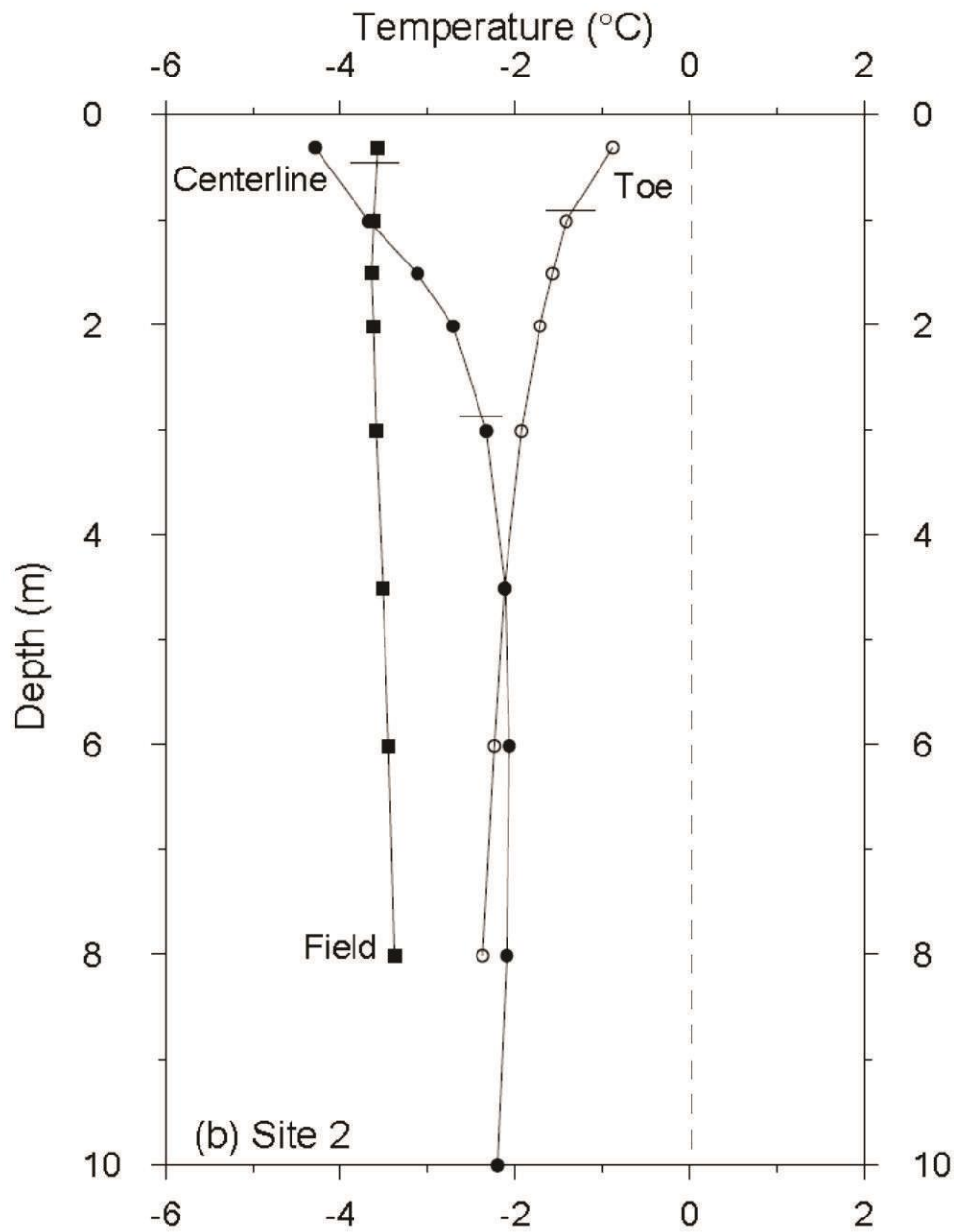
Figure 3.11.6 Annual mean temperature profiles from DH421 for March 1, 2014 – Feb. 28, 2015. Thaw depths are indicated by a horizontal line. Maximum temperatures were > 0 °C throughout the profile at the toe location (from Idrees et al. 2015).
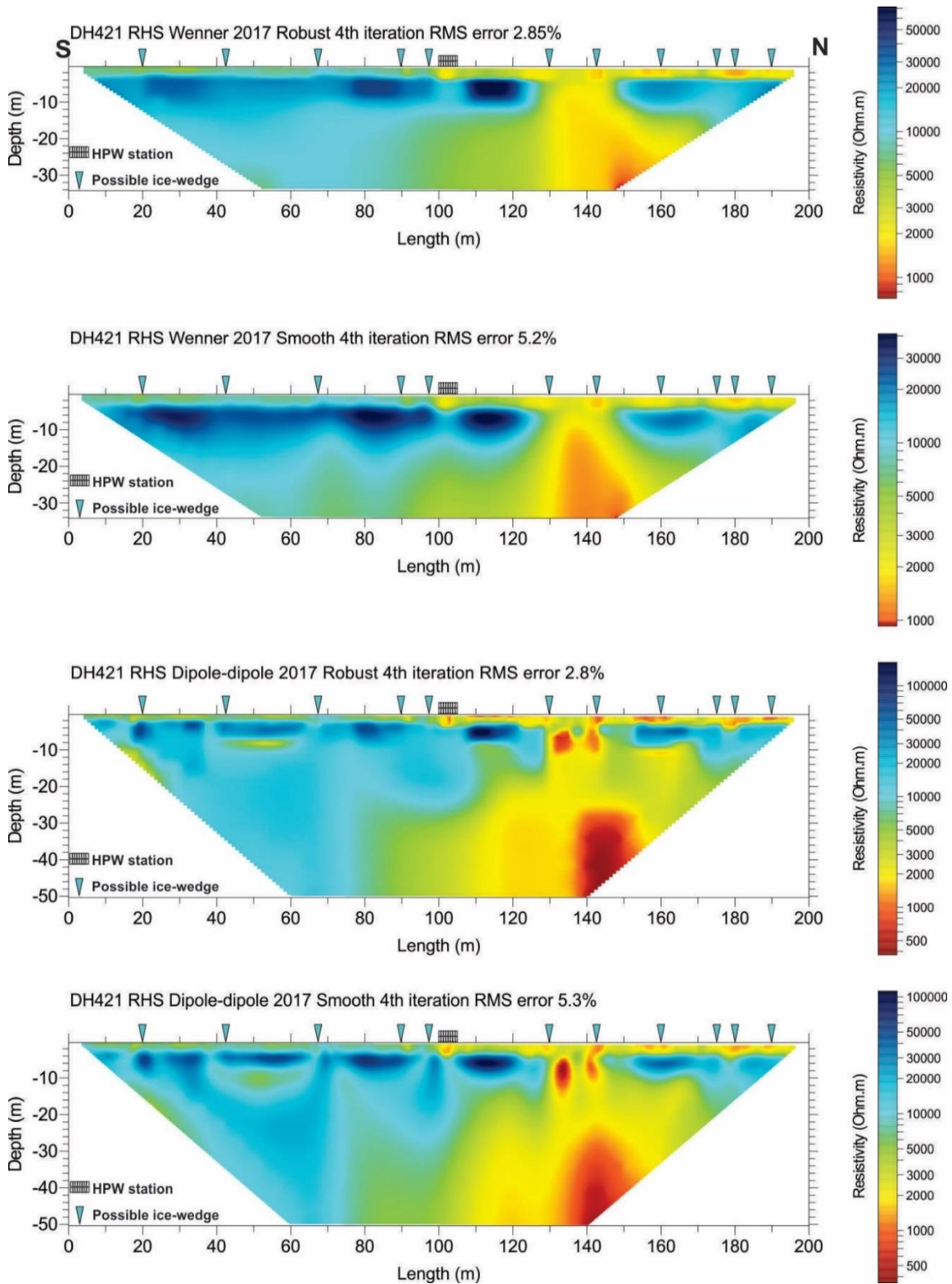
Figure 3.11.7 Wenner and dipole-dipole ERT surveys at site DH421, left-hand side (LHS), using robust and smoothed inversion processes.

3.12   SITE 12: DH424 – KM 424

Issues

- Slope movements and thermo-erosional features on both sides of the highway

- Subsidence, shoulder rotation, and a thermos-erosional cut into the embankment

Summary of Findings

- The ground at DH424 has low thaw sensitivity,

- It is possible that ice wedges are present deeper in the profile, but if they exist, they are scattered and low in number.

- The thermo-erosional features observed at DH424 could be singularly attributable to ground water movement degrading an ice-rich area or seeping sediment.

3.12.1   Introduction

This site is located at km 424, 3 km north of the previous site (DH421), in the Richardson Mountains, a physiographic unit between km 405 and 492. In this unit, thaw settlement has been identified as the principal permafrost related geohazard (Burn et al. 2015). Subsidence of the embankment due to thaw of ground ice is a principal hazard in this section.

At this site, slope movements and thermal erosion features have been observed at the left-hand side, a pond is present at the right-hand side (Fig. 3.12.1A), and shoulder rotation (Fig. 3.12.1B) and a thermo-erosional cut (Fig. 3.12.1C) are present at the left-hand side.

The field survey consisted of one shallow borehole drilled in the field at the right-hand side, and one ERT survey parallel to the road, also in the field at the right-hand side, using both Wenner and dipole-dipole arrays.

3.12.2   Geology

Site DH424 is located at the foot of the western escarpment of the Richardson Mountains. Based on the surficial geology map from the Yukon Geological Survey, the road runs on a colluvial deposit, a mix of coarse hetero granular material in a fine-grained matrix (Fig. 3.12.2). These types of materials are usually coarse in nature but the content of fine material can be

124

significant. The geological map shows the presence of a fine material (clay) 2 km north of the site.

3.12.3 Aerial imagery/field observation

The road runs across a slope covered by colluvium. Because the ground was not glaciated, the gentle gradient of the lower slopes is the result of colluvial deposition continuing over millennia. In this area ice wedge polygons are usually apparent, but their form is muted, with little development of bounding ridges and troughs. Burn et al. (2015) mention that the ground ice may occur as ice wedges or bodies of intrusive ice. However, surficial expression of ice formation may be covered by material deposited by hill slope movement during the extensive unglaciated period. This may be the case at site DH424, as there are few indicators of the presence of ice-wedges (Fig. 3.12.3).

Landslides are visible on the hillslope at the left-hand side of the road. Another notable feature is the presence of mud boils (AKA frost boils) which are upwellings of mud that occur through frost heave and cryoturbation in permafrost areas. Groups of them are visible at right-hand side of the road in the investigated area. These are good indicators of a fine-grained, frost-susceptible material, i.e. potentially ice-rich ground.

Beside the slides, there are no apparent signs of permafrost degradation in the aerial imagery.

3.12.4 Borehole geotechnical data

The Borehole DH424 BH1 was drilled in the field at the right-hand side; it reached a depth of 1.87 m, but cores were only collected down to 1.66 m depth. The thaw front was at 18 cm depth at the time of the drilling. The log (Fig. 3.12.4) shows a 0.30 m organic layer followed by a gray silty sand with gravel, alternating with gravelly sand with silt. A layer of organics occurs between 0.50 and 0.75 m. The borehole ends in dry gravelly sediment at 1.87 m, which could not be retrieved. Centimeter-scale ice lenses are only visible between 0.75 and 1 m; with volumetric excess ice content reaching 48%.

Overall, the borehole has a high volumetric excess ice content in the first meter of the profile, with a volumetric excess ice content of 35%, and does not represent a significant potential for thaw subsidence.

3.12.5 Ground temperature

The Borehole DH424 BH1 was not instrument for temperature monitoring due to lack of depth.

3.12.6 ERT survey

One ERT line was surveyed at DH421 in the field at right-hand side, parallel to the road using both Wenner and dipole-dipole arrays (Fig. 3.12.5). For each array, two profiles are shown. The first is produced using a robust inversion, and the second is created with a smoothness constraint in the inversion process. The robust inversion is typically used when sharp boundaries are expected, like in between ice and unfrozen ground, while a smoothness constraint tends to ensure that the resulting model shows a smooth variation in the resistivity values, usually producing a model with a larger apparent resistivity RMS error.

Both Wenner and dipole-dipole surveys show similar results, with slightly better-defined boundaries with the dipole-dipole array, but also higher resistivity values in the top of the resistivity spectrum. The robust inversion provides the sharpest boundaries for both arrays.

Generally, the resistivity values, are low all along the length of the survey and at various depths (red/orange areas). This may due to an ice-poor, possibly unfrozen ground. The highest resistivity values (dark blue areas), are concentrated in the first 6 m of the profiles, in a discontinuous way. Those are likely due to the presence of a cold ice-rich ground. The presence of wedge ice cannot be disproved, but there are no field indicators.

3.12.7 Synthesis

The borehole observations and the ERT survey suggest that the ground at DH424 has low thaw sensitivity. The borehole was drilled in one of the most resistive areas, and the thickness of frost susceptible material at this location does not exceed 2 m.

It is possible that ice wedges are present deeper in the profile, being covered by colluvial deposit through slope processes. But the ERT surveys suggest that if they exist, they are scattered and low in number.

The thermo-erosional features observed at DH424 could be singularly attributable to ground water movement degrading an ice-rich area or seeping sediment.
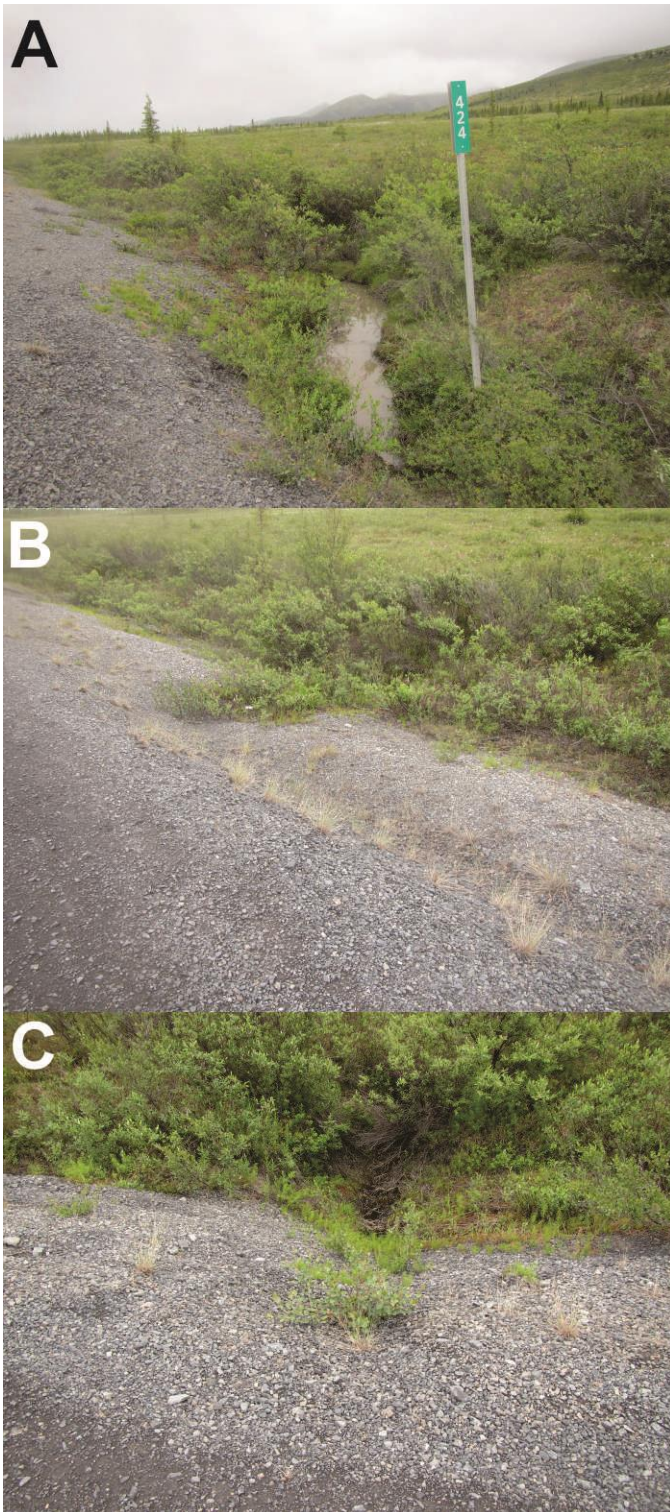
Figure 3.12.1 Degradation features observed at site DH424. A- pond at RHS; B- Shoulder rotation at LHS; C- Thermo-erosional cut at the toe of LHS.
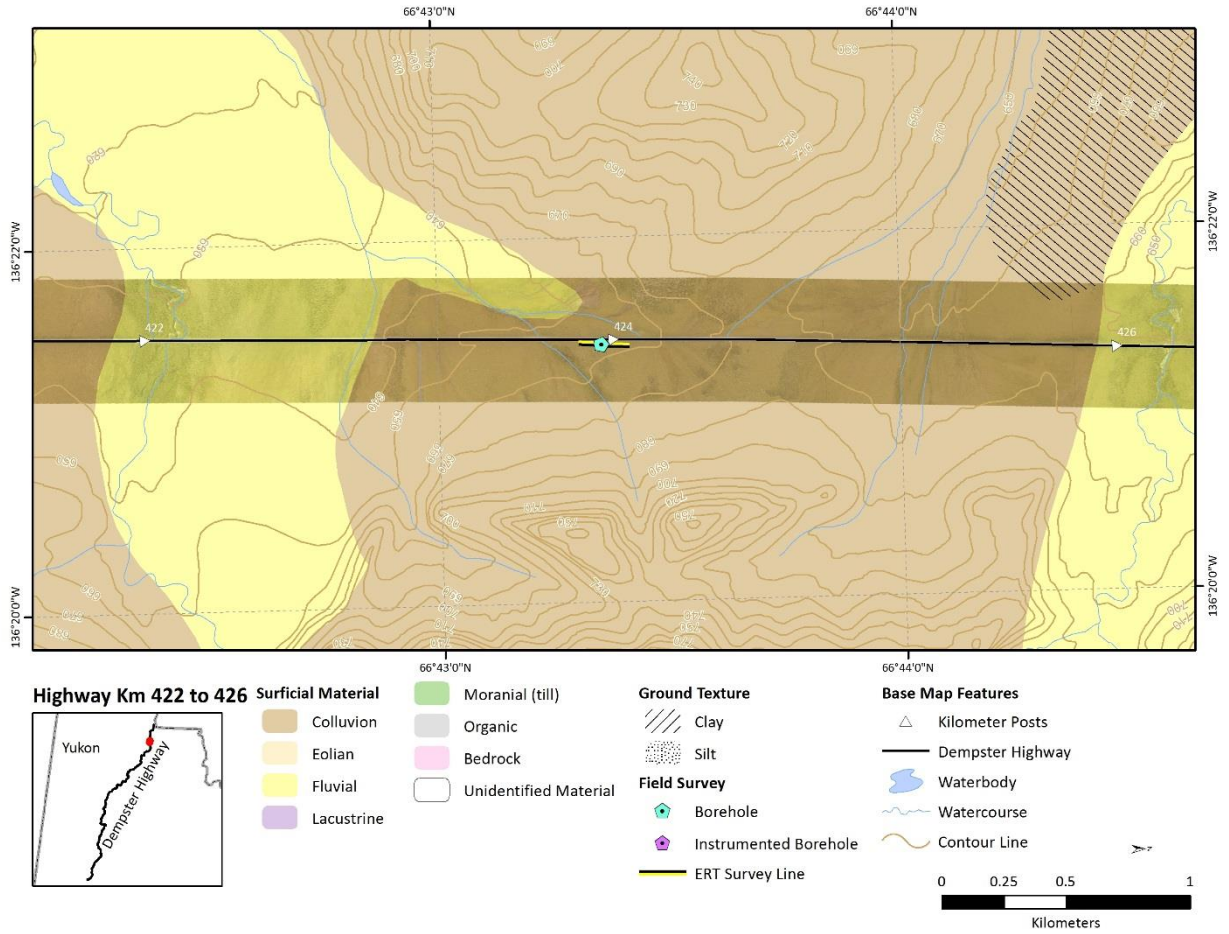
Figure 3.12.2 Surficial geology map of Site 12 DH424 area.
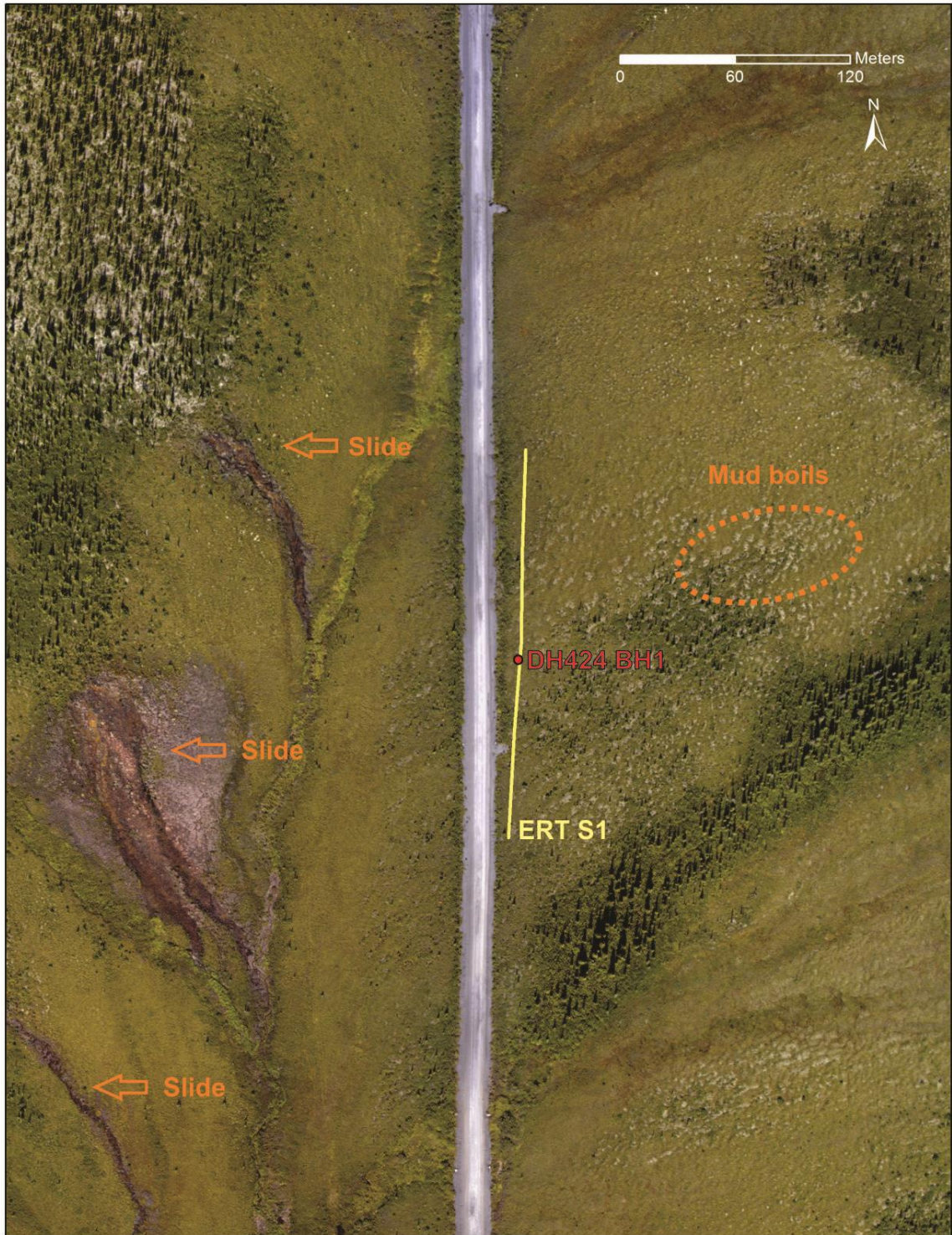
Figure 3.12.3 Aerial view of site DH424.
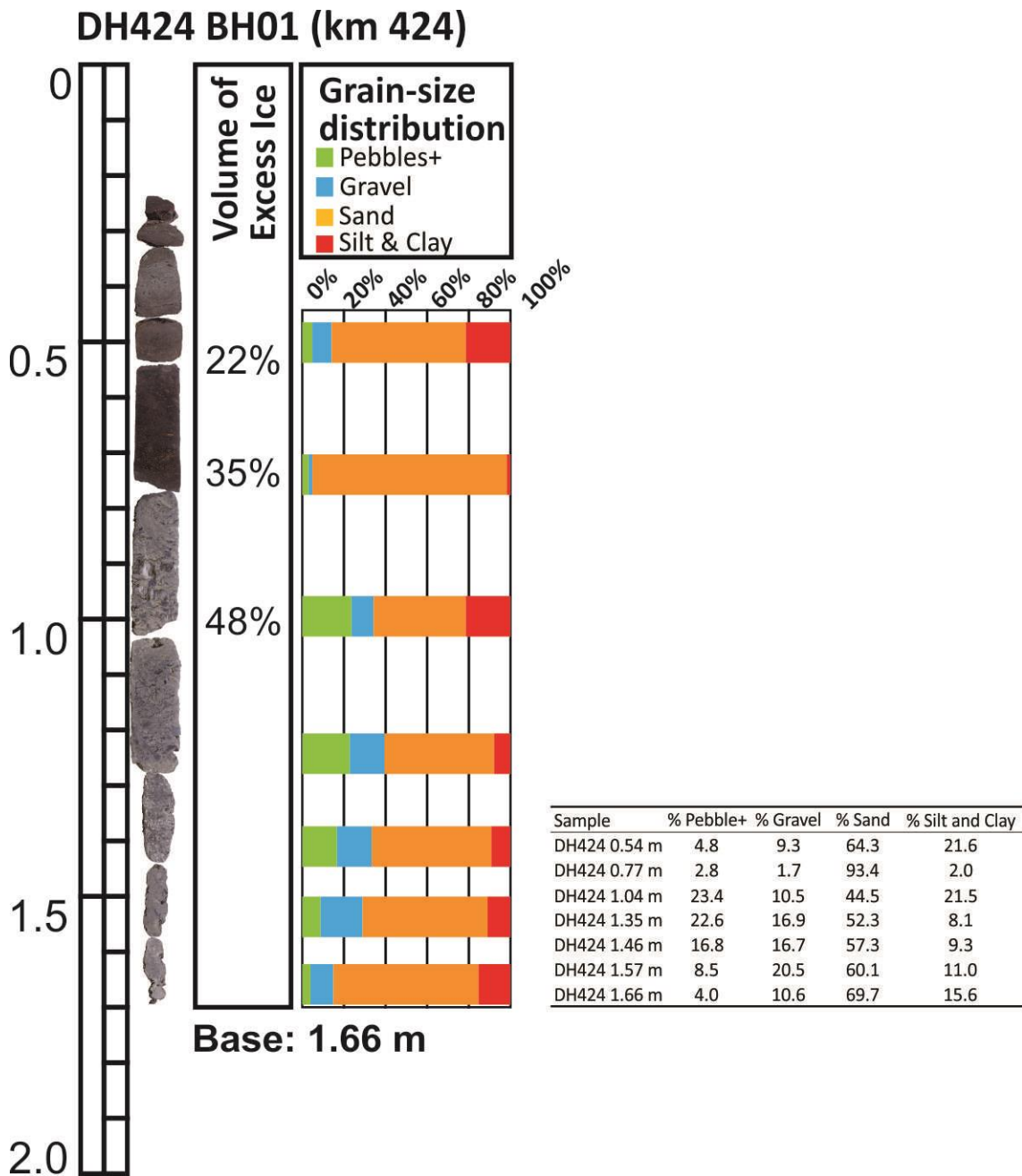
Figure 3.12.4 Log of borehole DH424 BH1 Field.

Sample	% Pebble+	% Gravel	% Sand	% Silt and Clay
DH424 0.54 m	4.8	9.3	64.3	21.6
DH424 0.77 m	2.8	1.7	93.4	2.0
DH424 1.04 m	23.4	10.5	44.5	21.5
DH424 1.35 m	22.6	16.9	52.3	8.1
DH424 1.46 m	16.8	16.7	57.3	9.3
DH424 1.57 m	8.5	20.5	60.1	11.0
DH424 1.66 m	4.0	10.6	69.7	15.6
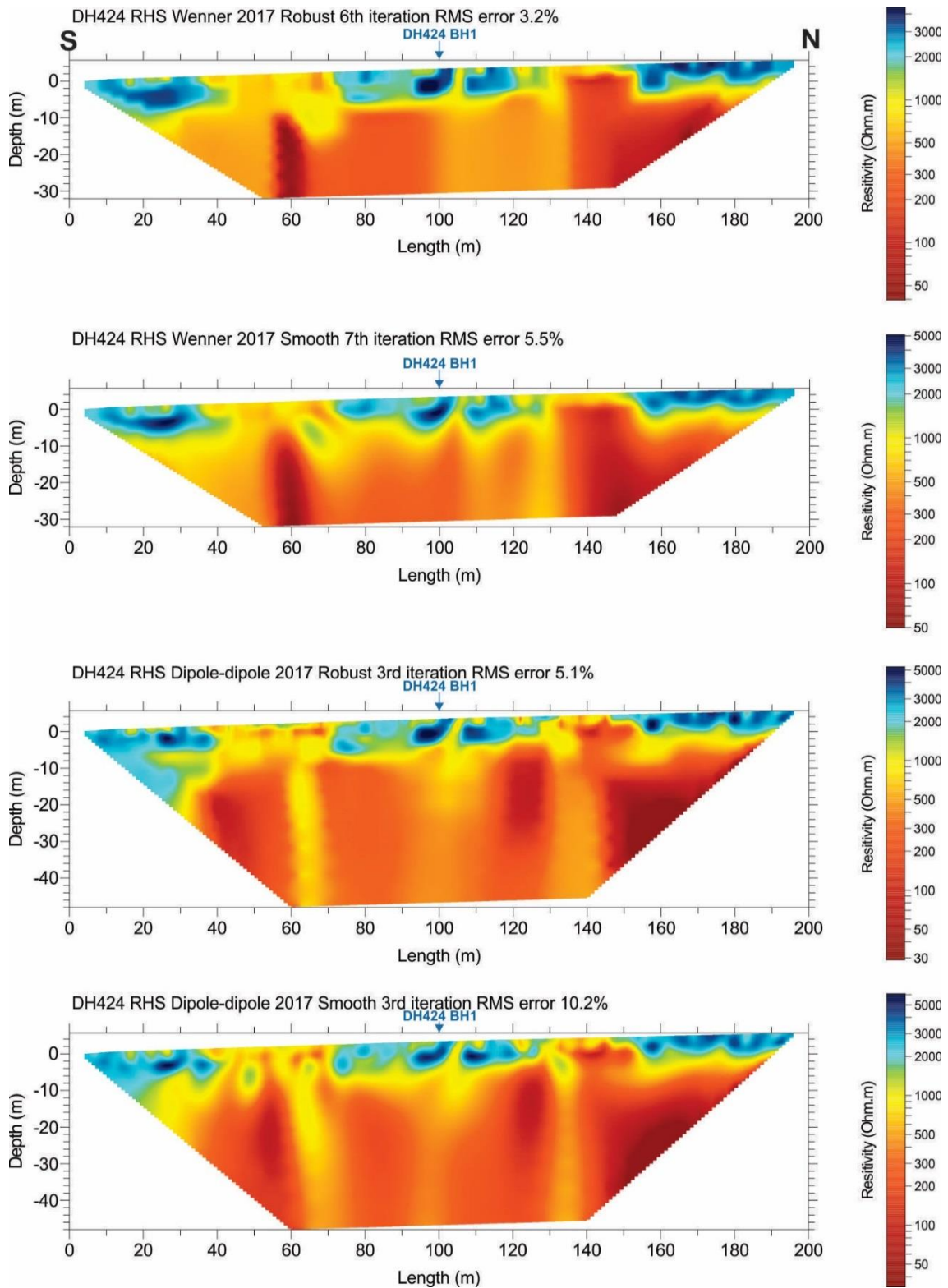
Figure 3.12.5 Wenner and dipole-dipole ERT surveys at site DH424, right-hand side (RHS), using robust and smoothed inversion processes.

3.13   Site 13: DH438 – km 438

Issues

- Subsidence on the embankment due to ground ice thaw

- The site contains a forested area, which provides an interesting vegetative difference to other sites in the Richardson Mountains

Summary of Findings

- The ground in wooded areas has a low thaw sensitivity.

- Permafrost could be relatively shallow or even non-existent at some locations within the wooded area.

- In the non-wooded area ice-rich permafrost is present, and potentially some ice wedges.

- Surficial and groundwater movement could be responsible for the permafrost degradation.

3.13.1   Introduction

This site is located at km 438, 14 km north of the previous site (DH424), in the Richardson Mountains, a physiographic unit between km 405 and 492. In this unit, thaw settlement has been identified as the principal-permafrost related geohazard (Burn et al. 2015). Subsidence of the embankment due to thaw of ground ice is a principal hazard in this section.

At total of 7 sites are in the Richardson Mountains physiographic unit. Site DH438 differs from the others in that it contains a forested area (Fig. 3.13.1). On site, thaw subsidence has been observed at the left-hand side in tundra vegetation.

As the site offered the opportunity to assess an area with a different type of vegetation cover, the field survey consisted of one shallow borehole drilled in the field, within the wooded area at the right-hand side, and one ERT survey parallel to the road, also in the field, at the right-hand side, using both Wenner and Dipole-dipole arrays, through forested and non-forested areas.

3.13.2   Geology

Site DH438 is located at the foot of the western escarpment of the Richardson Mountains. Based on the surficial geology map from the Yukon Geological Survey, the road runs on a

132

colluvial deposit, a mix of coarse hetero granular material in a fine-grained matrix (Fig. 3.13.2). These types of materials are usually coarse in nature but the content of fine material can be significant. The geological map does not show the presence of fine material in the vicinity.

3.13.3 Aerial imagery/field observation

The road runs across a slope covered by colluvium. Because the ground was not glaciated, the gentle gradient of the lower slopes is the result of colluvial deposition over millennia. In this area ice wedge polygons are usually apparent, but their form is muted, with little development of bounding ridges and troughs. Burn et al. (2015) mention that the ground ice may occur as ice wedges or bodies of intrusive ice. However, surface expression of the ice formation may be covered by material deposited by hill slope movement during the extensive unglaciated time. This may be the case at site DH438, as there are few indicators of the presence of ice wedges (Fig. 3.13.3).

The only evident periglacial features visible on the aerial imagery are smooth solifluction lobes occurring on the gentle hillslope at the left-hand side of the road. As said above, polygonal patterning is barely discernable in the aerial imagery except in very localized places. Yet it may be suspected that ice wedges are present in the field, in which case the center of the polygons would be areas in the tundra with a slightly lighter colour (likely drier).

3.13.4 Borehole geotechnical data

The Borehole DH438 BH1 was drilled in the field within a wooded area at the right-hand side, reaching a depth of 2.55 m. The thaw front was at 35 cm depth at the time of the drilling; the organic layer thickness was no more than few centimeters. The log (Fig. 3.13.4) shows a grey sand with silt and gravel all along the profile. The borehole ends at 2.55 m, the contact with a bed of gravelly sediment which was not sampled. The overall excess ice content is low, ranging from 3 to 35% with an average of 16% for the entire borehole. The ground ice is present in the shape of millimetric to centimetric ice lenses with a sub-horizontal orientation, parallel to ground surface.

Overall, the borehole does not indicate a significant potential for thaw subsidence, at least in the wooded area.

3.13.5 Ground temperature

Borehole DH438-BH1 was lined with PVC piping and instrumented with one 4-channel Hobo loggers to record ground temperatures at 0, 0.5, 1.0, 2.55 m depths. Ground temperature were recorded from July 4th to September 17th, 2017, the date of the last downloading (Fig. 3.13.5). Although very partial with only a two-month monitoring, the record shows that from July 15th to September 15th, the ground temperature at the deepest 2.5 m depth remains below -1 °C, between –0.9 and -0.6 °C. The active layer has a thickness of 140 cm on September 15th. Based on the short and shallow records, permafrost is relatively warms with temperature above -2.0 °C.

3.13.6 ERT survey

One ERT line was surveyed at DH438 parallel to the road, in the field at right-hand side, using both Wenner and dipole-dipole arrays (Fig. 3.13.6). For each array, two profiles are shown. The first is produced using a robust inversion, and the second is created with a smoothness constraint in the inversion process. The robust inversion is typically used when sharp boundaries are expected, like in between ice and unfrozen ground, while a smoothness constraint tends to ensure that the resulting model shows a smooth variation in the resistivity values, usually producing a model with a larger apparent resistivity RMS error.

Both Wenner and dipole-dipole surveys show similar results, with slightly better-defined boundaries with the dipole-dipole array, but also comparable resistivity values in term of range of value. The robust inversion provides the sharpest boundaries for both arrays.

Generally, starting from the south, from 0 to 120 m of the survey length, the resistivity values are low at various depths, showing as red/orange colours. There are higher resistivity areas (yellow/green colours) such as where DH438 BH1 was drilled, but these are sporadic. Based on the profile, the permafrost may not extend deeper than 10 m, likely less at some places.

The situation is different from 120 to 200 m, at the north end of the survey. There, some high-resistivity areas (blue) are present at various depths. These could mark the presence of frozen ice-rich and/or coarse material. We can hypothesize that the shallower resistive areas are attributable to the presence of wedge ices.

Between 140 and 160 m length, a low-resistivity area (yellow/orange colour) occurs between approximately 7 and 10 m depth. This could be due to the presence of ground water.

3.13.7   Synthesis

The borehole observations and the ERT survey suggest that the ground at DH438 has a low thaw sensitivity in the wooded areas. Permafrost could be relatively shallow or even non-existent at some locations.

From 120 to 200 m length, in the non-wooded area, ice-rich permafrost is present; and, although there is no field observation that can confirm it, ice wedges could be present, the thaw of which could result in damage to the road.

The ERT survey suggests that surficial as well as groundwater circulation could be responsible for the permafrost degradation.

Figure 3.13.1 Wooded area at site DH438.
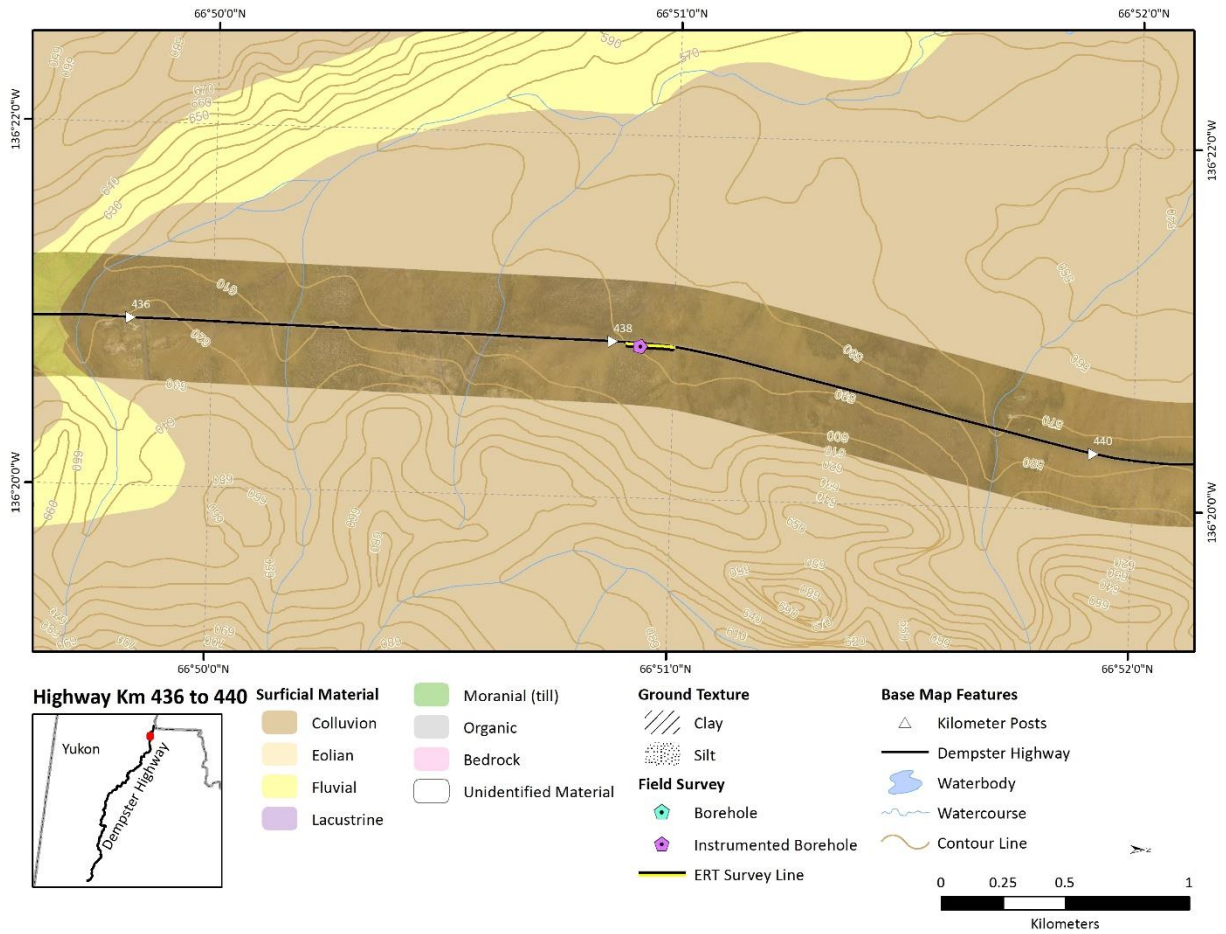
Figure 3.13.2 Surficial geology map of Site 13 DH438 area.

Figure 3.13.3 Aerial view of site DH438.

DH438 BH01 (km 438)

Sample	% Pebble+	% Gravel	% Sand	% Silt and Clay
DH438 0.52 m	7.6	4.0	64.6	23.7
DH438 0.79 m	9.2	4.7	69.9	16.3
DH438 1.08 m	5.5	3.9	57.3	33.3
DH438 1.32 m	10.0	6.8	60.7	22.4
DH438 1.51 m	1.6	6.4	66.5	25.5
DH438 1.72	1.8	8.6	63.4	26.2
DH438 1.90 m	6.7	10.2	62.9	20.3
DH438 2.01 m	6.6	4.3	66.7	22.5
DH438 2.15 m	5.7	14.2	67.9	12.2
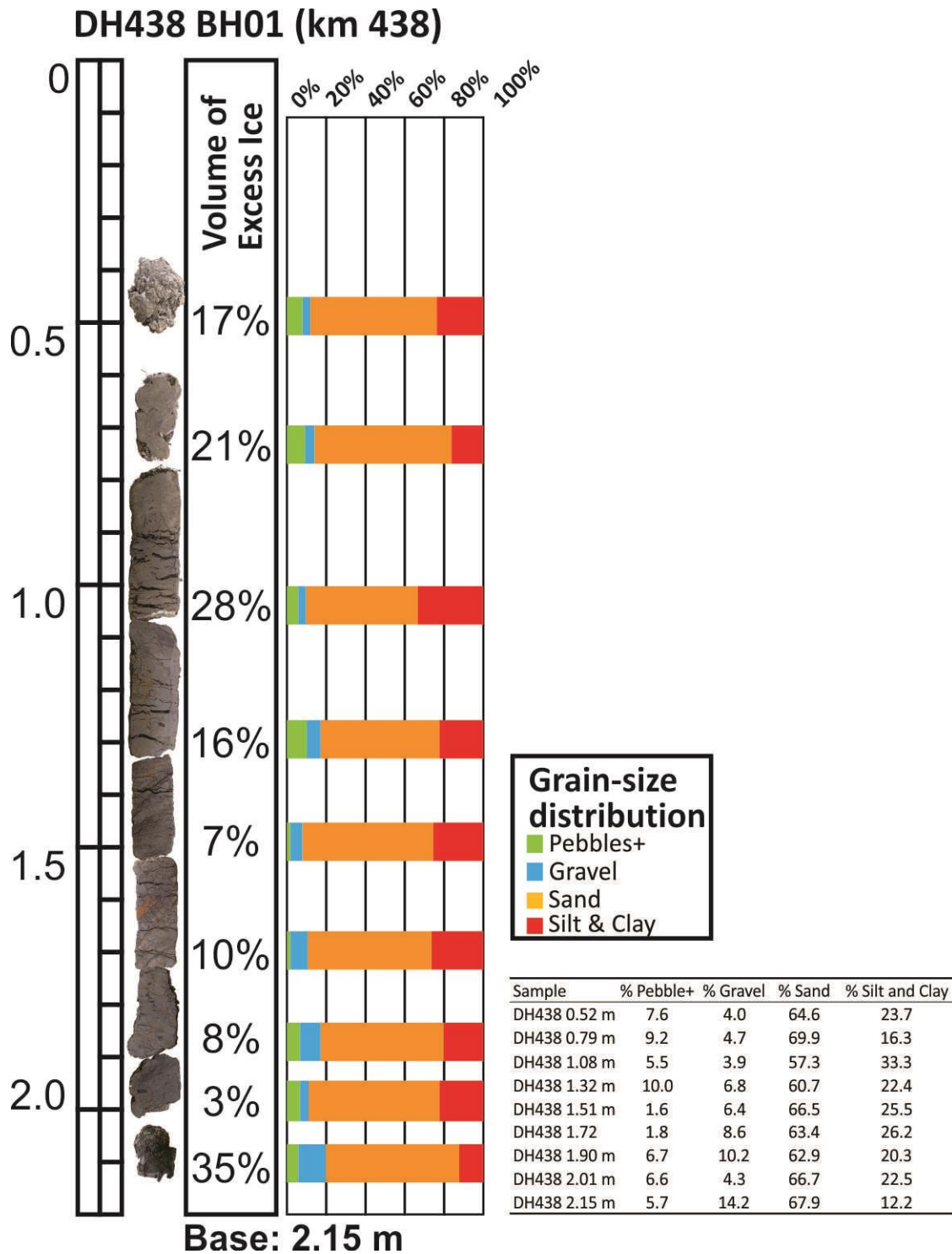
Figure 3.13.4 Log of borehole DH438 BH1 Field.
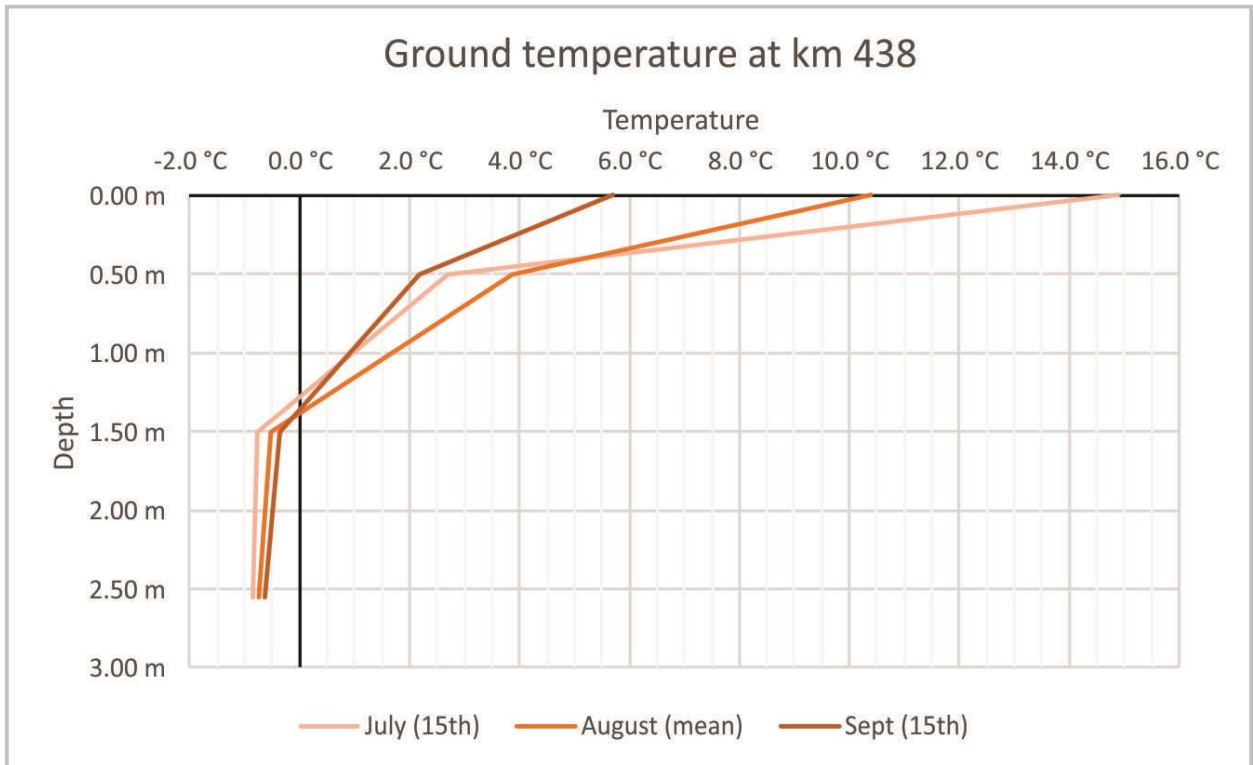
Depth	0.00 m	0.50 m	1.50 m	2.55 m
July (15th)	14.9 °C	2.7 °C	-0.8 °C	-0.9 °C
August (mean)	10.4 °C	3.9 °C	-0.5 °C	-0.7 °C
Sept (15th)	5.7 °C	2.2 °C	-0.4 °C	-0.6 °C

Figure 3.13.5 Ground temperature at site DH438, based on a record from July 15th to September 15th, 2017.
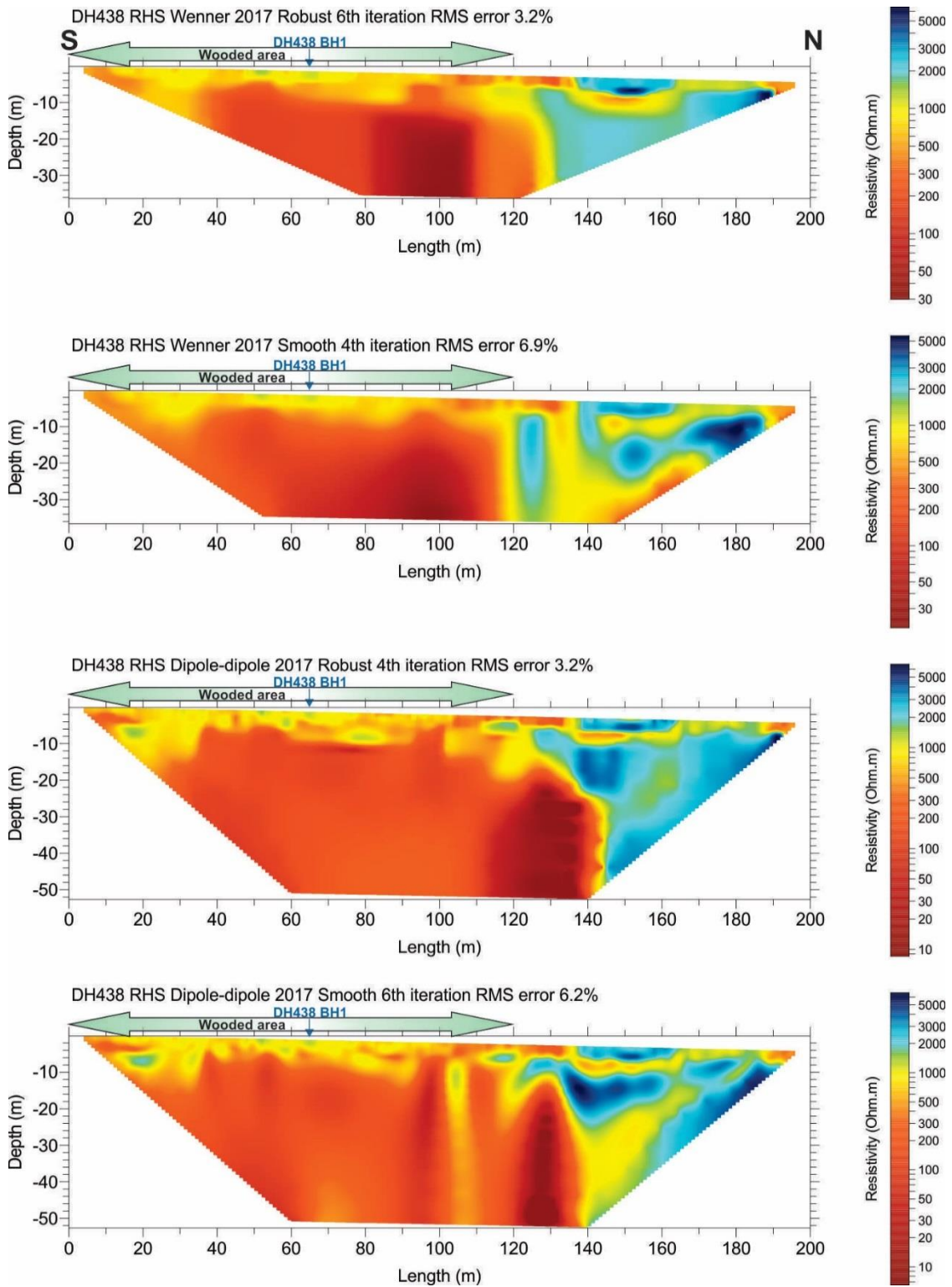
Figure 3.13.6 Wenner and dipole-dipole ERT surveys at site DH438, right-hand side (RHS), wooded and unwooded areas, using robust and smoothed inversion processes.

3.14   SITE 14: DH442 – KM 442

Issues

- Subsidence of the embankment due to thaw of ground ice

Summary of Findings

- The ground at this site is thaw sensitive due to the presence of ground ice at various levels in the profile.

- The permafrost is relatively warm with temperatures above -2.0 °C.

- Ice wedges are assumed to be shallowly concentrated along the profile.

- Permafrost could be relatively shallow or even non-existent at some locations.

- Water flow (surficial and groundwater) is likely the driving phenomenon responsible for the thaw.

3.14.1   Introduction

This site is located at km 442, 4 km north of the previous site (DH438), in the Richardson Mountains, a physiographic unit between km 405 and 492. In this unit, thaw settlement has been identified as the principal permafrost related geohazard (Burn et al. 2015). Subsidence of the embankment due to thaw of ground ice is the principal hazard in this section.

Thaw subsidence, or a similar process has been reported by HPW. The process is active on the right-hand side. At this site, the field survey consisted of one shallow borehole drilled in the field at the right-hand side, and one ERT survey parallel to the road, also in the field, right-hand side, using both Wenner and dipole-dipole arrays.

3.14.2   Geology

Site DH438 is located at the foot of the western escarpment of the Richardson Mountains. Based on the surficial geology map from the Yukon Geological Survey, the road runs on a colluvial deposit, a mix of coarse hetero granular material in a fine-grained matrix (Fig. 3.14.1). These types of materials are usually coarse in nature but the content of fine material can be significant. The geological map also shows the presence of fine material, clay, on site. This type of soil is highly frost susceptible, favouring ground ice formation, and also tends to be

142

associated with wetland, as the low hydraulic conductivity impedes good water drainage. Such soil may also be associated with the development of an organic layer favoring permafrost development.

3.14.3   Aerial imagery/field observation

The road runs across a slope covered by colluvium. Because the ground was not glaciated, the gentle gradient of the lower slopes is the result of colluvial deposition over millennia. In this area, ice wedge polygons are usually apparent, but their form is muted, with little development of bounding ridges and troughs. Burn et al. (2015) mention that the ground ice may occur as ice wedges or bodies of intrusive ice. At this site, the polygonal pattern is very visible, as runoff water has channelized the ice wedge troughs. However, surface expression of the ice wedge polygons has been affected by solifluction processes higher on the hill slope (Fig. 3.14.2).

The ice wedge polygons and solifluction are the dominant periglacial features visible in the aerial imagery. The polygons are good indicators of the presence of massive wedge ice.

3.14.4   Borehole geotechnical data

The Borehole DH442 BH1 was drilled in the field, at the right-hand side, reaching a depth of 2.88 m. The thaw front was at 30 cm depth at the time of the drilling, the organic layer thickness about the same thickness. The log (Fig. 3.14.3) shows a brown sand with silt or gravel, alternating with layers of organic material. The borehole ends at 3.00 m, the contact with a bed of gravelly sediment which was not sampled. The overall excess ice content ranges from 12 to 53% with an average of 35% for the entire borehole. The relatively high excess ice content represents a significant potential for thaw subsidence.

3.14.5   Ground temperature

Borehole DH442-BH1 was lined with PVC piping and instrumented with one 4-channel Hobo logger to record ground temperatures at 0, 0.5, 1.5, 3.0 m depths. Ground temperatures were recorded from July 4th to September 17th, 2017, the date of the last downloading (Fig. 3.14.4). Although very partial with only two months of monitoring, the record shows that from July 15th to September 15th the ground temperature at the deepest 3.0 m depth remained constantly below -1 °C, at –0.7 °C. The active layer had a thickness of 140 cm on September 15th. Based on the short and shallow records, permafrost is relatively warm with temperatures above -2.0 °C.

3.14.6   ERT survey

One ERT line was surveyed at DH442 parallel to the road, in the field at right-hand side, 7 to 10 m from the toe of the embankment (Fig. 3.14.5). The line was surveyed with Wenner and dipole-dipole ERT arrays. For each array, two profiles are shown. The first is produced using a robust inversion, and the second is created with a smoothness constraint in the inversion process. The robust inversion is typically used when sharp boundaries are expected, like in between ice and unfrozen ground, while a smoothness constraint tends to ensure that the resulting model shows a smooth variation in the resistivity values, usually producing a model with a larger apparent resistivity RMS error.

Both Wenner and dipole-dipole surveys show relatively similar results, with slightly better-defined boundaries with the dipole-dipole array, and slightly higher values in the resistivity spectrum scale. The robust inversion provides the sharpest boundaries for both arrays.

The ERT profiles cross a relatively wet area from the middle of the survey to its third quarter, resulting in low resistivity values (red/orange colours) likely representing a warm, degrading permafrost. On both sides of this area, two very high-resistivity areas (blue) are present: one at the south side comprised between 3 and 15 m depth approximately, and one in the north side comprised between 4-5 and 18 m depth approximately. At the south end, an area of bulk high-resistivity values is present between 15 and 25 m depth.

Finally, a second low-resistivity area is present deeper in the profile, below the first one, in the wet degraded area. It could be due to the presence of ground water.

The high-resistivity areas are likely due to the presence of frozen ice-rich and/or coarse material. It can be hypothesized that the shallower high-resistivity areas are attributable to the presence of wedge ice, yet the deeper ones could be due to a frozen gravel or bedrock, or an ice-rich sediment.

3.14.7   Synthesis

The borehole observations and the ERT survey suggest that the ground at DH442 is thaw sensitive due to the presence of ground ice at various levels in the profile. The permafrost is warm, which results in a faster rate of degradation. Water flow is likely the driving phenomenon responsible for the thaw.

The deepest high-resistivity values are intriguing, as ice wedges are assumed to be shallowly concentrated along the profile. Some low resistivity values suggest that permafrost could be relatively shallow or even non-existent at some locations.

The ERT survey suggests that surficial as well as groundwater circulation can be responsible for the permafrost degradation.
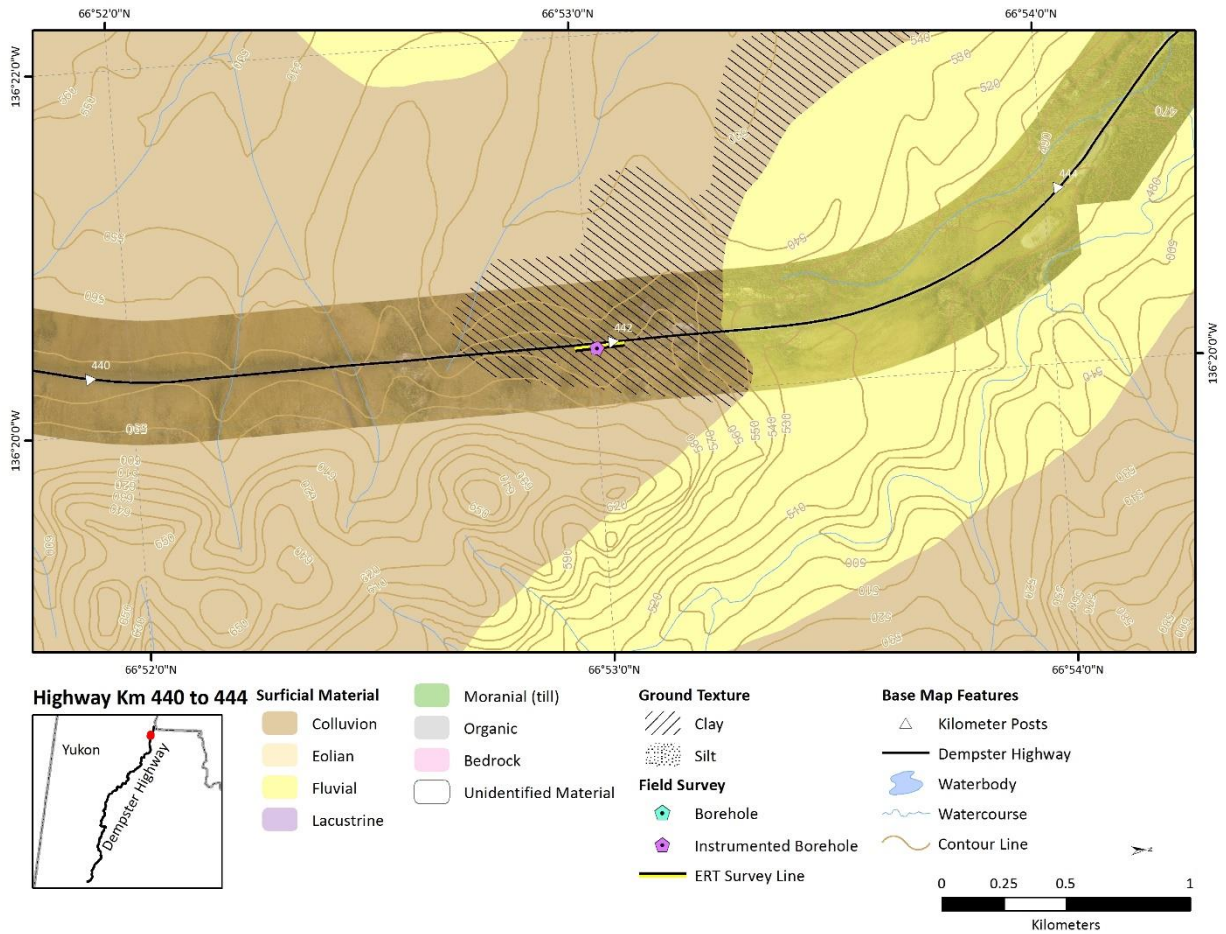
Figure 3.14.1 Surficial geology map of Site 14 DH442 area.
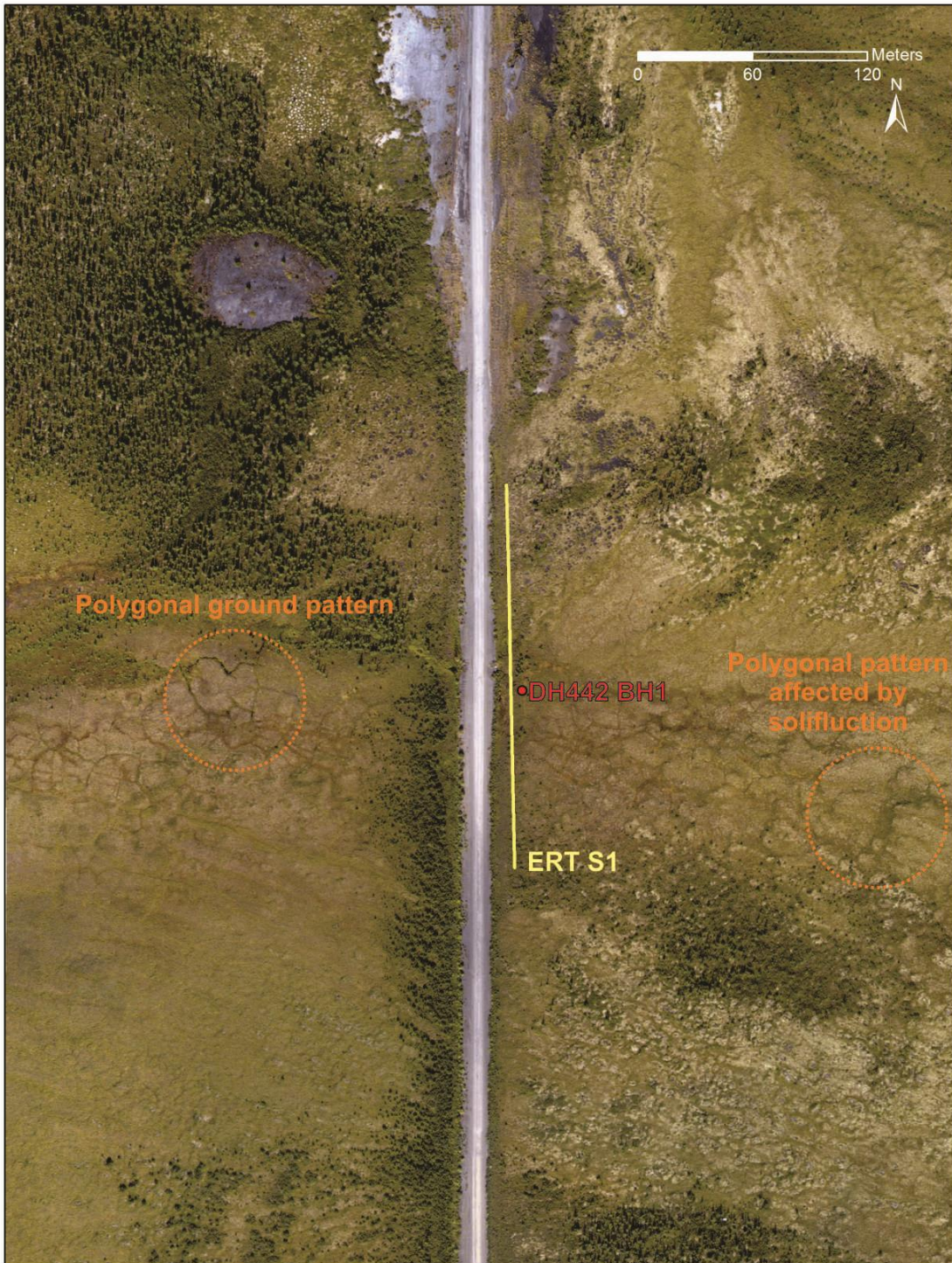
Figure 3.14.2 Aerial view of site DH442.

Sample	% Pebble+	% Gravel	% Sand	% Silt and Clay
DH442 0.55 m	0.7	4.2	90.0	5.0
DH442 0.88 m	11.4	16.8	69.6	2.2
DH442 1.18 m	29.4	9.2	46.5	14.9
DH442 1.44 m	1.3	3.3	92.5	3.0
DH442 1.76 m	6.9	14.2	76.7	2.2
DH442 2.10 m	1.9	9.0	86.6	2.5
DH442 2.33 m	1.6	3.0	75.2	20.3
DH442 2.56 m	16.6	19.1	63.0	1.3
DH442 2.88 m	15.1	9.3	41.4	34.2
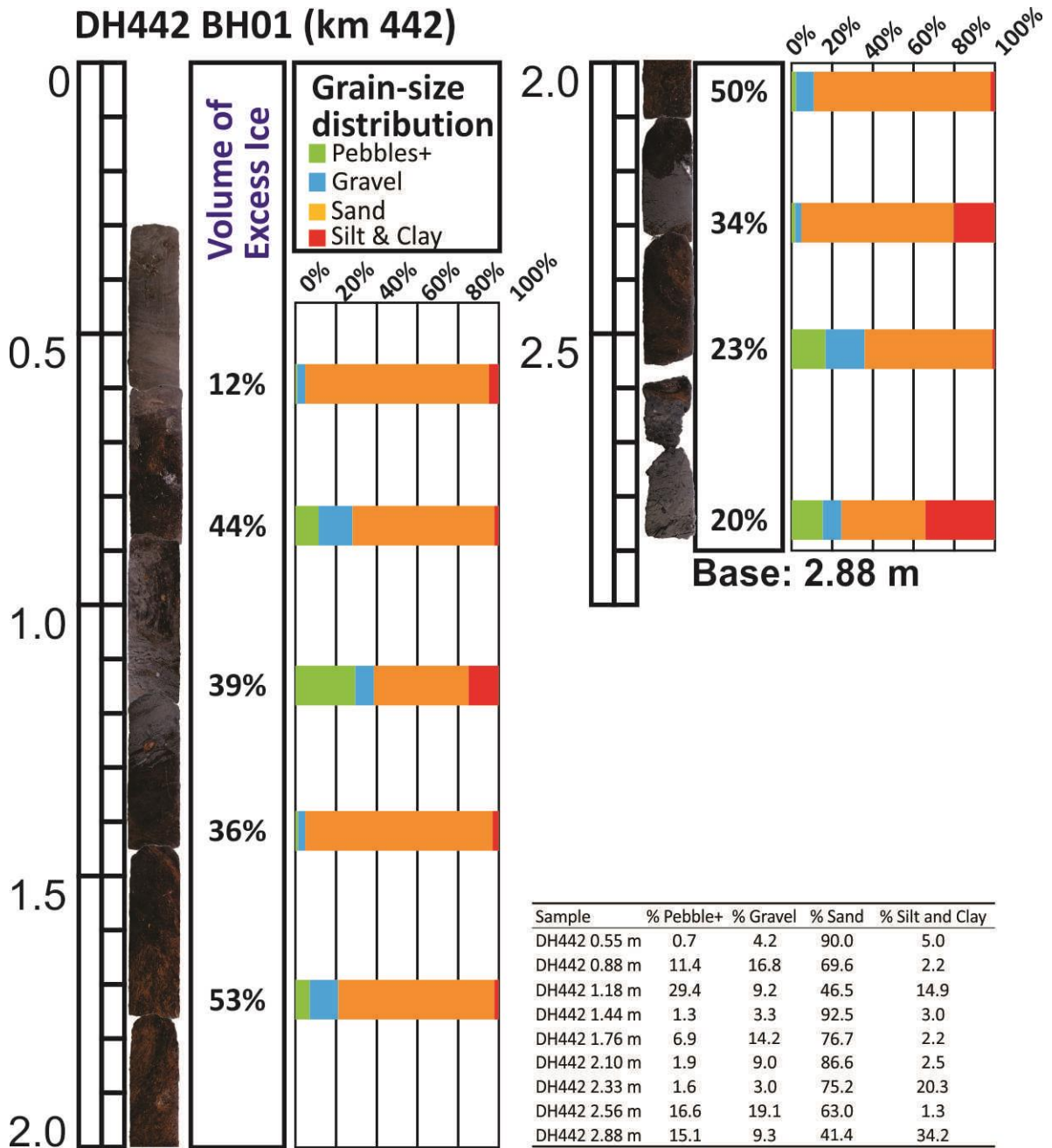
Figure 3.14.3 Log of borehole DH442 BH1 Field.
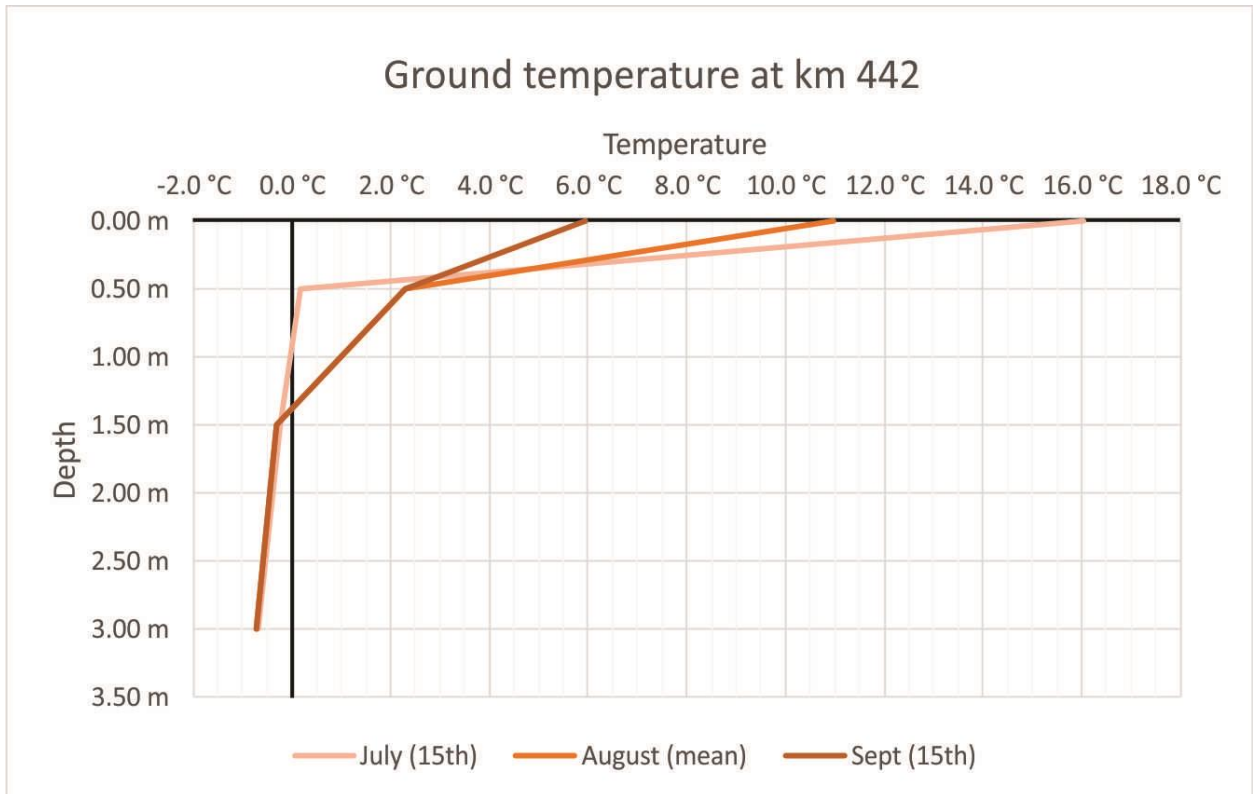
Depth	July (15th)	August (mean)	Sept (15th)
0.00 m	16.0 °C	11.0 °C	6.0 °C
0.50 m	0.2 °C	2.3 °C	2.3 °C
1.50 m	-0.2 °C	-0.3 °C	-0.3 °C
3.00 m	-0.7 °C	-0.7 °C	-0.7 °C

Figure 3.14.4 Ground temperature at DH442 site, based on a record from July 15th to September 15th, 2017.
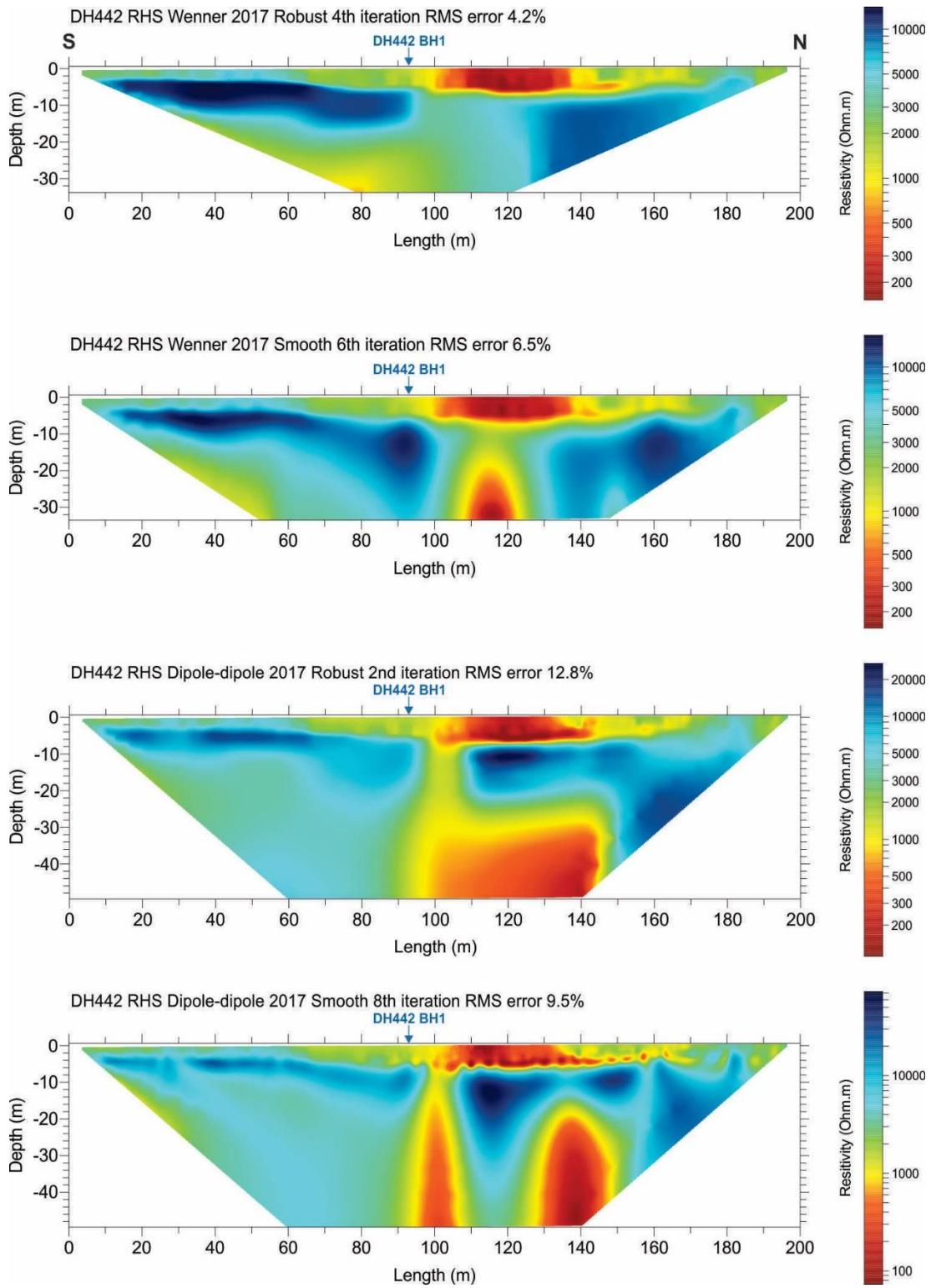
Figure 3.14.5 Wenner and dipole-dipole ERT surveys at site DH442, right-hand side (RHS), using robust and smoothed inversion processes.

3.15   SITE 15: DH447 – KM 447

Issues

- Sinkholes form in the road, requiring repeated repairs

- Tension cracks in the shoulder

- Crevices in the RoW, RHS

Summary of Findings

- The ground at this site is not particularly thaw sensitive; the soil is generally coarse, and unfrozen below 8 m.

- Some ice-rich areas are apparent to the north in the surveyed area.

- The nature of the ground ice is unclear, but it could be wedge ice or intrusive ice.

- No active processes such as frost heave or thermal cracking were reported.

- Permafrost in this area is likely warm and thin; its thaw should be relatively fast with only localized effects

3.15.1   Introduction

This site is located at km 447, 5 km north of the previous site (DH442), in the Richardson Mountains, a physiographic unit between km 405 and 492. In this unit, thaw settlement has been identified as the principal-permafrost related geohazard (Burn et al. 2015). Subsidence of the embankment due to thaw of ground ice is the principal hazard in this section.

Sinkholes are forming at this location. The HWP road manager has reported that despite numerous repairs, material keep "disappearing". The process seems to be especially active on the right-hand side. At the time of the investigation, tension cracks were visible in the shoulders (Fig. 3.15.1A), and some crevices were observed in the field near the road at the right-hand side (Fig. 3.15.1B). Surficial sediment is coarse, and bedrock is expected close to the surface, as observed on a nearby cut (Fig. 3.15.1C).

At this site, the field survey consisted one ERT survey in the field, parallel to the road, right-hand side, performed using both Wenner and dipole-dipole arrays. No borehole was made as no suitable site was available, the surficial material consisting of unfrozen gravelly sediment.

3.15.2 Geology

Site DH447 is located at the foot of the western escarpment of the Richardson Mountains. Based on the surficial geology map from the Yukon Geological Survey, at this site the road runs on fluvial material in its southern area, and on a colluvial deposit in its northern section. Fluvial material usually consists of a well sorted gravelly material (Fig. 3.15.1C), while colluvium is a mix of coarse hetero-granular material in a fine-grained matrix (Fig. 3.15.2). Both types of material are usually coarse in nature, but the content in fine material can be significant, especially in the case of colluvium. The geological map does show the presence of a fine material, clay, relatively close to the road about 2 km southward, at the left-hand site, but none is reported close to DH447.

3.15.3 Aerial imagery/field observation

This section of the road is located between the channels of two creeks which run adjacent to the highway in this site. One creek runs 250 m from the right-hand side (east) of the highway, and the other runs 120 m from the left-hand side (west). These streams likely are the source of the fluvial deposit located south of the site. The site is on an elevated plateau, the road slopes in a southward direction. The aerial imagery does not show landforms relating to the presence and/or degradation of permafrost. In this area ice-wedge polygons are usually apparent, but here their form is muted, with little development of bounding ridges and troughs. Burn et al. (2015) mention that the ground ice may occur as ice wedges or bodies of intrusive ice. No polygonal pattern is visible at this site. If ice wedges are present they would be located within the colluvium (Fig. 3.15.3). There are no apparent periglacial features or processes visible on the aerial imagery.

3.15.4 Borehole geotechnical data

No borehole was drilled at this site, but the site geotechnical materials were observed from the surface. The surficial material is coarse, angular, consisting of blocks and pebbles in a sandy matrix, which is consistent with the surficial geology map. A shallow shovel pit showed that the coarse material was present down to at least 0.7 m. The thaw front was not found at this depth which means that this material could be unfrozen even deeper. As shown in figure 3.15.1C, bedrock can occur close to the surface.

3.15.5 Ground temperature

No ground temperature data were collected at this site.

152

3.15.6   ERT survey

One ERT line was surveyed at DH447 in the field at the right-hand side of the road (Fig 3.15.4). The center of the survey line was aligned with the major tension cracks in the right-hand side of the embankment. Other tension cracks were observed north of this point, but not south.

The line was surveyed with Wenner and dipole-dipole ERT arrays. For each array, two profiles are shown; the first is produced using a robust inversion, and the second is created with a smoothness constraint in the inversion process. The robust inversion is typically used when sharp boundaries are expected, like in between ice and unfrozen ground, while a smoothness constraint tends to ensure that the resulting model shows a smooth variation in the resistivity values, usually producing a model with a larger apparent resistivity RMS error.

Both Wenner and dipole-dipole surveys show relatively similar results, with slightly better-defined boundaries with the dipole-dipole array, and slightly higher value in the resistivity spectrum scale. The robust inversion provides the sharpest boundaries for both arrays.

The substrate shows low resistivity values, less than 500 Ohm·m (Fig 3.15.4, red/orange colours), below 7-8 m depth. This could indicate unfrozen material, or material that is ice-poor, maybe bedrock.

Above the depth of 7-8 m, the south half of the profile shows slightly more highly-resistive material; while the north end of the profile shows several areas with higher-resistivity values, the most significant being located between 100 and 130 m of the survey length.

These high-resistivity areas could mark the presence of ground ice. Based on the surficial geology map, they are mostly located in the colluvium. Their occurrence matches the location of the observed tension cracks.

3.15.7   Synthesis

Field observations and the ERT survey suggest that the ground at DH447 is not especially thaw sensitive. The soil appears to be coarse in general and unfrozen below 8 m. Some ice-rich areas are apparent in the northern half of the ERT surveys. The nature of this ice is unclear due to the absence of any periglacial indicators. As it is within the colluvium, the ice could be ice wedges, but no polygonal ground was observed. It could also be intrusive ice, built from ground water movement. No active processes such as frost heave or thermal cracking were reported.

Based on observations at other neighbouring sites, permafrost is likely warm and thin. Its thaw at this site should be relatively fast with only localized effects.
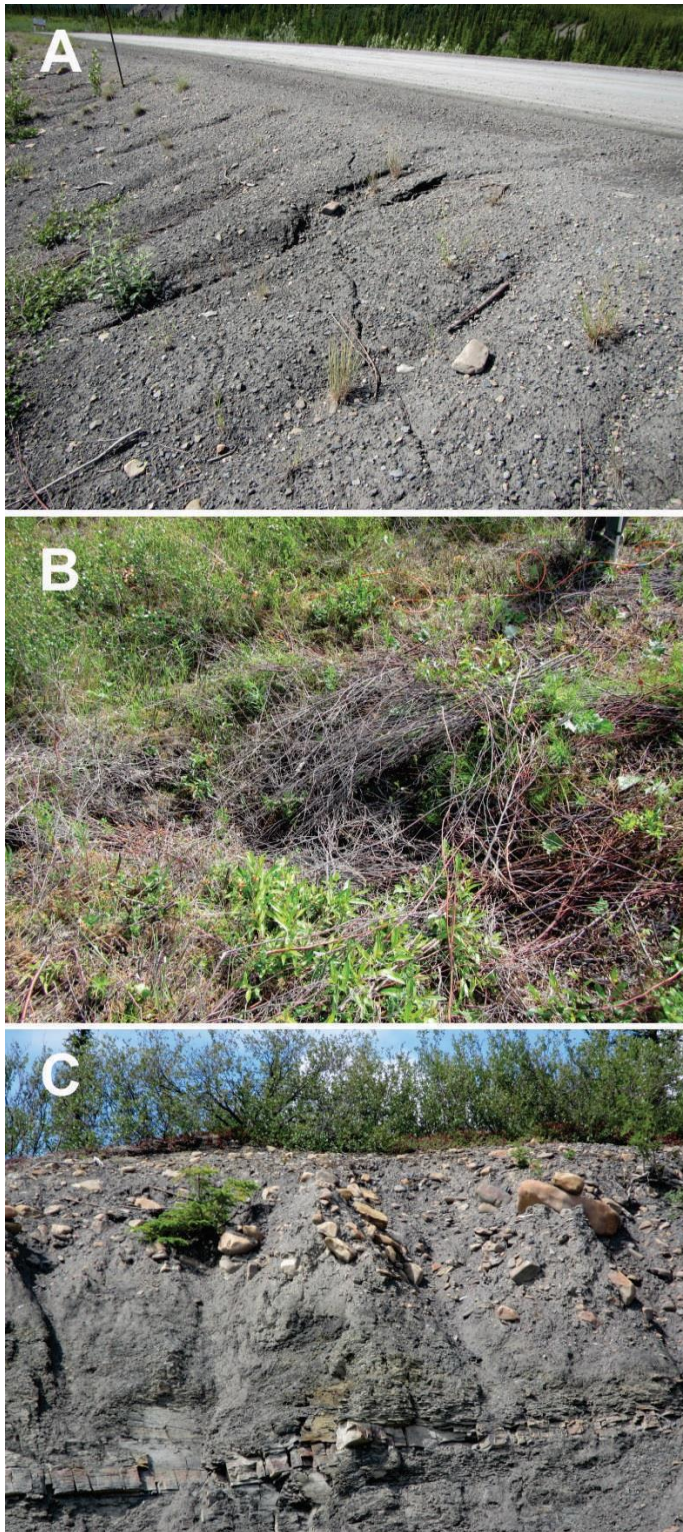
Figure 3.15.1 Observations at site DH447. A- Cracks in shoulder; B- Crevices in field; and C- Section showing fluvial sediment over bedrock.
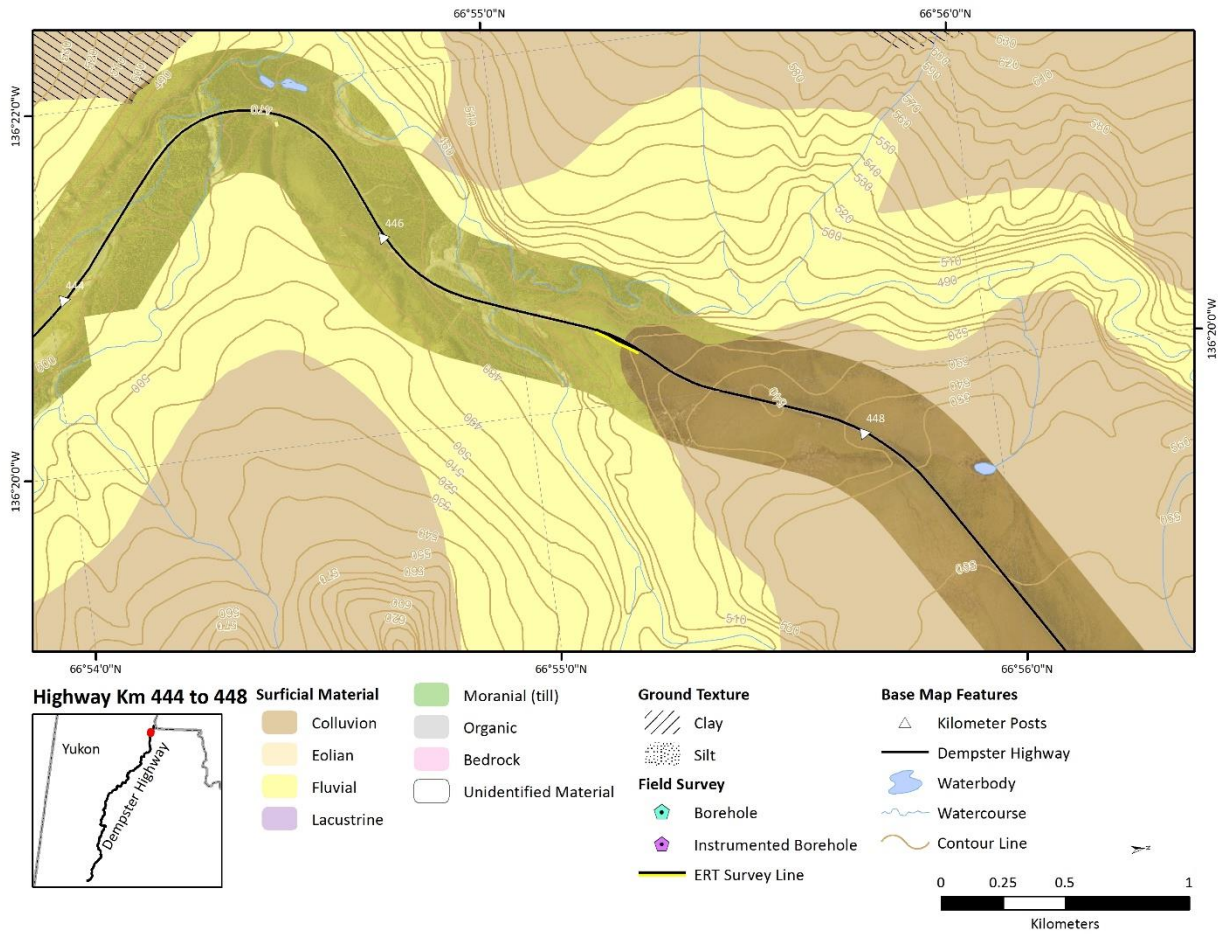
Figure 3.15.2 Surficial geology map of the site 15 DH447 area.

Figure 3.15.3 Aerial view of site DH447.
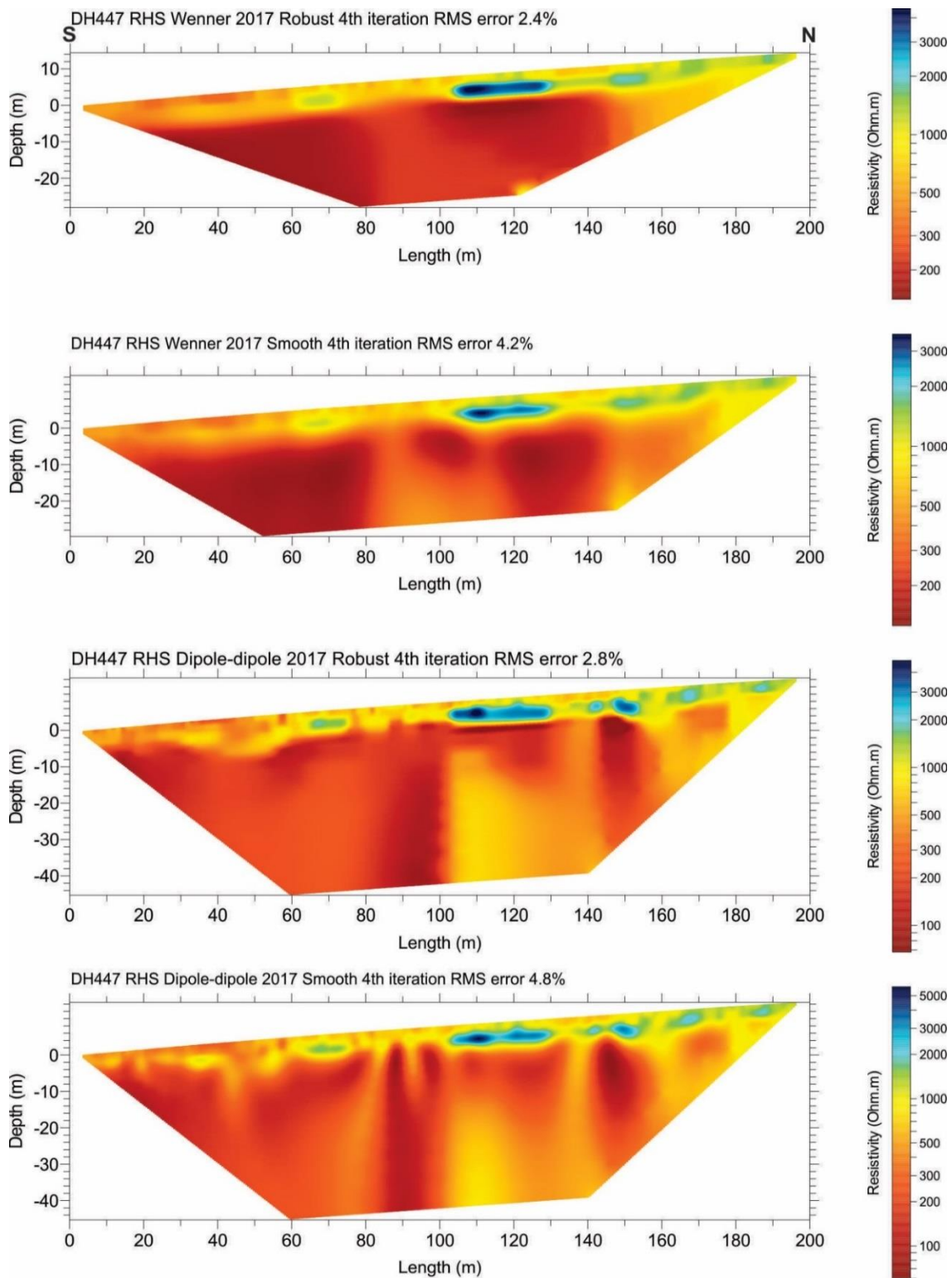
Figure 3.15.4 Wenner and dipole-dipole ERT surveys at site DH447, right-hand side (RHS), using robust and smoothed inversion processes.

3.16   SITE 16: DH454 – KM 454

Issues

- Major subsidence

- Tension cracks in the shoulder

- Ponding at the toe of the embankment

- Thaw lakes in the area

Summary of Findings

- The ground at DH454 could be thaw-sensitive due to the presence of ground ice, the nature of which is both wedge ice and segregated ice.

- It is hypothesized that previous excavations in the north end of the site removed thermal protections of affected ice wedges, leading to thawing and localized water flow, surface ponding, and thermal degradation of nearby permafrost.

3.16.1   Introduction

This site is located at km 454, 7 km north of the previous site (DH447), in the Richardson Mountains, a physiographic unit between km 405 and 492. In this unit, thaw settlement has been identified as the principal permafrost-related geohazard (Burn et al. 2015). Subsidence of the embankment due to thaw of ground ice is the principal hazard in this section.

HPW has reported major subsidence issues at this location. At the time of the survey, tension cracks were observed on the shoulders of the embankment. The process seems to be especially active on the right-hand side (Fig. 3.16.1A). Water ponding, likely due to permafrost thaw, was observed at the toe of the road on the right-hand side (Fig. 3.16.1B), and about 30 m from the road, an ice wedge polygon has already greatly degraded, with some water ponding in the formed depression (Fig. 3.16.1C). The field survey for the site consisted of one ERT survey in the field parallel to the road, right-hand side, performed using both Wenner and dipole-dipole arrays, and one shallow borehole drilled in the field, a few meters from the ERT survey at the approximate mid-point.

3.16.2   Geology

Site DH454 is located at the foot of the western escarpment of the Richardson Mountains. Based on the surficial geology map from the Yukon Geological Survey, at this site the road runs on colluvium, a mix of coarse hetero-granular material in a fine-grained matrix (Fig. 3.16.2). Both types of material are usually coarse in nature, yet the content of fine material can be significant. The geological map does show the presence of fine material, clay, relatively close to the road about 0.6-0.7 km to the south.

3.16.3   Aerial imagery/field observation

Several landforms are visible on the aerial imagery (Fig. 3.16.3). The most notable feature is a degraded polygon field located at the right-hand side of the road, starting about 30 m from the toe of the embankment. Depressions have formed in the troughs, leaving the center of the polygons standing at about similar ground level to that of unaffected areas. The difference of elevation between the top of the center of the polygon, and the bottom of the deepest depression (where a pond has formed, Fig. 3.16.1C) is 2.2 m. It can be assumed that this elevation represents the height of the now thawed ice wedges.

Except for areas where the ice wedges are degrading, polygons are hardly visible. In this area ice-wedge polygons are usually apparent, but their form is muted, with little development of bounding ridges and troughs. Their surface expression may be covered by material deposited by hill slope movement during the extensive unglaciated period (Burn et al. 2015).

A thaw lake is visible at the left-hand side, and another smaller one is seen at the right-hand side. The left-hand side lake has angular borders, being polygonal in shape, and is likely due to the degradation of ice wedges. Finally, mud boils (AKA frost boils) are present in the field, at both sides of the road. These are upwellings of mud that occur through frost heave and cryoturbation in permafrost areas; groups of them being visible north of the site. There are good indicators of a fine-grained, frost-susceptible material, i.e. potentially ice-rich ground.

Looking at a broader scale, there seems to be a degradation trend mainly following a downslope north-south axis. It seems to start from an excavated area at the left-hand side, swing to cross the road where the thaw lakes are present, and then end in the degrading polygons at the right-hand side.

160

3.16.4 Borehole geotechnical data

The Borehole DH454 BH1 was drilled in the field at the right-hand side, cores being collected down to 2.76 m depth. The thaw front was at 28 cm depth at the time of the drilling (July 2nd, 2017). The log (Fig. 3.16.4) shows a 0.30 m organic layer followed by a gray silty sand down to approximately 1 m depth. Below, the sediment becomes a silt with gravel and sand, and then changes to a silty sand again. The borehole ends in the gravel with silt and sand. Centimeter-scale ice lenses are visible at about 0.3 m depth, likely the location of the top of permafrost, the cryostructure being ice-rich and suspended along most of the profile. Volumetric excess ice content ranges from 14 to 62%. Overall, the borehole has a mean volumetric excess ice content of 44%. The soil is thaw sensitive down to the lowest investigated depth.

3.16.5 Ground temperature

Borehole DH454-BH1 was lined with PVC piping and instrumented with one 4-channel Hobo loggers to ground temperatures at 0, 0.5, 1.5, and 2.75 m depths. Ground temperature were recorded from July 4th to September 17th, 2017, the date of the last downloading (Fig. 3.16.5). Although very partial with a two-month monitoring, the record shows that from July 15th to September 15th, the ground temperature at the deepest 2.75 m depth warms from -2.3 to -1.6 °C. The active layer has a thickness of 100 cm on September 15th. Based on this partial record, permafrost seems relatively cold with temperature below -2.0 °C.

3.16.6 ERT survey

One ERT line was surveyed parallel to the road at DH454, in the field at the right-hand side, (Fig. 3.16.6). The center of the survey line was aligned with the major polygon degradation in the field.

The line was surveyed with Wenner and dipole-dipole ERT arrays. For each array, two profiles are shown, the first is produced using a robust inversion, and the second is created with a smoothness constraint in the inversion process. The robust inversion is typically used when sharp boundaries are expected, like in between ice and unfrozen ground, while a smoothness constraint tends to ensure that the resulting model shows a smooth variation in the resistivity values, usually producing a model with a larger apparent resistivity RMS error.

Both Wenner and dipole-dipole surveys show relatively similar results, with slightly better-defined boundaries with the dipole-dipole array, and slightly higher value in the resistivity spectrum scale. The robust inversion provides the sharpest boundaries for both arrays.

In general, highly resistive areas (shown as blue shades) are present in the first 7-8 m depth of the profile. These resistive zones are likely ice wedge complexes. The dipole-dipole array shows them more distinctly than the Wenner array.

Deeper in the profile the ground resistivity decreases. In the Wenner array, the northern part of the profile shows the lowest resistivity values in a single consolidated low-resistivity area. In the dipole-dipole surveys, things are more complex; several low-resistivity areas are present, concentrated mainly in the northern section. Deeper in the profile, below 25 m, a high-resistivity area is apparent in the middle of the survey.

The low-resistivity values (less than 700 Ohm·m, shown as red/orange), could indicate unfrozen or ice-poor material. In the dipole-dipole array, the low-resistivity areas could also relate to unfrozen groundwater.

The high-resistivity areas could be the markers of the presence of ground ice, yet it looks unlikely with the deepest areas. All together the results suggest a warming of the northern section of the survey area, likely driven by ground water movement.

3.16.7   Synthesis

Field observations, borehole data, and the ERT survey suggest that the ground at DH454 could be thaw-sensitive due to the presence of ground ice. The ice thickness is up to 2.2 m. The soil is generally coarse, and the permafrost temperature could be as cold as -2 °C or lower.

The nature of the ground ice is both wedge ice and segregated ice, as observed in the cores. The cause for the low resistivity values shown by dipole-dipole array in the deepest part on the profile is unclear: possibly more ice or frozen bedrock.

A hypothesis to explain the unusual resistivity profile observed at site DH454 is that material was excavated in the north end of the site, which was covering and protecting some ice wedges. Once uncovered, the ice wedges started to degrade. Runoff water from the wedge ice was channelized, and the degradation progressed underground, yet close to the surface, flowing to the south, forming thaw lakes, crossing through the road embankment and finding an outlet in the field where polygons are heavily degraded. There the run-off water connected with existing water tracks oriented with the slope.
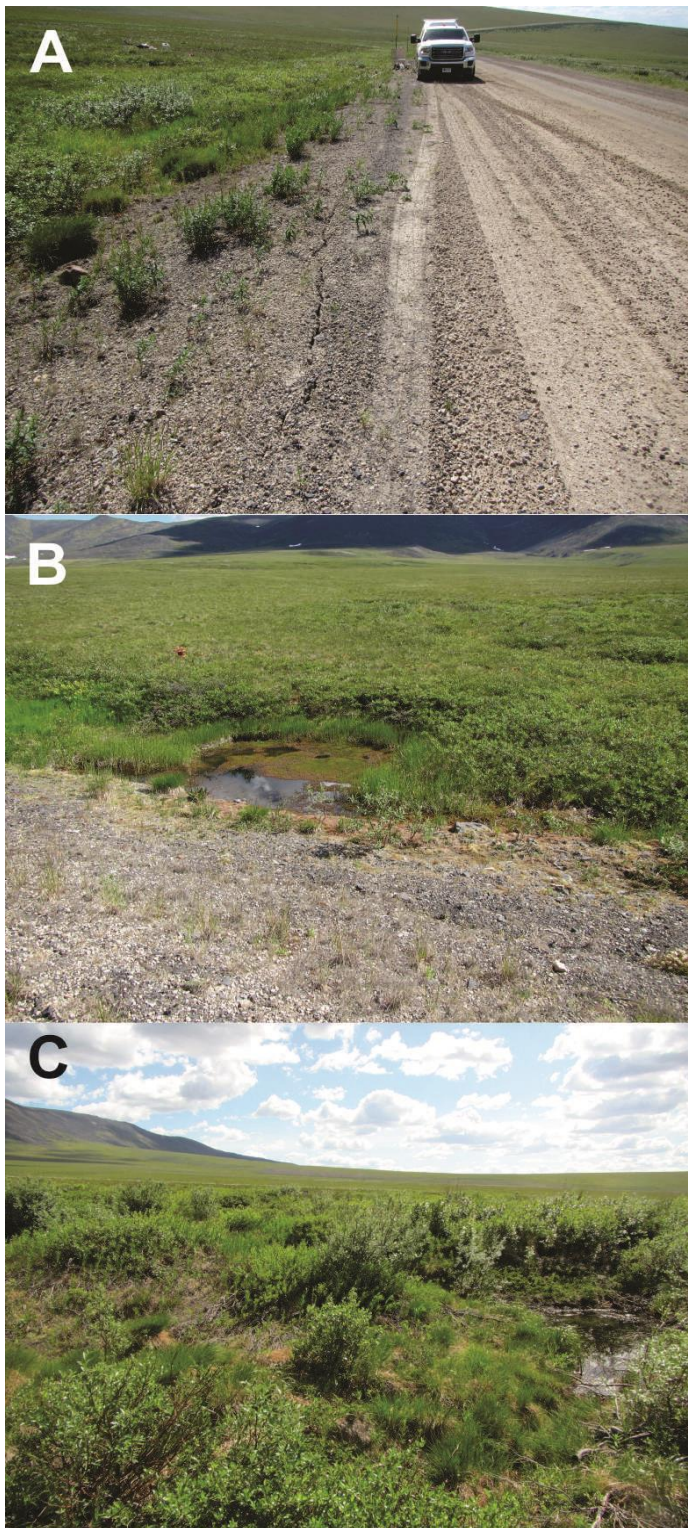
Figure 3.16.1 Observations at site DH454: A- cracks in the shoulder; B- ponding at the toe of the road; and, C- degraded ice-wedge polygons.
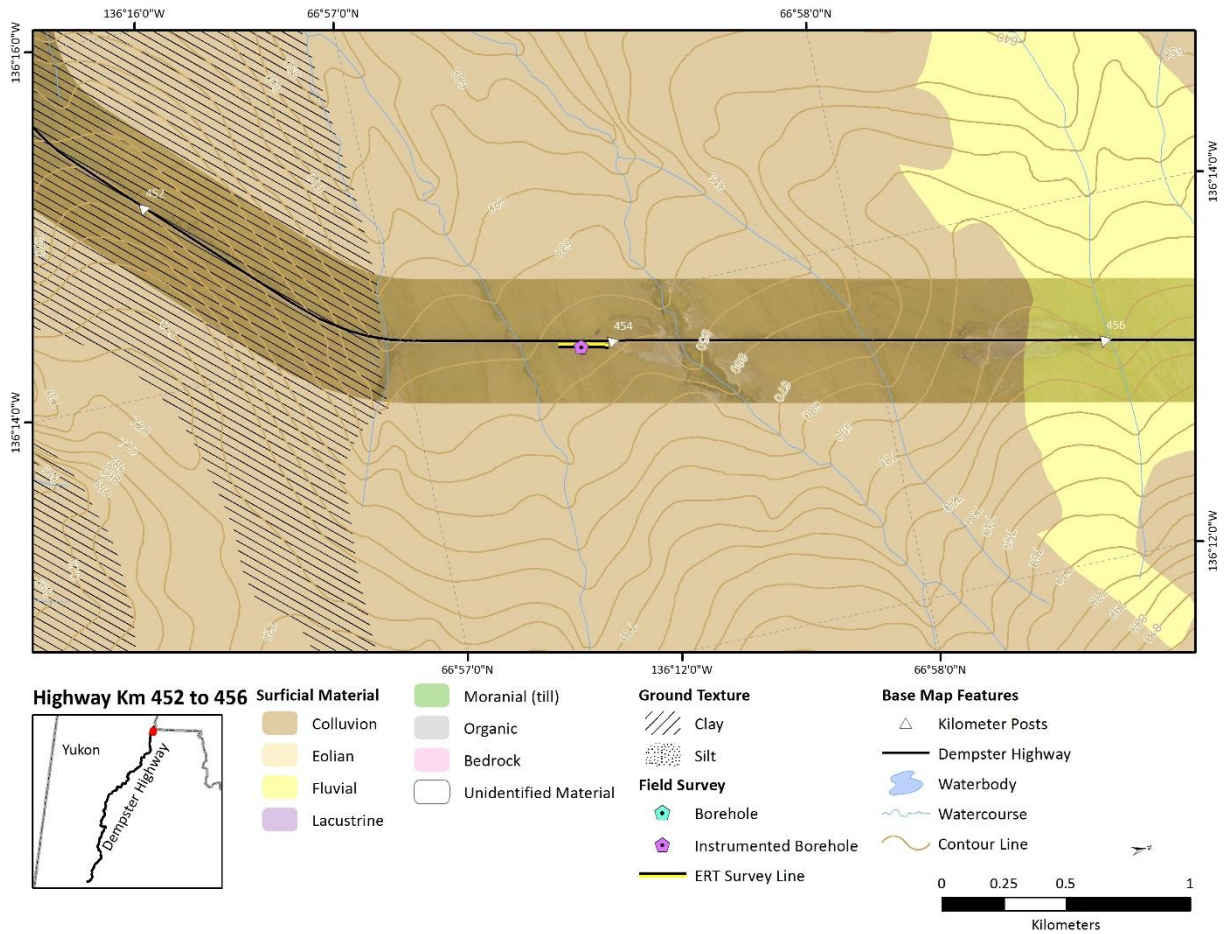
Figure 3.16.2 Surficial geology map of the site 16 DH454 area.
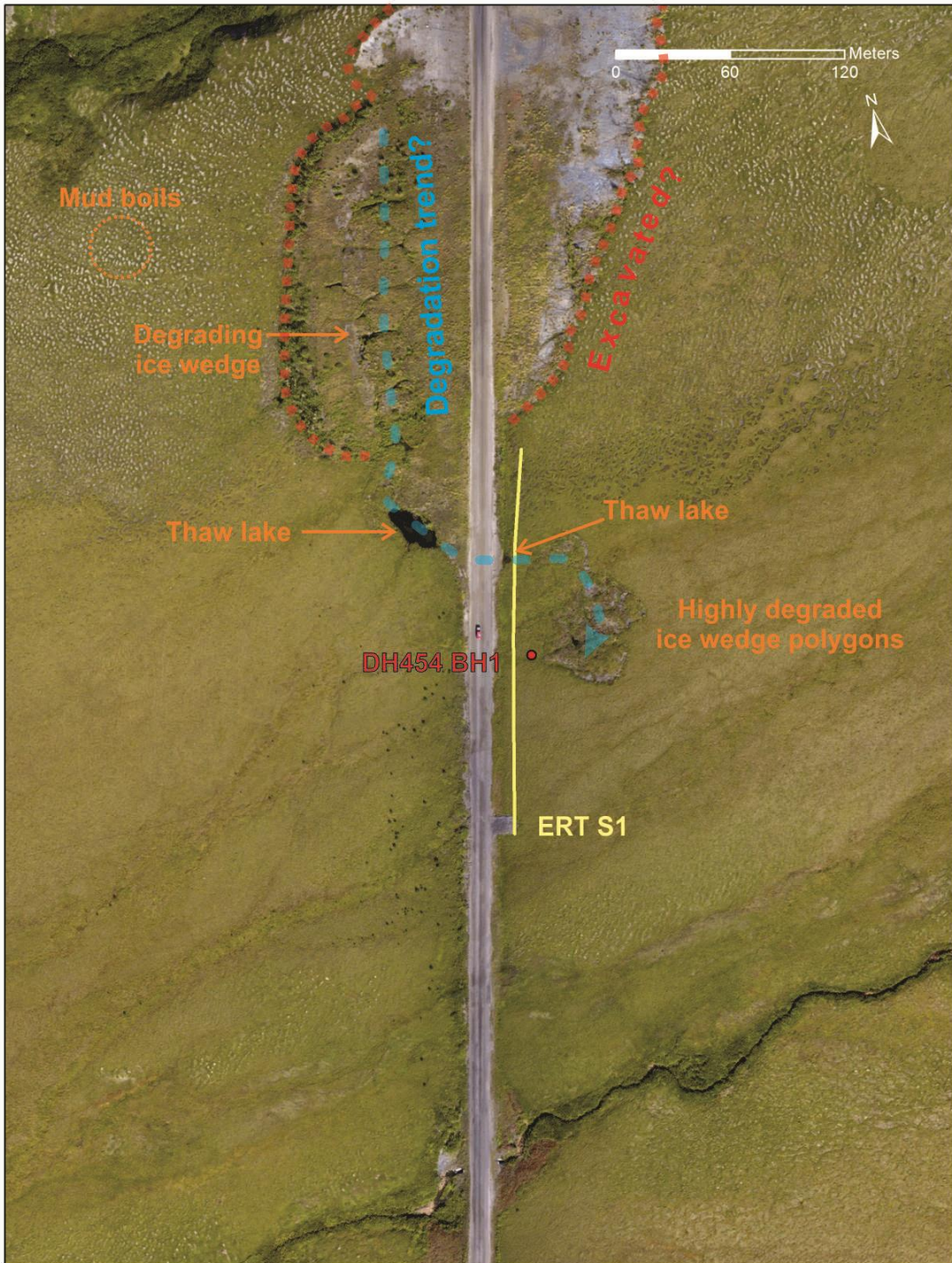
Figure 3.16.3 Aerial view of site DH454.
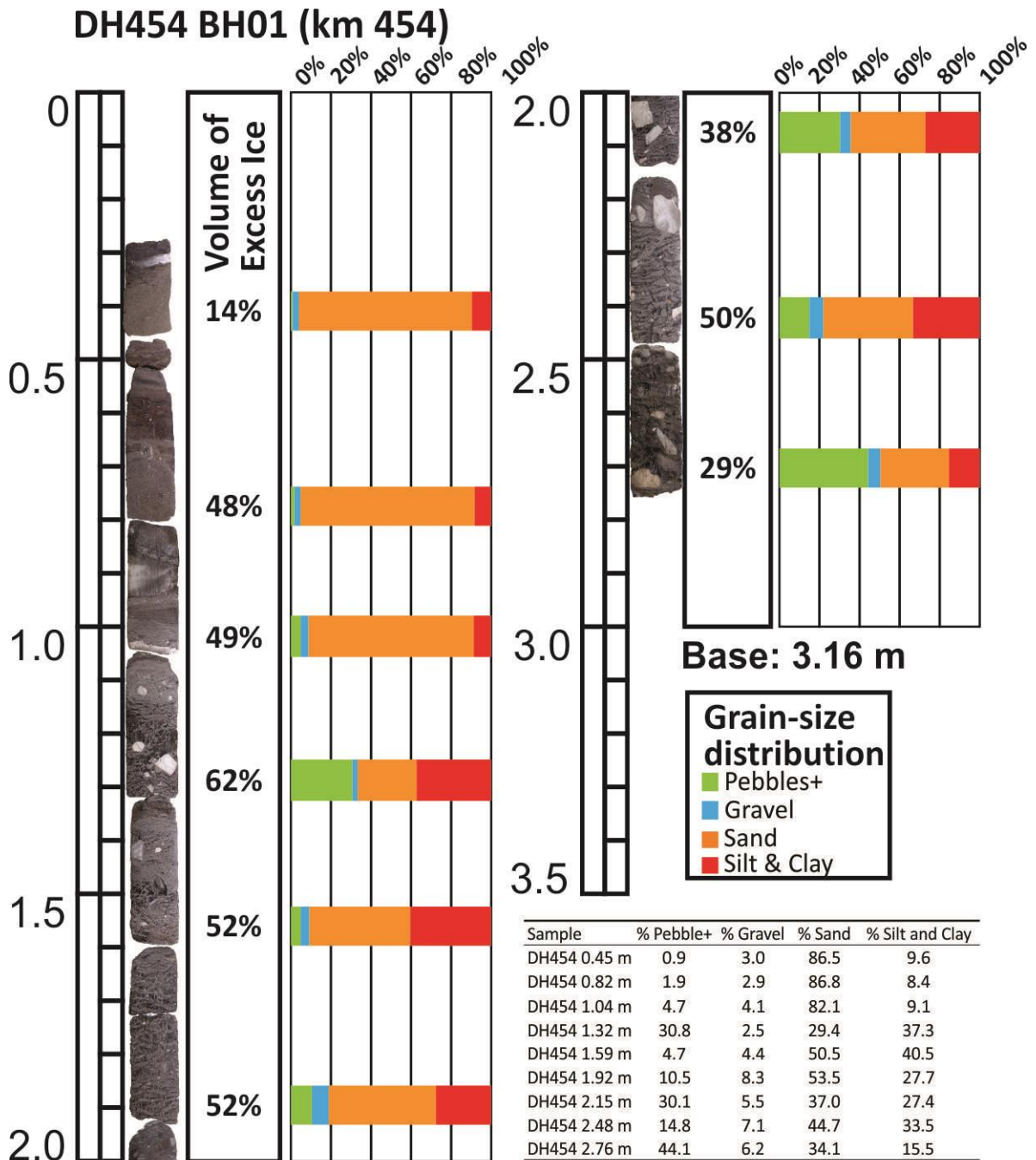
Figure 3.16.4 Logs of borehole DH454 BH1, with volumetric excess ice content and grain size distribution.

Sample	% Pebble+	% Gravel	% Sand	% Silt and Clay
DH454 0.45 m	0.9	3.0	86.5	9.6
DH454 0.82 m	1.9	2.9	86.8	8.4
DH454 1.04 m	4.7	4.1	82.1	9.1
DH454 1.32 m	30.8	2.5	29.4	37.3
DH454 1.59 m	4.7	4.4	50.5	40.5
DH454 1.92 m	10.5	8.3	53.5	27.7
DH454 2.15 m	30.1	5.5	37.0	27.4
DH454 2.48 m	14.8	7.1	44.7	33.5
DH454 2.76 m	44.1	6.2	34.1	15.5
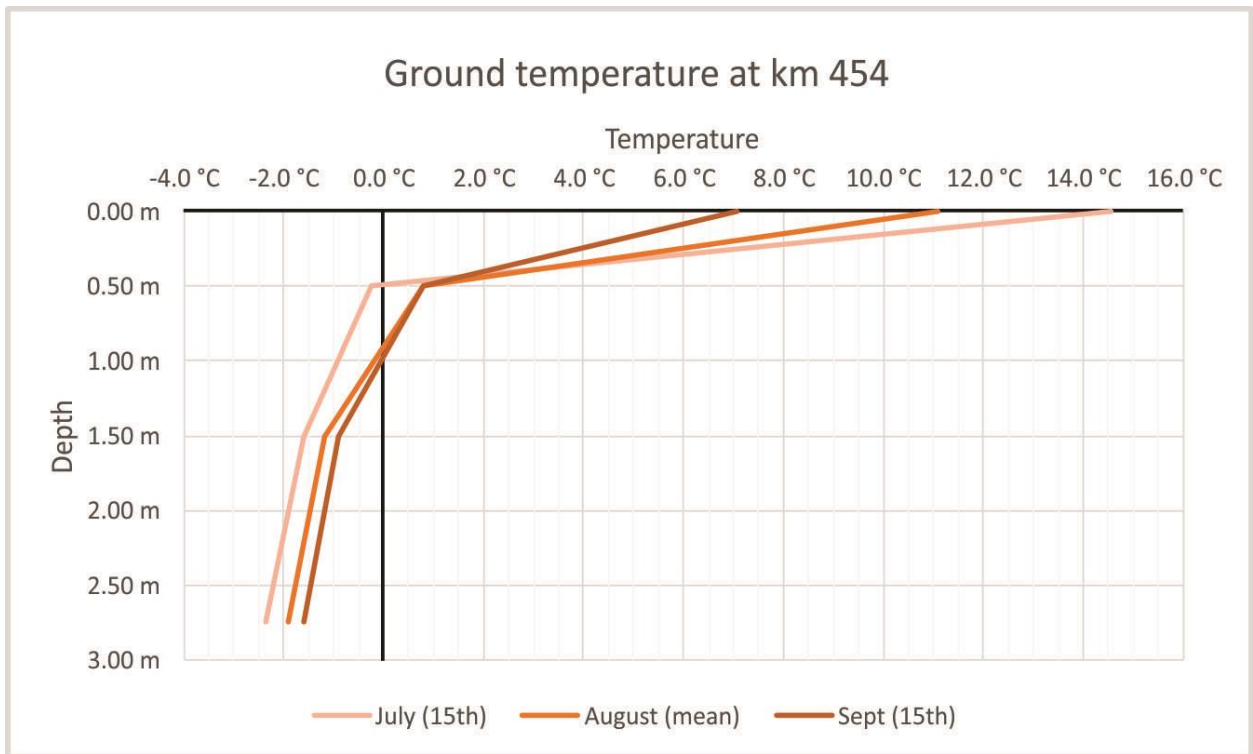
Depth	July (15th)	August (mean)	Sept (15th)
0.00 m	14.6 °C	11.1 °C	7.1 °C
0.50 m	-0.3 °C	0.8 °C	0.8 °C
1.50 m	-1.6 °C	-1.2 °C	-0.9 °C
2.75 m	-2.3 °C	-1.9 °C	-1.6 °C

Figure 3.16.5 Ground temperature at site DH454, based on a record from July 2017 to September 2017.
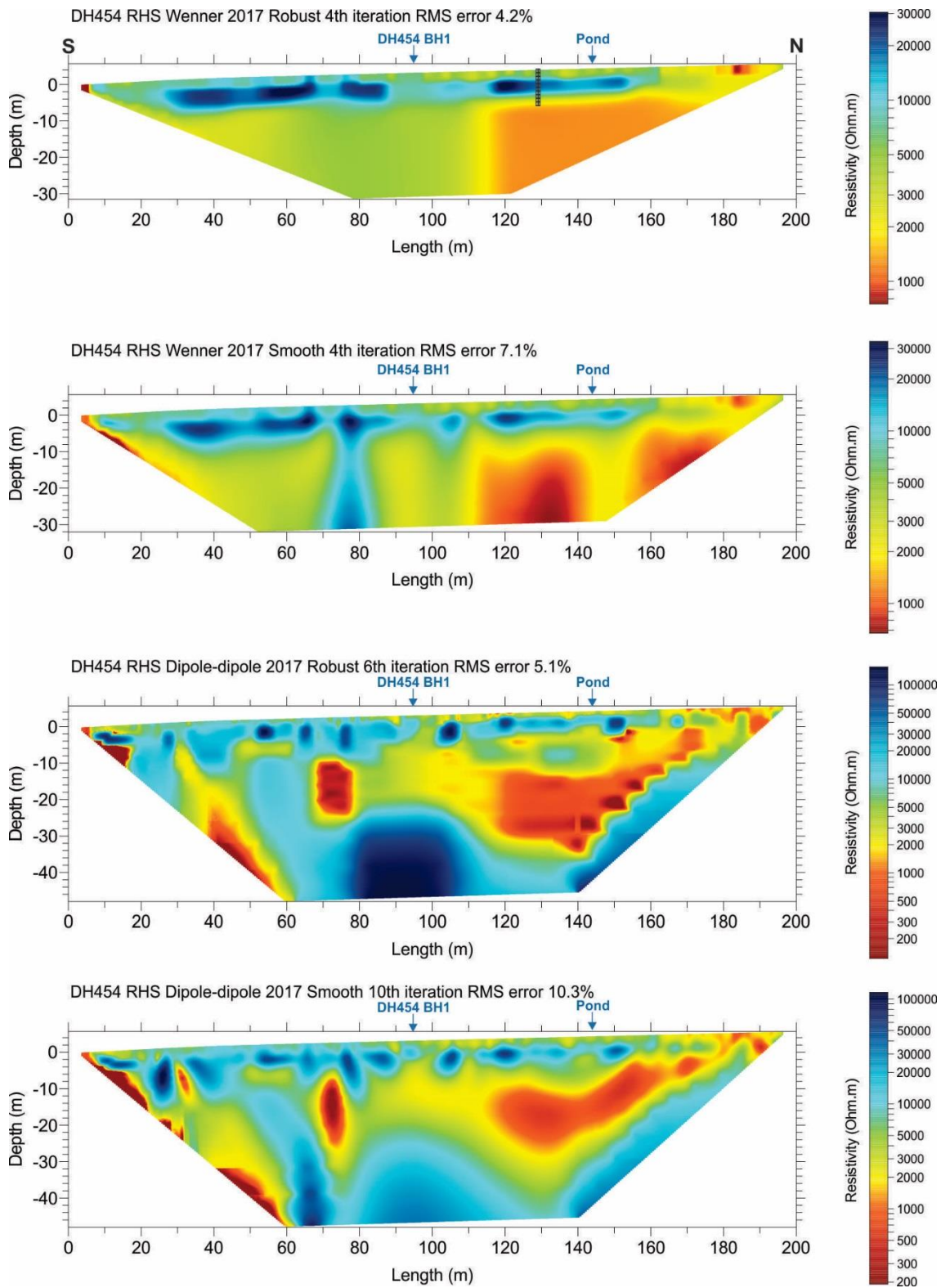
Figure 3.16.6 Wenner and dipole-dipole ERT surveys at site DH454, right-hand side (RHS), using robust and smoothed inversion processes.

3.17   SITE 17: DH458 – KM 458

Issues

- Major sinkholes

Summary of Findings

- the ground at DH458 could be thaw sensitive due to the presence of ground ice relatively close to the surface.

- Only segregated ice was observed in the cores; no evidence of wedge ice was found.

- Subsidence could be caused by a combination of ground ice thaw and fine sediment leaching through groundwater movement.

3.17.1   Introduction

This site is located at km 458, 4 km north of the previous site (DH454), in the Richardson Mountains, a physiographic unit between km 405 and 492. In this unit, thaw settlement has been identified as the principal permafrost-related geohazard (Burn et al. 2015). Subsidence of the embankment due to thaw of ground ice is the principal hazard in this section.

HPW has reported major sinkhole issues at this location. At the time of the survey, tension cracks and indicators of subsidence were observed on both sides of the embankment (Fig. 3.17.1A). Runoff water flows on the surface, at the right-hand side, and is collected by a culvert (Fig. 3.17.1B). On the left-hand side, a V-shaped depression has formed at the foot of the embankment. As of September 28th, 2017, snow was accumulating on the left-hand shoulder at this site, and in the V-shaped depression, but was not present on the right-hand side (Fig. 3.17.1C).

For this site, the field survey consisted of one ERT survey parallel to the road in the field, right-hand side, performed using both Wenner and dipole-dipole arrays. One shallow borehole was drilled in the field, at the approximate mid-point of the ERT survey.

3.17.2   Geology

Site DH454 is located at the foot of the western escarpment of the Richardson Mountains. Based on the surficial geology map from the Yukon Geological Survey, at this site the road runs

on colluvium, a mix of coarse hetero-granular material in a fine-grained matrix (Fig. 3.17.2). A creek runs crosses perpendicularly to the highway, passing through a culvert.

3.17.3   Aerial imagery/field observation

The aerial imagery from the site (Fig. 17.3) shows a wet area at the right-hand side where the creek crosses the road, as well as the V-shaped depression that has formed at the left-hand side. Shrub vegetation has established in the depression, likely because of the protective effect of the snow accumulating there.

Frost boils are present in the field at both side of the road. These are upwellings of mud that occur through frost heave and cryoturbation in permafrost areas. Groups of the frost boils are visible on the left-hand side, stretched by slope processes. Their presence is an indicator of fine-grained, frost-susceptible material, i.e. potentially ice-rich ground. At this site, stones and pebbles have accumulated on the top of the frost boils, having been cryo-expelled.

 In this area ice-wedge polygons are usually apparent, but here they are barely visible; their form is muted with little development of bounding ridges and troughs. The surface expression of the polygons may be covered by material deposited by hill slope movement during the extensive unglaciated period (Burn et al. 2015). However, their presence is revealed in the aerial imagery by their centers being a paler colour than the encircling troughs, which are usually greener.

3.17.4   Borehole geotechnical data

Borehole DH458 BH1 was drilled in the field at the right-hand side; cores were collected down to 2.29 m depth. The thaw front was at 20 cm depth at the time of the drilling (July 4th, 2017). The log (Fig. 3.17.4) shows a 0.50 m organic layer followed by a brown, organic rich silty sand down to approximately 2 m depth. The borehole ends in a gravel with cobbles. The cryostructure is micro-lenticular with millimeter-scale ice lenses from 0.5 to 1.7 m. Centimeter-scale ice lenses are visible from about 1.7 to 2.0 m depth. Some thick vertical ice lenses are present. Volumetric excess ice content ranges from 11 to 59%. Overall, the borehole has a mean volumetric excess ice content of 28%. The soil is moderately thaw sensitive down to the lowest investigated depth.

3.17.5 Ground temperature

Borehole DH458-BH1 was lined with PVC piping and instrumented with one 4-channel Hobo logger to record ground temperatures at 0, 0.5, 1.0, and 2.3 m depths. Ground temperatures were recorded from July 4th to September 17th, 2017, the date of the last downloading (Fig. 3.17.5). Although very partial with only two months of monitoring, the record shows that from July 15th to September 15th, the ground temperature at the deepest 2.30 m depth warms from -1.9 to -1.2 °C. The active layer has a thickness of about 1 m on September 15th. Based on this partial record, permafrost seems relatively cold with temperature probably less than -2.0 °C.

3.17.6 ERT survey

One ERT line was surveyed at DH458, located in the field, at right-hand side, 6-7 m away from and running parallel to the road (Fig. 3.17.6). The center of the survey line was located at the mid-point between the two culverts, to allow the deepest ERT assessment of the disturbed area.

The line was surveyed with Wenner and dipole-dipole ERT arrays. For each array, two profiles are shown; the first is produced using a robust inversion, and the second is created with a smoothness constraint in the inversion process. The robust inversion is typically used when sharp boundaries are expected, like in between ice and unfrozen ground, while a smoothness constraint tends to ensure that the resulting model shows a smooth variation in the resistivity values, usually producing a model with a larger apparent resistivity RMS error.

Both Wenner and dipole-dipole surveys show relatively similar results, with slightly better-defined boundaries with the dipole-dipole array, and slightly higher and lower values in the resistivity spectrum scale. The robust inversion provides the sharpest boundaries for both arrays.

In general, highly resistive areas (shown in blue), are present in the first 6-7 m depths of the profile. This resistive zone likely translates to the presence of ground ice complexes, wedge ice or others. The dipole-dipole seems to show this more distinctly than the Wenner array. Deeper in the profile, the ground resistivity decreases. In the Wenner array, the profile shows a relatively homogenous distribution of low-resistivity values (red/orange colours), with few lower-resistivity areas located just below 7 m (dark red). In the dipole-dipole surveys, the values are also low, but there is lateral and vertical variation, with some areas being lower in resistivity than others.

The low resistivity values, less than 400 or even 600 Ohm·m, could be an indicator of unfrozen material, or warm, ice-poor material. The dipole-dipole array suggests that the low-resistivity readings could also relate to unfrozen ground water.

3.17.7   Synthesis

Field observations, borehole data, and the ERT survey suggest that the ground at DH458 could be thaw sensitive due to the presence of ground ice relatively close to the surface. Ice wedges were not observed, and there is no clear indicator of their presence. However, other types of ground ice may be present, such as segregated ice and intrusive ice. The soil appears to be generally coarse, and the permafrost temperature could be as cold as -2 °C or lower.

Only segregated ice was observed in the cores, and the ERT survey suggests a limited vertical extent of the ice-rich material. Subsidence could be caused by a combination of ground ice thaw and fine sediment leaching through groundwater movement. Similar processes have been observed in DH82.
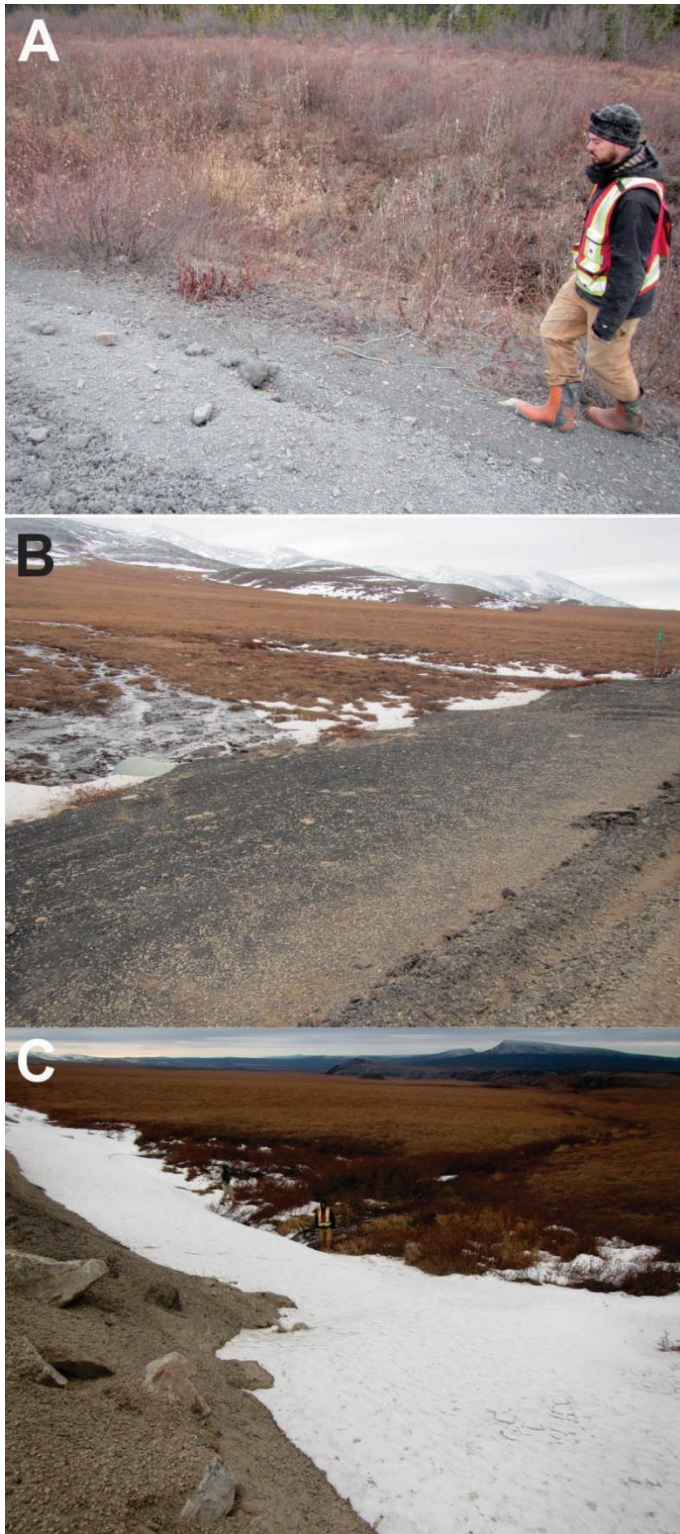
Figure 3.17.1 Observations at site DH458. A- Cracks in shoulder; B- water running on the ground surface on the right-hand side; and C- V-shaped depression filled with snow on the left-hand side.
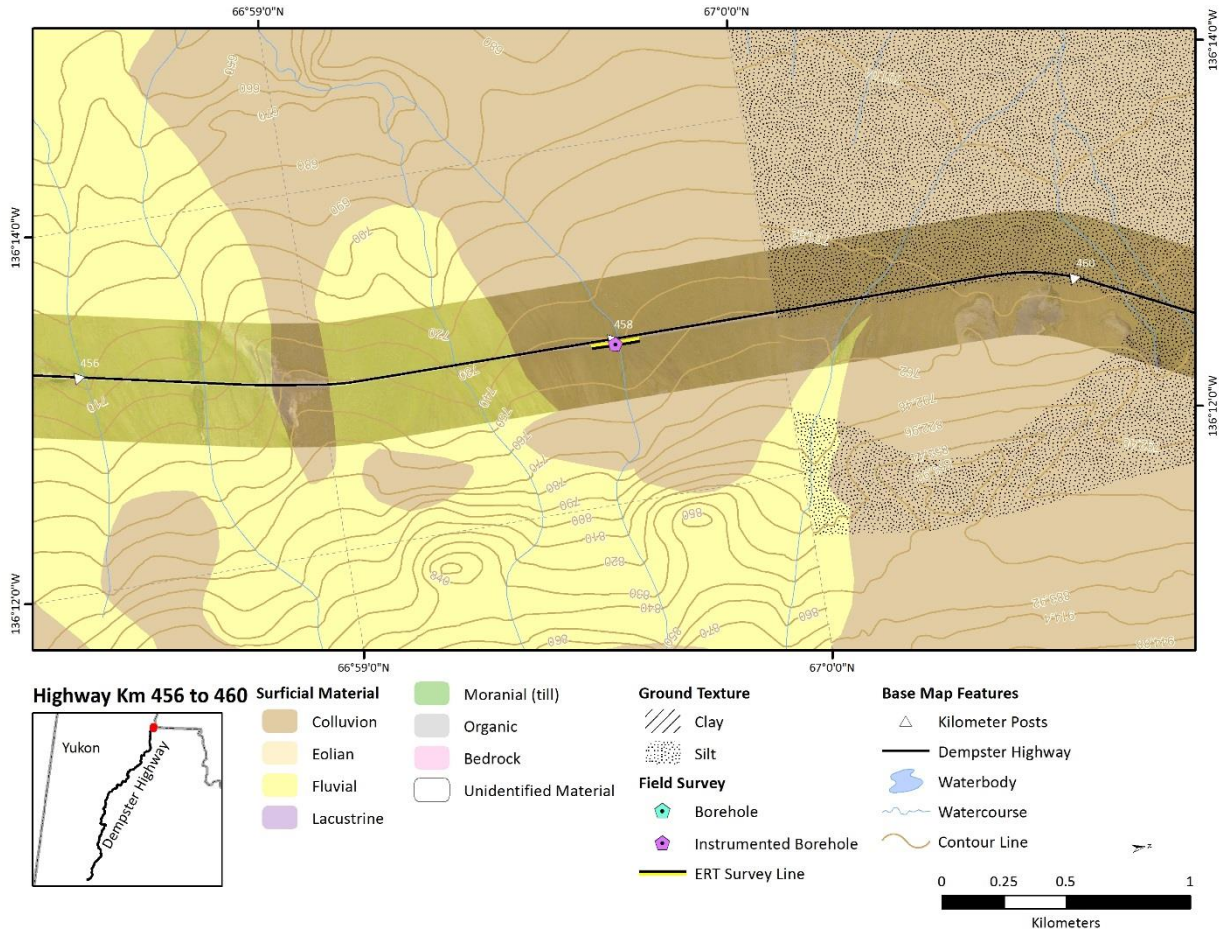
Figure 3.17.2 Surficial geology map of Site 17 DH458 area.
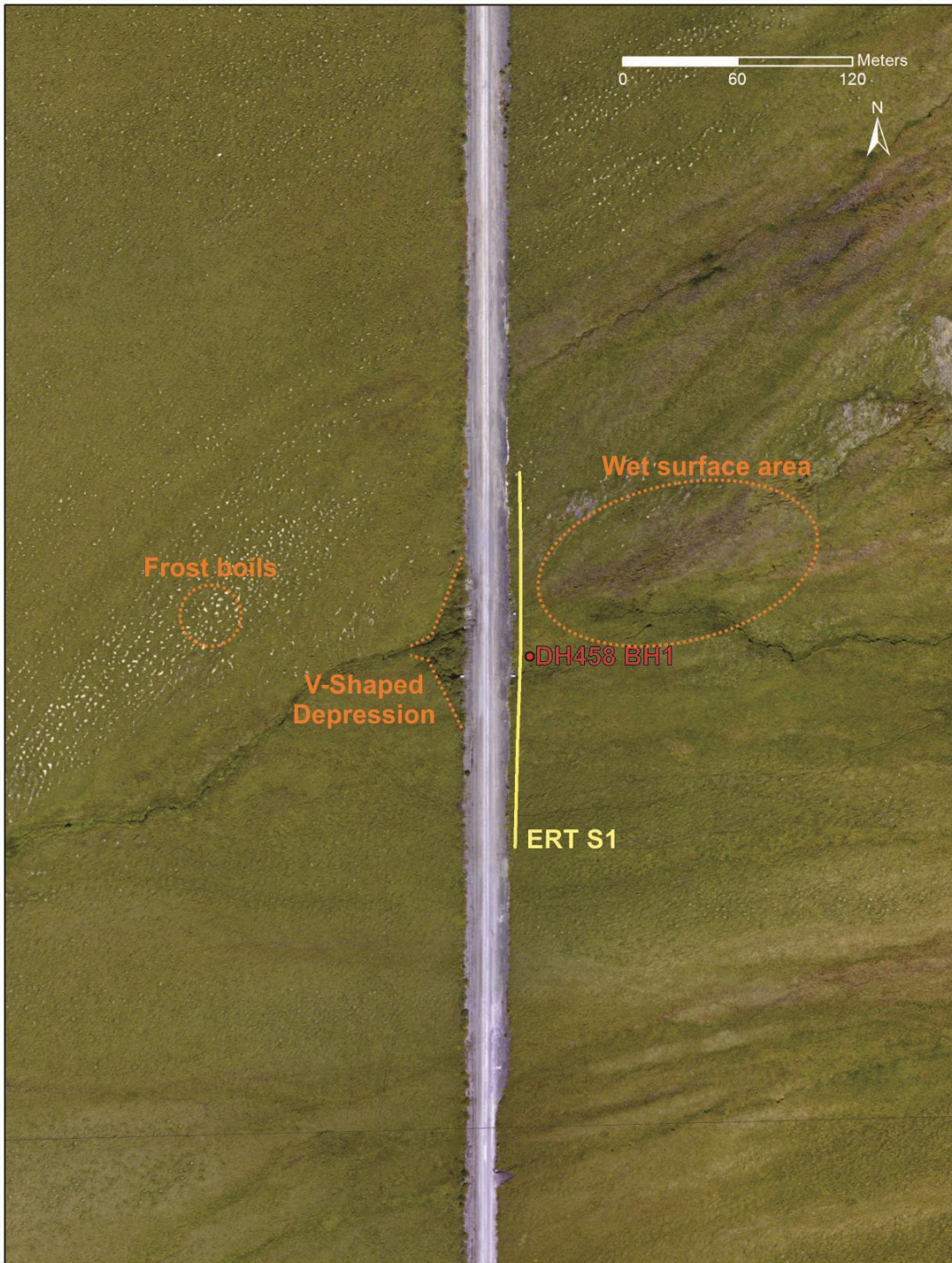
Figure 3.17.3 Aerial view from site DH458.
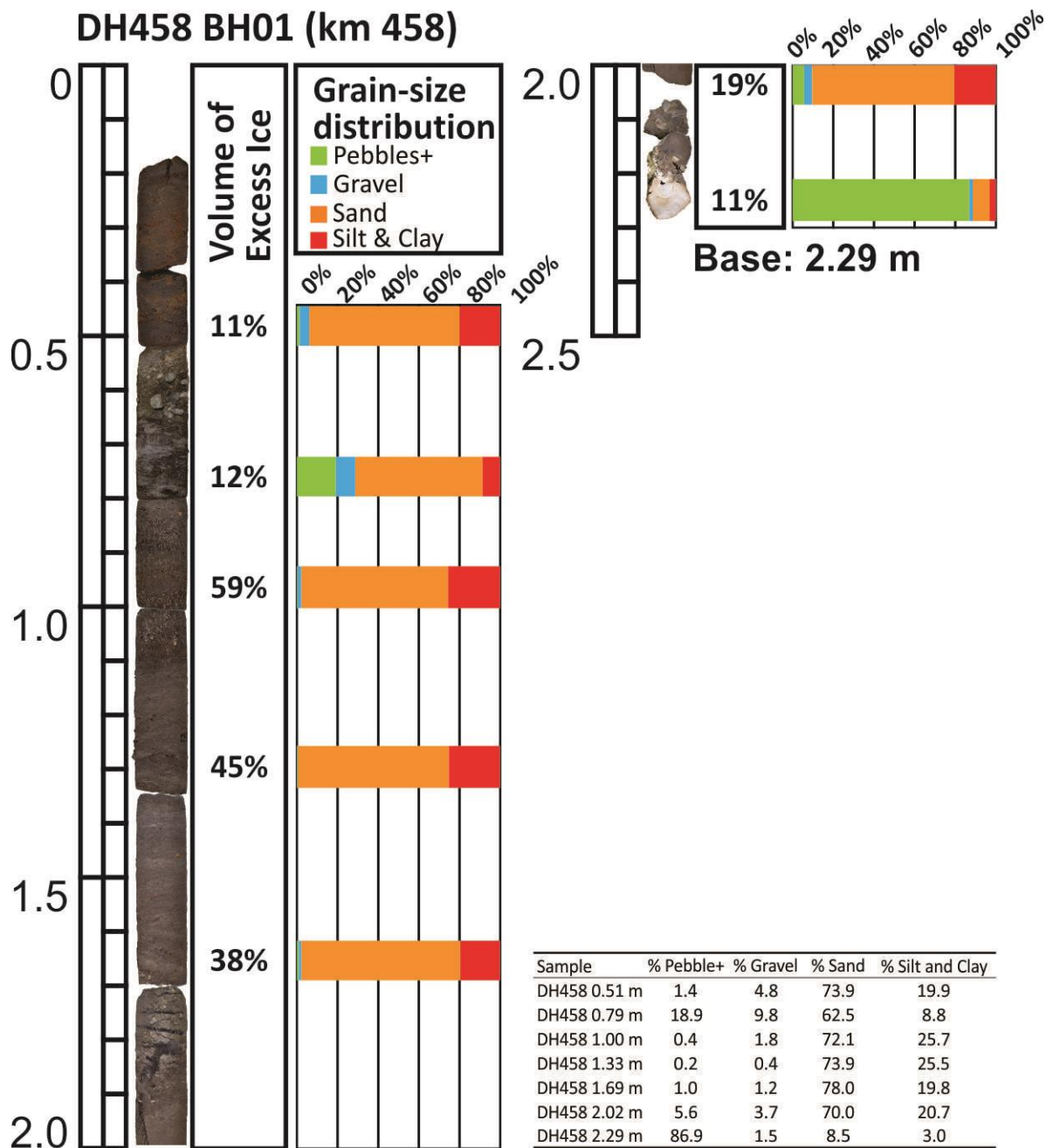
Figure 3.17.4 Logs of borehole DH458 BH1, with volumetric excess ice content and grain size distribution.

Sample	% Pebble+	% Gravel	% Sand	% Silt and Clay
DH458 0.51 m	1.4	4.8	73.9	19.9
DH458 0.79 m	18.9	9.8	62.5	8.8
DH458 1.00 m	0.4	1.8	72.1	25.7
DH458 1.33 m	0.2	0.4	73.9	25.5
DH458 1.69 m	1.0	1.2	78.0	19.8
DH458 2.02 m	5.6	3.7	70.0	20.7
DH458 2.29 m	86.9	1.5	8.5	3.0

Figure 3.17.5 Ground temperature at site DH458, based on a record from July 2017 to September 2017.
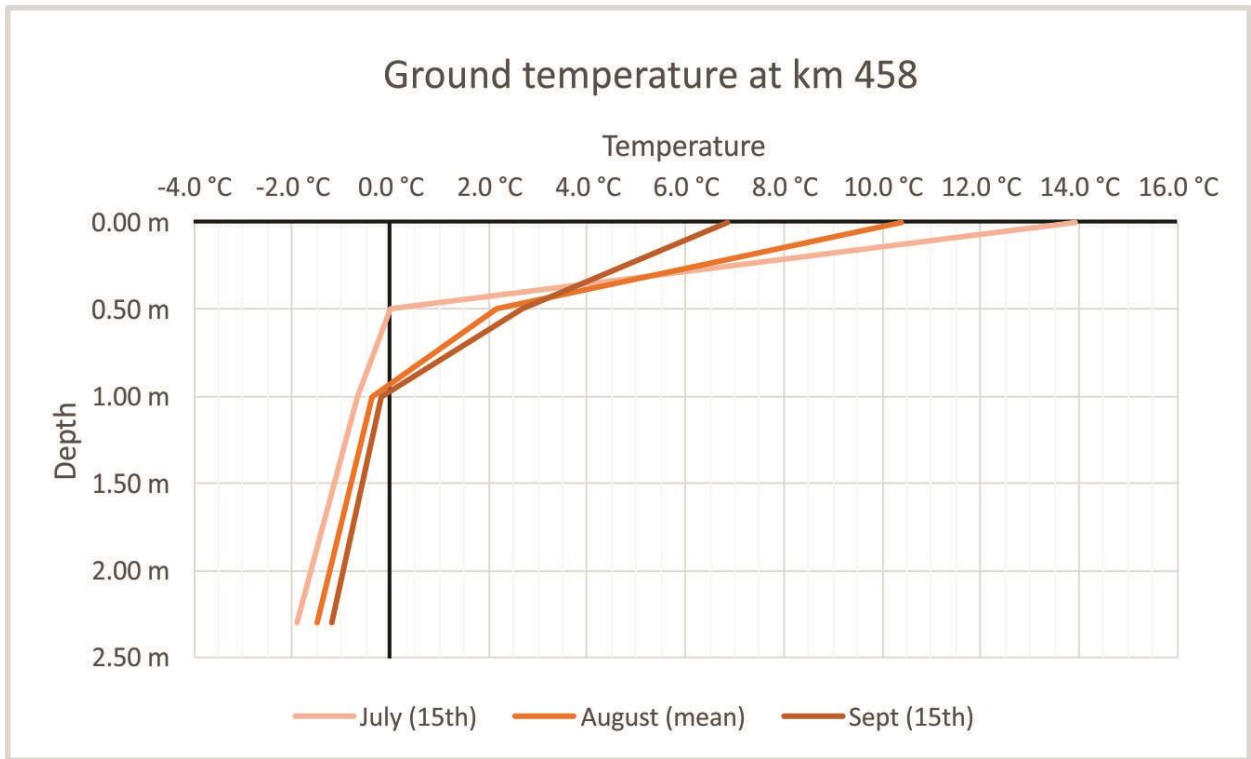
Depth	July (15th)	August (mean)	Sept (15th)
0.00 m	13.9 °C	10.4 °C	6.8 °C
0.50 m	0.0 °C	2.2 °C	2.7 °C
1.00 m	-0.7 °C	-0.4 °C	-0.2 °C
2.30 m	-1.9 °C	-1.5 °C	-1.2 °C
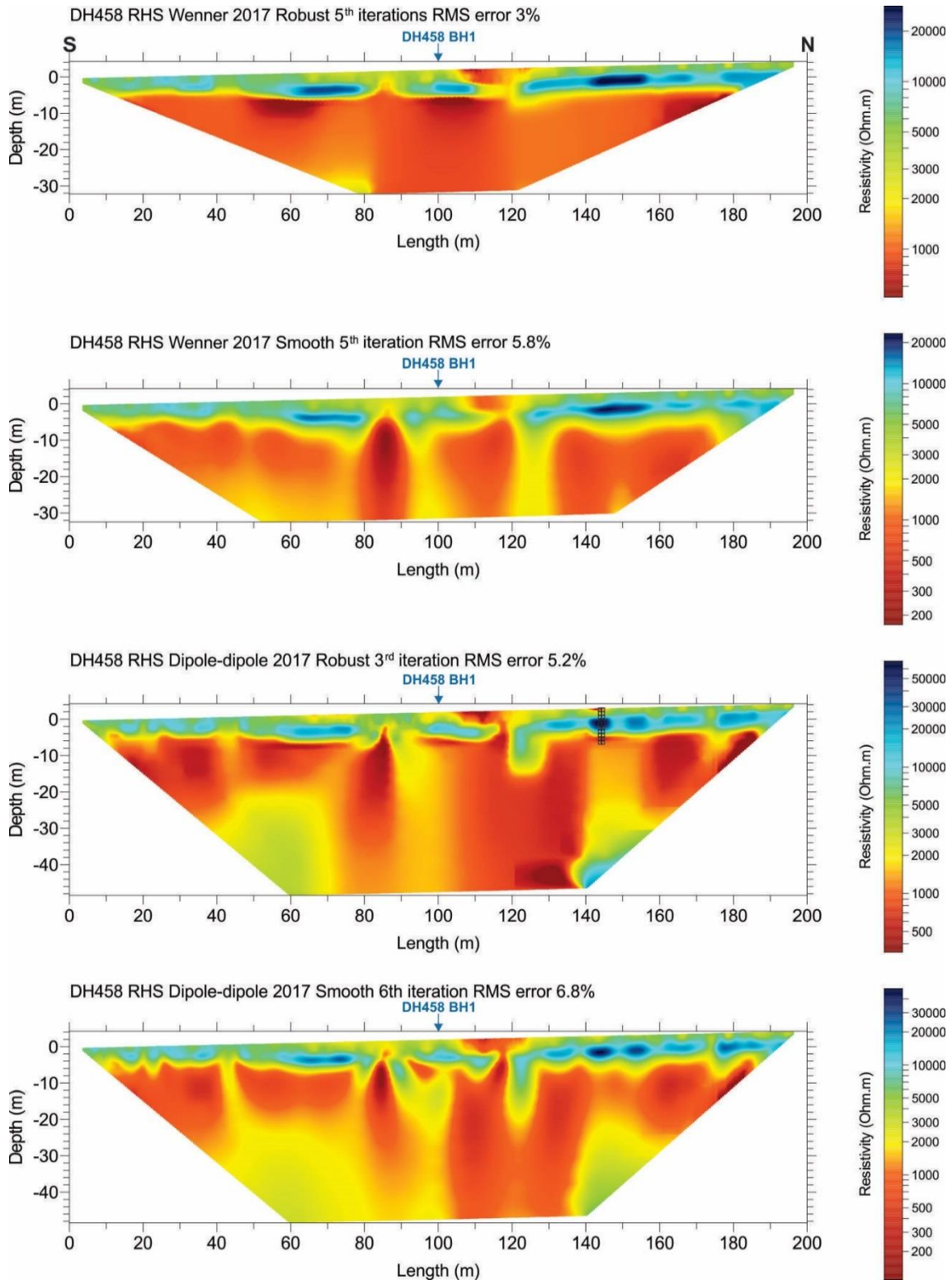
Figure 3.17.6 Wenner and dipole-dipole ERT surveys at site DH458, right-hand side (RHS), using robust and smoothed inversion processes.

4 DISCUSSION

4.1 GEOGRAPHICAL DISTRIBUTION OF THE SITES

The seventeen sites selected for investigation in this survey are distributed along two distinct areas; a southern area is located between km 82 and 126, in the Blackstone Uplands, and a northern area is located between km 375 and 458, from Eagle Plains to the Richardson Mountains (Fig. 1).

4.2 GENERAL GROUND TEMPERATURE AND GROUND ICE CONDITIONS

The assessment of the ground temperature condition is limited by: i- the short duration of the records, as many sites were instrumented in June and July 2017 and only a few months of data were available for this report; ii- the maximal depths of recording being generally shallow, i.e. less than 3 m.

Taking into account these limitations, ground temperature conditions were based on the warmest temperature recorded at the deepest depth of a borehole (Fig. 2A). The Blackstone Uplands section displays ground temperatures ranging between -3 and 0°C, with an average of -1.8°C; while the Eagle Plains/Richardson Mountains sector has ground temperatures ranging between -4.6 and -0.2°C, with an average at -1.6°C. Consequently, the ground temperatures appear to present a certain variability, but overall the permafrost at the investigated sites is warm (T>-2°C) in both areas, with the permafrost in the Blackstone Uplands area appearing to be slightly colder. Also, because the investigated sites were selected based on permafrost-related issues, their ground temperature may be more representative of that of degrading permafrost areas, rather than broader, regional permafrost conditions.

The assessment of the volumetric excess ice content (VEIC) is limited by the shallow depth of the geotechnical investigations. Figure 2B shows the average VEIC for each borehole plotted with respect to their location along the road. The VEIC does not include the content of massive ice such as wedge ice.

The Blackstone Uplands section shows VEIC ranging between 40 and 50%, with an average of 45%; the Eagle Plains/Richardson Mountains section has VEIC ranging between 15 and 45%, with an average of 33%. Accordingly, the VEIC appears to be higher in the Blackstone Uplands area, while the VEICs of the Eagle Plains/Richardson Mountains area are lower, and display a greater variability. Wedge ice, and other massive ice bodies were visually observed on cuts and sampled during drilling in the southern area, but not in the northern one; which puts an emphasis on the fact that the ground of the southern area is significantly more ice-rich than in the north.

4.3   NATURE AND EXTENT OF GROUND ICE

Blackstone Uplands area:

In the Blackstone Uplands, the major ground ice features are: i- ice wedges, and ii- buried ice bodies. The ERT surveys indicate the presence of these two types of ice (Fig. 3). The presence of the ice bodies is confirmed at site DH116, where ice wedges were observed along the cut and sampled in boreholes. The buried massive ice was sampled in one geotechnical borehole at a depth exceeding 14 m. Ice wedge exposure has also been observed at Two Moose Lake. The observed ice wedges are up to 3 m in width and 6 m in height. They can be found close to the surface and also to extend relatively deep in the profile (~10 m). The observed buried ice was located deep in the profile (>14 m), and its thickness may exceed 6 m.

Eagle Plains/Richardson Mountains area

In the Eagle Plains/Richardson Mountains area major ground ice bodies were not directly observed; their presence can only be inferred based on landforms (i.e. polygonal ground) and geophysical surveys. The ERT surveys show indications of the presence of wedge ice and other possible ice bodies (Fig. 4). Based on the observation of degraded polygonal ground, the ice wedges seem to be smaller, and have a lesser height (~2-3 m) than in the southern area. Based on the glacial history, the deeper ground ice is not likely buried glacier ice, but could be intrusive ice.

Geophysics suggests that permafrost is absent at some locations, and that ground water may be present at some sites. This is consistent with a warmer permafrost than that which is present in the Blackstone Uplands.

4.4   VULNERABILITY

Overall, the Blackstone Uplands appears to have greater vulnerability with respect to the impact of climate changes on permafrost, mainly because of the significant amount of ice present in the ground. In the Eagle Plains/Richardson Mountains area, permafrost appears to contain less ground ice and the permafrost may also be less extensive. Processes attributable to ground water movement are present in both areas.

The quantity of excess ice in the ground is likely to impact the volume of granulate that will be required to maintain the road over the coming decades. The loss of volume due to the ground ice melting must be compensated with a similar volume of granulate. In the Blackstone Uplands, ice wedge dimension and distribution will determine the required amount of granulate in the upper part of the ground profile.

The general distribution of ground ice is likely to control the timing of the degradation, as well as the required type of mitigation. The Chapman Lake site, DH116, is a perfect illustration of this fact.

Ground water movement will have an impact on sinkholes, landslides, and thermal erosion. Ground water originates either from melt water at freshet or summer precipitation. Increases in winter and summer precipitation in the future will result in more water infiltrating the ground surface, and increase the occurrence of the above-mentioned processes. In addition, increased snow precipitation will increase the insulating effect on permafrost where this snow accumulates.

4.5   MAINTENANCE VS. ADAPTATION

Four possible scenarios may occur in the future in terms of maintenance costs (without considering inflation).

In the first scenario, the cost of maintenance remains stable over time. This situation is likely to occur along sections of the highway where climate change will have no impact. i.e. where there is no permafrost, and where the road is not impacted by hydrologic processes (Fig. 5A).

In the second scenario, the cost of maintenance decreases over time. This situation is likely to occur along sections of the highway where permafrost and/or ground ice are disappearing under the influence of climate change, and where it is assumed that hydrologic processes are absent or under control (Fig. 5B). Some sites located in the Eagle Plains/Richardson Mountains will likely evolve in this direction.

In the third scenario, the cost of maintenance increases over time. This situation is likely to occur along sections of the highway where ice-rich permafrost is present. As the active layer thickens, the melt of ground ice will increase and ground may become more instable, with subsidence and the occurrence of slope processes increasing (Fig. 5C). Some sites located in the Blackstone Uplands will likely progress along this course as the melt of ice wedges and buried massive ice leads to more subsidence and ground water movement, contributing to the formation of sinkholes.

A fourth and last scenario can be applied to areas where regular maintenance will not be sufficient to control degradation processes. In this case, a remedial action is required to guarantee the continued integrity of the road over time. Such actions will likely be costly but may solve the maintenance issue for an undefined period (Fig. 5D). The Chapman lake area, DH116, is a good illustration of this type of site.

To chose the best strategy and select the most appropriate scenario for each area, a model linking biophysics and economics should be developed.
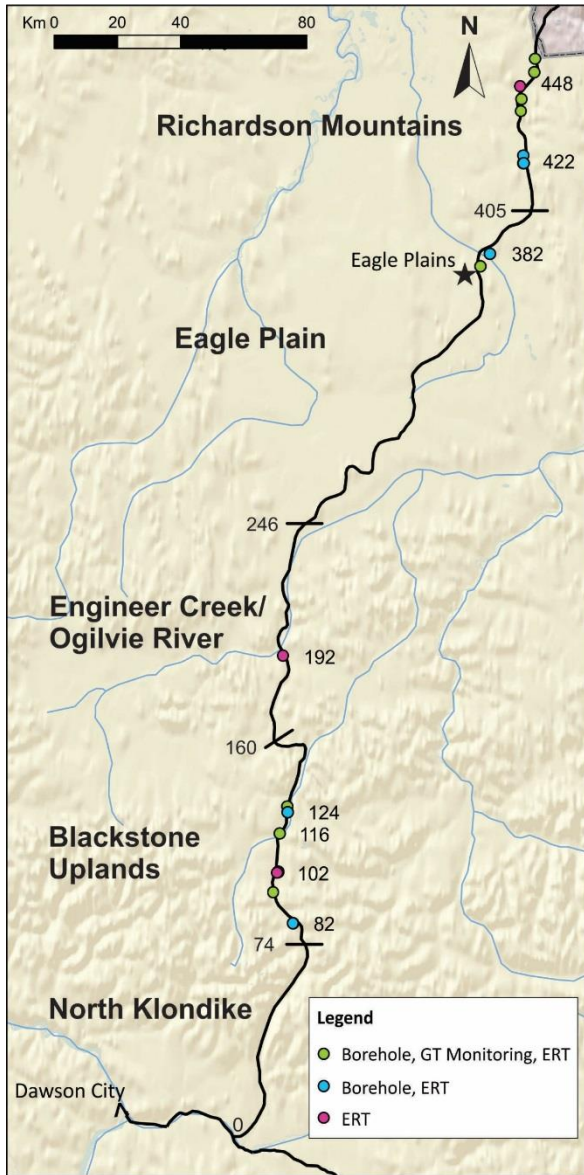
Figure 4.5.1 Site locations along the Dempster Highway
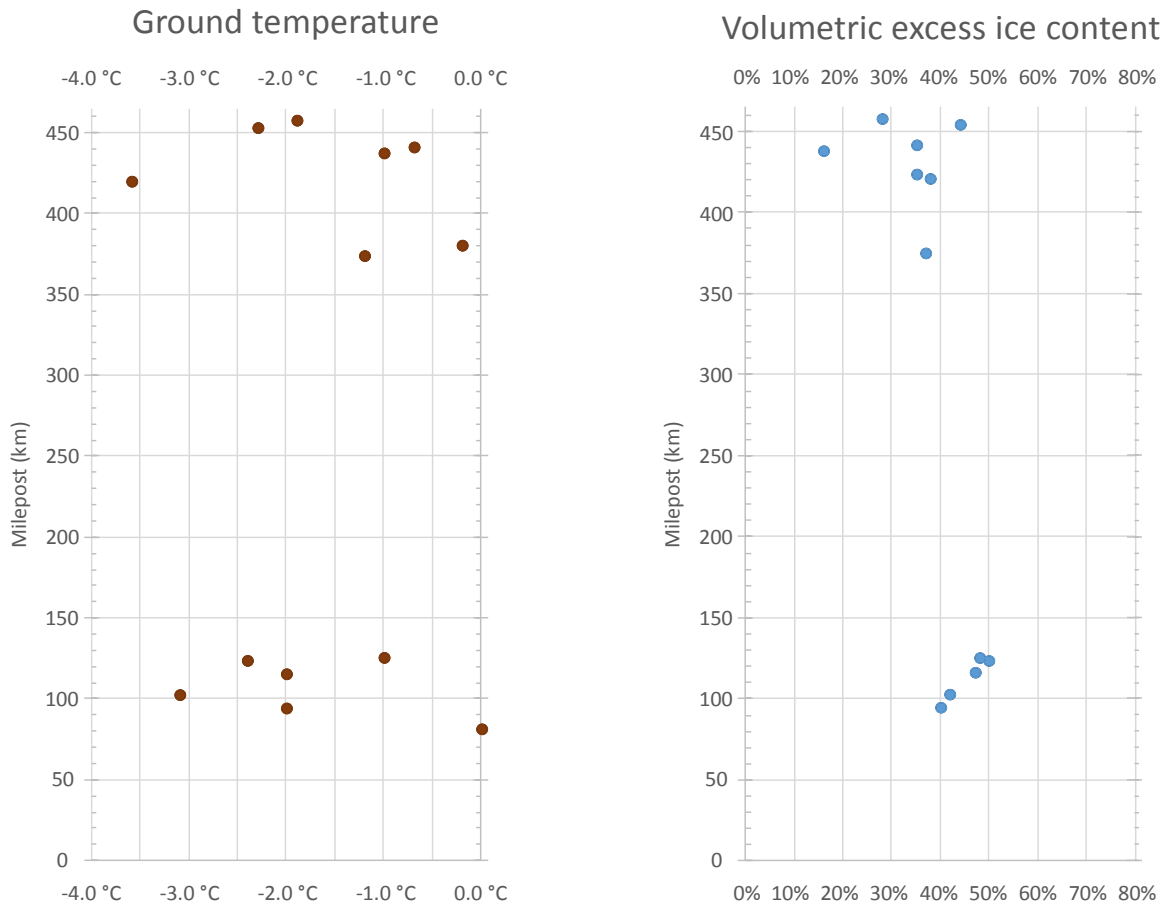
Figure 4.5.2 Ground temperature and ground ice conditions at investigated sites
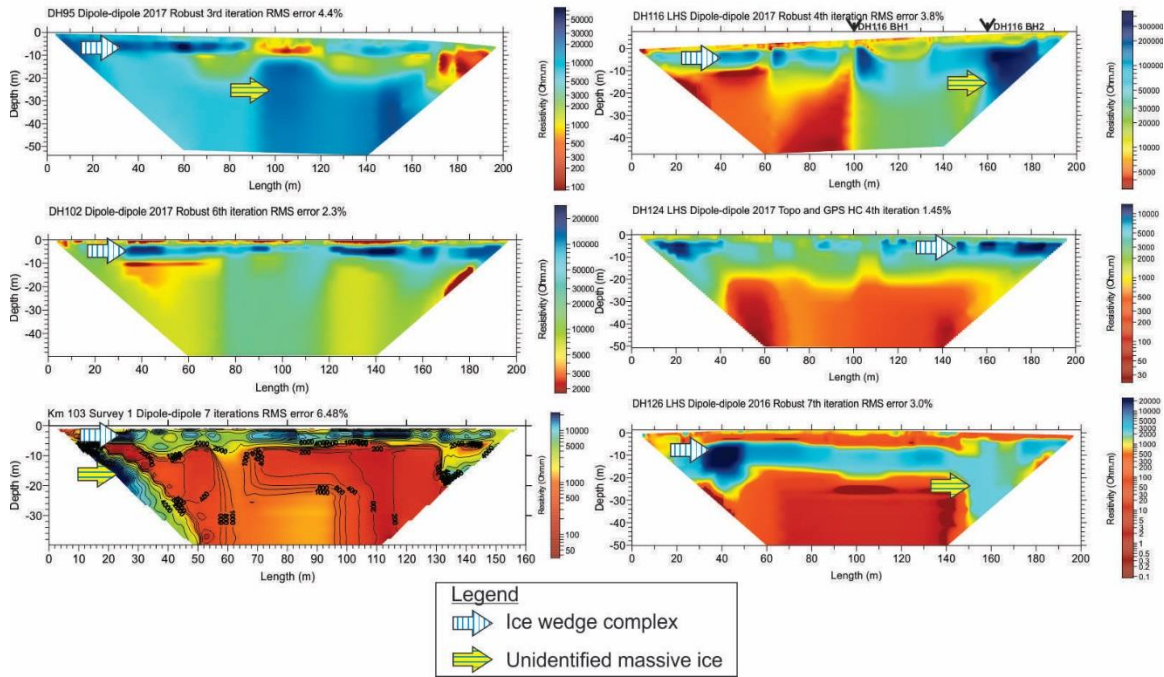
Figure 4.5.3 ERT surveys in the southern area with potential ground ice body locations
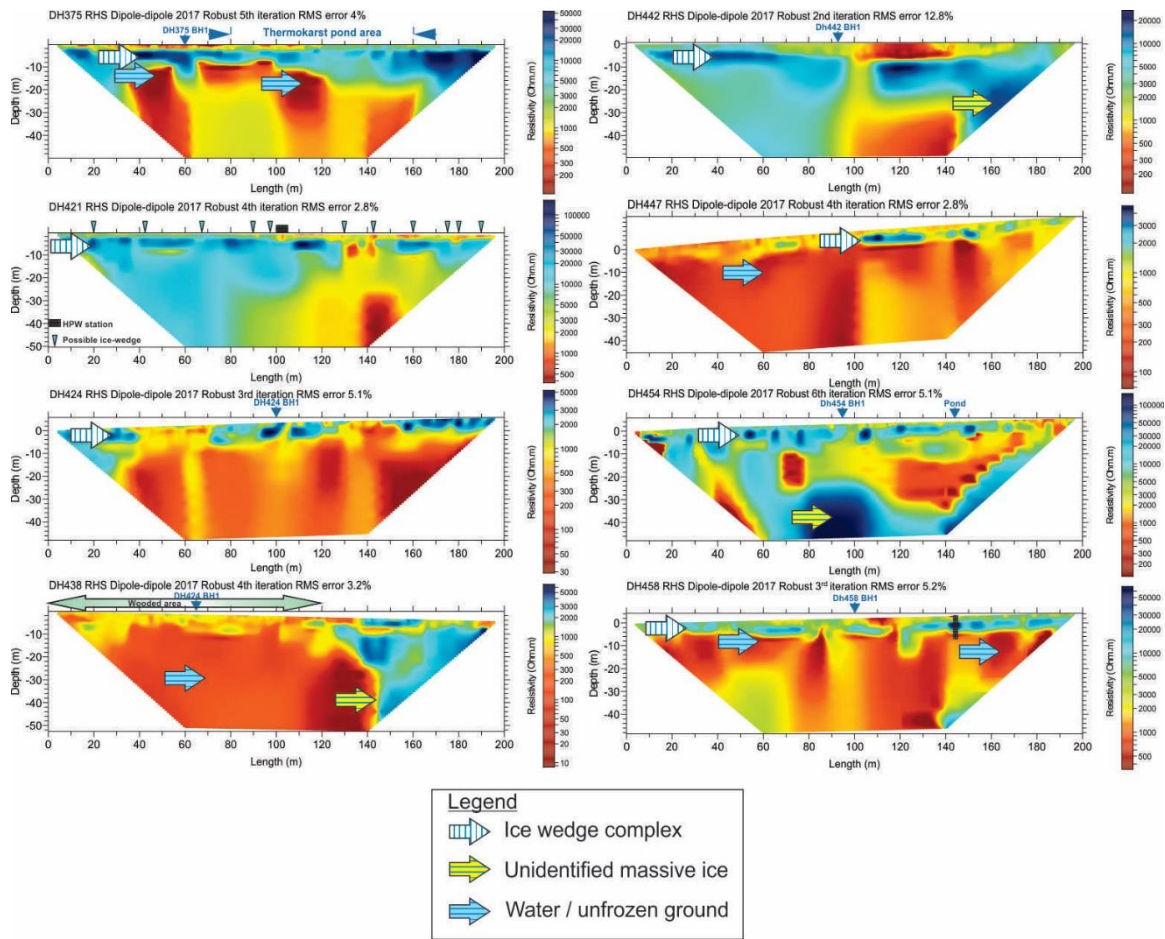
Figure 4.5.4 ERT surveys in the northern area with potential ground ice body locations

Scenario 1 - Maintenance remains stable over time

As time goes by...

Scenario 2 - Maintenance decreases over time

As time goes by...

Scenario 3 - Maintenance increases over time

As time goes by...

Scenario 4 - Requirement for mitigation measures

? ?

As time goes by...

Figure 4.5.5 Possible scenarios about the evolution of maintenance efforts due to climate change

5 REFERENCES

Andersland, O.B., Ladanyi, B. 2004. Frozen Ground Engineering. 2nd Edition. John Wiley & Sons, 384 p.

Burn, C., Moore, J., O'Neil, B., Hayley, D., Trimble, R., Calmels, F., Orban, S., and Idrees, M. 2015. Permafrost characterization of the Dempster Highway, Yukon and Northwest Territories. GEOQuébec2014: 64th Canadian Geotechnical Conference & 7th Canadian Permafrost Conference, Sept. 20-23, 2015, Québec, Québec. Canadian Geotechnical Society.

Calmels, F., Gagnon, O.; and Allard, M. 2005. A portable earth-drill system for permafrost studies. Permafrost and Periglacial Processes 16: 311-315.

Camels, F., Roy, L.P., Laurent, C. and Horton, B. 2017. Investigation of Dempster Highway Sinkholes: km 82 and Two Moose Lake. Yukon Research Centre, Yukon College, 66 p.

Idrees, M., Burn, C., Moore, J., and Calmels, F. 2015. Monitoring permafrost conditions along the Dempster Highway. GEOQuébec2014: 64th Canadian Geotechnical Conference & 7th Canadian Permafrost Conference, Sept. 20-23, 2015, Québec, Québec. Canadian Geotechnical Society.

Murton, J. and French, H. 1994. Cryostructures in Permafrost, Tuktoyaktuk Coastlands, Western Arctic Canada. Canadian Journal of Earth Sciences 31:737-747.

6   APPENDIX A: COPY OF BURN ET AL., 2015

Permafrost characterization of the Dempster Highway, Yukon and Northwest Territories

C.R. Burn, J.L. Moore, H.B. O'Neill
Department of Geography and Environmental Studies – Carleton University, Ottawa, ON, Canada
D.W. Hayley, J.R. Trimble
Hayley Arctic Geoconsulting, Kelowna, BC, and TetraTech EBA, Whitehorse, YT, Canada
F. Calmels
Northern Climate ExChange — Yukon Research Centre — Yukon College, Whitehorse, YT, Canada
S.N. Orban, M. Idrees
Transportation Engineering Branch — Highways and Public Works, Government of Yukon, Whitehorse, YT, Canada

GEOQuébec 2015
Challenges from North to South
Des défis du Nord au Sud

ABSTRACT
The Dempster Highway was built over permafrost to connect the western Arctic with the national highway system. Mean annual permafrost temperatures along the route are ≥ -4 °C. Most ground ice is found in glacial deposits, and in these materials the embankment is particularly prone to thaw subsidence. Extended periods of rain have led to debris flows blocking the road and wash outs in steep terrain and near rivers. Icings may impede drainage during freshet. These hazards are of varying relative importance along the route. The principal terrain units and permafrost-related hazards are: North Klondike, icing; Blackstone Uplands, thaw subsidence; Engineer Creek/Ogilvie River, debris flows and wash outs; Eagle Plains, relatively unaffected; Richardson Mountains and Peel Plateau, thaw subsidence; Northern Plains, icing.

RÉSUMÉ
L'autoroute Dempster a été construite sur le pergélisol, afin de connecter l'Arctique de l'Ouest avec le réseau autoroutier national. Les températures moyennes annuelles du pergélisol le long de la route sont de ≥ -4 °C. La majorité de la glace de sol est présente dans les dépôts glaciaires, matériaux sur lesquels le remblai routier est particulièrement sujet aux subsidences. Des périodes de pluie importantes ont mené à des coulées de débris bloquant la route et à des glissements de terrain sur les fortes pentes et à proximité des rivières. Des glaçages peuvent obstruer le drainage durant le dégel printanier. Ces risques varient en importance le long de la route. Les principales unités physiographiques et leurs dangers reliés au pergélisol sont: North Klondike, glaçage; Blackstone Uplands, subsidence au dégel; Engineer Creek/Ogilvie River, coulées de débris et glissements de terrain; Eagle Plains, relativement non-affecté; Richardson Mountains and Peel Plateau, subsidence au dégel, Northern Plains, glaçage.

1   INTRODUCTION

The Dempster Highway is the principal transportation artery for Canada's western Arctic. It is an all-season road opened in 1979 between Yukon Highway 2, the Klondike Highway, and Inuvik, NWT (Figure 1). The Dempster Highway was built on continuous permafrost for 90% of its 736 km. As a result, the road structure is an embankment, designed to maintain permafrost and prevent thaw subsidence (Huculak *et al.* 1978). For the first 75 km of its route, north from the junction with Klondike Highway, the road passes over discontinuous permafrost (Heginbottom *et al.* 1995).

Transport Canada (TC) has established a Network of Expertise in Northern Transportation Infrastructure Research to assist governments to adapt roads, airports, and marine facilities to challenges posed by climate change. One of the Network's projects concerns establishment of baseline data collection and assessment of permafrost response to climate warming alongside transportation infrastructure in Yukon and NWT. Given the strategic importance of the Dempster Highway and the record of climate warming in the region (e.g., Burn and

Kokelj 2009), the Network has invested considerable effort into this part of our northern transportation infrastructure. In a companion paper, we report a monitoring program to document baseline permafrost conditions and the thermal impact of the embankment on permafrost at key sites along the highway (Idrees *et al.* 2015).

In this paper, we present a summary of ground temperatures that have been collected along the highway from several sources: the TC monitoring program; Northwestel's microwave repeater stations; investigations sponsored by the NWT Cumulative Impacts Monitoring Program (CIMP) (e.g., O'Neill *et al.* 2015a); and the published literature. These data span most of the highway route (Figure 1). In addition, since 2005, significant research on ground ice conditions along the route has been published (e.g., Lacelle *et al.* 2007; Kokelj *et al.* 2013; Lacelle *et al.* 2015). This has accompanied recognition of terrain hazards due to ground ice thawing, and a

Figure 1. The Dempster Highway, Yukon and NWT, with locations mentioned in the text. Colours code data sources in Tables 2 and 3: yellow – Northwestel; green – Baseline study; purple – NWT CIMP; blue – Lacelle *et al.* (2009); black – communities and weather stations.

rehabilitation program for the highway in the NWT, from the territorial border to Tsiigehtchic (Figure 1), with particular effort west of the Peel River Crossing at NWT km 74. However, in several sections of the highway in Yukon, the primary terrain hazards are associated with hydrologic processes. We present a terrain vulnerability characterization for the route, combining knowledge of ground temperatures and ground ice conditions with the dominant geomorphic processes along the road.

2 PHYSIOGRAPHIC CHARACTERIZATION

For much of its length, the Dempster is a mountain highway that traverses Ogilvie and Richardson mountains of the northwestern Cordillera (Figure 2). In Ogilvie Mountains, the road follows valley floors (Figure 3), while in Richardson Mountains it crosses the ranges. The highest elevations occur in the southern sections (Figure 2). The road follows the rolling terrain of the upland Eagle Plain for about 180 km, and similarly crosses the uplands of Peel Plateau to the east of Richardson Mountains (Figure 4). From Peel River to Inuvik, the terrain is remarkably flat and at low elevation. As a result of changing elevation and latitude, the route passes through forest and tundra. Terrain units along the route are summarized in Table 1 and indicated in Figure 5.

2.1 Geological factors

The bedrock outcrops in the ranges of the Cordillera are of uplifted ocean floor deposits. The rocks are sandstones, shales and limestones, covered by veneers of glacial or colluvial deposits. The limestones have weathered mechanically to boulder size, while the sandstones and shales have been broken into finer-grained soils (Richardson and Sauer 1975).

2.2 Glacial legacy

Glaciation has left a variable imprint on the terrain. A central portion of the highway, km 116-495, passes through unglaciated terrain. As a result, some sections of the route are dominated by colluvial sediments, or weathered bedrock. In contrast, southern parts of the route, between about km 75 and km 116 km, experienced valley glaciation during the Wisconsinan period, while north and east of km 495 Peel Plateau and the plains of NWT were covered by the Laurentide ice sheet.
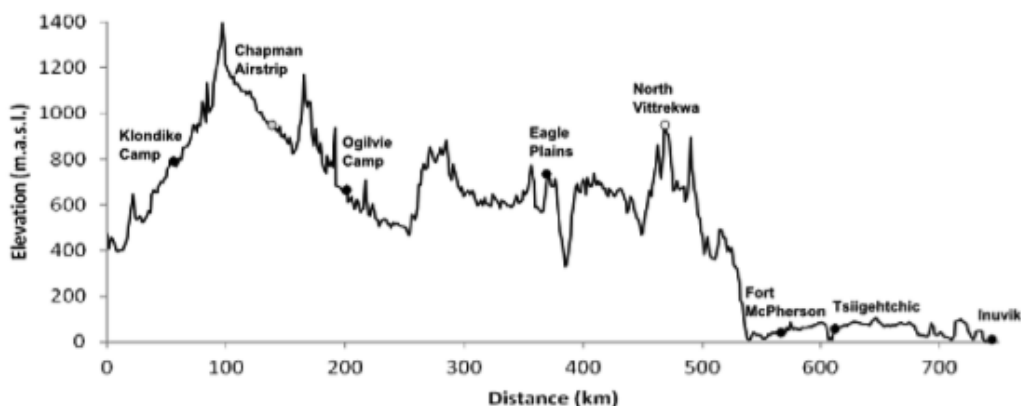
Figure 2. Schematic topographic profile for the Dempster Highway. Source: Google Earth.

Figure 3. Dempster Highway in the valley of Ogilvie River, at km 210, August 2011. Photo by S.N. Orban.

Figure 4. Peel Plateau, near NWT km 60, August 2012. Photo by H.B. O'Neill.

2.3 Climate

The region has a subarctic climate (Table 2), modified by the mountainous terrain of the region. Topographic shading and cold-air drainage lead to extremely low temperatures in valley bottoms during winter, as at Ogilvie Maintenance Camp. Air temperatures rise with elevation within atmospheric inversions, so that lapse rates in winter are less than in summer (Lewkowicz and Bonnaventure 2011; O'Neill et al. 2015b). Precipitation is reduced by the continental-scale rain shadow of St Elias Mountains, but rainfall has been increasing recently in the region (Kokelj et al. 2015). Blowing snow in tundra areas leads to significant accumulations alongside the embankment and where vegetation acts as a snow trap (O'Neill et al. 2015a).

Figure 5. Physiographic units along the Dempster Highway.

2.4 Permafrost

The area is almost entirely underlain by permafrost (Heginbottom et al. 1995). Ground water flow in the mountainous terrain modifies the condition of perennially frozen ground and may create considerable surface icing in winter (Idrees et al. 2015). Boreholes drilled at Chapman Airstrip (km 124) in glacial outwash penetrated through permafrost at only 7 m depth (Idrees et al. 2015). Ground water was observed in these boreholes, suggesting that convection in the ground water may restrict the thickness of permafrost. In the mountains, development of frost blisters at the base of hillslopes and accumulation of river icing demonstrate that ground water may emerge or freeze as intrusive ice within the active layer or at the ground surface throughout the winter (Pollard and French 1984; Hu and Pollard 1997).

Ground temperatures reported from the region indicate the annual mean temperature of permafrost within the boreal forest and taiga is ≥ -3.0 °C (Table 3) (Lacelle et al. 2009). In the taiga near Inuvik, annual mean ground temperatures ≥ -2.0 °C have been measured in peatlands, where the soils may have a long zero curtain due to high porosity, wet ground, and deep snow accumulation (Burn et al. 2009). Similar temperatures have been measured in shrubby tundra on Peel Plateau, due to the influence of atmospheric inversions and accumulation of blowing snow (O'Neill et al. 2015b). Below, we report recently compiled measurements of ground temperatures from a range of sites along the route.

191

Table 1. Physiographic units of the Dempster Highway. See Figure 5.

	Location (km) (NWT)	Terrain type	Surficial materials
North Klondike	0 - 74	Mountain hillsides	Colluvium and till
Blackstone Uplands	74 - 160	Valley floor	Till and outwash
Engineer/Ogilvie River	160 - 246	Narrow valleys	Colluvium and alluvium
Eagle Plain	246 - 405	Rolling uplands	Weathered bedrock
Richardson Mountains	405 – 492 (27)	Mountain slopes	Colluvium and alluvium
Peel Plateau	492 (27) – 539 (74)	Rolling plateau	Glacial till
Northern Plains	539 (74) – 732 (267)	Open plain	Glacial till

Table 2. Climate data for the Dempster Highway, 2004. Annual mean air temperature (AMAT), winter (D,J,F) mean air temperature (WMAT), summer (J,J,A) mean air temperature (SMAT), and precipitation are available for this year.

	km	Elevation (m)	AMAT (°C)	WMAT (°C)	SMAT (°C)	Rainfall (mm)	Snowfall (cm)
Dawson	0	346	-4.2	-18.9	15.6	78.6	237.4
Klondike Camp	65	966	-4.9	-19.2	12.3	243.3	304.3
Ogilvie Camp	195	588	-9.2	-29.7	13.2	104.4	176.5
Eagle Plains	369	729	-6.0	-24.3	14.8	81.1	94.0
Rock River	457	735	-6.8	-22.0	12.6	-	-
Fort McPherson	550	22	-8.7	-28.2	15.0	67.8	117.6
Inuvik	732	15	-9.4	-27.5	13.1	83.4	246.0
Tuktoyaktuk	-	0	-11.6	-28.5	10.4	56.0	151.3

3   PERMAFROST TEMPERATURES

Two complementary investigations have recently begun to yield new ground temperature information for terrain adjacent to the Dempster Highway. The first is from a series of boreholes drilled to approximately 10-m depth at microwave stations operated by Northwestel. The drilling and thermistor cable installation was by EBA Engineering, and data retrieval has been since 2009. Data are compiled by Northwestel and hosted online by Yukon College. Data acquisition has not been complete in all years. The second investigation has been sponsored by TC to obtain baseline information on permafrost temperature within the highway right-of-way, and, over time, to assess the impact of climate change on permafrost and the active layer within the embankment, at the toe, and in undisturbed ground. These sites were installed in late 2013, and data have been collected for one year. Temperature sensors were installed to 8 m below the surface in undisturbed ground. In addition, comparable data from undisturbed sites has been collected under CIMP. We have compiled data from these sources and the published literature in Table 3, where we report temperatures collected at depths ≥ 5 m.

3.1   Northwestel installations

The Northwestel stations are surrounded by a fence. The three cables at each site are located inside the fence, at the fence, and outside fence. We have compiled annual mean temperatures for each thermistor string for the most recent complete year of available data. We report the basal temperatures from outside the fence at each site in Table 3, since, of the data available, these are the best indicators of long-term undisturbed conditions. There is considerable surface disturbance at the Rengleng and Deep Water Lake stations. The annual mean temperature decreases with depth at these sites, indicating that permafrost is degrading. The values from North Fork and North Vittrekwa indicate relatively low ground temperatures at higher elevations along the route. The lowest annual mean temperature was recorded within the fence at North Vittrekwa (-5.8 °C), where infrastructure influences snow drifting and scouring.

3.2   Baseline characterization

Data collected during the characterization of baseline ground temperatures near and beneath the embankment are presented in Idrees et al. (2015). In Table 3 we present data from the undisturbed ground at two sites. The data collected from nearby Northwestel stations are consistent with measurements at these sites, even though the data in Idrees et al. (2015) are for 2014/15, and measurements at North Fork and North Vittrekwa were collected in 2013/14 and 2012/13, respectively.

The data presented in Table 3 do not display a consistent trend with latitude, as with annual mean air temperature (Table 2). There is a small difference between the annual mean ground temperatures collected in the forest/taiga and at tundra sites, with the difference between the two means, -2.0 and -3.0 °C, respectively, being significant at the 5% level under a one-tailed Student's t-test. The difference, 1 °C, represents the level of variation in ground temperature between tundra and taiga along the route.

Table 3. Annual mean ground temperatures and active-layer thicknesses in undisturbed terrain at sites along the Dempster Highway, Yukon and NWT. Data are from various sources described in the text. The Peel Plateau sites are in shrub tundra. Sites in the boreal forest or taiga are marked by *. Locations of sites are on Figure 1.

Site	Region	km post (NWT)	Depth (m)	MAGT (°C)	Active layer (cm)	Source
North Fork	Blackstone Uplands	98	10	-3.7	75	Northwestel (this paper)
Chapman Airstrip	Blackstone Uplands	124	1.0	-2.7	80	Idrees et al. (2015)
*Red Creek	Engineer/Ogilvie River	167	7.0	-2.5	110 (est.)	Lacelle et al. (2009)
*Ehnjuu Choo	Eagle Plain	347	10	-1.2	150	Northwestel (this paper)
Glacier Creek	Richardson Mountains	421	8.0	-3.6	40	Idrees et al. (2015)
North Vittrekwa	Richardson Mountains	465	10	-3.8	40	Northwestel (this paper)
Peel Plateau A	Peel Plateau	516 (51)	5.0	-1.8	70	O'Neill et al. (2015a)
Peel Plateau B	Peel Plateau	525 (60)	5.0	-2.6	75	O'Neill et al. (2015b)
Fort McPherson	Peel Plain	556 (91)	5.0	-2.5	40	O'Neill et al. (2015b)
Deep Water Lake	Peel Plain	572 (107)	10	-3.4	130	Northwestel (this paper)
Rengleng	Anderson Plain	645 (180)	10	-1.4	100	Northwestel (this paper)
Inuvik	Anderson Plain	722 (257)	5.0	-1.2	55	Burn et al. (2009)

4   GROUND ICE CONDITIONS

Ground ice conditions along the route are available from several reports that have been published recently, and for the boreholes that were drilled in the baseline characterization program (Idrees et al. 2015).

4.1   Buried ice

Buried glacier ice is increasingly recognized as an important component of the terrain close to the glacial limits of northwest Canada (Kokelj et al. 2013; Lacelle et al. 2013). Large retrogressive thaw slumps on Peel Plateau occur within the limit of Laurentide glaciation (Lacelle et al. 2015). At present, such slumps, although visible from the highway, have not yet posed a hazard to the road in NWT. Nevertheless, we may assume that thick masses of buried glacier ice may underlie some stretches of the road in Peel Plateau. Similarly, buried glacier ice has been exposed and described in the Chapman Lake moraine at km 116 (Lacelle et al. 2007).
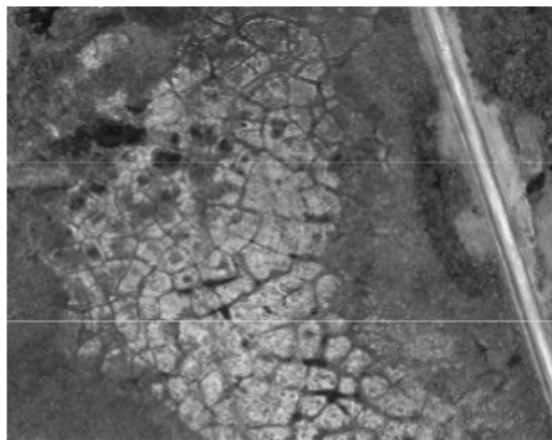
Figure 6. Ice-wedge polygons near the highway in Blackstone Uplands. Image from Google Earth.

4.2   Ice-wedge polygons

Ice-wedge polygons may be recognized along the route in many sections, as, for example, in Figure 6. These polygons characteristically have slight depressions above the wedges, and lack the raised rims formed by actively growing ice wedges. They are most commonly seen at tundra sites. The ice wedges are of massive ice (e.g., Idrees et al. 2015, Fig. 6).

4.3   Syngenetic segregated ice

The uppermost layers of permafrost terrain in unconsolidated, fine-grained sediments are commonly ice rich. The ground ice is in the form of segregated ice lenses that develop near the top of permafrost and remain there if the permafrost table rises (e.g., French and Shur 2010). The ice-rich zone has been called the transient layer of permafrost, to recognize that active-layer thickness may change as climate varies. Such a layer is common in frost-susceptible soils, as in the silty till cover of the Peel Plateau (site 4 of Idrees et al. 2015, Fig. 6). However, a similarly ice-rich zone may develop as a result of sedimentation and aggradation of the surface. Unglaciated parts of the highway route contain both sites of long-term erosion, and sites of long-term deposition. At the latter, a thick layer of ice-rich ground may have developed in aggrading deposits, as at Glacier Creek (site 2 of Idrees et al. 2015, Fig. 6).

4.4   Intrusive ice

Intrusive ice is most commonly recognized as a seasonal form, developed within the active layer (e.g., Pollard and French 1984). In mountainous terrain, such as along the Dempster Highway, it is associated with hydraulic gradients due to elevation. Frost blisters are best known from the Blackstone Uplands, but Richardson Mountains provide similar terrain conditions for the development of massive intrusive ice. Intrusive ice may occur as sheets of pure ice as well as the commonly identified frost blisters.

4.5 Icing

Development of surface icing over winter is apparent in spring after snow melt, because extensive masses of ice may linger in river beds. Icings develop in the rivers of Ogilvie Mountains because of groundwater systems that have developed in limestone bedrock. Intrusive ice is commonly associated with discharge through the active layer, but icings that continue to form throughout winter may originate from deeper, sub-permafrost circulation. Icings occur when water flows over surface ice, allowing greater thicknesses to form than by downward freezing alone (Hu and Pollard 1997).

5   VULNERABILITY CLASSIFICATION

The principal terrain hazards along the route stem from the nature of the mountainous terrain and the presence of ground ice in permafrost. A key hazard in all permafrost environments is the potential for thaw subsidence from melting of ground ice. This varies along the Dempster Highway because ground-ice occurrence is associated with the different glacial histories along the route. In narrow valleys, the embankment is subject to blockage by mass movements and erosion by rivers in flood where the road abuts watercourses. The likelihoods that both of these hazards may occur during periods of rainfall are magnified by the impermeability of permafrost terrain. Groundwater discharge in winter leads to extensive river icing, blocked culverts, and, if water overtops the embankment, a dangerous driving surface.

The highway route may be divided into several physiographic regions, in each of which permafrost-related terrain hazards differ in their importance. Throughout the length of the road, annual mean permafrost temperatures are ≥ -4 °C, indicating that all soils with massive ice have a high sensitivity to disturbance either due to changes in surface conditions or climate (Hayley and Horne 2008).

Figure 7. Culvert at km 32.5 (North Klondike River valley), filled with icing, May 2014. Photo by C.R. Burn.

5.1   North Klondike – Surface icing

The principal terrain hazard in the first 80 km of the route is development of icings that block culverts and impede drainage (Figure 7). If discharge continues through the winter, the embankment may be insufficiently high to retain the accumulating water (ice), and it may flow onto the driving surface. This is a principal hazard in winter, but in freshet, blocked culverts may lead to alternate routing of surface water and washout of the embankment.

5.2   Blackstone Uplands – Thaw subsidence

Buried glacier ice has been identified in the moraine at Chapman Lake (km 116) (Lacelle et al. 2007). In 2006, Yukon Highways realigned the road in this area because erosion of the riverbank threatened the integrity of the embankment. The new alignment was built as a cut in order to reduce vertical curvature. The cut was in ice-rich till containing buried glacier ice. Deterioration of the embankment was observed shortly after construction. Remedial work on the section has been necessary almost continuously since then.

Two Moose Lake (km 102) is within the glacial limits in Blackstone Valley, and is surrounded by moraine. Thermokarst development of the lake has brought the shoreline to the road embankment, so that temperatures beneath the road are now affected by the lake (Figure 8). Continual maintenance has been required at this point.
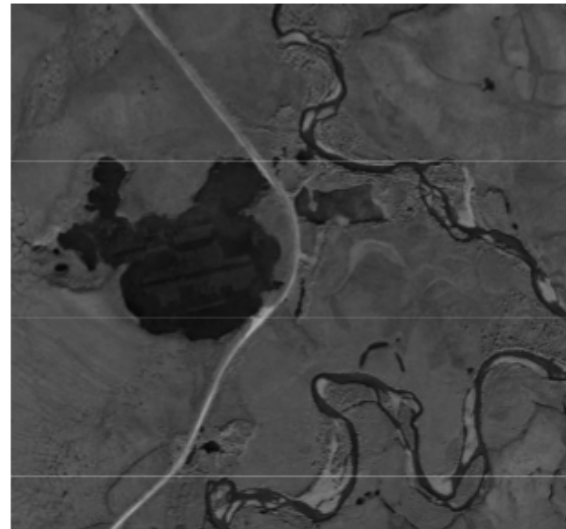
Figure 8. Thermokarst expansion of Two Moose Lake has brought it to the highway embankment. Image from Google Earth.

5.3   Engineer Creek/Ogilvie River – Mass movement

The road follows the narrow valleys of Engineer Creek and Ogilvie River. Where the bedrock is carbonate, rock falls are a recognized hazard, as the slopes are bare of

soil. In clastic bedrock, a surface veneer of soil rests on permafrost. During heavy rain, landslides and debris flows may block the road (Figure 9), with the occurrence facilitated by the relatively impermeable permafrost.

High discharge and coarse bedload in the streams during freshet and following rain storms may erode the riverbank supporting the highway and bridge abutments, requiring reconstruction of the road bed (Figure 10). Drainage structures may appear to be over designed in summer for the magnitude of flow, but even these may still be damaged in the spring flood.

Figure 9. Debris flow at km 244, August 2010. Photo by C.R. Burn.

Figure 10. Wash out of the road by Ogilvie River at km 245, June 2013. Photo by S.N. Orban

5.4   Eagle Plain – relatively unaffected

The highway route follows the upper surface of Eagle Plain. The route avoids many hazards associated with permafrost due to the shallow soils and absence of water courses. The Eagle River crossing is a short exceptional section, due to the abundance of water and frost-susceptible, floodplain deposits.

5.5 Richardson Mountains – Thaw settlement

Subsidence of the embankment due to thaw of ground ice is a principal hazard in this section (Figure 11). The ground ice is localized, because the mountains were not glaciated. It may occur as ice wedges or bodies of intrusive ice. However, given the extensive time available for hill slope movement, any surface expression of the ice formation may have been covered by subsequent deposits. Figure 11 shows thaw subsidence of the road embankment at km 27. Degradation of the driving surface is generally managed through routine maintenance along the route. Shoulder rotation due to thaw settlement of the toe may be observed in several places.

Figure 11. Thaw subsidence of the embankment at NT km 27, August 2011. Photo by C.R. Burn.

5.6 Peel Plateau – Thaw settlement

Thaw settlement is the principal hazard on Peel Plateau because of the ice-rich till that covers the terrain unit and the buried glacier ice that underlies some sections of the landscape.

5.7 Northern Plains – Surface icing

The northern plains are covered by a veneer of till, and in places thaw subsidence is a hazard. However, massive ice is not as prevalent as in Peel Plateau, and so the hazard is reduced. Drainage is locally awkward where creeks flow out of lakes for a long portion of the freezing season, and icing accumulates beside the road.

6   CONCLUSIONS

(1) For most of the Dempster Highway, with the exception of Eagle Plain and North Klondike River valley, the ground is highly sensitive to disturbance, either by surface modification or from climate warming, because the temperature of permafrost is ≥ -4 °C and the area has ice-rich soil. Thaw subsidence is the primary terrain hazard for much of the route.

(2) In the Engineer Creek/Ogilvie River valleys, the principal hazards are related to the impermeability of permafrost terrain heightening runoff, and hence flooding, and also increasing the potential for mass movement on hill slopes.

(3) Throughout the mountainous terrain of the route, ground water discharge in winter leads to surface icing and blockage of culverts, threatening the integrity of the embankment during freshet.

REFERENCES

Burn, C.R., and Kokelj, S.V. 2009. The environment and permafrost of the Mackenzie Delta area, *Permafrost and Periglacial Processes*, 20: 83-105.

Burn, C.R., Mackay, J.R., Kokelj, S.V. 2009. The thermal regime of permafrost and its susceptibility to degradation in upland terrain near Inuvik, N.W.T., *Permafrost and Periglacial Processes*, 20: 221-227.

French, H., and Shur, Y. 2010. The principles of cryostratigraphy, *Earth-Science Reviews*, 101: 190-206.

Hayley, D.W., and Horne, B. 2008. Rationalizing climate change for design of structures on permafrost: a Canadian perspective. *9th International Conference on Permafrost*, Institute of Northern Engineering, University of Alaska Fairbanks, AK, USA. Vol. 1: 681-686.

Heginbottom, J.A., Dubreuil, M.A., and Harker, P.A.1995. Canada-Permafrost In *National Atlas of Canada*, 5th ed., Natural Resources Canada, Ottawa, ON, Canada. Plate 2.1 MCR 4177.

Hu, X.G., and Pollard, W.H. 1997. The hydrologic analysis and modeling of river icing growth, North Fork Pass, Yukon Territory, Canada, *Permafrost and Periglacial Processes*, 8: 279-294.

Huculak, N.A., Twach, J.W., Thomson, R.S., and Cook, R.D. 1978. Development of the Dempster Highway north of the Arctic Circle. *3rd International Conference on Permafrost*, National Research Council of Canada, Edmonton, AB, Canada. Vol. 1: 798-805.

Idrees, M., Burn, C.R., Moore, J., and Calmels, F. 2015. Monitoring permafrost conditions along the Dempster Highway. *7th Canadian Permafrost Conference, GeoQuébec 2015*, Canadian Geotechnical Society, Québec City, QC, Canada. (This conference)

Kokelj, S.V., Lacelle, D., Lantz, T.C., Tunnicliffe, J., Malone, L., Clark, I.D., and Chin, K.S. 2013. Thawing of massive ground ice in mega slumps drives increases in stream sediment and solute flux across a range of watershed scales, *Journal of Geophysical Research (Earth Surface)*, 118: 681-692.

Kokelj, S.V., Tunnicliffe, J., Lacelle, D., Lantz, T.C., Chin, K.S., and Fraser, R. 2015. Increased precipitation drives mega slump development and destabilization of ice-rich terrain, northwestern Canada, *Global and Planetary Change*, 129: 56-68.

Lacelle, D., Lauriol, B., Clark, I.D., Cardyn, R., and Zdanowicz, C. 2007. Nature and origin of a Pleistocene-age massive ground-ice body exposed in the Chapman Lake moraine complex, central Yukon Territory, Canada, *Quaternary Research*, 68: 249-260.

Lacelle, D., St-Jean, M., Lauriol, B., Clark, I.D., Lewkowicz, A., Froese, D.G., Kuehn, S.C., and Zazula, G. 2009. Burial and preservation of a 30,000 year old perennial snowbank in Red Creek valley, Ogilvie Mountains, central Yukon, Canada, *Quaternary Science Reviews*, 28: 3401-3413.

Lacelle, D., Lauriol, B., Zazula, G., Ghaleb, B., Utting, N., and Clark, I.D. 2013. Timing of advance and basal condition of the Laurentide Ice Sheet during the last glacial maximum in the Richardson Mountains, N.W.T., *Quaternary Research*, 80: 274-283.

Lacelle, D., Brooker, A., Fraser, R.H., and Kokelj, S.V. 2015. Distribution and growth of thaw slumps in the Richardson Mountains-Peel Plateau region, northwestern Canada, *Geomorphology*, 235: 41-50.

Lewkowicz, A.G. and Bonnaventure, P.P. 2011. Equivalent elevation: a new method to incorporate variable surface lapse rates into mountain permafrost modelling, *Permafrost and Periglacial Processes*, 22: 153–162.

O'Neill, H.B., Burn, C.R., and Kokelj, S.V. 2015a. Field measurement of permafrost conditions beside the Dempster Highway embankment, Peel Plateau, NWT. *7th Canadian Permafrost Conference, GeoQuébec 2015*, Canadian Geotechnical Society, Québec, QC, Canada. (This conference)

O'Neill, H.B., Burn, C.R., Kokelj, S.V., and Lantz, T.C. 2015b. "Warm" tundra: atmospheric and near-surface ground temperature inversions across an alpine tree line in continuous permafrost, western Arctic, Canada, *Permafrost and Periglacial Processes*, 26: doi: 10.1002/ppp.1838.

Pollard, W.H., and French, H.M. 1984. The groundwater hydraulics of seasonal frost mounds, North Fork Pass, Yukon Territory, *Canadian Journal of Earth Sciences*, 23: 543-549.

Richardson, N.W., and Sauer, E.K. 1975. Terrain evaluation of the Dempster Highway across the Eagle Plain and along the Richardson Mountains, Yukon Territory. *Canadian Geotechnical Journal*, 12: 296-319.

7 APPENDIX B: COPY OF IDREES ET AL., 2015

Monitoring permafrost conditions along the Dempster Highway

GEOQuébec
2015

Challenges from North to South
Des défis du Nord au Sud

M. Idrees
Transportation Engineering Branch — Highways and Public Works, Government of Yukon, Whitehorse, YK, Canada
C.R. Burn, J.L. Moore
Department of Geography and Environmental Studies — Carleton University, Ottawa, ON, Canada
F. Calmels
Northern Climate ExChange — Yukon Research Centre — Yukon College, Whitehorse, YK, Canada

ABSTRACT

The Dempster Highway, which connects the western Arctic to the national highway network, is built almost entirely on permafrost. Four long-term permafrost monitoring sites were established on the highway in 2013-14 to determine baseline thermal conditions and to follow changes in ground temperatures driven by climate change. The sites are at km 124 and 421 in Yukon and km 8.5 and 51.5 in NWT. Boreholes, up to 10 m in depth, were drilled at each site in the highway centerline, at the embankment toe, and in undisturbed ground. Data have been retrieved from thermistor cables at these sites since February 2014. The embankment toe is the warmest location at each site. In undisturbed ground, annual mean temperatures range from -3.6 to -1.1 °C. The centerline is relatively cold, with annual mean temperatures ranging from -3.9 to -2.4 °C. The permafrost at km 124 is unexpectedly thin due to groundwater movement.

RÉSUMÉ

L'autoroute Dempster connecte l'Arctique de l'ouest au réseau autoroutier national. Elle est presque entièrement construite sur le pergélisol. Quatre sites ont été instrumentés le long de la route en 2013-2014 afin de fournir un suivi thermique des conditions du pergélisol dans le contexte des changements climatiques. Les sites sont localisés aux km 124 et 521 au Yukon et aux km 8.5 et 51.5 au TNO. Des trous ont été forés à chaque site au milieu de la route, au pied du talus et dans le terrain non-perturbé jusqu'à une profondeur maximale de 10 m. Les données sont enregistrées par des câbles à thermistances depuis février 2014. Le pied du talus est l'endroit le plus chaud. Les températures moyennes annuelles du terrain non-perturbé s'échelonnent de −3.6 à −1.1 °C. Le centre de la route est relativement froid avec des températures s'échelonnant de -3.9 à -2.4°C. Le pergélisol au km 124 est étonnamment mince à cause des mouvements d'eau souterraine.

1 INTRODUCTION

The Dempster Highway is a critical component of Canada's transportation infrastructure, because it is the only all-weather road connecting the western Arctic to the national highway network (Figure 1). For about 90% of its 736 km length, the highway is on continuous permafrost. Transport Canada (TC) has established a Network of Expertise in Northern Transportation Infrastructure Research to assist governments to adapt roads, airports, and marine facilities to challenges posed by climate change. One of the Network's projects concerns establishment of baseline data collection and assessment of permafrost response to climate warming alongside transportation infrastructure in Yukon and NWT.

This paper describes four long-term monitoring sites on the Dempster Highway that were established in 2013-14 to characterize permafrost conditions and follow changes in ground temperatures due to climate change and the thermal influence of the embankment. The sites were selected at locations anticipated to be sensitive to long-term disturbance due to evidence of near-surface ice-rich permafrost. Ground conditions at the sites are described and one year's ground temperatures are presented in order to characterize mean annual permafrost temperatures (T_p) along the route. The thermal differences between undisturbed terrain and ground affected by the embankment are examined.

2 BACKGROUND

The Dempster Highway connects the Klondike Highway (Yukon Highway 2), 40 km east of Dawson City, Yukon, to Inuvik, NWT. The first 80 km of the route lies in the extensive discontinuous permafrost of North Klondike River valley (Heginbottom et al. 1995). In this section, the road climbs from about 400 m a.s.l. to over 1200 m a.s.l. at the continental divide. The route traverses continuous permafrost north of the divide. Latitude and elevation vary so that the highway route passes through forest and tundra.

The route covers a series of physiographic units with varying surficial materials (Burn et al. 2015). Glacial history is a key influence on ground materials, including ground ice content. The terrain was glaciated from km 0 to the vicinity of Chapman Lake (km 116) in Yukon, and northeast of km 30 on Peel Plateau and in the plains of NWT. In these sections, surficial materials are dominated by till (Beierle 2002; Lacelle et al. 2013). The remainder of the route was unglaciated, and the surficial materials are glacial outwash, alluvial, and colluvial deposits in valleys and a weathered colluvial veneer in the uplands of Eagle Plain. Massive ground ice has been observed in glacial deposits near Chapman Lake and in the Peel Plateau (Lacelle et al. 2007, 2013). Ice-wedge polygons are prevalent in the terrain of the Blackstone River valley,

from km 85 to 130, and in other tundra areas. Icings are common in the discontinuous permafrost section. Extensive sheets of river icing develop in the Blackstone and North Klondike river channels (Figure 2) (Hu and Pollard 1997).
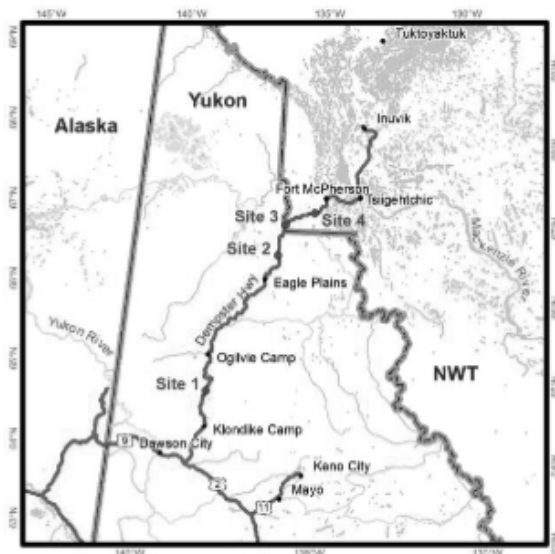
Figure 1. Location map for permafrost monitoring sites on the Dempster Highway, Yukon and NWT.

Figure 2. Blackstone River near Chapman Lake, showing extensive river icing, May 2014.

The 1981-2010 climate normal mean annual air temperature (T_a) varies from -4.1 °C at Dawson to -8.2 °C at Inuvik (Environment Canada 2015). The coldest location on the route is the steep and incised terrain near the Ogilvie River, where shading and cold-air drainage promote severe cooling in winter. T_a at Ogilvie Camp (km 200) is comparable to Inuvik, although there are insufficient data for calculation of a 30-year average. Recently, O'Neill et al. (2015a) have shown that air temperature inversions create significantly warmer winter

conditions on Peel Plateau than on low-lying Peel Plain at Fort McPherson.

Since 2009, ground temperatures have been collected near NorthwesTel's microwave towers along the highway route. These data are discussed in a companion paper, but the key observations are of relatively low T_p (~ -4 °C) in the tundra of the Blackstone Uplands and in the Richardson Mountains at the Yukon-NWT border (Burn et al. 2015). The ground is warmer on Peel Plateau (T_p ~ -2 °C) (O'Neill et al. 2015a), and the warmest observed permafrost is in taiga near Inuvik, with T_p ~ -1.6 °C (Burn et al. 2009). Smith et al. (1998) recorded little difference in T_p between forest sites spread as far apart as Takhini River valley near Whitehorse, YK, and Inuvik. The observed T_p indicate that atmospheric inversions and snow accumulation are important modifiers of ground temperature. The effects of snow are important for permafrost adjacent to road embankments in tundra regions, where there is commonly a significant supply of blowing snow. Accumulation of snow on the embankment slopes may lead to permafrost degradation at the toe, where increased wetness commonly promotes the growth of shrubs, fertilized by road dust (Gill et al. 2014). Trapping of snow by shrubs further amplifies snow depth (e.g., Roy-Léveillée et al. 2014).

Climate warming, particularly in autumn and winter, has been observed in Canada's western Arctic since 1970 (Burn and Kokelj 2009), and near-surface permafrost is warming at a rate that has been reconciled with observed atmospheric warming (Burn and Zhang 2009, 2010). Coincidental rehabilitation since 2005 of the Dempster Highway in the NWT through Richardson Mountains and Peel Plateau has cost approximately $65M. Much of this construction has been designed to reduce the effects of permafrost degradation on the driving surface. The project described in this paper is explicitly intended to gather information on permafrost temperatures beneath and adjacent to the highway embankment in tundra sections of the route and to install equipment that will be used to monitor long-term changes in permafrost conditions.

3   SITE SELECTION

Four sites were selected for monitoring of permafrost conditions along the highway (Figure 1). The sites were chosen to span much of the route, and were located in tundra areas in order to examine conditions where the effects of snow on embankment stability are likely greatest. In addition, installation disturbance is less in such terrain than in the forest, where trees must be removed for access by drilling equipment. Sites were identified with evidence of near-surface ground ice, either observed in the field or known from historical investigations. Two sites were selected in Yukon and two in NWT. The specific locations were determined during a field investigation and reconnaissance survey along the highway in late August 2013. The four locations are in the Blackstone Uplands at the Chapman Lake airstrip (Yukon km 124); near Glacier Creek, on the slopes of Richardson Mountains north of the Arctic Circle (Yukon km 421); in Richardson Mountains near the Yukon-NWT border (NWT

Table 1. Monitoring site characteristics

Site	Informal Name	Km post	N	W	Surface conditions
1	Chapman Lake airstrip, YT	124	64.903	138.278	Mosses and lichens; ice-wedge polygons; flat
2	Glacier Creek, YT	421	66.701	136.358	Mosses and lichens; ice-wedge polygons; gentle cross slope
3	Territorial border, NWT	8.5	67.109	136.088	Mosses, lichens and dwarf birch; inclined with road
4	Midway airstrip, NWT	51.5	67.241	135.263	Alder bushes, mosses and sedges; inclined with road

km 8.5); and on Peel Plateau, 1.8 km west of the emergency airstrip near at Midway Lake (NWT km 51.5). Coordinates of the sites and brief site descriptions are given in Table 1, and photographs of the sites are presented in Figure 3.

Site 1 is in the northernmost portion of the Blackstone Uplands, where the road follows the broad Blackstone River valley (Figure 3a). The site is north of the glacial limit (Beierle 2002). A gravel pit 1 km south of the airstrip indicates the surficial materials are mostly glaciofluvial outwash, covered by a veneer of silt. The site has well developed networks of ice-wedge polygons. These are outlined at the ground surface by slight depressions in the moss and lichen surface vegetation. Numerous willow bushes have grown adjacent to the road at the toe of the embankment. In 2005-2010, ground temperatures were measured with HOBO H-008 miniature data loggers and TMC6-HA sensors at three locations in this flat valley floor, about 500 m from the road. T_p at 1-m depth at the three sites were -4.7, -4.5, and -5.0 °C (Burn et al. 2015). The glaciofluvial terrace surface at the site is about 30 m above the Blackstone River, which flows north, subparallel to the road, about 200 m to the east.

Site 2 is 15 km north of the Arctic Circle crossing, at the foot of the western escarpment of Richardson Mountains (Figure 3b). The road runs across the slope at the site. The vegetation cover is dominated by mosses and lichens, with few bushes. The ground was not glaciated, so the gentle gradient of the lower slopes is the result of colluvial deposition continuing over millennia. Ice-wedge polygons are apparent, but their form is muted, with little development of bounding ridges and troughs.

Site 3 is on the NWT side of the territorial border (Yukon km 465) in the high Richardson Mountains (Figure 3c). It is near the location of a serious accident caused by collapse of the roadbed following thermal erosion of an ice wedge beneath the embankment. The site is on a slope descending westwards. The area is covered by dwarf birch bushes growing in mosses and lichens. The area was not glaciated, so the surficial materials are dominantly the result of colluvial processes. Bedrock exposures are visible from the road, but not at the precise location of the monitoring site. In June 2014 a large frost blister was examined on the south side of the road near the site, indicating the efficacy of water movement through the active layer at this site.

Site 4 is in Peel Plateau (Figure 3d), within the area glaciated by the Laurentide Ice Sheet. The region is underlain by extensive deposits of buried glacier ice. The rolling terrain is covered by shrub tundra, and dense alder thickets have grown alongside the highway since it was built in the 1970s (Gill et al. 2014). Tills cover much of the region (Lacelle et al. 2013). Permafrost in the Peel Plateau is remarkably warm for a tundra environment in the western Arctic (O'Neill et al. 2015a).

The embankment height is variable between the sites, being least at site 1 and greatest at site 4 (Table 2). Snow accumulation along the embankment slope is evident in Figure 4, which presents views of the embankment at site 2 in summer and winter.

4 METHODS

The four monitoring sites were established in late November and December 2013. At the highway centerline, holes were drilled to reach 10 m below grade. At the toe and at the undisturbed ("field") sites, the nominal intentional depth was 8.5 m. The holes were drilled by Marl M4CT and Sandvik Marlin M5 rigs. Surficial materials and any unfrozen ground were penetrated by auger, but in frozen ground a 4-inch CRREL barrel was used. Cores were retrieved with the CRREL barrel, but only grab samples were recovered when drilling with the auger. The ground materials retrieved from the holes were logged, with some samples returned to Whitehorse for laboratory examination. Grain-size and moisture content analyses were by Tetra Tech EBA. A one-inch, capped PVC tube was installed in the holes as casing for thermistor cables. The holes were backfilled with dry sand. Figure 5 is a schematic diagram of the installation at the sites.

Unanticipated conditions were encountered at sites 1 and 3. At Site 1 the materials were largely unfrozen and water logged, and impenetrable boulders required redrilling of the holes at the toe and beneath the centerline. This was completed in January 2014. At Site 3 the holes were drilled to bedrock, which was closer to the surface than the intended depths of drilling. Table 2 presents the depth of boreholes and embankment materials, and the height of the embankment at each site. Thermistor cables were installed in the borehole casings in late February 2014. The sensors (YSI 44007) have a tolerance of ±0.2 °C below 0 °C. The nominal depths of sensors are 0.3, 1.0, 1.5, 2.0, 3.0, 4.5, 6.0, 8.0, (and 10.0) m below the surface. The number of sensors varies between cables, being 9 at the centerline and 8 elsewhere, except at Site 3. There the cables terminate at 3.0, 6.0, and 8.0 m with 5, 7, and 8 sensors at the field, toe, and centerline positions respectively (Table 2).

Table 2. Depth of boreholes and embankment fill, and height of road surface above toe at each site (m).

Site	Field	Toe	Centerline	Fill	Height
1	8.53	8.53	10.00	1.80	1.15
2	8.53	8.84	10.00	2.40	1.85
3	3.20	6.10	8.40	4.00	2.30
4	8.40	8.23	10.06	2.00	1.70
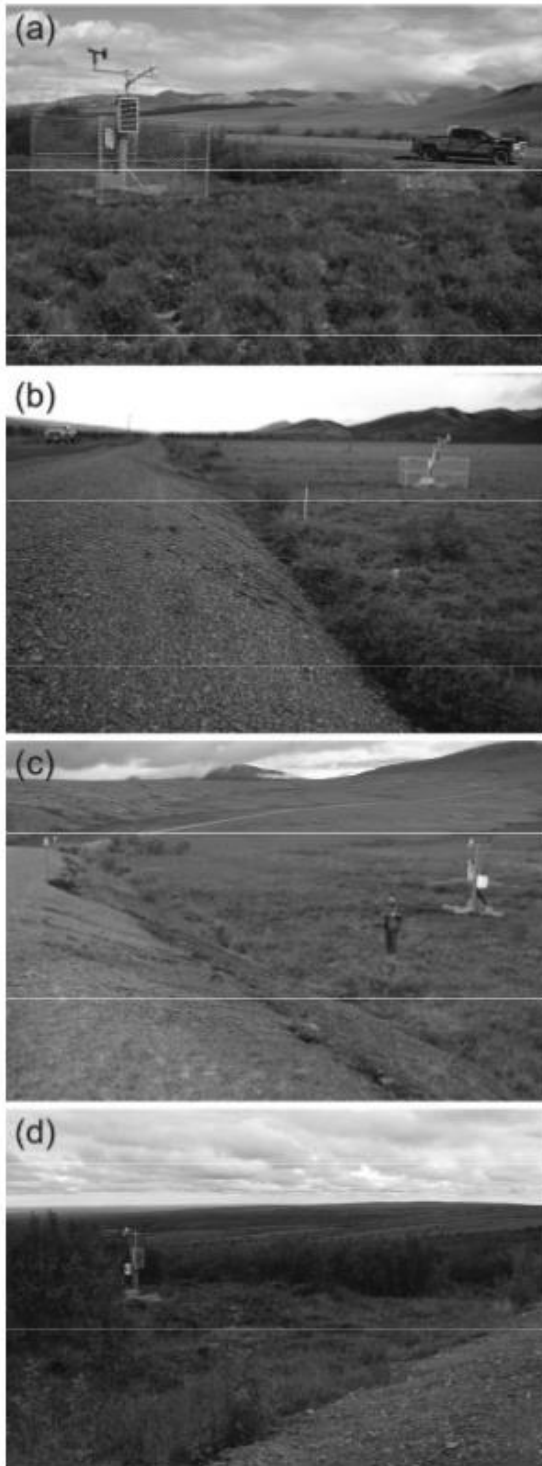
Figure 3. Permafrost monitoring sites along the Dempster Highway, late July 2014. (a) Chapman Lake airstrip; (b) Glacier Creek; (c) Territorial border; (d) Midway airstrip.

Figure 4. Site 2 shown (a) in summer and (b) in winter to illustrate the accumulation of snow beside the road embankment.

A weather station was erected at the field installations, 15 m from the toe of the embankment (Figure 3). This station includes Campbell Scientific HC2-S3-L air temperature and relative humidity sensors, and an anemometer and wind direction sensor (RM Young 05103AP-10-L). Data from these atmospheric sensors and the thermistors are collected by a Campbell Scientific CR1000-55 data logger via a multiplexer board (AM 16/32B XT). Weather data are stored on an hourly basis; ground temperatures are collected every four hours. As from early June 2014, data from sites 1 and 2 have been relayed by GOES satellite to a server in Whitehorse. Data are stored at sites 3 and 4 until collected.

Surface disturbance during drilling was minimal at sites 2 and 3, and moderate at site 1, where two attempts were required for completion of the installation (Figure 3). Disturbance was greatest at site 4, due to the need to clear alders and other bushes (Figure 3d).

Ground and air temperatures were recovered from all sites in June 2014. Further recovery was made in March 2015. Data are available at the time of writing from sites 1, 2 and 3 for a full year, but at site 4 data were not downloaded successfully.

200
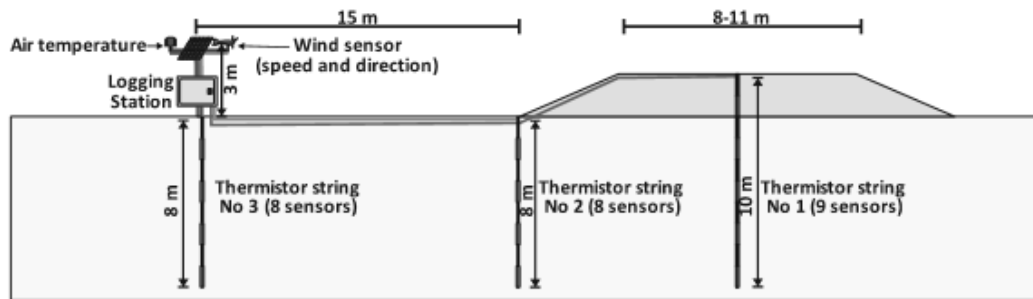
Figure 5. Schematic diagram of drill holes and meteorological equipment at each site.

Table 3. Summary of undisturbed ground conditions at the monitoring sites

Site	Ground	Surficial materials	Excess Ice content
1	Unfrozen below ~7 m	Veneer of silt above outwash gravel	Wedge ice and intrusive ice in upper 3 m
2	Frozen	Organic-rich silt above colluvial diamicton	Wedge and aggradational ice in upper 3.5 m
3	Frozen	Colluvial silt and weathered bedrock	Wedge and aggradational ice in upper 4.0 m
4	Frozen	Stoney silt and clay till	Ice-rich throughout

5 RESULTS

The drilling program and installation of sensors provide some of the few well documented data on permafrost conditions beneath and adjacent to the Dempster Highway.

5.1 Ground materials

Table 3 presents a summary of ground materials at each site. Excess ice was encountered in the uppermost 3.5 m of the field borehole at each site. The stratigraphy of these boreholes is presented in Figure 6. Full stratigraphic data, including photographs of retrieved core, are in Northern Climate ExChange (2014).

5.1.1 Site 1, km 124, Chapman Lake airstrip

Permafrost was anticipated in the surficial materials at site 1 because of the low near-surface annual mean ground temperatures (< -4.0 °C) measured nearby. Surprizingly, unfrozen ground and free water were encountered at depth in all drill holes at this site. A thin layer of permafrost was penetrated at the field installation and in the embankment. At the field site, foliated massive ice, interpreted as wedge ice, was recovered in silts (Mod. USC - ML) above gravel, and a 0.35-m layer of pool ice was found within the permafrost (Figure 6a). The silts were ice rich, with two tested samples giving excess ice contents of 49 and 69 %. The outwash gravels included a range of clast sizes, including boulders that terminated initial drilling. Groundwater discharge through the gravel into Blackstone River channel leads to surface icing in winter (Figure 2). The exceptionally thin permafrost for a site with T_p of < -4 °C is likely due to convective heat transfer in the ground water.

5.1.2 Site 2, km 421, Glacier Creek

Ice-poor gravelly diamicton is overlain at the site by a layer of ice-rich organic silt and clay (Mod. USC – CL), 1 – 2 m thick (Figure 6b). The diamicton is interpreted as a colluvial deposit that originated from the nearby slopes of Richardson Mountains (Figure 3b). The restriction of ice enrichment to the uppermost 3.5 m suggests that the excess ice is associated with permafrost aggradation during deposition of the fine-grained materials. Excess ice content in this material ranged from 20 – 50 %. Wedge ice was recovered in the toe borehole. The organic content of the upper 2 m indicates burial by surface deposition or cryoturbation.

5.1.3 Site 3, km 8.5, Territorial border

Schist bedrock is close to the surface at this site. The lower surficial material is dominantly weathered rock. Ice-rich sediment and massive ice were found in the near surface (Figure 6c). The materials are sand and silt sized at the surface (Mod. USC – ML), becoming coarser with depth (MH), reaching gravel size. The ice is a combination of wedge ice, intrusive ice, and aggradational ice. Excess ice contents of 25 – 52% were measured in the ice-rich material, but relatively few samples were collected due to the shallow holes.

5.1.4 Site 4, km 51.1, Midway airstrip

The terrain is covered by diamicton (till), dominated by silt and clay with numerous stones (Figure 6d). Some beds of clay and silty clay were encountered in the drill holes (Mod. USC – Cl), but samples of diamicton tested also contained up to 10% gravel. It is ice-rich throughout, with excess ice contents of up to 57%, but generally in the range of 40 – 50 %. No massive icy bodies were encountered in the drill holes.
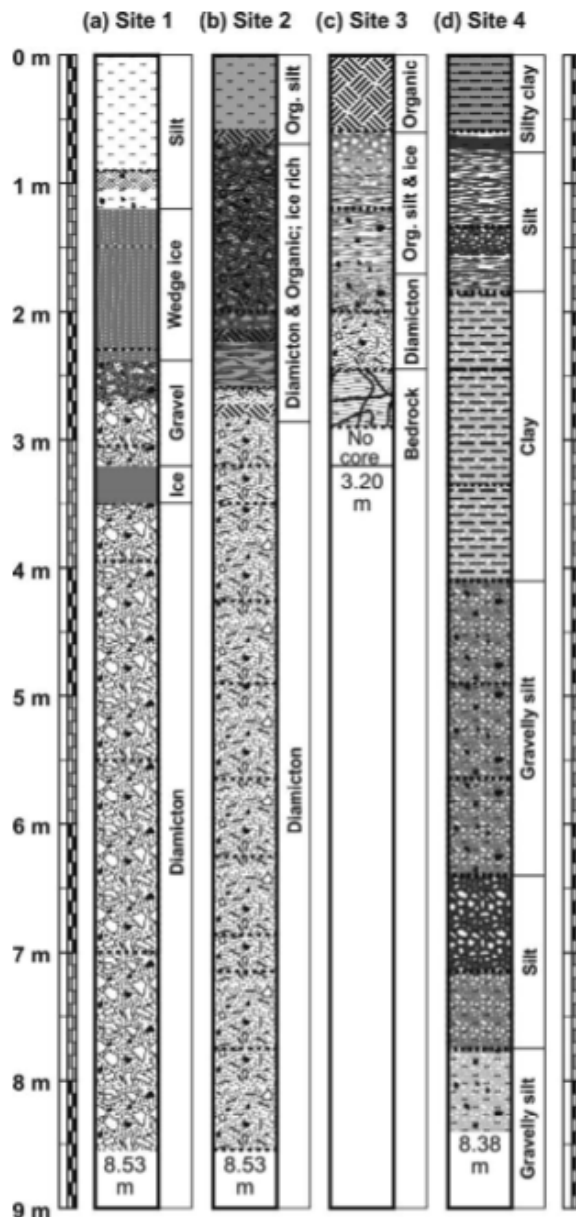
Figure 6. Representative stratigraphy of boreholes drilled in undisturbed ground (field) at the monitoring sites. The base of permafrost at site 1 is at approximately 7 m depth.

5.2 Ground thermal regime

Table 4 presents summary data on ground thermal conditions at each site. Data for sites 1 to 3 are derived from a full year of observations, but the information for site 4 is interpreted from only 3 months' data. There is considerable other thermal information from Peel Plateau that is consistent with these values (e.g., O'Neill et al. 2015a, b). Figures 7a-c present mean annual ground temperature profiles from the field, toe and embankment cables at sites 1-3, and Table 5 presents snow depths measured at sites 1-4 in mid-March 2015. We note several general characteristics: (1) ground temperatures are highest at the toe in association with a snow bank that accumulates there each winter; (2) the temperatures at the centerline are cooler at the surface than in the field sites; (3) the temperature profile of the embankment appears to converge at depth with the profile from the toe.

5.2.1 Site 1, km 124, Chapman Lake airstrip

T_a at site 1 was the lowest recorded in this study (Table 4), and is consistent with the relatively low T_p recorded previously in Blackstone River valley (Burn et al. 2015). Near-surface T_p at the field site was low, as anticipated. However, we did not anticipate that permafrost would be < 8 m thick at this site, or that it would have degraded completely beneath the toe of the embankment (Figure 7a). Maximum temperatures measured over the year indicate the base of permafrost is at about 7 m depth at both field and centerline sites. We attribute the thin layer of permafrost to heat transfer in groundwater flowing through the glacial outwash at the site. The extensive icing in Blackstone River is derived from groundwater discharge throughout winter (Figure 2). Permafrost at the toe cannot be sustained, due to snow accumulation at the edge of the road from ploughing and trapping of blown snow in willows and alder bushes (Figure 3a) (Table 5). Within the embankment, at the centerline, permafrost is sustained, and T_p, just below the active layer is comparable with the field site (-2.4 °C) (Table 4).

5.2.2 Site 2, km 421, Glacier Creek

Permafrost is sustained at site 2, but has been warmed at depth beneath the road and toe, due to the deep snow banks that accumulate on the side slopes (Figure 4) (Table 5). The field site appears to be located away from thermal disturbance associated with the embankment. The site is exemplary because it demonstrates (1) overall warming of permafrost by the road; (2) relatively cold conditions in the embankment; (3) relatively warm conditions at the toe.

5.2.3 Site 3, km 8.5, Territorial border

Bedrock was encountered near the surface at site 3, reducing the depths at which ground temperatures have been measured. The embankment at centerline is relatively cold at the site (Figure 7c), but the similarity between conditions at the toe and field sites suggests that the influence of the snow bank created by the road extends away from the embankment (Table 5). Permafrost appears to be degrading at the toe, as indicated by annual mean temperature above 0 °C

202

Table 4. Annual mean air temperature (Ta, °C), annual mean temperature at the top of permafrost (T_p, °C), thaw depths (m), and permafrost state at sites 1-3, 1 Mar 2014 - 28 Feb 2015. Data for site 4 interpreted from deepest thermistor and only for 24 Feb – 3 June 2014.)

Site	T_a	T_p Centerline	T_p Toe	T_p Field	Thaw depth Centerline	Toe	Field	Permafrost state Centerline	Toe	Field
1	-6.8	-2.4	-	-2.7	2.9	-	0.8	Aggrading	Degraded	Equilibrium
2	-4.9	-2.3	-1.4	-3.6	2.8	0.9	0.4	Aggrading	Degrading	Equilibrium
3	-5.4	-3.9	-1.0	-1.1	2.9	1.4	0.9	Aggrading	Degrading	Equilibrium
4	-5.2	-4.3	-1.1	-0.7	1.9	1.4	0.9	Aggrading	Degrading	Degrading
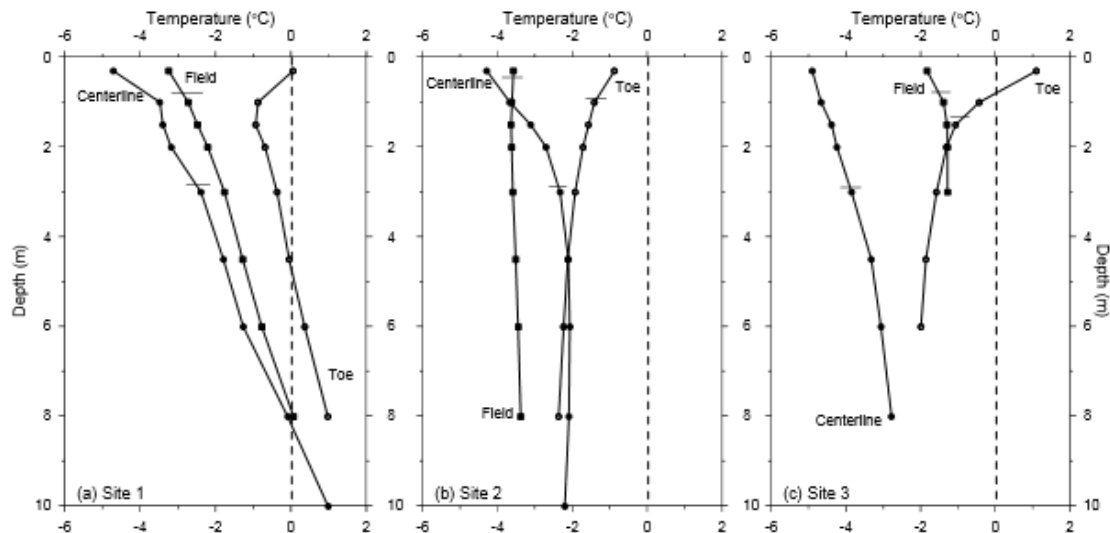
Figure 7. Annual mean temperature profiles from sites 1 – 3 for 1 Mar. 2014 – 28 Feb. 2015. Thaw depths are indicated by a horizontal line at each site. Maximum temperatures were > 0 °C throughout the profile at the toe location of site 1.

within the active layer, which is 0.5 m thicker than at the field location.

5.2.4 Site 4, km 51.1, Midway airstrip

Thermal data at site 4 are presented in Table 4 from only 3 months of observations. The values for T_p, measured at the 8 and 10-m boreholes, are consistent with the relatively warm permafrost conditions interpreted for Peel Plateau by O'Neill et al. (2015a). We do not compare these values with data for site 3 here because of the limited time for data collection, but we note that the time of observation corresponds with a relatively cold period of the year at depth, and therefore we expect mean annual values to be higher than those presented for information purposes in Table 4.

Table 5. Snow depth (m) at the four study sites, 16-17 March 2015.

Site	Field	Toe	Centerline
1	0.80	1.00	-
2	1.00	1.50	-
3	1.20	1.25	-
4	1.40	1.40	-

6   CONCLUSIONS

From the data presented above we note the following:

(1)   Permafrost is stable and aggrading beneath the centerline of the embankment of the Dempster Highway at the three sites from which a year's ground temperatures have been collected.

(2)   Permafrost has degraded or is degrading beneath the toe of the embankment at these three sites.

(3)   Thin permafrost has been measured at the site with lowest air temperature in association with groundwater movement.

(4)   The integrity of the embankment along the highway appears to be related to the abundance of near-surface ground ice, because conclusion (2) implies that side slope failure is inevitable where the ground is thaw sensitive.

203

REFERENCES

Beierle, B.D. 2002. Late Quaternary glaciation in the Northern Ogilvie Mountains: revised correlations and implications for the stratigraphic record, *Canadian Journal of Earth Sciences*, 39: 1709-1717

Burn, C.R., and Kokelj, S.V. 2009. The environment and permafrost of the Mackenzie Delta area, *Permafrost and Periglacial Processes*, 20: 83-105.

Burn, C.R., and Zhang, Y. 2009. Permafrost and climate change at Herschel Island (Qikiqtaruk), Yukon Territory, Canada, *Journal of Geophysical Research (Earth Surface)*, 114: F02001.

Burn, C.R., and Zhang, Y. 2010. Sensitivity of active-layer development to winter conditions north of treeline, Mackenzie delta area, western Arctic coast, *6th Canadian Permafrost Conference*, Canadian Geotechnical Society, Calgary, AB, Canada: 1458-1465.

Burn, C.R., Mackay, J.R., and Kokelj, S.V. 2009. The thermal regime of permafrost and sensitivity to disturbance near Inuvik, N.W.T., *Permafrost and Periglacial Processes*, 20: 221-227.

Burn, C.R., Moore, J.L., O'Neill, H.B., Hayley, D.W., Trimble, J.R., Calmels, F., Orban, S.N., and Idrees, M. 2015. Permafrost characterization for the Dempster Highway, *7th Canadian Permafrost Conference*, Canadian Geotechnical Society, Québec, QC, Canada.

Environment Canada. 2015. http://climate.weather.gc.ca/ Accessed 2 March 2015.

Gill, H.K., Lantz, T.C., O'Neill, H.B., Kokelj, S.V. 2014. Cumulative Impacts and Feedbacks of a Gravel Road on Shrub Tundra Ecosystems in the Peel Plateau, Northwest Territories, Canada, *Arctic, Antarctic, and Alpine Research*, 46: 947-961.

Heginbottom, J.A., Dubreuil, M.A., and Harker, P.A. 1995. Canada-Permafrost In *National Atlas of Canada*, 5th ed., Natural Resources Canada, Ottawa, ON, Canada. Plate 2.1 MCR 4177.

Hu, X.G., and Pollard, W.H. 1997. The hydrologic analysis and modeling of river icing growth, North Fork Pass, Yukon Territory, Canada, *Permafrost and Periglacial Processes*, 8: 279-294.

Kokelj, S.V., Lacelle, D., Lantz, T.C., Tunnicliffe, J., Malone, L., Clark, I.D., and Chin, K.S. 2013. Thawing of massive ground ice in mega slumps drives increases in stream sediment and solute flux across a range of watershed scales, *Journal of Geophysical Research (Earth Surface)*, 118: 681-692.

Lacelle, D., Lauriol, B., Clark, I.D., Cardyn, R., and Zdanowicz, C. 2007. Nature and origin of a Pleistocene-age massive ground-ice body exposed in the Chapman Lake moraine complex, central Yukon Territory, Canada, *Quaternary Research*, 68: 249-260.

Lacelle, D., Lauriol, B., Zazula, G., Ghaleb, B., Utting, N. and Clark, I.D. 2013. Timing of advance and basal condition of the Laurentide Ice Sheet during the last glacial maximum in the Richardson Mountains, N.W.T., *Quaternary Research*, 80: 274-283.

Northern Climate ExChange. 2014. *Final report: Dempster Highway permafrost assessment*, Report to Highways and Public Works, Government of Yukon, Yukon College: Whitehorse.

O'Neill, H.B., Burn, C.R., Kokelj, S.V., and Lantz, T.C. 2015a. "Warm" tundra: atmospheric and near-surface ground temperature inversions across an alpine tree line in continuous permafrost, western Arctic, Canada, *Permafrost and Periglacial Processes*, 26: doi: 10.1002/ppp.1838.

O'Neill, H.B., Burn, C.R., and Kokelj, S.V. 2015b. Field measurement of permafrost conditions beside the Dempster Highway embankment, Peel Plateau, NWT. *7th Canadian Permafrost Conference*, Canadian Geotechnical Society, Québec, QC, Canada.

Roy-Léveillée, P., Burn, C.R., and McDonald, I.D. 2014. Vegetation-permafrost relations within the forest-tundra ecotone near Old Crow, northern Yukon, Canada, *Permafrost and Periglacial Processes*, 25: 127-135.

Smith, C.A.S., Burn, C.R., Tarnocai, C., and Sproule, B. 1998. Air and soil temperature relations along an ecological transect through the permafrost zones of northwestern Canada, *7th International Conference on Permafrost*, Nordicana, Yellowknife, N.W.T., Canada: 1009-1016